

## RAI Responses 28-32

**RESPONSE TO RAI COMMENT 28  
ROADMAP TO REFERENCES**

<b>REFERENCED DOCUMENT</b>	<b>*EXCERPT LOCATION</b>	<b>REMARK</b>
Bohm 1979	Representative excerpt(s) enclosed following response	Entire book details difficulty in collection of root data on perennial woody species. All methods of excavation and sub-sampling have limitations that must be recognized. Table of Contents provided.
Buol 1973	Representative excerpt(s) enclosed following response	
Burns and Hondala 1990	Excerpt enclosed following response	Provides description of general rooting habit of loblolly pine (assumed to be predominant invader in the region) on page 7.
Cook et al. 2005 (WSRC-TR-2005-00074)	Excerpt enclosed following response	Section 1.2, Section A.2.1, A.2.3.1, A.2.3.2
Goldman et al. 1986	Excerpt enclosed following response	
Hillel 1982	Representative excerpt(s) enclosed following response	
Ludovici 2002	Representative excerpt(s) enclosed following response	Used as basis for modeling of decomposition of root components of loblolly pine based on years since death of tree. Important data is summarized as total tap biomass in figure 5 (page 1681) over time for estimating decomposition.
McRae 1988	Representative excerpt(s) enclosed following response	
Phifer and Nelson 2003 (WSRC-TR-2003-00436)	Excerpt enclosed following response	Sections 2.0, 4.0, 5.0, and 6.0, and Appendix K

**RESPONSE TO RAI COMMENT 28  
ROADMAP TO REFERENCES**

Puls et al. 1992	Excerpt enclosed following response	
Taylor 1974	Representative excerpt(s) enclosed following response	Used as reference on root development when horizontal soil anomalies exist (geotextile layer, water saturation zone, etc.) in the soil profile, especially on pages 284-286.
Ulrich 1981	Representative excerpt(s) enclosed following response	Used as estimates of root growth periodicity and root turnover rates. Research summaries on rates of biomass accumulation during tree growth for several species are discussed, especially on pages 321-325.
USEPA 1987	Representative excerpt(s) enclosed following response	
USEPA 1994a	Excerpt enclosed following response	Section 1
USEPA 1994b	Excerpt enclosed following response	Sections 1 and 2
Walkinshaw 1999	Representative excerpt(s) enclosed following response	Used as reference for the rate of root cell death and decomposition after cutting (death) of tree. Beginning of root decomposition is not immediate, see discussion section on pages 575-576.
Wilcox 1968	Representative excerpt(s) enclosed following response	Used as reference for seasonal root growth pattern and source of root anatomy and branching habits. Plantation trees are described in last paragraph on page 248 - 250.

7/15/2005

2/3

**RESPONSE TO RAI COMMENT 28**  
**ROADMAP TO REFERENCES**

**\*Excerpt Locations:**

1. Excerpt included within response: The excerpt is included within the text of the response or is appended to the response.
2. Excerpt enclosed following response: The excerpt is enclosed on a separate sheet or sheets following the response.
3. Representative excerpt(s) enclosed following response: Representative excerpts from a document that is wholly or largely applicable are enclosed following the response.
4. Other

APPROVED for Release for  
Unlimited (Release to Public)

## Chapter 4

# Surface-Charge Repulsive Effects on the Mobility of Inorganic Colloids in Subsurface Systems

Robert W. Puls<sup>1</sup> and Robert M. Powell<sup>2</sup>

<sup>1</sup>Robert S. Kerr Environmental Research Laboratory, U.S. Environmental  
Protection Agency, Ada, OK 74820

<sup>2</sup>ManTech Environmental Technology, Inc., Ada, OK 74820

Batch and column experiments using natural aquifer material investigated the specific adsorption of anions onto charged inorganic colloidal surfaces in terms of enhanced colloid stability and transport in subsurface model systems. Variables in the study included flow rate, pH, ionic strength, aqueous chemical composition, colloid concentration and size. Specific adsorption of some anions resulted in enhanced colloid stability and transport of Fe<sub>2</sub>O<sub>3</sub> particles due to increases in charge repulsion between the particles in suspension and between the particles and the immobile column matrix minerals. Extent of particle breakthrough was dependent upon a complex variety of parameters; however, the highest statistical correlation was observed with particle size and ionic composition of the supporting electrolyte.

The hydrogeochemical significance of colloidal-size particles in subsurface systems has only been realized during the past few years. This realization has resulted from field studies that show contaminant migration over distances and at concentrations greater than model predictions would allow. These models generally perform predictive calculations by assuming the contaminants interact with the mobile aqueous and immobile solid phases, and occasionally include the possibilities of contaminant free-phase and co-solvency effects. They account for solubility, speciation, ion-exchange, adsorption-desorption and diffusion reactions within and between these phases but do not consider the possibility of these interactions with a potential additional phase, mobile colloidal solids. Should such a phase be present in sufficient quantity, exhibit high sorption reactivity, remain stable in suspension, and be capable of avoiding attachment to the immobile solid phase, it might serve as an important mechanism for contaminant transport.

Colloids are particles that are sufficiently small that the surface free

4.

el  
p  
o  
cl  
di  
de  
si  
su  
bu  
or  
so  
su  
ve

Es  
hi  
su

in t  
sub  
ion.  
trar

gro  
ma  
ads  
con  
by  
Cs,

ACS SYMPOSIUM SERIES 491

# Transport and Remediation of Subsurface Contaminants

## Colloidal, Interfacial, and Surfactant Phenomena

**David A. Sabatini, EDITOR**  
*University of Oklahoma*

**Robert C. Knox, EDITOR**  
*University of Oklahoma*

Developed from a symposium sponsored  
by the Division of Colloid and Surface Chemistry  
of the American Chemical Society  
at the 65th Annual Colloid and Surface Science Symposium,  
Norman, Oklahoma,  
June 17-19, 1991

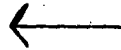


American Chemical Society, Washington, DC 1992

# Erosion and Sediment Control Handbook

---

**Steven J. Goldman**  
*California Tahoe Conservancy*



**Katharine Jackson**  
*Consultant*

**Taras A. Bursztynsky, P.E.**  
*Association of Bay Area Governments*

**McGraw-Hill Publishing Company**

New York St. Louis San Francisco Auckland Bogotá  
Caracas Hamburg Lisbon London Madrid Mexico Milan  
Montreal New Delhi Oklahoma City Paris San Juan  
São Paulo Singapore Sydney Tokyo Toronto

12/11/91

26

7C  
423  
.G1

**Library of Congress Cataloging-in-Publication Data**  
**Goldman, Steven J.**

**Erosion and sediment control handbook.**

Includes bibliographies and index.

1.Sediment control—United States—Handbooks, manuals, etc. 2.Soil erosion—United States—Handbooks, manuals, etc. 3.Soil conservation—United States—Handbooks, manuals, etc. I.Jackson, Katharine.

II.Buraztynsky, Taras A. III.Title.  
TC423.G645 1986 627'.52 85-15371  
ISBN 0-07-023655-0

Copyright © 1986 by McGraw-Hill, Inc. Printed in the United States of America. Except as permitted under the United States Copyright Act of 1976, no part of this publication may be reproduced or distributed in any form or by any means, or stored in a data base or retrieval system, without the prior written permission of the publisher.

234567890 HDHD 99876543210

**ISBN 0-07-023655-0**

The editors for this book were Joan Zaeleczky and Galen H. Fleck; the designer was Mark E. Safran; and the production supervisor was Thomas G. Kowalczyk. It was set in Century Schoolbook by University Graphics, Inc.

Printed and bound by Halliday Lithograph

28/284

**Handbook**

Technical Paper  
No. 147, 1961.

*Soil Loss in Small  
Farm Culture, Soil*

*Atlas of the  
Soil Conservation Division, U.S.  
Department of Com-  
merce, Weather Ser-*

*San Fran-  
cisco, U.S.G.S.,*

*Facilities in  
San Francisco, Calif.,*

*Engineering*

*Small Dams,*

*and Sediment*

*Control, Denver*

## Estimating Soil Loss with the Universal Soil Loss Equation

Soil conditions are a principal factor in determining the erosion potential at a site. Yet although estimating runoff is a common practice, estimating soil loss is not, particularly in urban areas.

Soil loss estimates have three important applications for erosion control planning:

1. To identify erosion-prone areas on a site
2. To compare the effectiveness of different control measures
3. To estimate the volume of sediment storage needed in a sediment basin

Thus, by estimating soil loss, the erosion control planner will be able to avoid disturbing highly erodible areas, select the most effective control measures for a site, and avoid costly oversizing or undersizing of sediment basins.

A number of methods for assessing soil loss have been developed. They range from simple, qualitative models to elaborate watershed simulations. Qualitative models rely on subjective evaluation of a series of criteria. Watershed simulation models are often very theoretical. Several empirical models also are available. Most models are best suited to estimating erosion from very large areas (more than 1 mi<sup>2</sup>) and lack the accuracy for use on small sites such as construction sites.

cost, and need for permanence. Calculate velocity and depth of flow as described in Chap. 4. Common lining materials include:

- Earth
- Rock
- Grass
- Grass and rock combination
- Fabric
- Pavement

### 7.7a Unlined Channels

Table 7.1 lists the maximum permissible velocities in unlined channels according to soil type. Generally, sandy, noncohesive soils tend to be very erodible, mixtures of sand, clay, and colloids are moderately erodible, and large-grained gravel, clay, and silt mixtures are erosion-resistant.

Channels with slopes less than 3 percent may remain unlined; but unless the channel is a small swale, a lining is advisable if the channel is expected to serve throughout an entire season. Figure 7.28 shows an unlined diversion that became a deep channel in the course of an average rainy season.

### 7.7b Rock Linings

Gravel or rock is the simplest kind of lining. Rock linings can be made to withstand most velocities if the proper size of rock is selected. Basically, the sequence of construction is to place a filter layer on the soil and then place a layer of riprap on top of the filter layer. The filter layer is important to prevent soil movement out through the riprap, which would result in the settling and eventual failure of the lining. The filter may be a special filter cloth or properly graded layers of sand and gravel.

#### *Sample Design Procedure to Determine Stone Size for Riprap-Lined Channels (14)*

The design procedure for riprap-lined channels is adapted from the National Cooperative Highway Research Program Report No. 108, entitled *Tentative Design Procedure for Riprap-Lined Channels (14)*. It is based on the tractive force method and covers the design of riprap in two basic channel shapes: trapezoidal and triangular.

*Note:* This procedure is for uniform flow in channels and is *not* to be used for design of riprap energy dissipators. See Sec. 7.8 for design guidelines for outlet protection and energy dissipators.

The procedure is based on the assumption that the channel is already designed and the remaining problem is to determine the riprap size that would

be stable in  
by the use of  
determined  
spounding n

#### TRAPEZOIDAL

1. Calculate the ratio
2. Enter  $F_i$  median  $r$  by weigh
3. Enter  $F_i$  2. If the another t or small return to

Wolfgang Böhm

# Methods of Studying Root Systems

With 69 Figures



Springer-Verlag Berlin Heidelberg New York 1979

Dr. WOLFGANG BÖHM  
Institut für Pflanzenbau und Pflanzenzüchtung  
der Universität Göttingen  
v.-Siebold-Straße 8, 3400 Göttingen/FRG

ISBN 3-540-09329-X Springer-Verlag Berlin Heidelberg New York  
ISBN 0-387-09329-X Springer-Verlag New York Heidelberg Berlin

Library of Congress Cataloging in Publication Data. Böhm, Wolfgang, 1936-. Methods of studying root systems. (Ecological studies; v. 33). Bibliography: p. Includes indexes. 1. Roots (Botany)-Research. 2. Botany-Ecology-Methodology. I. Title. II. Series. QK644.B63. 581.1. 79-9706

This work is subject to copyright. All rights are reserved, whether the whole or part of the material is concerned, specifically those of translation, reprinting, re-use of illustrations, broadcasting, reproduction by photocopying machine or similar means, and storage in data banks.

Under § 54 of the German Copyright Law where copies are made for other than private use, a fee is payable to the publisher, the amount of the fee to be determined by agreement with the publisher.

© by Springer-Verlag Berlin-Heidelberg 1979  
Printed in Germany.

The use of registered names, trademarks, etc. in this publication does not imply, even in the absence of a specific statement, that such names are exempt from the relevant protective laws and regulations and therefore free for general use.

Typesetting, printing, and binding: Brühlische Universitätsdruckerei, Lahn-Gießen.  
2131:3130-543210

specially, but  
its. In spite of  
th workers in  
ter ecological  
research.

elped me with  
to record my  
lands), G.H.  
) W. Ehlers  
r (Denmark),  
rd (USA), H.  
R. Steinhardt

his excellent  
ts of the text.  
and critical  
tion to write  
nany) for his  
U. Köpke  
d gave criti-  
aries at Göt-  
terature.

o use photos  
ng the entire  
it for reading  
publication.  
anks also to  
port to study

ile help and  
he publisher  
f the book.

GANG BÖHM

## Contents

<b>1. Root Ecology and Root Physiology</b>	<b>1</b>
<b>2. General Survey of Root-Study Methods</b>	<b>2</b>
2.1 Historical Development . . . . .	2
2.2 Principles of Classification . . . . .	4
2.3 Selection of the Best Method . . . . .	4
<b>3. Excavation Methods</b>	<b>5</b>
3.1 Introduction . . . . .	5
3.2 Outline of the Classical Method . . . . .	5
3.2.1 Selection of the Plant . . . . .	5
3.2.2 Digging the Trench . . . . .	5
3.2.3 Excavating the Root System . . . . .	6
3.2.4 Drawings and Photographs . . . . .	8
3.2.5 Preparation and Storage of Excavated Root Systems . . . . .	10
3.2.6 Review of Applications . . . . .	12
3.2.7 Advantages and Disadvantages . . . . .	12
3.3 Modifications of the Classical Method . . . . .	14
3.3.1 Excavations with Water Pressure . . . . .	14
3.3.2 Excavations with Air Pressure . . . . .	15
3.3.3 Excavations in a Horizontal Plane . . . . .	16
3.3.4 Sector Method . . . . .	18
<b>4. Monolith Methods</b>	<b>20</b>
4.1 Introduction . . . . .	20
4.2 Simple Spade Methods . . . . .	20
4.3 The Common Monolith Method . . . . .	21
4.3.1 Square Monoliths . . . . .	21
4.3.2 Round Monoliths . . . . .	25
4.4 Box Methods . . . . .	26
4.5 Cage Methods . . . . .	29

4.6 Needleboard Methods . . . . .	30	7.3.4
4.6.1 General Survey . . . . .	30	7.3.5
4.6.2 Construction and Preparation of the Needleboards . . . . .	31	7.4 Root
4.6.3 Excavating the Monoliths . . . . .	32	7.5 Evalu
4.6.4 Washing Procedure . . . . .	33	
4.6.5 Photographing and Sectioning . . . . .	34	
4.6.6 Special Modifications . . . . .	35	
4.6.7 Evaluation of the Methods . . . . .	38	
5. Auger Methods . . . . .	39	8. Indirect P
5.1 Specific Features . . . . .	39	8.1 Intro
5.2 Sampling Techniques . . . . .	39	8.2 Dete
5.2.1 Techniques with Hand Augers . . . . .	39	8.2.1
5.2.1.1 Sampling Procedure . . . . .	39	8.2.2
5.2.1.2 Number or Replications . . . . .	41	8.3 Stair
5.2.1.3 Special Technique for Studying Tree Roots . . . . .	41	8.4 Upt
5.2.2 Mechanized Techniques . . . . .	42	8.5 Rad
5.2.3 Core-Sampling Machines . . . . .	43	8.5.1
5.3 The Core-Break Method . . . . .	45	8.5.2
5.4 Advantages and Drawbacks . . . . .	47	8.5.3
		8.5.4
		8.5.5
		9. Other M
6. Profile Wall Methods . . . . .	48	9.1 M
6.1 General Survey . . . . .	48	9.2 M
6.2 The Traditional Trench Profile Method . . . . .	48	9.3 M
6.2.1 Digging the Trench . . . . .	48	9.4 R
6.2.2 Preparing the Profile Wall . . . . .	50	9.5 R
6.2.3 Exposing the Roots . . . . .	52	9.6 M
6.2.4 Mapping and Counting Procedure . . . . .	53	9.7 R
6.2.4.1 Determination of Root Number . . . . .	53	9.8 R
6.2.4.2 Determination of Root Length . . . . .	56	9.9 El
6.3 The Foil Method . . . . .	56	9.10 D
6.4 Technique in a Horizontal Plane . . . . .	59	9.11 In
6.5 Evaluation and Applications . . . . .	59	9.12 D
		9.13 D
		10. Contain
7. Glass Wall Methods . . . . .	61	10.1
7.1 Introduction . . . . .	61	10.2
7.2 Glass-Faced Profile Walls . . . . .	61	10.3
7.3 Root Laboratories . . . . .	64	
7.3.1 General Survey . . . . .	64	
7.3.2 Features of Their Design . . . . .	64	
7.3.3 Methods of Recording . . . . .	68	

Contents

XI

30	7.3.4 Light Sensitivity of Roots . . . . .	71
30	7.3.5 Recent Research in Root Laboratories . . . . .	71
31	7.4 Root Observations with Glass Tubes . . . . .	72
32	7.5 Evaluation of the Methods . . . . .	75
33		
34		
35	8. Indirect Methods . . . . .	77
38		
	8.1 Introduction . . . . .	77
	8.2 Determination of Soil Water Content . . . . .	77
39	8.2.1 Gravimetric Method . . . . .	78
	8.2.2 Neutron Method . . . . .	79
39	8.3 Staining Techniques . . . . .	79
39	8.4 Uptake of Non-Radioactive Tracers . . . . .	80
39	8.5 Radioactive Tracer Methods . . . . .	80
39	8.5.1 General Survey . . . . .	80
41	8.5.2 Soil Injection Technique . . . . .	81
41	8.5.3 Plant Injection Technique . . . . .	83
42	8.5.4 Root Studies with <sup>14</sup> C . . . . .	86
43	8.5.5 Critical Evaluation . . . . .	86
45		
47		
	9. Other Methods . . . . .	88
48	9.1 Measuring Root-Pulling Strength . . . . .	88
	9.2 Measuring Root-Clump Weight . . . . .	88
48	9.3 Measuring Root Tensile Strength . . . . .	89
48	9.4 Root Measurements Using Soil Sections . . . . .	90
48	9.5 Root-Detecting Method . . . . .	90
50	9.6 Mesh Bag Method . . . . .	91
52	9.7 Root Replacement Method . . . . .	91
53	9.8 Root Investigations with Paper Chromatography . . . . .	92
53	9.9 Electrical Methods . . . . .	92
56	9.10 Determination of Growth Rings in Tree Roots . . . . .	93
56	9.11 Investigations of Root Hairs . . . . .	93
59	9.12 Determination of Root Nodules . . . . .	94
59	9.13 Determination of Mycorrhizae . . . . .	94
61	10. Container Methods . . . . .	95
61	10.1 General Features . . . . .	95
61	10.2 Rooting Volume and Container Size . . . . .	95
64	10.3 Types of Containers . . . . .	96
64	10.3.1 Small Pots . . . . .	96
64	10.3.2 Boxes and Tubes . . . . .	97
64	10.3.3 Glass-Faced Containers . . . . .	99
68	10.3.4 Flexible Tubes . . . . .	102

10.4	Rooting Media . . . . .	104	12.7	Root
10.5	Filling the Containers . . . . .	105	12.7	12.7
10.6	Seed Technique . . . . .	107	12.7	12.7
10.7	Irrigation Problems . . . . .	107	12.7	12.7
10.8	Special Washing Procedures . . . . .	108	12.8	Root
10.9	Modified Container Methods . . . . .	109	12.8	12.8
	10.9.1 Cage Method . . . . .	109	12.8	12.8
	10.9.2 Needleboard Method . . . . .		12.9	Shc
	10.9.3 Root Training by Plastic Tubes . . . . .			
	10.9.4 Split-Root Technique . . . . .	112		
	10.9.5 Undisturbed Soil Monoliths . . . . .	112		
10.10	Root Studies in Nutrient Solutions . . . . .	113	13.0	Some Fu
10.11	Root Studies in Mist Chambers . . . . .	114		
10.12	Comparability of Results from Container Experiments with field Data . . . . .	114		References
				Subject Ind
11.	Techniques of Root Washing . . . . .	115		
	11.1 Dry Sieving . . . . .	115		
	11.2 Storing Soil-Root Samples Before Washing . . . . .	115		
	11.3 Chemicals for Facilitating Root Washing . . . . .	116		
	11.4 Washing Roots by Hand . . . . .	117		
	11.5 Flotation Method . . . . .	119		
	11.6 Root-Washing Machines . . . . .	121		
	11.7 Nutrient Losses from Roots During Washing . . . . .	122		
	11.8 Cleaning Roots from Debris . . . . .	122		
	11.9 Storing Roots After Washing . . . . .	124		
12.	Root Parameters and Their Measurement . . . . .	125		
	12.1 General Aspects . . . . .	125		
	12.2 Root Number . . . . .	125		
	12.3 Root Weight . . . . .	126		
	12.3.1 Determination of Fresh Weight . . . . .	126		
	12.3.2 Determination of Dry Weight . . . . .	126		
	12.3.3 Advantages and Critical Objections . . . . .	127		
	12.4 Root Surface . . . . .	128		
	12.4.1 Calculation from Other Parameters . . . . .	128		
	12.4.2 Photoelectric Measurements . . . . .	128		
	12.4.3 Adsorption Methods . . . . .	129		
	12.5 Root Volume . . . . .	130		
	12.5.1 Calculation from Other Parameters . . . . .	130		
	12.5.2 Displacement Technique . . . . .	130		
	12.6 Root Diameter . . . . .	130		
	12.6.1 Measurements . . . . .	130		
	12.6.2 Applications in Tree Root Studies . . . . .	131		



*Soil Genesis  
& and  
Classification*

S. W. Buol

F. D. Hole

R. J. McCracken

*The Iowa State University Press, Ames*

1973

Car 34818  
Cir 37818

S  
591  
B887

STANLEY WALTER BUOL, professor of Soil Science at North Carolina State University, Raleigh, holds the B.S., M.S., and Ph.D. degrees from the University of Wisconsin. He is a member of Alpha Zeta, Sigma Xi, Soil Science Society of America, American Society of Agronomy, North Carolina Soil Science Society, and the Soil Conservation Society of America. Besides this book, Dr. Buol has authored and coauthored Agricultural Experiment Station Technical Bulletins at the University of Arizona and North Carolina State University and published articles in various journals, including *Soil Science*, *Soil Science Society of America Proceedings*, *Southeastern Geology*, *Journal of Soil and Water Conservation*, and *Progressive Agriculture in Arizona*.

FRANCIS D. HOLE, professor of Soil Science and Geography and chairman of the Soil Survey Division of the Wisconsin Geological and Natural History Survey at the University of Wisconsin, Madison, holds the B.A. degree from Earlham College, the M.A. degree from Haverford College, and the Ph.D. degree from the University of Wisconsin. Dr. Hole is a Fellow of the American Society of Agronomy, the Geological Society of America, the Indiana Academy of Science, the American Association for the Advancement of Science; a member of the Soil Science Society of America, the Society for Social Responsibility in Science, and the Wisconsin Academy of Sciences, Arts and Letters. Besides this book, Dr. Hole has coauthored *Soil Resources and Forest Ecology of Menominee County, Wisconsin* and many other county soil survey maps and reports, and has published articles in various journals, including the *Soil Science Society of America Proceedings*, *Soil Science*, and the *Transactions of the Wisconsin Academy of Sciences, Arts and Letters*.

RALPH J. MCCRACKEN is currently assistant director of research in the School of Agriculture and Life Sciences, North Carolina State University, Raleigh. During the period of 1963 to 1970, he was head of the Department of Soil Science; from 1956 to 1963, he was associate professor and professor of Soil Science at that University. He was associate agronomist, University of Tennessee, 1954 to 1956. He served as soil scientist with the United States Department of Agriculture, 1947 to 1954, with leaves of absence for graduate training. During this period, he served as soil surveyor in California, Western Pacific Islands, New York, and Iowa. He is past president of the Soil Science Society of America and the Soil Science Society of North Carolina. He is a Fellow of the American Society of Agronomy and the American Association for Advancement of Science.

We dedicate  
JAMES  
soil scientist  
teacher, scholar  
and letters  
world citizen

Library of Congress Cataloging in Publication Data

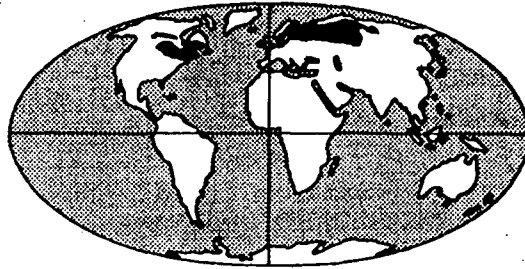
author Buol, S W  
Title Soil genesis and classification.  
Includes bibliographies.  
SWS 1. Soil science. 2. Soil formation. 3. Soils-Classification. I. Hole, Francis Doan, 1913- joint  
author. II. McCracken, R. J., joint author. III. Title. 631.4 72-3434  
S591.B887  
ISBN 0-8138-1460-X 3d auth

© 1973 The Iowa State University Press  
Ames, Iowa 50010. All rights reserved

Composed and printed by  
The Iowa State University Press

First edition, 1973

6/19/73 - 3/6/31



CHAPTER 20

*Spodosols: Soils with Subsoil  
Accumulations of Sesquioxide and Humus \**

THE "WHITE EARTHS," the Spodosols, contrast sharply with the "black earths," the Borolls (Chernozems) (see Chapter 19). Spodosols encompass most but not all soils named Podzol—from the Russian terms *pod* (beneath) and *zol* (ash).

Spodosols are widely known as acid ashy gray sands over dark sandy loams. These two contrasting horizons, with an abrupt boundary between them, place these soils among the most eye-catching and photogenic in the world. Many scientists take pleasure in studying Spodosols, which respond quickly to changes in vegetation, and which have the appearance of a chromatographic column. The development of these soils in quartzose sand is favored by the presence of a vegetative cover under which acid litter accumulates. Moved by percolating water, organic compounds from the litter clean the quartz grains in the first horizon and coat them with a dark mixture of iron oxide and humus in the second. The great variety of Spodosols, and their distribution in very different climatic zones, suggest that this first impression of these soils is far too simple.

**SETTING.** Not every "white" A2 (albic) horizon that one sees signifies a Spodosol. The wide application of the term "podzolization" to many soils with bleached surface or subsurface horizons is not followed here. Albaquolls and Albaqualfs (salt-affected soils and Planosols), Eutroboralfs (Gray Wooded soils), and many Hapludalfs (Gray-Brown Podzolics) are loci of active podzolization but are not Spodosols. Neither is the pseudopodzol of Madagascar, the albic horizon of which is a 1- to 30-cm-thick accumulation of opal phytoliths under acacias and bamboos (Riquier 1960). Thus, it is fortunate that the albic horizon is not considered a diagnostic horizon, whereas the spodic horizon is. This black to strong brown subsoil horizon is the essential feature by which a Spodosol is identified, whether the topsoil is a dark plow layer or ashy gray sand.

The setting in which such a soil is produced is one in which the combination of factors of soil formation yields the necessary conditions—

*Spodosols*

the accumulative horizon. Many organic compounds but litter from fostering such (*Tsuga canadensis*, *Pinus australis*) of *Ne* and *Erica* sp.) correlated with of heath plants *Pinus*, *Larix*, (including *Vaccinium* 1965). This in tainous lands t ometers of land soils is propitio O horizon and

On the co: Aquods (Group associated unde

The giant Bhir horizon sand. The me fall is 2,300 m and November present savann this soil first fo

A 2-m-deep in ecological e Bragg area of Spodosols (less Whittig 1960) Shanks, and Cl

The great can be expecte on any minera of the youthfu definition of horizon, the zo and is quite di

Tree-tip r some Spodosol storms. They r trees with stro shallow root sy fred, Olson, an of the forest fl



S \*

Spodosols, contrast  
ns) (see Chapter 19).  
dzol—from the Rus-

ids over dark sandy  
t boundary between  
and photogenic in  
Spodosols, which re-  
ave the appearance  
se soils in quartzose  
der which acid litter  
omponents from the  
at them with a dark  
he great variety of  
matic zones, suggest  
e.

one sees signifies a  
tion" to many soils  
ollowed here. Alba-  
, Eutroboralfs (Gray  
odzolics) are loci of  
is the pseudopodzol  
t-cm-thick accumula-  
iquier 1960). Thus,  
diagnostic horizon,  
own subsoil horizon  
ed, whether the top-

one in which the  
ecessary conditions—

the accumulation of iron, aluminum, and/or organic matter in a subsoil horizon. Many kinds of vegetation, including grasses, can yield certain organic compounds that speed podzolization under laboratory conditions, but litter from a certain few species of plants is particularly capable of fostering such accumulations. Among these plants are the hemlock tree (*Tsuga canadensis*) in forests of northern latitudes, the kauri tree (*Agathis australis*) of New Zealand (see Chapter 11), and heath (*Calluna vulgaris* and *Erica* sp.) of northern Europe. Individual Spodosol soil bodies may be correlated with single kauri trees or groups of hemlocks or communities of heath plants. Spodosols do occur under a wide variety of trees (*Picea*, *Pinus*, *Larix*, *Thuja*, *Populus*, *Quercus*, *Betula*) and understory plants (including *Vaccinium*) in climatic zones that are cool (McFee and Stone 1965). This includes the taiga and similar plant communities of mountainous lands that together may occupy more than 38 million square kilometers of land in the world. Apparently the moisture regime in these soils is propitious for the formation of requisite organic compounds in the O horizon and their delivery, under a flushing regime, to the subsoil.

On the coastal plain of southeastern United States extensive areas of Aquods (Groundwater Podzols) are developed under *Quercus*, *Pinus*, and associated understory plants.

The giant Podzol of Surinam (Eyck 1957) has a 25-cm-thick sandy Bhir horizon on schist-derived clay under nearly 3 m of gray to white sand. The mean annual temperature is 26 C (79 F) and mean annual rainfall is 2,300 mm (92 in.), which includes a relatively dry period in October and November when monthly precipitation is about 75 mm (3 in.). The present savanna vegetation may be quite different from that under which this soil first formed.

A 2-m-deep Typic Sideraquod (Groundwater Podzol with iron pan) is in ecological equilibrium with a pigmy forest 1.5 to 3 m tall in the Fort Bragg area of coastal California (Jenny, Arkley, and Schultz 1969). Dwarf Spodosols (less than 45 cm deep) are reported from Alaska (Kubota and Whittig 1960) and heath balds of the Great Smoky Mountains (McCracken, Shanks, and Clebsch 1962).

The great "Russian generalization" that the climate of the boreal zone can be expected to impress, via organisms, the O-A2-Bhir horizon sequence on any mineral material, including calcareous clay, has validity because of the youthfulness of landscapes in this zone. But because of the precise definition of properties of the Spodosol order, emphasizing the spodic horizon, the zonal pattern of Podzols is only partially realized as Spodosols, and is quite discontinuous.

Tree-tip mounds, sometimes called cradle knolls, are numerous in some Spodosol polypedons. They are formed by uprooting of trees in storms. They may have a relief of as much as 1 m and length of 3 m. Tall trees with strong trunks that will not snap in a wind, and a somewhat shallow root system, produce these features during storms (Baxter, in Milfred, Olson, and Hole 1967). Cradle knolls occupy about 20% of the area of the forest floor in parts of the Great Lakes region of North America.

Macrotopography is variable. Spodosols are extensive on nearly level to undulating sand plains, but some are reported on slopes approaching 90% in mountainous areas (Bouma et al. 1969), with best solum development on slopes facing away from the equator.

It is generally conceded that Spodosols may form relatively quickly. Estimates range from a few hundred years (Soil Survey Staff 1967) to several thousand years (Franzmeier and Whiteside 1963a). The movement of organic and mineral colloids from surface soil to subsoil in coarse sandy material to the point of equilibrium with the environment should not take an inordinate amount of time and energy. Burges and Drover (1953) reported evidence that 200 years were required to leach calcite from beach sand in New South Wales, 2,000 years to produce an iron-Podzol, and 3,000 years to produce an iron-humus Podzol with pH as low as 4.5. A Podzol buried under peat in northern Ireland was dated by artifacts and paleobotany as being formed between 3,000 and 2,000 B.C. (Proudfoot 1958). Franzmeier and Whiteside (1963a, b) studied a 10,000-year-long chronosequence of Spodosols in Michigan and concluded that between 3,000 and 8,000 years were necessary for the formation of a Spodosol. The age of a Typic Sideraquod of coastal California has been estimated at about 1 million years (Jenny, Arkley, and Schultz 1969).

**NATURE OF PEDOGENIC PROCESSES.** Podzolization is a bundle of processes (Gerasimov 1960; Ponomareva 1964; Stobbe and Wright 1959) which brings about translocation, under the influence of the hydrogen ion (Hallsworth, Costin, and Gibbons 1953) and organic compounds (Bloomfield 1953a, b; 1954), of organic matter, iron, and aluminum (and a small amount of phosphorus) from the upper part of the mineral solum to the lower part. If clay is also transported in suspension, this may be considered atypical as a pedogenic process in this order, although it is actually a fairly common accompaniment of podzolization. This is evidenced by clay accumulation in spodic horizons (Franzmeier and Whiteside 1963a) and in argillic horizons below them (Milfred, Olson, and Hole 1967). Free iron:clay ratios are not constant with depth as they are in Alfisols and Ultisols (Soil Survey Staff 1967). "Purest" Spodosols may be expected to have formed in initial material containing little or no clay and receiving little if any by wind action during pedogenesis.

Processes of Spodosol formation may be considered under the following headings: accumulation of organic matter; leaching and acidification; weathering; translocation of Fe and Al (with some P, Mn, and clay) from the A to B horizon; immobilization of humic and fulvic acids (and some clay) in the B; pelleting of humus coatings; reduction in bulk density; cementation.

Accumulation of organic matter in the solum of a Spodosol is concentrated in the O and Bh or Bh (Spodic) horizons. In dry weight per acre, the total organic matter in the Spodosol sequum increased steadily to 30 tons over a period of 10,000 years, in a chronosequence studied by Franzmeier and Whiteside (1963b). In well-developed, well-drained Spodosols, proliferation of tree roots tends to be in both the O and spodic horizons.

FIG. 20.1. Diagram of a cross section of a Spodosol in Wisconsin that is a bisecting

The O horizon containing an abundance of organic debris, and podzols. The bacteria. The (where it resembles numerous in the Annelidae (Earthworms) oxygen consuming that in mull (K three times as smaller and in the ratio of volume in the litter layer (O<sub>2</sub>).

Leaching of available cations, C prerequisite to about 1/20,000 soil under a k and Erickson containing mo

The amount than has been side 1963b). The horizon, therefore feldspars, illite below 5.0, and 1969). The pa

1. Personal communication

sive on nearly level slopes approaching best solum develop-

relatively quickly. (Staff 1967) to sev-

The movement of oil in coarse sandy ent should not take 1 Drover (1953) recalcite from beach n-Podzol, and 3,000 w as 4.5. A Podzol artifacts and paleo- (Proudfoot 1958). year-long chronose- between 3,000 and osol. The age of a ted at about 1 mil-

ion is a bundle of and Wright 1959) f the hydrogen ion ompounds (Bloom- inum (and a small neral solum to the may be considered is actually a fairly denced by clay ac- side 1963a) and in : 1967). Free iron: dfisols and Ultisols expected to have and receiving little

under the follow- ; and acidification; 4n, and clay) from ic acids (and some 1 in bulk density;

Spodosol is concen- ry weight per acre, sed steadily to 30 studied by Franz- drained Spodosols, id spodic horizons.

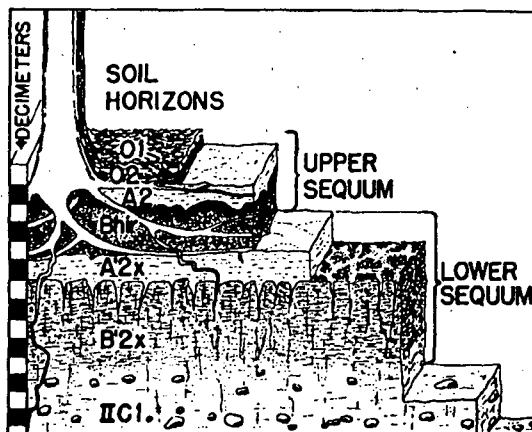


FIG. 20.1. Diagrammatic cross section of a Spodosol in Wisconsin that is a bisequal soil.

The O horizons of a Spodosol constitute a mor layer (Fig. 20.1) containing an abundance of fungi, the hyphae of which permeate the material at certain seasons. The decomposition of this acid mat is slowed by freezing, drought, low summer temperatures, acidity, resistant nature of the plant debris, and possibly by antibiotics produced by fungi, actinomycetes, and bacteria. The mor may be thicker than 1 m adjacent to a kauri tree trunk (where it resembles a Folist). *Collembola* (springtails) and *Acarina* (mites) are numerous in these horizons, along with many other Arthropods and some Annelidae (Eaton and Chandler 1942; Macfadyen 1963). Although total oxygen consumption of the biomass in mor may be only about a third of that in mull (Kevan 1955), its respiration rate per gram of biomass is nearly three times as fast. This is presumably because the microfauna in mor are smaller and individually more intensely active than those in mull. In mor, the ratio of volume of living organisms to volume of litter is about 1:30,000 in the litter layer (O1) and 1:15,000 in the fermenting and humus layer (O2).

Leaching of carbonates and significant replacement of the exchangeable cations,  $\text{Ca}^{++}$ ,  $\text{Mg}^{++}$ ,  $\text{K}^+$ , and  $\text{Na}^+$ , by  $\text{H}^+$  and  $\text{Al}^{+++}$  in the A horizon are prerequisite to mobilization of organic matter, and with it, of  $\text{Fe}^{+++}$ , Al, and about 1/20,000 as much P, and some Mn. Thorp<sup>1</sup> observed a Rendzinalike soil under a kauri tree growing in unleached material. Bailey, Whiteside, and Erickson (1957) noted collapse of sola developed in initial materials containing more than 12% of acid-soluble mineral matter.

The amount of Fe and Al accumulated in a Spodosol may be far more than has been biocycled in the history of the soil (Franzmeier and Whiteside 1963b). The source of the bulk of these two elements in the spodic horizon, therefore, has come from weathering of ferromagnesian minerals, feldspars, illite, and chlorite in the A horizon, where pH usually drops below 5.0, and in one case went as low as 2.8 (Jenny, Arkley, and Schultz 1969). The particles of weatherable minerals may not by any means have

1. Personal communication, 1962.

all been present in the initial material. If iron is not present in appreciable amounts, the spodic horizon is composed largely of quartz sand coated with humus, as in Humods (Edelman, 1950).

The albic horizon of a Spodosol is the site of accumulation of both (1) resistant minerals and of (2) difficultly soluble products of decomposition. The resistant minerals include quartz with small amounts of montmorillonite and beidellite (Bouma et al. 1969). The second category of materials includes silica in various forms such as dehydrated silicic acid or secondary quartz with small amounts of titanium oxide and barium sulfate in some soils. The albic horizon is pink (5YR 6/3, moist) under forest cover and gray (10YR 6/2) under heath (Schuylenborgh 1962). "Bleicherde" is the German term for the albic horizon.

Illuviation of clay, a process called lessivage (Duchaufour 1958) or illmerization (Fridland 1957), is sometimes viewed as a precursor of podzolization. After clay is eluviated from surficial horizons, albic and spodic horizons can form in the coarser residue. Tonguing of Spodosol sola into older degrading horizons is not uncommon. In some Spodosols lessivage may, however, be concurrent with podzolization. Franzmeier, Whiteside, and Mortland (1963) observed in a spodic horizon very thin birefringent free-grain argillans coated with thick (1.08 mm) amorphous organics (organic cutans) with some included clay.

Chemical eluviation in these soils includes reduction and translocation of Fe (McKenzie, Whiteside, and Erickson 1960) by chelates (Atkinson and Wright 1957) and complexing compounds of branching structure, such as polyphenols (Bloomfield 1957). The maximum accumulation of Al is commonly below that of Fe in the spodic horizon. Aaltonen and Mattson (after Jenny 1941) found evidence that the Podzol B may form from the bottom up, the zone of maximum colloid accumulation shifting from a depth of about 40 cm to 15 cm over a period of 5,000 years. Burges and Drover (1953), on the contrary, observed that this boundary shifted downward with time.

Precipitation of illuviated sesquioxides in the spodic horizon, Orterde and Orstein, in German parlance (referring by corruption to "Ertz" or ore), may be mechanical, chemical, or biological. Insufficiency of percolating water, from individual storms, to carry the colloids and solutes farther down may force precipitation in the B horizon. Sieving action can be mechanical. Colloids clog pores. When this process is important, the spodic horizon may grow upward into the albic horizon, a trend suggested by data of Franzmeier, Whiteside, and Mortland (1963). Bacteria may destroy the chelating and complexing organic compounds which mobilized the Fe and Al. Negative charges on thin clay films may immobilize the positively charged ions of Fe and Al. Polyphenols, organic acids, and reducing sugars were found to be major active components in mobilizing Fe and Al in a North Carolina study (Malcolm and McCracken 1968). In this study it was concluded that a major source of mobile organic matter for mobilization of Fe and Al in the podzolization process comes from tree canopy drip. They also concluded from their studies that precipitation and immobiliza-

tion took place. Solubility products were not found. Kawaguchi and others reported that the precipitation of iron by a chelating agent immobilized iron. Presumably, so did Malcolm and others and immobilized iron by podzolization.

Humic acids increase in oxygen content into the spodic horizon. They readily accumulate at the top of the soil around sand drougths. They sift down into soil. This may be with ultimate amorphous fil-

Much of the iron (Erickson 1956) in water Podzols is translocated.

This whole process increases in volume (Erickson 1957) 1.21 g/cc (A2 silty one were consin. McFe a mor weighi crop and over observed tong latter into the down tree-roc

Cementa' Survey Staff 1. material is la reddish brow the *placic hor* in tropical as the spodic ho (1961) reports 2% to 15%

resent in appreciable quartz sand coated

accumulation of both products of decomposition amounts of montmorillonite second category of hydrated silicic acid or ferric and barium sulfate (moist) under forest (Borchgrevink 1962). "Blei-

schäufel (1958) or precursor of podzols, albic and spodic of Spodosol sola into Spodosols lessivage (Zechmeister, Whiteside, 1967). Thin birefringent amorphous organic

matter and translocation of clay (Atkinson and 1967) structure, such as fixation of Al is common in podzols and Mattson may form from the iron shifting from a podzolic horizon (10 to 20) years. Burges and Mattson shifted down-

podzolic horizon, Orterde on to "Ertz" or ore), intensity of percolating and solutes farther moving action can be important, the spodic trend suggested by bacteria may destroy which mobilized the Fe which mobilize the positively charged and reducing sugars and Fe and Al in a podzolic horizon. In this study it is a matter for mobilization under tree canopy drip. Iron and immobiliza-

tion took place when sufficient Al and/or Fe was present to exceed the solubility product believed to prevail in incipient spodic horizons. Calcium was not found to affect mobilization and immobilization in this study. Kawaguchi and Matsuo (1960) also report studies showing that the movement of iron in the soil is regulated by the ratio of the amount of the mobilizing agent to the amount of iron to be mobilized, relating this to the immobilization of Fe in a Spodic horizon due to presence of excess iron. Presumably, similar relationships exist with respect to Al, based on data of Malcolm and McCracken (1968). This mechanism, then, of mobilization and immobilization seems to provide the basis for a reasonable process for "podzolization" and development of spodic horizons.

Humic acids may convert to fulvic acids in the albic horizon by increase in oxygen-containing functional groups. These acids move down into the spodic horizon where they are bonded to the  $Fe^{++}$  and  $Al^{+++}$  already accumulated there. The nearly black organic subhorizon now forms at the top of the spodic horizon. As the films of organic matter thicken around sand grains, the films become susceptible to cracking during droughts. This results in pelleting of the films. The amorphous pellets sift down into voids, increasing the available water-holding capacity of the soil. This may foster a forest succession from conifers to deciduous trees, with ultimate degradation of the Spodosol. Some clay is occluded in the amorphous films and pellets.

Much of what has been said about cheluviation (Swindale and Jackson 1956) in well-drained Spodosols can also be said of Aquods (Groundwater Podzols) in which a fluctuating water table is an important agent of translocation.

This whole process of formation of a Spodosol entails an overall decrease in bulk density of the mineral portion of the solum. A 13% increase in volume is reported for Michigan Spodosols (Bailey, Whiteside, and Erickson 1957). Reductions in bulk density from 1.67 g/cc (C horizon) to 1.21 g/cc (A2 horizon) in a sandy Spodosol and from 1.62 to 1.13 g/cc in a silty one were reported by Hole and Schmude (1959) from northern Wisconsin. McFee and Stone (1965) reported a bulk density of 0.14 g/cc for a mor weighing 108 T/a (87 T of organic matter) under a 70-T standing crop and over 71 T of organic matter in the mineral solum. The commonly observed tonguing of the albic horizon into the spodic horizon, and the latter into the C horizon, may have been formed by flow of soil and water down tree-root channels.

Cementation may be striking in a Spodosol solum. *Durinodes* (Soil Survey Staff 1967) are cemented portions of the albic horizon. The cementing material is largely silica. A thin (1 to 10 mm) wavy or involuted black to reddish brown iron pan within 50 cm (20 in.) of the soil surface is called the *placic horizon* (Soil Survey Staff 1967). This horizon has been observed in tropical as well as subarctic regions. Cementation of a thicker mass of the spodic horizon to a rocklike consistency is called an Ortstein. Pol'skii (1961) reports analyses from this material showing 5% to 21%  $Fe_2O_3$  and 2% to 15% MnO. P. E. Müller distinguished several kinds of Ortsteins

(Muir 1961), including a black peatlike Ortstein, a brown humus Ortstein, and two concretionary Ortsteins, one in quartz sand converted to a pseudo-sandstone, and one in peat, called Raseneisenstein, that contains about 90% iron hydroxide and is porous and slaglike in appearance.

Under the spodic horizon of many Spodosols (Nygard, McMiller, and Hole 1952) is a reversibly and weakly cemented horizon called the fragipan (Fig. 20.1). It has been suggested that the invisible, reversible cement is silica, or alumina, or illite. This seems reasonable in the light of calculations of Rode (quoted by Russell 1956) that losses from a Spodosol during 10,000 years arranged the elements in the following order of diminishing quantity:  $Si > Al > Fe > K > Mg > Ca > Na$ . This seems to reflect the abundance of elements in the initial materials. The fabric of a fragipan is one of packing of finer particles in voids between larger ones to yield a bulk density (oven dry) as high as 1.92 g/cc (Hole et al. 1962). Vesicular, platy, and prismatic structures are present and may have been produced by frost action not involving cryopedoturbation. Repeated movement of a freezing front down through this horizon may have swept fines out of the horizon, increasing its close packing and fragile brittleness. Silty and clayey coatings on the upper surfaces of stones in the subjacent C horizon below support this idea. The fragipan is a barrier to root growth and downward water movement. Lateral movement of water over its surface is common on slopes.

Shifting of ecotones may enhance or diminish podzolization. In south central Alaska forests have encroached on grasslands, converting Cryandepts into Cryorthods (Rieger and DeMent 1965). Removal of hemlock from hemlock hardwood forests in northern Wisconsin results in fading of the spodic B horizon in the soils (Milfred, Olson, and Hole 1967). Lateral growth of sphagnum moss bogs in the taiga of northern Canada may bury Spodosols under Histosols.

**USES.** Spodosols are used for forestry, pasture, hay land, and cultivated crops. The soilscape shown in Figure 20.2 is covered for the most part with poor quality pine-oak woodland, but some level areas are used for truck crops (and the peat for cranberries). Three centuries of haying on sparsely stable-manure-fertilized alpine meadows have converted Spodosols to a "Brown" soil (Inceptisol) in parts of Switzerland (Bouma et al. 1969). In the north central region of the United States, crop rotations on Spodosols include silage corn, oats, rye, potatoes, red clover, flax, strawberries, and raspberries. Spodosols provide the major sites for commercial blueberry production in the coastal plain of North Carolina. Fertilization and cultivation raise the nutrient levels of these soils and lead to soil compaction, mixing of O and A2 horizons, and some degradation of spodic horizons by aeration and leaching, particularly in irrigated potato fields. Recreational activities are on the increase on these soils, as larger numbers of city people vacation in the forests near lakes and streams. Spodosol terrain includes extensive wildlife preserves.

**CLASSIFICATION.** Once the spodic horizon (or iron-cemented placic horizon over a fragipan) of a profile has been identified as meeting the



FIG. 1  
Glow  
Cour

requirements,<sup>2</sup>  
(see Fig. 20.3) w

1. Aquods  
least down to t  
ficially drained  
epipedon, (b) r  
duripan in the

2. Limits of the s  
amounts of amor  
layer lattice clay:  
than 20% and le  
cutans and pellets  
or more.

FIG. 20.3. Diagr  
showing some re  
ships between st  
of Spodosols.

own humus Ortstein, inverted to a pseudogley, contains about 90% ice.

gard, McMiller, and Enfield called the fragipan reversible cement is the light of calculation a Spodosol during order of diminishing to reflect the abundance of a fragipan is one ones to yield a bulk (2). Vesicular, platy, produced by frost movement of a freeze-thaw in silts out of the horizons. Silty and clayey in the C horizon below the surface and downward surface is common on

zolitization. In southern New England, Cryandepths of hemlock forest results in fading of the soil (Hole 1967). Lateral movement in Canada may bury

and, and cultivated for the most part areas are used for pastures of haying on converted Spodosols (Bouma et al. 1969). Plantations on Spodosols for strawberries, and commercial blueberry production and cultivated to soil compaction of spodic horizons in potato fields. Recreation numbers of city Spodosol terrain in-

on-cemented placic horizons as meeting the

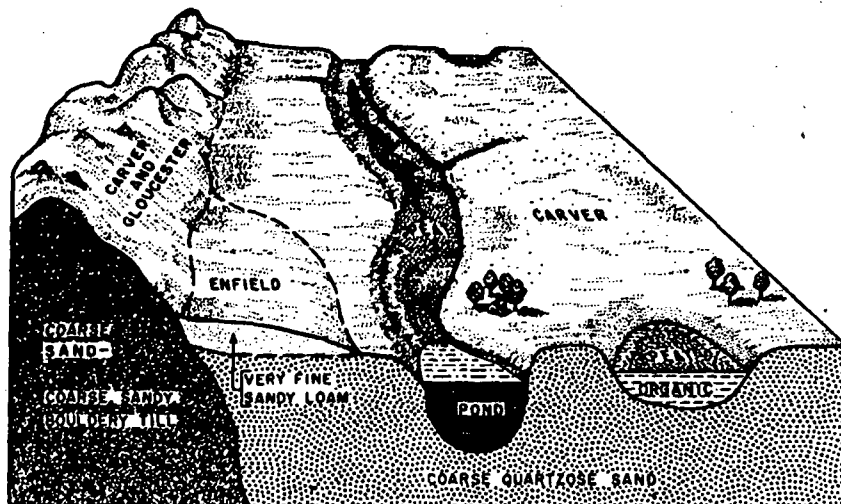


FIG. 20.2. Soilscape pattern of Entic Haplorthods (Carver, Gloucester, Enfield) with Histosols (Peat) in Plymouth County in eastern Massachusetts. (After Upham 1969.)

requirements,<sup>2</sup> the Spodosol may be classified into one of four suborders (see Fig. 20.3) which are briefly defined as follows:

1. Aquods are Spodosols that are commonly saturated with water (at least down to the placic horizon or duripan if such is present) or, if artificially drained, display such evidences of former wetness as (a) a histic epipedon, (b) mottling in the albic and upper spodic horizons, and (c) a duripan in the albic horizon.

2. Limits of the spodic horizon (see Soil Survey Staff 1967 for details) include: substantial amounts of amorphous material including carbon, iron, and aluminum; relatively little layer lattice clay; a thickness of at least 1 cm to this horizon; a 15-bar water content of less than 20%, and less than 60% glassy volcanic ash (20 to 200 $\mu$ ); presence of amorphous cutans and pellets; hue of 10YR or redder and either value less than 3 or chroma of 3 or more.

FIG. 20.3. Diagram showing some relationships between suborders of Spodosols.

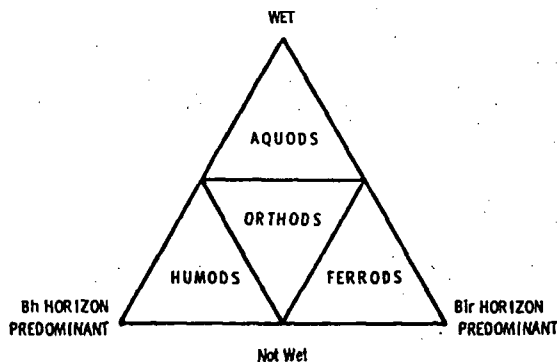


TABLE 20.1 Suborders and great groups in the Spodosol order

Suborder	Great Group
Aquods	FragiAquods—have a fragipan below the spodic horizon but no placic horizon Cryaquods—MAST* <8 C (47 F) Duraquods—indurated albic horizon in which dry peds will not slake in water Placaquods—have a placic horizon that rests on a spodic horizon and a fragipan Tropaquods—MAST >8 C (47 F) and <5 C (9 F) summer to winter temperature change Haplaquods—have spodic horizons where >50% of the horizon turns redder upon ignition Sideraquods—other Aquods
Humods:	Placohumods—have a placic horizon in the spodic horizon Tropohumods—MAST >8 C (47 F) and summer to winter temperature difference <5 C (9 F) Fragihumods—have fragipan below spodic horizon Cryohumods—MAST <8 C (47 F) Haplohumods—other Humods
Orthods:	Placorthods—have a placic horizon in or above the spodic horizon Fragiorthods—have a fragipan below the spodic horizon Cryorthods—MAST <8 C (47 F) Haploorthods—other Orthods
Ferrod:	No great groups

\* MAST = mean annual soil temperature.

2. Ferrod are Spodosols that are not as wet as Aquods and have more than six times as much free (elemental) iron as carbon in the spodic horizon.

3. Humods are Spodosols that are not as wet as Aquods and have spodic horizons containing dispersed organic matter and aluminum but little free iron (less than 0.5% of the fine earth).

4. Orthods are Spodosols that are not as wet as Aquods and have in the spodic horizon a content of free iron not more than six times that of carbon, usually much less.

These suborders are divided into 16 great groups (Table 20.1) on the basis of several factors: mean annual soil temperature and range of soil temperature; degree of cementation of the albic horizon with silica; degree of accumulation of iron in the spodic horizon; degree of development of a fragipan; presence of an umbric epipedon.

No reference is made in this classification to buried (thaptic) Spodosols such as were observed by Bryson, Irving, and Larsen (1965) in a tension zone between tundra and taiga in Canada.

Some Haploorthods with ochric epipedons resting on the spodic horizon (without albic horizon) have been called Brown Podzolics in the past (Nygard, McMiller, and Hole 1952).

The terms maximal, medial, and minimal Spodosols have been used by some workers (Hole and Schmude 1959) to indicate degrees of profile development within a region.

## LITERATURE

- Atkinson, H. J., soil constitutions of podzols
- Bailey, H. H., E. tion of glacial Podzol, Graygan. Soil Sci Soc. Am. Proc. 1953. 17: 1-10
- Bloomfield, C. I. aluminum by the soil. 1953b. A. 17: 1-10
- . 1954. A. 18: 1-10
- . 1957. T. Food Agr. 8: 1-10
- Bouma, J., J. H. and morphological evidence of formation of the Woy podzol. 1953. 17: 1-10
- Bryson, R. A., V. dence of formation of the Woy podzol. 1965. 19: 1-10
- Burges, A., and of the Woy podzol. 1953. 17: 1-10
- Duchaufour, P. tional des E. 1953. 17: 1-10
- Eaton, T. H., Jr in New York. 1953. 17: 1-10
- Edelman, C. H. sterdam, H. 1953. 17: 1-10
- Eyk, J. J. Van cthesis. Wageningen. 1963b. 36.
- Franzmeier, D. I. of Podzols and net changes. Quart. Bull. Soil. Soc. Am. 1966. 30: 1-10
- Fridland, V. M. 1966. 30: 1-10
- Gerasimov, I. P. tion of bina. 1953. 17: 1-10
- Hallsworth, E. C. in New South Wales. 1953. 17: 1-10
- Hole, F. D., and Univ. Wis. 1952. 16: 1-10
- Hole, F. D., G. of Florence. 1952. 16: 1-10
- Jenny, H. 1941. 15: 1-10
- Jenny, H., R. J. system and development. 1959. 23: 1-10
- Kawaguchi, K., 1953. 17: 1-10

## LITERATURE CITED

- er
- on but no placic horizon
- Is will not slake in water  
dic horizon and a fragi-
- mer to winter tempera-
- he horizon turns redder
- izon  
inter temperature differ-
- dic horizon  
n
- uods and have more  
the spodic horizon.  
s Aquods and have  
and aluminum but
- Aquods and have in  
an six times that of
- ps (Table 20.1) on  
ature and range of  
horizon with silica;  
degree of develop-
- (thaptic) Spodosols  
(1965) in a tension
- the spodic horizon  
dzolics in the past
- ols have been used  
e degrees of profile
- Atkinson, H. J., and J. R. Wright. 1957. Chelation and the vertical movement of soil constituents. *Soil Sci.* 84:1-11.
- Bailey, H. H., E. P. Whiteside, and A. E. Erickson. 1957. Mineralogical composition of glacial materials as a factor in the morphology and genesis of some Podzol, Gray Wooded, Gray-Brown Podzolic and Humic-Gley soils in Michigan. *Soil Sci. Soc. Am. Proc.* 21:433-41.
- Bloomfield, C. 1953a. A study of podzolization. I. The mobilization of iron and aluminum by Scots pine needles. *J. Soil Sci.* 4:5-16.
- . 1953b. A study of podzolization. II. The mobilization of iron and aluminum by the leaves and bark of *Agathis australis* (Kauri). *J. Soil Sci.* 4:17-23.
- . 1954. A study of podzolization. III. The mobilization of iron and aluminum by Rimu (*Dacrydium cupressium*). *J. Soil Sci.* 5:39-45.
- . 1957. The possible significance of polyphenols in soil formation. *J. Sci. Food Agr.* 8:389-92.
- Bouma, J., J. Hoeks, L. Van der Plas, and B. van Scherrenburg. 1969. Genesis and morphology of some Alpine Podzol profiles. *J. Soil Sci.* 20:384-98.
- Bryson, R. A., W. N. Irving, and J. A. Larsen. 1965. Radiocarbon and soil evidence of former forest in the southern Canadian Tundra. *Science* 147:46-48.
- Burges, A., and D. P. Drover. 1953. The rate of Podzol development in sands of the Woy Woy district, N.S.W. *Australian J. Botany* 1:83-94.
- Duchaufour, P. 1958. Dynamics of forest soils under Atlantic climate. *Ecole Nationale des Eaux et Forêts*. Nancy, France.
- Eaton, T. H., Jr., and R. F. Chandler, Jr. 1942. The fauna of forest-humus layers in New York. *Cornell Agr. Exp. Sta. Memoir* 247.
- Edelman, C. H. 1950. Soils of the Netherlands. North-Holland Pub. Co., Amsterdam, Holland.
- Eyk, J. J. Van der. 1957. Reconnaissance soil survey in northern Surinam. Ph.D. thesis. Wageningen.
- Franzmeier, D. P., and E. P. Whiteside. 1963a. A chronosequence of Podzols in northern Michigan. I. Ecology and description of pedons. *Mich. State Univ. Agr. Exp. Sta. Quart. Bull.* 46:2-20.
- . 1963b. A chronosequence of Podzols in northern Michigan. II. Physical and chemical properties. *Mich. State Univ. Agr. Exp. Sta. Quart. Bull.* 46:21-36.
- Franzmeier, D. P., E. P. Whiteside, and M. M. Mortland. 1963. A chronosequence of Podzols in northern Michigan. III. Mineralogy, micromorphology, and net changes occurring during soil formation. *Mich. State Univ. Agr. Exp. Sta. Quart. Bull.* 46:37-57.
- Fridland, V. M. 1957. Podzolization and illmerization. *Dokl. Akad. Nauk.* 115:1006-9.
- Gerasimov, I. P. 1960. Gleyey pseudo-Podzols of central Europe and the formation of binary surface deposits. *Soils Fertilizers* 23:1-7.
- Hallsworth, E. G., A. B. Costin, and F. R. Gibbons. 1953. Studies in pedogenesis in New South Wales. VI. On the classification of soils showing features of Podzol morphology. *J. Soil Sci.* 4:241-56.
- Hole, F. D., and K. O. Schmude. 1959. Soil survey of Oneida County, Wisconsin. *Univ. Wis. Geol. Nat. Hist. Survey Bull.* 82.
- Hole, F. D., G. W. Olson, K. O. Schmude, and C. J. Milfred. 1962. Soils survey of Florence County, Wisconsin. *Univ. Wis. Geol. Nat. Hist. Survey Bull.* 84.
- Jenny, H. 1941. *Factors of soil formation*. McGraw-Hill, New York.
- Jenny, H., R. J. Arkley, and A. M. Schultz. 1969. The pygmy forest-Podzol ecosystem and its dune associates in the Mendocina Coast. *Madrono.* 20:60-74.
- Kawaguchi, K., and Y. Matsuo. 1960. The principle of mobilization and immobili-

- zation of iron oxide in soils and its application to the experimental production of podzolic soil profiles. *Trans. 7th Intern. Congr. Soil Sci. (Madison, Wis.)* 4:305-13.
- Kevan, D. K. McE. (ed.). 1955. *Soil zoology; proceedings of the University of Nottingham Second Easter School in Agricultural Science*. Academic Press, New York.
- Kubota, J., and L. D. Whittig. 1960. Podzols in the vicinity of Nelchina and Tazlina glaciers, Alaska. *Soil Sci. Soc. Am. Proc.* 24:133-36.
- Malcolm, R. L., and R. J. McCracken. 1968. Canopy drip: A source of mobile soil organic matter for mobilization of iron and aluminum. *Soil Sci. Soc. Am. Proc.* 32:834-38.
- McCracken, R. J., R. E. Shanks, and E. E. C. Clebsch. 1962. Soil morphology and genesis at higher elevations of the Great Smoky Mountains. *Soil Sci. Soc. Am. Proc.* 26:384-88.
- Macfadyen, A. 1963. *Animal ecology: Aims and methods*. Pitman, New York.
- McFee, W. W., and E. L. Stone. 1965. Quantity, distribution and variability of organic matter and nutrients in a forest Podzol in New York. *Soil Sci. Soc. Am. Proc.* 29:432-36.
- McKenzie, L. J., E. P. Whiteside, and A. E. Erickson. 1960. Oxidation-reduction studies on the mechanism of B horizon formation in Podzols. *Soil Sci. Soc. Am. Proc.* 24:300-305.
- Milfred, C. J., G. W. Olson, and F. D. Hole. 1967. Soil resources and forest ecology of Menominee County, Wisconsin. *Soil Series 60*. Univ. Wis. Geol. Nat. Hist. Survey Bull. 85.
- Muir, A. 1961. The Podzol and Podzolic soils. *Adv. Agron.* 13:1-56.
- Nygaard, I. J., P. R. McMiller, and F. D. Hole. 1952. Characteristics of some Podzolic, Brown Forest, and Chernozem of the northern portion of the lake states. *Soil Sci. Soc. Am. Proc.* 16:123-29.
- Pol'skii, B. N. 1961. The question of the chemistry of Ortsteins of sod-podzolic soils. *Pochvovedeniye* N.2:93-96.
- Ponomareva, V. V. 1964. Theory of podzolization (*Izdatel'stvo Nauka*). (Transl. by A. Gourevitch.) *Israel Prog. for Sci. Trans.*, Jerusalem, 1969. Available from U.S. Dept. Commerce, Springfield, Va.
- Proudfoot, V. B. 1958. Problems of soil history. Podzol development at Goodland and Torr Townlands, County Antrim, Northern Ireland. *J. Soil Sci.* 9:186-98.
- Rieger, S., and J. A. DeMent. 1965. Cryorthods of the Cook Inlet-Susitna Lowland, Alaska. *Soil Sci. Soc. Am. Proc.* 29:448-53.
- Riquier, J. 1960. Les phytolithes de certains sols tropicaux et des Podzols. *Trans. 7th Intern. Congr. Soil Sci. (Madison, Wis.)* 4:425-31.
- Russell, E. W. 1956. *Soil conditions and plant growth*. Longmans, Green and Co., London.
- Schuylenborgh, J. van. 1962. On soil genesis in temperate humid climate. I. Some soil groups in the Netherlands. *Neth. J. Agr. Sci.* 10:127-44.
- Soil Survey Staff. 1967. *Supplement to Soil classification, a comprehensive system—7th approximation*. U.S. Dept. Agr. U.S. Govt. Printing Office, Washington.
- Stobbe, P. C., and J. R. Wright. 1959. Modern concepts of the genesis of Podzols. *Soil Sci. Soc. Am. Proc.* 23:161-64.
- Swindale, L. D., and M. L. Jackson. 1956. Genetic processes in some residual podzolized soils of New Zealand. *Trans. 6th Intern. Congr. Soil Sci.*, pp. 233-39.
- Upham, C. W. 1969. *Soil survey of Plymouth County, Massachusetts*. Soil Conserv. Serv., U.S. Dept. Agr. U.S. Govt. Printing Office, Washington.

## Alfisols: Hi

in the B horizon the more high requisite soil p although the n the order are al subtropical regi

**SETTING.** Tv erate abundanc enough to produ acid conditions the absence of other diagnosti of the soil. Alt are most exten land surfaces th erosion for at l to retain nota available plant forest lands an on old alluvial landscapes is co sociated Ultiso clays in which argillans.

Gardner a Alfisols in glaci New York, Cli to highly leach (Udalf) → Brov

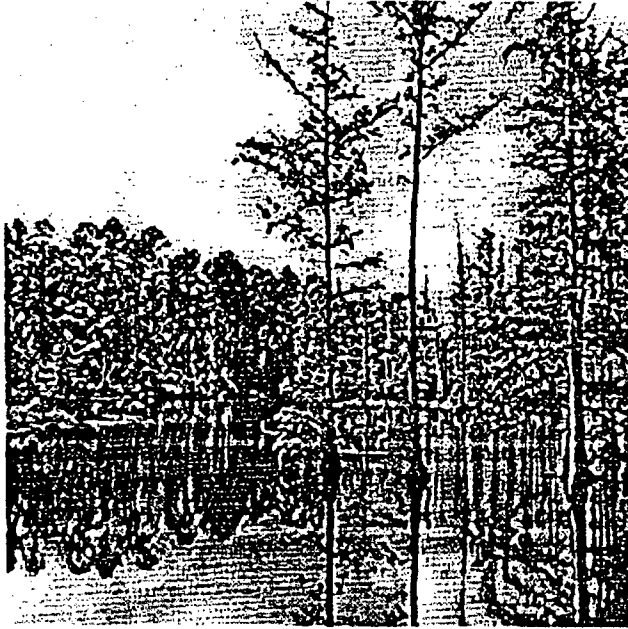
United States  
Department of  
Agriculture

# Silvics of North America

Forest Service

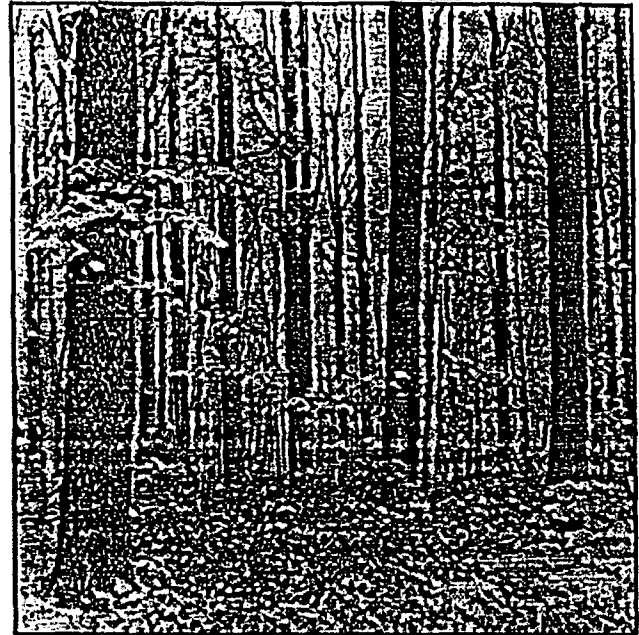
Agriculture  
Handbook 654

Volume 1: Conifers



[Click here for Table of Contents](#)

Volume 2: Hardwoods



[Click here for Table of Contents](#)

---

Russell M. Burns and Barbara H. Honkala  
Technical Coordinators  
Timber Management Research

Agriculture Handbook 654

(Supersedes Agriculture Handbook 271,  
Silvics of Forest Trees of the United States, 1965)

Forest Service  
United States Department of Agriculture

Washington, DC

December 1990

Burns, Russell M., and Barbara H. Honkala, tech. coords. 1990. Silvics of North America: 1. Conifers; 2. Hardwoods. Agriculture Handbook 654.

Burns + Hardin 1990

## *Pinus taeda* L

# Loblolly Pine

Pinaceae Pine family

James B. Baker and O. Gordon Langdon

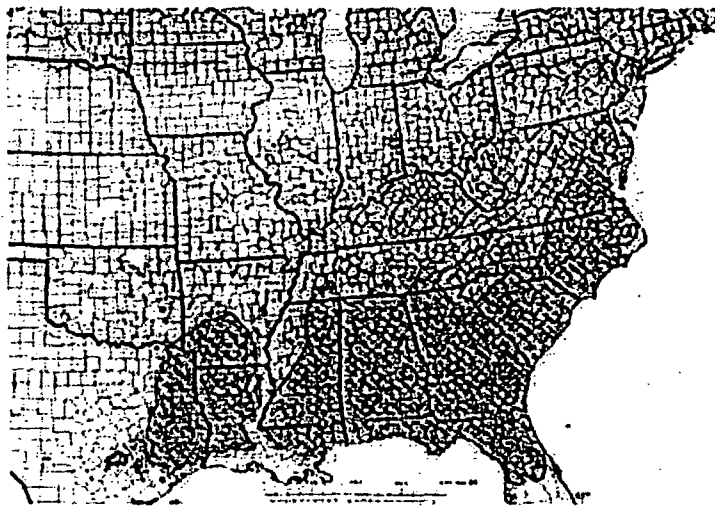
Loblolly pine (*Pinus taeda*), also called Arkansas pine, North Carolina pine, and oldfield pine, is the most commercially important forest species in the southern United States, where it is dominant on about 11.7 million ha (29 million acres) and makes up over one-half of the standing pine volume. It is a medium-lived, intolerant to moderately tolerant tree with rapid juvenile growth. The species responds well to silvicultural treatments and can be managed as either even-aged or uneven-aged natural stands, or can be regenerated artificially and managed in plantations.

### Habitat

#### Native Range

The native range of loblolly pine extends through 14 States from southern New Jersey south to central Florida and west to eastern Texas. It includes the Atlantic Plain, the Piedmont Plateau, and the southern extremities of the Cumberland Plateau, the Highland Rim, and the Valley and Ridge Provinces of the Appalachian Highlands. Loblolly pine does not grow naturally in the Mississippi River flood plain and is scarce in the deep, coarse sands of the lower Atlantic Plain and sandhills of North and South Carolina; it is important only in localized areas in southeastern Georgia and northern Florida (37,55,69).

Loblolly pine is an adaptable species that has been successfully planted along the periphery of its natural range and has been introduced on other continents with varying degrees of success.



The native range of loblolly pine.

#### Climate

The climate over most of the loblolly pine range is humid, warm-temperate with long, hot summers and mild winters. Average annual rainfall varies from 1020 to 1520 mm (40 to 60 in). The frost-free period varies from 5 months in the northern part of the range to 10 months along the southern coastal States. Mean annual temperatures range from 13° to 24° C (55° to 75° F); average July temperature is 27° C (80° F) and frequently exceeds 38° C (100° F). January temperature averages 4° to 16° C (40° to 60° F) and occasionally drops to -23° C (-10° F) in the northern and western parts of the range (69).

During both winter and summer, weather within the range of loblolly pine differs from that immediately outside the

the disease (60). The loblolly x pitch cross has growth characteristics of loblolly pine and cold resistance of pitch pine, making the hybrid more suitable for plantings in the north (30).

#### Literature Cited

1. Amateis, Ralph L., Harold E. Burkhart, Bruce R. Knoebel, and Peter T. Sprinz. 1984. Yields and size class distributions for unthinned loblolly pine plantations on cutover site-prepared lands. School of Forestry and Wildlife Resources Publication No. FWS-2-84. Virginia Polytechnic Institute and State University, Blacksburg, VA. 69 p.
2. Androlot, A. E., L. P. Blackwell, and P. Y. Burns. 1972. Effects of thinning on yield of loblolly pine in central Louisiana. Louisiana Tech. University, Bulletin 6. Ruston. 145 p.
3. Ashe, W. W. 1915. Loblolly or North Carolina pine. North Carolina Geological and Economic Survey, Bulletin 24. Raleigh. 176 p.
4. Bailey, Robert L., Galen E. Grider, John W. Rhency, and Leon V. Pienaar. 1985. Stand structure and yields for site-prepared loblolly pine plantations in the Piedmont and upper coastal plain of Alabama, Georgia, and South Carolina. The University of Georgia College of Agriculture Experiment Stations Research Bulletin 328. The University of Georgia, Athens. 118 p.
5. Baker, James B. 1986. The Crossett farm forestry forties after 41 years of selection management. Southern Journal of Applied Forestry 10(4):233-237.
6. Baker, James B., and William E. Balmer. 1983. In Silvicultural systems for the major forest types of the United States. Russell M. Burns, tech. comp. p. 148-152. USDA Forest Service, Agriculture Handbook 445. Washington, DC.
7. Baker, Whiteford L. 1972. Eastern forest insects. U.S. Department of Agriculture, Miscellaneous Publication 1175. Washington, DC. 642 p.
8. Baldwin, V.C., Jr., and D. P. Feduccia. 1987. Loblolly pine growth and yield prediction for managed West Gulf plantations. USDA Forest Service, Research Paper SO-236. Southern Forest Experiment Station, New Orleans, LA. 27 p.
9. Balmer, W. E., E. G. Owens, and J. R. Jorgenson. 1975. Effects of spacings on loblolly pine growth 15 years after planting. USDA Forest Service, Research Note SE-211. Southeastern Forest Experiment Station, Asheville, NC. 7 p.
10. Balmer, W. E., K. A. Utz, and O. G. Langdon. 1978. Financial return from cultural work in natural loblolly pine stands. Southern Journal of Applied Forestry 24:111-117.
11. Barnett, J. P. 1970. Germination inhibitors unimportant in dormancy of southern pine seeds. USDA Forest Service, Research Note SO-112. Southern Forest Experiment Station, New Orleans, LA. 4 p.
12. Bassett, J. R. 1964. Tree growth as affected by soil moisture availability. Soil Science Society of America Proceedings 28:436-438.
13. Blair, R. M., and H. G. Enghardt. 1976. Deer forage and overstory dynamics in a loblolly pine plantation. Journal of Range Management 29(2):104-108.
14. Box, B. H. 1967. A study of root extension and biomass in a six-year-old pine plantation in southeast Louisiana. Thesis (Ph.D.). Duke University, School of Forest Resources, Durham, NC. 178 p.
15. Boyer, William D. 1970. Shoot growth patterns of young loblolly pine. Forest Science 16(4):472-482.
16. Boyer, William D. 1978. Heat accumulation: an easy way to anticipate the flowering of southern pines. Journal of Forestry 76(1):20-23.
17. Brender, E. V. 1973. Silviculture of loblolly pine in the Georgia Piedmont, Georgia Forest Research Council, Report 33. Macon. 74 p.
18. Brender, E. V., and J. L. Clutter. 1970. Yield of even-aged natural stands of loblolly pine. Georgia Forest Research Council, Report 23. Macon. 7 p.
19. Brown, Claud L. 1976. Forests as energy sources in the year 2000: what man can imagine, man can do. Journal of Forestry 74(1):7-12.
20. Brunswig, N. L., and A. S. Johnson. 1972. Bobwhite quail foods and populations in the Georgia Piedmont during the first seven years following site preparation. Proceedings Southeastern Association of Game and Fish Commissioners 26:96-107.
21. Burkhart, Harold E., and Peter T. Sprinz. 1984. A model for assessing hardwood competition effects on yields of loblolly pine plantations. School of Forestry and Wildlife Resources Publication No. FWS-3-84. Virginia Polytechnic Institute and State University, Blacksburg, VA. 55 p.
22. Burkhart, Harold E., Quang V. Cao, and Kenneth D. Ware. 1981. A comparison of growth and yield prediction models for loblolly pine. School of Forestry and Wildlife Resources Publication No. FSW-2-81. Virginia Polytechnic Institute and State University, Blacksburg, VA. 59 p.
23. Burkhart, Harold E., Kenneth D. Farrar, Ralph L. Amateis, and Richard F. Daniels. 1987. Simulation of individual tree growth and stand development in loblolly pine plantations on cutover, site-prepared areas. School of Forestry and Wildlife Resources Publication No. FWS-1-87. Virginia Polytechnic Institute and State University, Blacksburg, VA. 47 p.
24. Cain, M. D., and W. F. Mann, Jr. 1980. Annual brush control increases early growth of loblolly pine (*Pinus taeda*). Southern Journal of Applied Forestry 4(2):67-70.
25. Cao, Quang V., Harold E. Burkhart, and Ronald C. Lemin, Jr. 1982. Diameter distributions and yields of thinned loblolly pine plantations. School of Forestry and Wildlife Resources Publication No. FWS-1-82. Virginia Polytechnic Institute and State University, Blacksburg, VA. 62 p.

range. There are a greater number of days with rain, a greater frequency of effective amounts of rain, that is, more than 13 mm (0.5 in), and higher average winter temperatures. In spring and autumn, the weather within and outside the range is more nearly the same (37).

The main factor limiting northern extension of the species is probably low winter temperature with associated damage from ice, snow, and sleet and cold damage during flowering. Lack of adequate growing-season precipitation probably limits western extension of loblolly pine in Oklahoma and Texas (37).

### Soils and Topography

Soils within the native range of loblolly pine are predominantly Ultisols. Small areas of Entisols and Spodosols are found in the Southeastern States and there are some Alfisols throughout the region. Loblolly pine grows on a wide variety of these soils, ranging from the flat, poorly drained Aquults and Aquods of the coastal portion of the Atlantic Plain to the relatively dry Psammets, Udults, and Udalfs of the inland portion of the Atlantic Plain, Piedmont, and upland Provinces (107). Best growth is on moderately acid soils with imperfect to poor surface drainage, a thick medium-textured surface layer, and a fine-textured subsoil. These soils are common in the uplands of the Atlantic Plain and on the flood plains and terraces of rivers and streams. Poorest performance is on shallow soils, eroded soils and very wet or waterlogged sites (37).

Some typical examples of Ultisols on which loblolly pine grows include the Coxville, Bladen, Beauregard, Wahee, Dunbar, Ruston, Norfolk, Orangeburg, and Smithdale series found in the Atlantic Plain; the Cecil, Davidson, and Appling series in the Piedmont; and the Hartsells and Linker series in the upland Provinces. Ultisols have a site index measured at base age 50 years for loblolly pine of 23 to 30 m (75 to 100 ft) in the Coastal Plain, 20 to 29 m (65 to 95 ft) in the Piedmont, and 18 to 24 m (60 to 80 ft) in the upland Provinces. Typical Entisols on which loblolly pine is found include deep sands (Chibley, Eustis, and Lakeland series) and alluvial soils (Alpin and Osier series), with a site index ranging from 20 to 30 m (65 to 100 ft). Representative Spodosols include the Leon and Lynn Haven series, with a site index of 18 to 26 m (60 to 85 ft). Within the Atlantic Plain but confined to a strip on each side of the Mississippi River are loessial soils represented by the Memphis, Grenada, Providence, Calhoun, and Henry series. These loessial soils, as well as Caddo, Wrightsville, Meggett, and Bude series, all having a site index ranging from 23 to 34 m (75 to 110 ft), are some representative Alfisols on which loblolly pine grows.

In the Atlantic Plain, the productivity of mineral soils generally decreases with improvement in surface drainage. Productivity is sensitive to soil fertility, however, and if fertility is low on poorly drained sites, productivity decreases (63). The presence of a spodic horizon within the rooting zone, as in the Leon series, frequently is associated with low productivity. Deep, excessively drained sands are also very low in site quality unless a water table or a clay lens which holds moisture lies within reach of the tree roots (37).

In the Piedmont Plateau, where surface drainage is well developed, physical characteristics of the soil, rather than surface drainage, determine the availability of moisture, nutrients, and aeration. Here uneroded soils with a thick surface layer and a friable subsoil have a site index of 24 to 27 m (80 to 90 ft). Common series in this category are Appling, Durham, Davidson, Georgeville, and Cecil. The least productive sites are eroded soils with a very plastic subsoil such as the Orange and Iredell series. When the A horizon is gone, site index is less than 12 m (40 ft) (37).

In the Ridge and Valley Provinces loblolly pine site index of 18 to 26 m (60 to 85 ft) generally increases from ridge tops to bottoms. This variation is related to landform, slope position and aspect, and geology. Soil features that determine site quality, such as soil temperatures, surface soil thickness, subsoil consistency, and soil moisture, are correlated with topography. However, past land use, differences in soil parent material, and other factors also affect soil profile development and cause variations in site quality independent of topography (92).

Perhaps as significant as the soils on which loblolly pine grows are those soils in the region where loblolly pine does not grow. These are principally Mollisols of the Blackbelt, Entisols of calcareous river bottoms and terraces (that is, soils in the Louisa, Miller, and Precris series characterized by high base saturation and high pH) and Alfisols of the Coastal Prairie of Louisiana and Texas with moderately high base saturation. These soils may also have other unidentified properties which exclude pine (72).

The topography throughout the loblolly pine range varies from flat near the coast to mountainous in the interior highlands. The topography can best be related to the physiographic regions within the loblolly pine range.

The Atlantic Plain is generally flat near the coast but becomes rolling and hilly inland with elevations ranging up to 150 m (500 ft). The Piedmont Plateau is more rolling, with highly developed drainage patterns and generally finer textured soils. Elevations range up to 305 m (1,000 ft) in Georgia. The Ridge and Valley Province is about 64 km (40 mi) wide and extends into the loblolly pine range from southeastern Tennessee into northern Georgia and Alabama. The topography is characterized by a group of valley floors separated by long, narrow, zigzagging ridges; elevations range from about 185 m (600 ft) to about 365 m (1,200 ft). The Cumberland Plateau, which lies just west of the Ridge

and Valley Province, is underlain by massive sandstone and its topography is characterized by winding narrow-crested ridges and narrow valleys. In some places the sandstone has given rise to local upland flats and mesa-like forms or knobs. Elevations range from 150 m (500 ft) in the southern part of the region and in the valley floors to 305 m (1,000 ft) at the northern end of the region and on ridge tops. The topography of the Highland Rim that extends into south-central Tennessee and northern Alabama is undulating with depressions and low domes where elevations range from 150 to 245 m (500 to 800 ft).

### Associated Forest Cover

Loblolly pine is found in pure stands and in mixtures with other pines or hardwoods, and in association with a great variety of lesser vegetation. When loblolly pine predominates, it forms the forest cover type Loblolly Pine (Society of American Foresters Type 81) (31). Within their natural ranges, longleaf, shortleaf, and Virginia pine (*Pinus palustris*, *P. echinata*, and *P. virginiana*), southern red, white, post, and blackjack oak (*Quercus falcata*, *Q. alba*, *Q. stellata*, and *Q. marilandica*), sassafras (*Sassafras albidum*), and persimmon (*Diospyros virginiana*) are frequent associates on well-drained sites. Pond pine (*Pinus serotina*), spruce pine (*P. glabra*), blackgum (*Nyssa sylvatica*), red maple (*Acer rubrum*), and water oak (*Quercus nigra*), willow oak (*Q. phellos*), and cherrybark oak (*Q. falcata* var. *pagodifolia*) are common associates on moderately to poorly drained sites. In the southern part of its range, loblolly frequently is found with slash pine (*Pinus elliotii*) and laurel oak (*Quercus laurifolia*).

In east Texas, southern Arkansas, Louisiana, and the lower Piedmont, loblolly and shortleaf pine are often found in mixed stands. In Loblolly Pine-Shortleaf Pine (Type 80), loblolly predominates except on drier sites and at higher elevations. When shortleaf pine predominates, the mixture forms Shortleaf Pine (Type 75).

In fertile, well-drained coves and along stream bottoms, especially in the eastern part of the range, yellow-poplar (*Liriodendron tulipifera*), American beech (*Fagus grandifolia*), and white and Carolina ash (*Fraxinus americana* and *F. caroliniana*) are often found in the Loblolly Pine-Shortleaf Pine cover type.

Loblolly pine also grows in mixture with hardwoods throughout its range in Loblolly Pine-Hardwood (Type 82). On moist to wet sites this type often contains such broadleaf evergreens as sweetbay (*Magnolia virginiana*), southern magnolia (*M. grandiflora*), and redbay (*Persea borbonia*), along with swamp tupelo (*Nyssa aquatica*), red maple, sweetgum, water oak, cherrybark oak, swamp chestnut oak (*Quercus michauxii*), white ash, American elm (*Ulmus americana*), and water hickory (*Carya aquatica*). Occasionally, slash, pond, and spruce pine are present.

In the Piedmont and in the Atlantic Plain of northern Virginia and Maryland, loblolly pine grows with Virginia Pine (Type 79). In northern Mississippi, Alabama, and in Tennessee it is a minor associate in the eastern redcedar-hardwood variant of Eastern Redcedar (Type 46). On moist lower Atlantic Plain sites loblolly pine is found in Longleaf Pine (Type 70), Longleaf Pine-Slash Pine (Type 83), and Slash Pine-Hardwood (Type 85).

In the flood plains and on terraces of major rivers (except the Mississippi River) loblolly pine is a minor associate in Swamp Chestnut Oak-Cherrybark Oak (Type 91). On moist, lower slopes in the Atlantic Plain it is an important component in the Sweetgum-Yellow Poplar (Type 87). In bays, ponds, swamps, and marshes of the Atlantic Plain it is a common associate in Pond Pine (Type 98), the cabbage palmetto-slash pine variant of Cabbage Palmetto (Type 74), and Sweetbay-Swamp Tupelo-Red Bay (Type 104).

There is a great variety of lesser vegetation found in association with loblolly pine. Some common understory trees and shrubs include flowering dogwood (*Cornus florida*), American holly (*Ilex opaca*), inkberry (*I. glabra*), yaupon (*I. vomitoria*), hawthorn (*Crataegus* spp.), southern bayberry (*Myrica cerifera*), pepperbush (*Clethra* spp.), sumac (*Rhus* spp.), and a number of ericaceous shrubs. Some common herbaceous species include bluestems (*Andropogon* spp.), panicums (*Panicum* spp.), sedges (*Carex* spp. and *Cyperus* spp.), and fennels (*Eupatorium* spp.).

### Life History

#### Reproduction and Early Growth

**Flowering and Fruiting-** Loblolly pine is monoecious; male flowers form in clusters at the tip of the preceding year's growth and female flowers form on the new year's growth. The pollen-bearing staminate flowers are catkin-like in appearance; they range from 2.5 to 3.8 cm (1.0 to 1.5 in) in length and vary from light green to red and yellow depending on stage of development. The pistillate flowers are generally ovoid and range from 1.0 to 1.5 cm (0.4 to 0.6 in) in length. They vary from light green through shades of pink to red depending on stage of development.

Flowering of loblolly pine is initiated in July and August in a quiescent bud that is set from middle June to early July. The male strobili form in this bud in late July and the female in August, but they are not differentiated into

recognizable structures until late September or October. In October the staminate buds develop at the base of a vegetative bud and the pistillate buds develop at the apex of a vegetative bud a few weeks later; both remain dormant until early February (37,41). The date of peak pollen shed depends on the accumulation of 353° C (636° F) day-heat units above 13° C (55° F) after February 1 (16). Flowering is also related to latitude, beginning earlier at lower latitudes than at higher ones, and it can occur between February 15 and April 10. Staminate flowers on a given tree tend to mature before the pistillate flowers, which helps to reduce self-pollination. Fertilization of the pistillate strobili takes place in the spring of the following year (37).

Loblolly pine does not normally flower at an early age, although flowering has been induced on young grafts with scion age of only 3 years. The phenomenon of inducing such early flowering in seedlings is dependent on reducing vegetative shoot growth so that quiescent buds are formed in the latter part of the growing season to allow for the initiation and differentiation of reproductive structures. The formation of quiescent buds in seedlings and saplings does not usually occur during that period because four to five growth flushes are common for trees of this age. As a loblolly pine tree ages, the number of growth flushes decreases, which accounts in part for increased flowering of trees at older ages. Flowering is also genetically controlled and is influenced by moisture (May-July rainfall) and nutrient stresses.

**Seed Production and Dissemination-** Seed production of loblolly pine varies according to physiographic region, climatic factors, and tree or stand condition. In the southern coastal portions of the Atlantic Plain, loblolly is generally a prolific and consistent seed producer, but in some of the inland portions of the Atlantic Plain, the Piedmont, and in the western extremities of its range, seed production is often lower and more erratic. Year-to-year variations in seed crops can range from failure to bumper crops. For example, in 27 years of seedfall records in the Atlantic Plain of South Carolina, there was one seed-crop failure but there were three seed crops of more than 2.5 million sound seeds per hectare (1 million/acre) with the other crops falling between these extremes. At most locations where seed-crop records have been kept, however, such wide annual variations have not been observed.

Despite fluctuations in seed production, loblolly usually produces some seeds every year and good seed crops normally occur at intervals of 3 to 6 years. More than 198,000 sound seeds per hectare (80,000/acre) is considered a good seed crop; 74,000 to 198,000/ha (30,000 to 80,000/acre) is an average crop, and less than 74,000/ha (30,000/acre) is considered marginal, depending on seedbed characteristics and weather conditions.

Throughout the range of loblolly pine, usually cones mature and seeds ripen by the second October after flowering or about 26 months after the strobili are initiated. The mature cones are light reddish brown and range from 7.5 to 15.0 cm (3 to 6 in) in length. They are narrowly conical to ovoid-cylindrical. Each cone scale is tipped with a stout triangular spine. Mature cones have a specific gravity of 0.89 or less (they float in SAE 20 oil). Individual cones may contain from less than 20 to more than 200 seeds, and the percentage of sound seeds may vary from about 15 percent to nearly 100 percent. Loblolly seeds vary in size from 27,100/kg (12,300/lb) to 58,200/kg (26,400/lb) and average 40,100/kg (18,200/lb) (37,88).

Seed production of individual trees increases with tree age, size, and freedom from crown competition. By age 25, enough seeds may be produced in widely spaced trees to regenerate a stand; however, trees at 40 years generally produce three to five times more. Rotations shorter than 30 years usually do not lend themselves to natural regeneration.

In well-stocked and overstocked stands, cone production of loblolly pine can be stimulated threefold to tenfold by releasing the seed trees from competitors at least three growing seasons before the seed is needed. If seed-tree release is delayed later than May 1, seed-crop stimulation will be delayed 1 year. In overstocked stands, if seed trees are not released before a harvest cutting, then seed-crop stimulation will be delayed 2 or 3 years, depending on the season of the harvest cut (37,61,95).

Seedfall usually begins in October, and the bulk of the seeds are released in November and early December. Seedfall is hastened by dry, warm, windy weather and retarded by cool, wet weather. Seed dispersal in or adjacent to a stand varies with height and stocking level of the seed-source trees, magnitude of the seed crop, terrain, and weather conditions at the time of seedfall. The effective seeding distance ranges from 61 to 91 m (200 to 300 ft) in a downwind direction from the seed source and 23 to 30 m (75 to 100 ft) in other directions. Viability of seeds varies with seed-crop size and the month that the seed is dispersed. Seed viability is often lower in years of poor seed crops and in seeds dispersed late in the season (37).

Loblolly pine seeds generally go through a stage of dormancy after seedfall, which lasts longer than that of any other southern pine. Seed dormancy is related to the impermeable properties of the seedcoat that constrain water imbibition and oxygen uptake; chemical germination inhibitors do not play a significant role (11,73). Dormancy is broken naturally as the seeds overwinter on the forest floor. Germination is epigeal (88). Natural seed germination usually begins in March when daytime temperatures range between 18° and 27° C (65° and 80° F). Few seeds remain viable (not more than 0.1 percent) on the forest floor for germination in the second year after seedfall (70). Secondary seed dormancy can be induced during seed handling procedures. Cold, moist stratification of the seed for 30 to 90 days at

temperatures 3° to 5° C (37° to 41° F) are generally recommended to artificially break dormancy for direct seeding or for nursery sowing (74).

**Seedling Development-** Moisture is a critical factor in seed germination and seedling establishment; the amount of rainfall in the spring is related directly to seedling catches. Scarifying the seedbed exposes mineral soil and increases contact of the seeds with moist soil surfaces. Failure of the root radicle to penetrate compacted or puddled soil surfaces reduces seedling establishment, especially on major skid trails and log decks. Soil compaction and puddling also reduce root growth, seedling survival, and shoot growth (36,37,40,61).

Seedbed preparation by scarification or burning greatly increases seed germination and seedling survival, which reduces the number of seeds required to produce one seedling. For example, undisturbed seedbeds with a litter depth of 8 to 10 cm. (3 to 4 in) require 5 to 6 times more seeds to produce the number of seedlings produced in disturbed seedbeds.

Seed germination decreases with age of seedbed and increases with clay content of the soil. Two-year-old seedbeds require 3 to 4 times more seed for successful establishment than do 1-year-old seedbeds, and 3-year-old seedbeds require 9 to 14 times more seed than is needed in the first year. Thus, favorable seedbeds usually exist for only 1 year after disturbance, after which they rapidly deteriorate. Heavier textured soils provide better seedbeds which results in higher seedling survival than do lighter textured soils (37,104).

Drought is a major cause of mortality for planted loblolly pine seedlings, especially in areas with low rainfall during the growing season. Improper care, handling, and planting of nursery stock and inadequate site preparation for control of competing vegetation also contribute to poor survival by indirectly increasing moisture stress (34,57).

Height growth of loblolly pine seedlings occurs annually in a series of two to five growth flushes and is dependent on variables such as temperature, day length, soil moisture, nutrients, competition, and genetics. Temperature has a dominant influence on the initiation of height growth in the spring. High day temperatures increase height growth, but high night temperatures decrease it. When day and night temperatures differ by 12° to 13° C (54° to 55° F), the best height growth occurs (15,43).

Soil moisture influences growth of loblolly pine by its effect on internal water relations and vital physiological processes. Growth is reduced with increasing water deficits. For example, at a soil moisture tension of 1520 mm of mercury (2 atm), height growth of loblolly pine seedlings is greatly reduced and at 2660 mm of mercury (3.5 atm), height growth ceases. Height and diameter growth are significantly reduced by a late spring and summer drought, which also reduces early height growth the following year (37,98,116).

Growth of loblolly pine seedlings in a natural stand is inversely related to overstory stocking of pine and hardwoods. As the proportion of hardwoods increases for a given pine stocking, loblolly pine seedling growth decreases. Size and shape of openings affect seedling growth up to 9 m (30 ft) from edges of openings. Seedlings growing beneath overstory hardwoods are not likely to survive more than a few years and if they do survive their growth will be slow. Growth and survival of loblolly pine seedlings during the first 7 years after a stand is regenerated may be reduced by 80 percent because of the faster growth of competing hardwood sprouts and shrubs. Pine seedlings not overtopped by hardwoods at age 3 or older have an excellent chance to outgrow the hardwood competition (37).

Photosynthesis in loblolly pine seedlings is related to light and soil moisture conditions, which in turn are affected by competing hardwoods. Photosynthetic rates of many hardwoods are inherently higher than those of loblolly pine at relatively low light intensities and with low soil moisture (37).

Fertilization often increases seedling growth in waterlogged soils. In some instances where specific nutrients are limiting growth, fertilization results in growth equal to or greater than that with drainage. Loblolly pine grows well on wet, fertile sites because of the effects of moisture on nutrient availability (63,101).

**Vegetative Reproduction-** Young loblolly pine seedlings up to 3 years of age may sprout from buds in axils of primary needles if tops are clipped off, but older trees will not produce basal sprouts at root collars if stems are cut or top-killed by fire, nor do they produce root sprouts. Rooting is related to tree age and is more successful with cuttings from younger trees. Techniques and materials used to root cuttings are of critical importance. For example, a fine mist over the rooting bench is better than a heavy mist, and Hare's powder is a better compound to use than indolebutyric acid when rooting loblolly pine cuttings. Although needle bundles and buds of loblolly pine have been rooted, the success rate has been low. Air layering, a modification of rooting cuttings, has been the more successful method of the two. Success rates have been high for young trees but older trees are more difficult to air layer (29,42,48,110).

Grafting is the most common method of vegetative propagation used to produce genetically uniform trees, especially in seed orchards. Grafting success is usually high but varies with scion material because problems may develop from

incompatibility of scion and root stock (29,37,66).

Producing genetically uniform plantlets from tissue cultures is a promising technique, and research is underway to develop procedures for the commercial production of loblolly pine clones (19,94).

### Sapling and Pole Stages to Maturity

**Growth and Yield-** Growth of loblolly pine stands is inherently good when compared to most hardwood competitors and on many sites doubles or triples the production of common associates (108). Growth is influenced by the physical and chemical properties of soils (texture, compaction, aeration, moisture, pH, nutrients), light, temperature, photoperiod, allelopathy, precipitation and its seasonal pattern, and intra- and inter-species competition for space and essential elements. Because many of these factors interact, it is difficult to specify the most limiting one. Consequently, these biotic and environmental effects are commonly expressed as the average height of dominant trees at age 50 years, that is, site index.

Yield estimates for natural, even-aged loblolly pine in fully stocked stands were first made more than 50 years ago (3,106). Additional estimates have been made in more recent years for stands of various stocking levels (18,81,90,99).

Normal yields of natural, even-aged loblolly pine stands on average sites, such as those with a site index of 27 m (90 ft), have ranged from 133.0 m<sup>3</sup>/ha (1,900 ft<sup>3</sup>/acre) in trees 9 cm (3.6 in) and larger in d.b.h. including 29.4 m<sup>3</sup>/ha (2,100 fbm/acre) in trees 24 cm (9.6 in) and larger d.b.h. at age 20 to 427.7 m<sup>3</sup>/ha (6,110 ft<sup>3</sup> or 40,000 fbm/acre) at age 60 (all board-foot volumes reported in International quarter-inch rule). Mean annual cubic volume growth generally culminates at about age 40 on these sites with approximately 8.0 m<sup>3</sup>/ha (115 ft<sup>3</sup>/acre). As a result of larger sawtimber merchantability limits, mean annual board-foot growth culminates at about age 50 at a rate of 9.5 m<sup>3</sup>/ha (680 fbm/acre).

Growth of loblolly pine may be affected adversely by drought, excess moisture (flooding), and nutrient deficiencies. Growth of this species is highly correlated with departure from the normal rainfall of April through October. Extreme negative and positive departures (-117 vs. 229 mm or -4.6 vs. 9.0 in) in seasonal rainfall over 21 years resulted in differences of nearly 2.1 m<sup>3</sup> (74 ft<sup>3</sup>) of annual growth (12,39,65). Drainage (including bedding) and fertilization have been shown to increase dominant height and basal-area growth, resulting in dramatic increases in volume growth (45,63,76,101).

Growth of planted loblolly pine is affected by the same factors affecting natural stands. Sites are usually prepared before planting on cutover lands, and some are fertilized to correct nutrient deficiencies. Such practices are applied to control competition and to supply nutrients at optimum levels to establish vigorous, uniform stands at spacings that will fully utilize site potentials.

Yields of planted loblolly pine vary with plantation age, site quality, number of trees planted, and interactions of these variables. Yields generally increase with increasing age and site quality. Yields also increase with higher planting density or closer spacing; however, on some sites, moderately wide spacing of 2.4 by 2.4 m (8 by 8 ft) or 3.0 by 3.0 m (10 by 10 ft) outproduce both wider and closer spacing. Mean annual increment culminates at younger ages on better sites than on poorer ones. Better sites can carry more stocking than poor sites; consequently, initial spacing can be closer (9,77,93).

Closer spacing tends to produce higher total cubic volumes at younger ages than does wider spacing; however, average tree sizes are larger on wider spacings than on closer ones. If sawtimber is a primary management objective, then wider spacing or lower density would be advantageous. Although thinning seldom increases cubic volume yield of loblolly pine, light thinnings that salvage suppressed and moribund trees have increased net yields by as much as 20 percent in 50 years. Thinnings usually result in increased diameter growth of residual trees and allow the growth to be put on the better trees in the stand. Another benefit is that thinnings provide intermediate returns on investment (2,17).

Average total solid-wood yields of unthinned loblolly pine planted at 1,730 seedlings per hectare (700/acre) on non-old-field sites at various locations within its range were predicted to increase from approximately 155 m<sup>3</sup>/ha (2,200 ft<sup>3</sup>/acre) at age 15 to 300 m<sup>3</sup>/ha (4,200 ft<sup>3</sup>/acre) at age 30. Mean annual increment at age 30 was about 10 m<sup>3</sup>/ha (145 ft<sup>3</sup>/acre) (1,4,27,33,67). Estimates are also available for a variety of site and stand conditions and geographic areas (8,21,22,23,25,44,68,71).

Growth and yield in natural uneven-aged loblolly pine stands is dependent on stand structure, stocking, and site quality. To optimize average annual growth on average sites with a site index of 27 m (90 ft), stand structure should be manipulated so that approximately 70 percent of the merchantable cubic volume is in the saw-log portion of the stand, that is, trees 25 cm (10 in) in d.b.h. and larger. On average sites, stands with approximately 17 m<sup>3</sup>/ha (75 ft<sup>3</sup>/acre) of basal area, or 140 m<sup>3</sup>/ha (2,000 ft<sup>3</sup>/acre) total merchantable volume, or 10,000 fbm saw-log volume at the end of the

cutting cycle would be considered well stocked (5,84,86).

On good sites in southern Arkansas, with a site index of 27 m (90 ft) managed uneven-aged loblolly pine stands that are well stocked have averaged 0.7 m<sup>3</sup>/ha (3 ft<sup>3</sup>/acre) of basal-area growth, 5.6 m<sup>3</sup>/ha (80 ft<sup>3</sup>/acre) of merchantable volume growth, or 432 fbm/acre of saw-log volume growth per year for a 29-year period. On somewhat poorer sites in the Georgia Piedmont with a site index of 23 m (75 ft), annual growth has averaged 5.3 m<sup>3</sup>/ha (76 ft<sup>3</sup>/acre) or 319 fbm/acre over a 21-year period (5,17,82,85,86).

In sapling stands, differences in growth rate of individual loblolly pines are evident at early ages when competition between trees begins. The growth differentiation process begins at earlier ages on better sites or at higher levels of stocking; it begins later on poor sites or at low levels of stocking (51). The result is separation of trees into crown classes. Growth in height is a critical factor in the occupation of available space. Loblolly pine is a species in which individual trees tend to express dominance at an early age, and the most vigorous individuals that are best adapted to the microsite environment become dominants as the stand ages.

Faster growing trees develop larger live-crown ratios than do slower growing trees. Diameter growth of individual trees generally increases as crown surface area and crown ratio increase, with optimal diameter growth occurring when trees have at least a 40 percent live-crown ratio. Diameter increment does not occur uniformly on portions of the bole. Annual diameter growth is greatest within the crown and decreases with increased distance below the crown. This phenomenon causes the bole of loblolly pine trees to become cylindrical with increasing age. Height growth is not as sensitive as diameter growth to differences in crown size. Height growth of codominants is significantly less, however, in dense stands of trees with small crowns than in low-density stands of trees with larger crowns (37,38,51).

Loblolly pine is a medium-lived tree. Maximum recorded age of one tree in a small stand of 20 trees in North Carolina was 245 years, with the group averaging 240 years. The largest tree in this stand was 135 cm (53 in) in d.b.h. and 45.7 m (150 ft) tall. Currently, the champion for the species in the "National Register of Big Trees" is located near Urania, LA, and is 143 cm (56.3 in) in d.b.h. and 49.7 m (163 ft) tall (52).

**Rooting Habit-** The rooting habit of loblolly pine is strongly influenced by tree age, soil, and the soil environment. A young tree develops a short taproot but in most cases it ceases growth in favor of an extensive lateral-root system. A taproot 1.5 to 2.0 m (5.0 to 6.5 ft) long is often produced on deep, sandy or loamy soils. On heavy clay soils, the taproot tends to be stout and short. Taproots of loblolly pines are much smaller and shorter than those of shortleaf and longleaf pines. On excessively wet sites or when a water table or an impenetrable hardpan confines the roots to surface layers of soil, lateral roots are prominent in a superficial system (3,50,108).

In a 6-year-old loblolly pine plantation in southeast Louisiana, 83 percent of total root weight was in the upper 46 cm (18 in) of soil. In a 31-year-old natural stand in North Carolina, the majority of the feeder roots less than 2.5 mm (0.1 in) in diameter were concentrated in the 15-cm (6-in) deep-A horizon; practically no lateral roots were found below the 15- to 53-cm (6- to 21-in) depth of the B horizon (14,59).

Roots of loblolly generally spread laterally farther than their crowns. As a result, root grafting is a common occurrence both in natural stands and closely spaced plantations. Roots grow at all times of the year, but most root growth occurs in April and May, and in late summer and early fall (37,80,89,108).

**Reaction to Competition-** Loblolly pine is moderately tolerant when young but becomes intolerant of shade with age. Its shade tolerance is similar to that of shortleaf and Virginia pines, less than that of most hardwoods, and more than that of slash and longleaf pines (31,37,108). Loblolly pine is most accurately classed as intolerant of shade.

Succession in loblolly pine stands that originate in old fields and cutover lands exhibit a rather predictable pattern. The more tolerant hardwoods (including various species of oaks and hickories, sweetgum, blackgum, beech, magnolia, holly, and dogwood) invade the understory of loblolly pine stands and, with time, gradually increase in numbers and in basal area. The hardwoods finally share dominance with each other and with loblolly pine (37,83,100).

The climax forest for the loblolly pine type has been described as oak-hickory, beech-maple, magnolia-beech, and oak-hickory-pine in various parts of its range (28,37). Others view the climax forest as several possible combinations of hardwood species and loblolly pine. There is evidence that within the range of loblolly pine several different tree species could potentially occupy a given area for an indefinite period of time and that disturbance is a naturally occurring phenomenon. If this is so, then the climax for this southern forest might best be termed the southern mixed hardwood-pine forest (83).

Competition affects the growth of loblolly pine in varying degrees depending on the site, the amount and size of competing vegetation, and age of the loblolly pine stand. Across the southern region, average loss of volume production resulting from hardwood competition has been estimated at 25 percent in natural stands and 14 percent in

plantations (35). In a North Carolina study, residual hardwoods after logging reduced cubic-volume growth of a new stand of loblolly pine by 50 percent at 20 years, and where additional small hardwoods of sprout and seedling origin were present, growth was reduced by another 20 percent by age 20 (10,64). Similar growth responses in young seedling and sapling stands have been observed in Arkansas, Louisiana, and Texas (24,26,39). Although several short-term studies (5 years or less) of the effects of understory hardwoods on growth of older loblolly pine did not show measurable effects (58), a long-term study (11 to 14 years) showed growth increases of 20 to 43 percent in cubic volume and 21 to 54 percent in board-foot volume after removal of understory vegetation (39). Control of both residual overstory and understory hardwoods is a financially attractive silvicultural treatment for loblolly pine management (10).

Silvicultural practices such as prescribed burns, the use of herbicides, and mechanical treatments arrest natural succession in loblolly pine stands by retarding the growth and development of hardwood understories. Prescribed fire is effective for manipulating understory vegetation, reducing excessive fuel (hazard reduction), disposing of logging slash, preparing planting sites and seedbeds, and improving wildlife habitat. Responses of the understory to prescribed fire varies with frequency and season of burning. Periodic winter burns keep hardwood understories in check, while a series of annual summer burns usually reduces vigor and increases mortality of hardwood rootstocks (62). In the Atlantic Coastal Plain, a series of prescribed burns, such as a winter burn followed by three annual summer burns before a harvest cut, has been more effective than disking for control of competing hardwood vegetation and improvement of pine seedling growth after establishment of natural regeneration (103,104).

**Loblolly pine expresses dominance early, and various crown classes develop rapidly under competition on good sites; but in dense stands on poor sites, expression of dominance and crown differentiation are slower (37).**

Dense natural stands of loblolly pine usually respond well to precommercial thinning. To ensure the best volume gains, stocking should be reduced to 1,235 to 1,730 stems per hectare (500 to 700/acre) by age 5. When managing for sawtimber, thinnings increase diameter growth of residual trees and allow growth to be put on the better trees in the stand, thus maximizing saw-log volume growth and profitability (56,78).

Loblolly pines that have developed in a suppressed condition respond in varying degrees to release. Increases in diameter growth after release are related to live-crown ratio and crown growing space, but trees of large diameter generally respond less than trees of small diameter. Trees with well-developed crowns usually respond best to release. Trees long suppressed may also grow much faster in both height and diameter after release but may never attain the growth rate of trees that were never suppressed (37,75).

**Loblolly pine can be regenerated and managed with any of the four recognized reproduction cutting methods and silvicultural systems. Even-aged management is most commonly used on large acreages; however, uneven-aged management with selection cutting has proved to be a successful alternative.**

**Damaging Agents-** Agents that cause periodic damage to individual trees or stands of loblolly pine include wind, lightning, temperature extremes, ice, drought, flooding, insects, and diseases. Voluminous literature about the effects of these agents in loblolly pine stands on a range of sites, soils, and stand conditions is available; a brief summary follows.

Large dominant trees usually are more vulnerable to high winds than smaller trees, and trees with large cankers caused by rust disease break more readily than sound trees. In general, damage resulting from severe winds associated with hurricanes or thunderstorms is caused primarily by windthrow or blowdown. Windthrow is most common on shallow soils with coarse-textured profiles. Wind damage is also more likely to occur in recently thinned stands (37,105).

Direct losses to lightning are small, averaging only about 5 trees per 100 hectares (2/100 acres) per year. Large, dominant, open-grown trees are generally the most vulnerable to lightning strikes. Probably more important than the direct damage caused by lightning is the possibility that a lightning-struck tree will become a center for insect infestation (37).

Damage or seedling mortality caused by low or freezing temperatures occurs primarily in the northern extremities of the loblolly pine range. Older, vigorous trees can usually withstand occasional low temperatures (37,79). Greater damage frequently occurs from ice or glaze storms. This damage is normally associated with branch and stem breakage, severe bending and, in some cases, uprooting. Ice damage is usually more severe in recently thinned (particularly row thinned) plantations and in heavily stocked stands made up of slender, small-crowned trees (37,91). Extremely high summer temperatures and drought often cause mortality of seedlings and, in some cases, of larger trees. Heat and drought more often cause stress and a resultant loss of vigor and growth in larger trees, which can lead to more serious problems with insect infestations.

**Loblolly pine seedlings or saplings cannot withstand prolonged flooding. Complete inundation for more than 2 weeks during the growing season often results in significant mortality. Larger trees are classed as moderately tolerant of**

flooding; typically they can survive one season but usually succumb during the second growing season if continuously in 0.3 m (1 ft) or more of water (37,113).

A comprehensive review of insects associated with loblolly pine is provided by Baker (7). Loblolly pine serves as host to a multitude of insect pests; however, insect outbreaks vary greatly in frequency, area, and duration. The majority of outbreaks are small and short-lived and usually consist of only one or a few spots in a stand, but some may expand until they encompass hundreds of hectares and last for several years before subsiding. With only a few exceptions, the majority of the insects that attack loblolly pine are insignificant in terms of damage or mortality.

The most serious insect pests to loblolly pine are bark beetles, particularly the southern pine beetle (*Dendroctonus frontalis*), whose attack may result in extensive mortality, and pine engraver beetles (*Ips* spp.), that can cause death of isolated or small groups of trees; pine tip moths (*Rhyacionia* spp.), that often infest young trees; seedling debarking weevils (*Hyllobius* spp. and *Pachylobius* spp.), that sometimes result in girdling and death of young seedlings up to 13 mm (0.5 in) in d.b.h.; and cone and seed feeders (*Dioryctria* spp. and *Leptoglossus* spp.), that can seriously reduce seed crops. Loblolly pine is generally the preferred host of the southern pine beetle, which is the most destructive insect for this species (102). Most infestations originate in stands that are under stress because of poor site, adverse weather, overstocking, or overmaturity. Once a buildup of southern pine beetle occurs, adjacent well-managed stands may also be attacked. Preventive measures include avoidance of planting offsite and maintenance of vigorous stands through silvicultural practices such as controlling density through thinning and harvesting trees at or before maturity (6,102).

A general account of diseases associated with loblolly pine is provided by Hepting (54). The most common disease problems in loblolly pine are related to seedling susceptibility to black root rot (*Fusarium* spp., *Macrophomina* spp., and possibly others) and fusiform rust (*Cronartium quercuum* f. sp. *fusiforme*); sapling susceptibility to fusiform rust; root rot by *Heterobasidion annosum* in thinned stands; and heart rot in old stands with *Phellinus pini* in the bole and *Phaeolus schweinitzii* primarily in the butt.

Nursery seedlings are subject to root rot in soils with pH above 6.0 under moist conditions; however, root rot becomes severe only if soil temperatures remain above 32° C (90° F) for long periods. Fusiform rust is also a major nursery disease in many parts of the South, requiring rigid spray programs to keep infections low.

The most serious stem disease is fusiform rust, which kills and disfigures young trees from Virginia to Texas. Saplings and older trees, especially if planted, are subject to attacks by *Heterobasidion annosum* in stands where some cutting has taken place. It is considered a disease problem in plantation management second only to fusiform rust. Losses in natural stands or in the absence of some cutting are generally negligible.

*Phaeolus schweinitzii* causes a root and butt rot, usually after basal or root injuries, and in the Deep South it has caused more loss in some areas than *Heterobasidion annosum*. Red heart (*Phellinus pini*), entering almost entirely through dead branch stubs, is rarely a factor under the age of 60 years. However, when large branches that have heartwood begin to die, red heart can set in and destroy much of a tree.

## Special Uses

Natural loblolly pine stands as well as intensively managed plantations provide habitat for a variety of game and nongame wildlife species. The primary game species that inhabit pine and pine-hardwood forests include white-tailed deer, gray and fox squirrel, bobwhite quail, wild turkey, mourning doves, and rabbits (94). Some of these species utilize the habitat through all stages of stand development, while others are attracted for only a short time during a particular stage of development. For example, a loblolly pine plantation can provide forage for deer only from the time of planting to crown closure. Without modifying management practices, this usually occurs in 8 to 10 years (13). Bobwhite tend to use the plantation until a decline in favored food species occurs (20). As the habitat deteriorates, deer and quail usually move to mature pine or pine-hardwood forests (47) or to other newly established plantations. Management modifications such as wider planting spacing and early and frequent thinnings will delay crown closure, and periodic prescribed burns will stimulate wildlife food production.

Wild turkeys inhabit upland pine and pine-hardwood forests and do particularly well on large tracts of mature timber with frequent openings and where prescribed burning is conducted (96,97).

Pine lands are the chief habitat for some birds such as the pine warbler, brown-headed nuthatch, and Bachman's warbler. Old-growth stands are very important to the existence of the red-cockaded woodpecker. Large loblolly pine trees are favorite roosting places for many birds and provide an important nesting site for ospreys and the bald eagle (46).

In urban forestry, loblolly pines often are used as shade trees and for wind and noise barriers throughout the South.

They also have been used extensively for soil stabilization and control of areas subject to severe surface erosion and gullyng. Loblolly pine provides rapid growth and site occupancy and good litter production for these purposes (114,115).

Biomass for energy is currently being obtained from precommercial thinnings and from logging residue in loblolly pine stands. Utilization of these energy sources will undoubtedly increase, and loblolly pine energy plantations may become a reality.

## Genetics

### Population Differences

Many studies of racial and geographical variation in loblolly pine have been carried out since research with loblolly pine began in the early part of this century. Provenance studies have shown differences in survival, growth, disease resistance, drought hardiness, and cold hardiness attributable to source of the seed. The many findings of geographical differences (some of which show continuous, others discontinuous variation with geographic location) have led geneticists to consider some differences to be racial. Although distinct races of loblolly pine have not been named and described, recommended zones for collecting seed for planting of seedlings in a given geographic area have been established. Seed orchards for producing seed for specific areas have been established (29,30,111).

Resistance of certain families of loblolly pine to fusiform rust and the geographic variation in susceptibility of loblolly pine to the rust are important research findings now in use. Special rust-resistant seed orchards have been established with the most rust-resistant clones producing seed for specific geographic areas. Rust resistance of seedlings is low from seed sources in some areas such as east Texas and high for those in other areas such as Georgia and South Carolina. Rust resistance seems to be clinal and is strongly related to longitude of the seed source—the westerly sources are more resistant than the easterly ones (30,109,117).

Loblolly pine from the Lost Pines area of east Texas is more drought resistant than those with more easterly seed sources. The use of drought-hardy strains of loblolly pine for planting in drought-prone areas is most important. Cold hardiness is also an important characteristic to be considered, especially if loblolly is to be planted north or inland of its natural range. As expected, the more northerly sources of loblolly pine are more cold resistant (29,37).

Seed source affects yields of loblolly pine. These yield differences are usually attributable to the combined effects of seed source on survival, height and diameter growth, and susceptibility to fusiform-rust infection. Clinal effects in growth also are evident in the data, with trees from coastal areas growing faster than those from inland sources, except in northerly plantings. Loblolly pine trees within a seed source also vary in growth. Progeny tests of half-sib families (most of which are less than 10 years old) have shown significant differences in height growth with differences between races and families being additive. Nursery-bed selections of plus-seedlings have been effective in producing height growth gains for loblolly pine of 45 percent at age 10, and volume of the average plus-tree was 3.4 times that of the control. Although gains in other traits are not consistent, nursery-bed selection appears to be an effective first step in choosing fast-growing seedlings (30,53,109,112).

Wood characteristics of loblolly pine have been extensively investigated. Specific gravity generally decreases from southeast to northeast and from the coastal areas to the Piedmont. Wide tree-to-tree variation also has been found for specific gravity, tracheid length, fiber angle, and cellulose type. A most important research result for geneticists has been that wood quality characteristics and growth rate at older ages are not highly correlated and, more important, not negatively correlated, which allows breeding for several traits (30).

### Hybrids

The best-known southern pine hybrid is Sonderegger pine (*Pinus x sondereggeri* H. H. Chapm.), a cross between longleaf and loblolly pine. This natural hybrid occurs quite frequently in Louisiana and east Texas. It is conspicuous in nursery beds and plantings of longleaf pine because the hybrid gains height growth in the first year in contrast to longleaf seedlings, which do not. Natural hybrids of pond and loblolly pine have been observed in North Carolina, and those of pond, loblolly, and pitch pine have been recognized and studied in New Jersey, Delaware, and Maryland (37,87). Natural hybrids of loblolly and shortleaf are known to occur in Oklahoma and east Texas (29,37,49), and based on observations of tree characteristics intermediate between loblolly and shortleaf, they probably also occur in Louisiana and Arkansas in areas where the two species commonly occur together. Hybridization between these two species is thought to contribute to the fusiform-rust resistance of loblolly pine from those sources (29).

Artificial hybrids of loblolly pine and the other southern yellow pines have been produced. Two crosses—loblolly x shortleaf pine and loblolly x pitch pine—show considerable promise for use on a commercial scale. The loblolly x shortleaf cross will be used in areas with high fusiform-rust incidence for breeding a strain of loblolly pine resistant to

- Clason, T. R. 1978. Removal of hardwood vegetation increases growth and yield of a young loblolly stand. *Southern Journal of Applied Forestry* 2(3):96-97.
27. Clutter, Jerome L., William R. Harms, Graham H. Brister, and John W. Rheney. 1984. Stand structure and yields of site-prepared loblolly pine plantations in the lower coastal plain of the Carolinas, Georgia, and north Florida. USDA Forest Service, General Technical Report SE-27. Southeastern Forest Experiment Station, Asheville, NC. 173 p.
  28. Delcourt, H. R., and P. A. Delcourt. 1977. Presettlement magnolia-beech climax of the Gulf coastal plain: quantitative evidence from the Apalachicola river bluffs, north-central Florida. *Ecology* 55:1085-1093.
  29. Dorman, Keith W. 1976. The genetics and breeding of southern pines. U. S. Department of Agriculture, Agriculture Handbook 471. Washington, DC. 407 p.
  30. Dorman, Keith W., and B. J. Zobel. 1973. Genetics of loblolly pine. USDA Forest Service, Research Paper WO-19. Washington, DC. 21 p.
  31. Eyre, F. H., ed. 1980. Forest cover types of the United States and Canada. Society of American Foresters, Washington, DC. 148 p.
  32. Farrar, Robert M., Jr., Paul A. Murphy, and R. Larry Willett. 1984. Tables for estimating growth and yield of uneven-aged stands of loblolly-shortleaf pine on average sites in the West Gulf area. Arkansas Agricultural Experiment Station Bulletin 874. University of Arkansas, Fayetteville, AR. 21 p.
  33. Feduccia, D. P., T. R. Dell, W. F. Mann, Jr., T. E. Campbell, and B. H. Polmer. 1979. Yields of unthinned loblolly pine plantations on cutover sites in the West Gulf region. USDA Forest Service, Research Paper SO-148. Southern Forest Experiment Station, New Orleans, LA. 88 p.
  34. Ferguson, E. R. 1956. Causes of first-year mortality of planted loblolly pines in east Texas. In *Proceedings, Annual Meeting, Society of American Foresters, 1956*. p. 89-92.
  35. Fitzgerald, Charles H., Fred A. Peevy, and Darwin E. Fender. 1973. Rehabilitation of forest land: the Southern Region. *Journal of Forestry* 71(3):148-162.
  36. Foil, R. R., and C. W. Ralston. 1967. The establishment and growth of loblolly pine seedlings on compacted soils. *Soil Science Society of America Proceedings* 31(4):565-568.
  37. Fowells, H. A., comp. 1965. Silvics of forest trees of the United States. U.S. Department of Agriculture, Agriculture Handbook 271. Washington, DC. 762 p.
  38. Grano, Charles X. 1969. Precommercial thinning of loblolly pine. *Journal of Forestry* 67(11):825-827.
  39. Grano, C. X. 1970. Small hardwoods reduce growth of pine overstory. USDA Forest Service, Research Paper SO-55. Southern Forest Experiment Station, New Orleans, LA. 9 p.
  40. Grano, C. X. 1971. Conditioning loessial soils for natural loblolly and shortleaf pine seeding. USDA Forest Service, Research Note SO-116. Southern Forest Experiment Station, New Orleans, LA. 4 p.
  41. Greenwood, M. S. 1978. Flowering induced on young loblolly pine grafts by out-of-phase dormancy. *Science* 201(4354):443-444.
  42. Greenwood, M. S., T. M. Marino, R. D. Meier, and K. W. Shahan. 1980. The role of mist and chemical treatments in rooting loblolly and shortleaf pine cuttings. *Forest Science* 26(4):651-655.
  43. Griffing, Charles G., and William W. Elam. 1971. Height growth patterns of loblolly pine saplings. *Forest Science* 17:52-54.
  44. Hafley, W. L., W. D. Smith, and M. A. Buford. 1982. A new yield prediction model for unthinned loblolly pine plantations. Southern Forest Research Center, School of Forest Resources Technical Report No. 1. North Carolina State University, Raleigh. 65 p.
  45. Haines, L. W., T. E. Maki, S. G. Sanderford, and others. 1975. The effect of mechanical site preparation treatments on soil productivity and tree (*Pinus taeda* & *P. elliotii*) growth. In *Forest soils and forestland management, Proceedings, Fourth North American Forest Soils Conference*. p. 379-386. Laval University Press, Quebec, PQ.
  46. Halls, Lowell K., ed. 1977. Southern fruit-producing woody plants used by wildlife. USDA Forest Service, General Technical Report SO-16. Southern Forest Experiment Station, New Orleans, LA. 235 p.
  47. Halls, L. K., and J. J. Stransky. 1971. Atlas of southern forest game. USDA Forest Service, Southern Forest Experiment Station, New Orleans, LA. 24 p.
  48. Hare, R. C. 1965. Breaking and rooting of fascicle buds in southern pines. *Journal of Forestry* 63:544-546.
  49. Hare, R. C., and G. L. Switzer. 1969. Introgression with shortleaf pine may explain rust resistance in western loblolly pine. USDA Forest Service, Research Note SO-88. Southern Forest Experiment Station, New Orleans, LA. 7 p.
  50. Harlow, W. M., E. S. Harrar, and F. M. White. 1978. Textbook of Dendrology. 6th ed. McGraw-Hill, New York. 510 p.
  51. Harms, William R., and O. Gordon Langdon. 1976. Development of loblolly pine in dense stands. *Forest Science* 22(3):331-337.
  52. Hartman, Kay. 1982. National register of big trees. *American Forests* 88(4):17-31, 34-48.
  53. Hatchell, Glyndon E., Keith W. Dorman, and O. Gordon Langdon. 1972. Performance of loblolly and slash pine nursery selection. *Forest Science* 18(4):308-313.
  54. Hepting, George H. 1971. Diseases of forest and shade trees of the United States. U.S. Department of Agriculture, Agriculture Handbook 386. Washington, DC. 658 p.
  55. Hunt, C. B. 1967. Physiography of the United States. W. H. Freeman Company, San Francisco, CA. 480 p.
  56. Jones, E. P. 1974. Precommercial thinning for slash and loblolly pines. In *Proceedings, Symposium on Management of Young Pines*. p. 229-233. USDA Forest Service, Southeastern Area State and Private Forestry, Atlanta, GA.
  57. Jones, Leroy, and Sam Thacker. 1965. Survival. In *A guide to loblolly and slash pine plantation management*

- in southeastern USA. p. 68-73. Georgia Forest Research Council, Report 14. Macon.
58. Klawitter, R. A. 1966. Diameter growth of mature loblolly unaffected by understory control. *Southern Lumberman* 213(2656):154-155.
  59. Korstian, C. F., and T. S. Coile. 1938. Plant competition in forest stands. Duke University School of Forest Resources, Bulletin 3. Durham, NC. 125 p.
  60. Kraus, J. F., and T. LaFarge. 1977. The use of *Pinus echinata x taeda* hybrids for the development of *P. taeda* resistant to *Cronartium fusiforme*. In *Intraspecific hybridization in plant breeding*. p. 377-381. Proceedings of 8th EUCARPIA Congress. (Madrid, Spain)
  61. Langdon, O. Gordon. 1979. Natural regeneration of loblolly pine. In *Proceedings, National Silviculture Workshop*. p. 101-116. USDA Forest Service, Washington, DC.
  62. Langdon, O. G. 1981. Some effects of prescribed fire on understory vegetation in loblolly pine stands. In *Prescribed Fires and Wildlife in Southern Forests: Proceedings of a Symposium*; April 6-8, Myrtle Beach, SC. Gene W. Wood, ed. p. 143-154. Belle Baruch Forest Institute, Georgetown, SC.
  63. Langdon, O. G., and W. H. McKee, Jr. 1981. Can fertilization of loblolly pine on wet sites reduce the need for drainage? In *Proceedings, First Biennial Southern Silvicultural Research Conference*. p. 212-218. USDA Forest Service, General Technical Report SO-34. Southern Forest Experiment Station, New Orleans, LA.
  64. Langdon, O. G., and K. B. Trousdell. 1974. Increasing growth and yield of natural loblolly pine by young stand management. In *Proceedings, Symposium on Management of Young Pines*. p. 288-296. USDA Forest Service, Southeastern Area State and Private Forestry, Atlanta, GA.
  65. Langdon, O. G., and K. B. Trousdell. 1978. Stand manipulation: effects on soil moisture and tree growth in southern pine and pine-hardwood stands. In *Proceedings, Symposium on Soil Moisture-Site Productivity*, Myrtle Beach, SC. p. 221-236. USDA Forest Service, Southeastern Area State and Private Forestry, Atlanta, GA.
  66. Lantz, C. W. 1973. Survey of graft incompatibility in loblolly pine. In *Proceedings, Twelfth Southern Forest Tree Improvement Conference*. p. 79-85.
  67. Ledbetter, Julia R., Alfred D. Sullivan, and Thomas G. Matney. 1986. Yield tables for cutover site-prepared loblolly pine plantations in the Gulf coastal plain. Mississippi Agricultural and Forestry Experiment Station Technical Bulletin 135. Mississippi State University, Mississippi State. 31 p.
  68. Lenhart, David J. 1988. Diameter-distribution yield-prediction system for unthinned loblolly and slash pine plantations on non-old-fields in East Texas. *Southern Journal of Applied Forestry* 12(4):239-242.
  69. Little, Elbert L., Jr. 1971. Atlas of United States trees. vol. 1. Conifers and important hardwoods. U.S. Department of Agriculture, Miscellaneous Publication 1146. Washington, DC. 9 p., 313 maps.
  70. Little, S., and H. A. Somes. 1959. Viability of loblolly pine seed stored in the forest floor. *Journal of Forestry* 57(11):848-849.
  71. Matney, T. G., A. D. Sullivan, and J. R. Ledbetter. 1986. Diameter distributions and merchantable volumes for planted loblolly pine in cutover site-prepared land in the West Gulf coastal plain. Mississippi Agricultural and Forestry Experiment Station Technical Bulletin 132. Mississippi State University, Mississippi State. 12 p.
  72. McKee, W. F., Jr. 1981. Personal communication. USDA Forest Service, Southeastern Forest Experiment Station, Asheville, NC.
  73. McLemore, B. F. 1964. Light during stratification hastens dark-germination of loblolly pine seed. *Forest Science* 10(3):348-349.
  74. McLemore, B. F. 1966. Temperature effects on dormancy and germination of loblolly pine seed. *Forest Science* 12(3):284-289.
  75. McLemore, B. F. 1987. Development of intermediate and suppressed loblolly pines following release. In *Proceedings, Fourth Biennial Southern Silvicultural Research Conference*. p. 439-444. USDA Forest Service, General Technical Report SE-42. Southeastern Forest Experiment Station, Asheville, NC.
  76. Maki, T. E. 1971. Drainage: effect on productivity. In *Proceedings, Annual Meeting, Society of American Foresters, Applied Section*. p. 16-23.
  77. Mann, W. F., Jr., and T. R. Dell. 1971. Yields of 17-year-old loblolly pine planted on cutover site at various spacings. USDA Forest Service, Research Paper SO-70. Southern Forest Experiment Station, New Orleans, LA. 9 p.
  78. Mann, W. F., Jr., and R. E. Lohrey. 1974. Precommercial thinning of southern pine. *Journal of Forestry* 42(9):557-560.
  79. Mignery, A. L. 1967. Winter injury to loblolly pine in Tennessee related to seed origin. *Southern Lumberman* 215(2680):146.
  80. Miller, L., and F. W. Woods. 1965. Root-grafting in loblolly pine. *Botanical Gazette* 126:252-255.
  81. Murphy, Paul A. 1983. Merchantable and sawtimber volumes for natural even-aged stands of loblolly pine in the West Gulf region. USDA Forest Service, Research Paper SO-194. Southern Forest Experiment Station, New Orleans, LA. 38 p.
  82. Murphy, P. A., and R. M. Farrar. 1982. Interim models for basal area and volume projection of uneven-aged loblolly-shortleaf pine stands. *Southern Journal of Applied Forestry* 6(2):115-119.
  83. Quarterman, E., and C. Keever. 1962. Southern mixed hardwood forest: climax in the southeastern coastal plain United States of America. *Ecological Monographs* 32(2):167-185.
  84. Reynolds, R. R. 1959. Eighteen years of selection timber management on the Crossett Experimental Forest. U.S. Department of Agriculture, Technical Bulletin 1206. Washington, DC. 68 p.
  85. Reynolds, R. R. 1969. Twenty-nine years of selection timber management on the Crossett Experimental Forest. USDA Forest Service, Research Paper SO-40. Southern Forest Experiment Station, New Orleans, LA. 19 p.

86. Reynolds, R. R., James B. Baker, and Timothy T. Ku. 1984. Four decades of selection management on the Crossett farm forestry forties. Arkansas Agricultural Experiment Station Bulletin 872. University of Arkansas, Fayetteville, AR. 43 p.
87. Saylor, L. C., and K. W. Kang. 1973. A study of sympatric populations of *Pinus taeda* L. and *Pinus serotina* Michx. in North Carolina. Journal of the Elisha Mitchell Scientific Society 89:101-110.
88. Schopmeyer, C. S., tech. coord. 1974. Seeds of woody plants in the United States. U.S. Department of Agriculture, Agriculture Handbook 450. Washington, DC. 883 p.
89. Schultz, Robert P., and Frank W. Woods. 1967. The frequency and implications of intraspecific root-grafting in loblolly pine. Forest Science 13:226-239.
90. Schumacher, F. X., and T. S. Coile. 1960. Growth and yield of natural stands of the southern pines. T. S. Coile, Inc. Durham, NC. 115 p.
91. Shepard, R. K., Jr. 1974. Ice storm damage to thinned loblolly pine plantations in northern Louisiana. Southern Journal of Applied Forestry 2(3):83-85.
92. Smalley, G. W. 1979. Classification and evaluation of forest sites on the southern Cumberland Plateau. USDA Forest Service, General Technical Report SO-23. Southern Forest Experiment Station, New Orleans, LA. 59 p.
93. Smalley, G. W., and R. L. Bailey. 1974. Yield tables and stand structure for loblolly pine plantations in Tennessee, Alabama, and Georgia highlands. USDA Forest Service, Research Paper SO-96. Southern Forest Experiment Station, New Orleans, LA. 81 p.
94. Smeltzer, R. H., R. L. Mott, and A. Mehra-Polta. 1977. Influence of parental tree genotype in the potential for in vitro cloning progenation from loblolly pine embryos. In Forest biology wood chemical conference, 1977. p. 5-8. Tappi Press, Atlanta, GA.
95. Stewart, J. T. 1965. Regenerating loblolly pine with four seed trees. Virginia Forests 20(2):14-15, 26, 28.
96. Stoddard, H. L. 1963. Maintenance and increase of the eastern wild turkey on private lands of the Coastal Plain of the Deep Southeast. Tall Timbers Research Station, Bulletin 3. Tallahassee, FL. 49 p.
97. Stransky, J. J., and L. K. Halls. 1967. Timber and game food relations in pine-hardwood forests of the southern United States. In Proceedings, Fourteenth International Union of Forestry Research Organizations Congress. p. 208-217.
98. Stransky, J. J., and D. R. Wilson. 1964. Terminal elongation of loblolly and shortleaf pine seedlings under soil moisture stress. Soil Science Society of America Proceedings 28:439-440.
99. Sullivan, Alfred D., and Jerome L. Clutter. 1972. A simultaneous growth and yield model for loblolly pine. Forest Science 18(1):76-86.
100. Switzer, G. L., M. G. Shelton, and L. E. Nelson. 1979. Successional development of the forest floor and soil surface on upland sites of the East Gulf Coastal Plain. Ecology 60(6):1162- 1171.
101. Terry, T. A., and J. H. Hughes. 1975. The effects of intensive management on planted loblolly pine (*Pinus taeda* L.) growth on poorly drained soils of the Atlantic Coastal Plain. In Forest soils and forest land management. Proceedings, Fourth North American Forest Soils Conference. p. 351-377. Laval University Press, Quebec, PQ.
102. Thatcher, R. C., J. L. Searcy, J. E. Coster, and others, eds. 1980. The southern pine beetle. U.S. Department of Agriculture, Technical Bulletin 1631. Washington, DC. 267 p.
103. Trousdell, K. B. 1970. Disking and prescribed burning: sixth year residual effects on loblolly pine and competing vegetation. USDA Forest Service, Research Note SE-133. Southeastern Forest Experiment Station, Asheville, NC. 6 p.
104. Trousdell, Kenneth B., and O. Gordon Langdon. 1967. Disking and prescribed burning for loblolly pine regeneration. Journal of Forestry 65(5):548-551.
105. Trousdell, Kenneth B., Wilfred C. Williams, and Thomas C. Nelson. 1965. Damage to recently thinned loblolly pine stands by Hurricane Donna. Journal of Forestry 63(2):96-100.
106. U.S. Department of Agriculture, Forest Service. 1929. Volume, yield, and stand tables for second-growth southern stands. U.S. Department of Agriculture, Miscellaneous Publication 50. Washington, DC. 202 p.
107. U.S. Department of Agriculture, Soil Conservation Service. 1975. Soil taxonomy: a basic system of soil classification for making and interpreting soil surveys. Soil Survey Staff, coords. U.S. Department of Agriculture, Agriculture Handbook 436. Washington, DC. 754 p.
108. Wahlenberg, W. G. 1960. Loblolly pine: its use, ecology, regeneration, protection, growth, and management. Duke University, School of Forestry, Durham, NC. 603 p.
109. Wakeley, Philip C., and T. E. Bercaw. 1965. Loblolly pine provenance test at age 35. Journal of Forestry 63:168-174.
110. Wells, D. W., and M. Reines. 1965. Vegetative propagation of needle bundles of pines. Georgia Forest Research Council, Report 26. Macon. 8 p.
111. Wells, O. O. 1969. Results of the southwide pine seed source study through 1968-69. In Proceedings, Tenth Southern Forest Tree Improvement Conference. p. 117-129.
112. Wells, O. O., and P. C. Wakeley. 1966. Geographic variation in survival, growth, and fusiform-rust infection of planted loblolly pine. U.S. Department of Agriculture, Monograph 11. Washington, DC. 40 p.
113. Williston, H. L. 1962. Loblolly seedlings survive twelve days' submergence. Journal of Forestry 60:412.
114. Williston, H. L. 1971. Guidelines for planting and maintaining loblolly pine and other cover for road bank stabilization. Tree Planters Notes 22(2):14-17.
115. Williston, H. L., and S. J. Ursic. 1979. Planting loblolly pine for erosion control: a review. Tree Planters' Notes 30(2):15-18.
116. Zahner, R. 1968. Water deficits and the growth of trees. In Water deficits and plant growth, vol. 2. Plant water

- consumption and response. p. 191-254. Academic Press, New York.
117. Zobel, Bruce J., Roger Blair, and Marvin Zoerb. 1971. Using research data: disease resistance. *Journal of Forestry* 69:486-489.

APPROVED for Release for  
Unlimited (Release to Public)  
6/6/2005

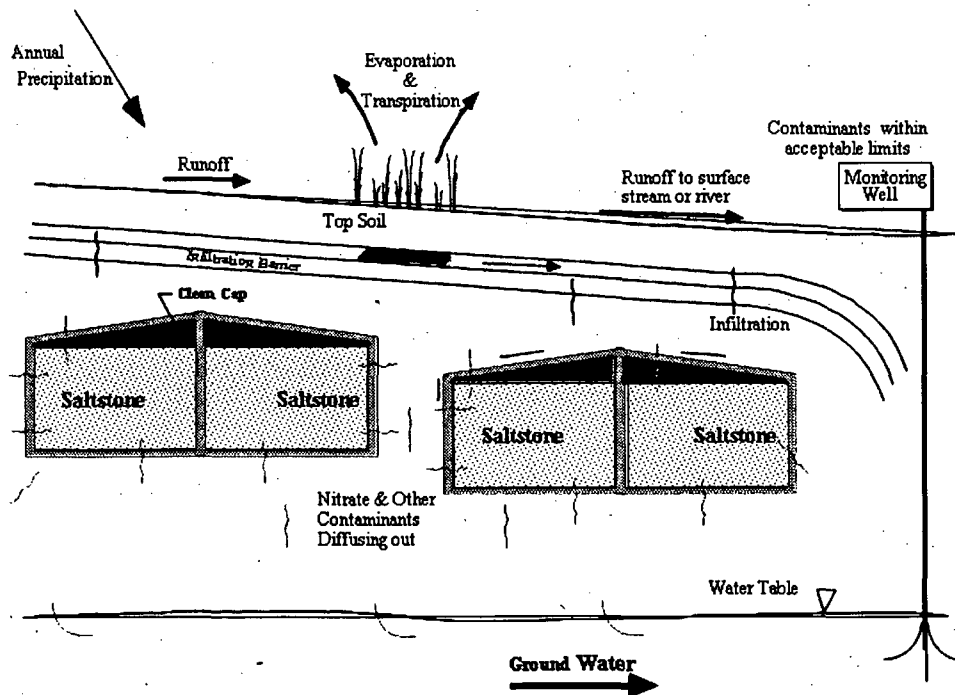
WSRC-TR-2005-00074  
Revision 0

KEY WORDS: Performance Assessment  
Low-level Radioactive Waste Disposal

**SPECIAL ANALYSIS:  
REVISION OF SALTSTONE VAULT 4 DISPOSAL LIMITS (U)**

PREPARED BY:  
James R. Cook  
Elmer L. Wilhite  
Robert A. Hiergesell  
Gregory P. Flach

MAY 26, 2005



Westinghouse Savannah River Company  
Savannah River Site  
Aiken, SC 29808

Prepared for the U.S. Department of Energy Under  
Contract Number DE-AC09-96SR18500



The currently active vault (Vault #4) has the dimensions of approximately 200 feet wide, by 600 feet in length, by 26 feet in height. The vault is divided into 12 cells, with each cell measuring approximately 100 ft. x 100 ft. The vault is covered with a sloped, permanent roof that has a minimum thickness of 4 inches, and a minimum slope of 0.24 inches/foot. The vault walls are approximately 1.5 feet thick, with the base mat having a thickness of 2 feet. Operationally, the cell of the vault will be filled to a height of approximately 25 feet with Saltstone, and then a layer of uncontaminated grout, with an average thickness of 2 feet, will be poured to fill in the space between the Saltstone and the sloped roof. Figure 1-1 is an aerial view of Vaults 1 and 4.

## **1.2 SDF Closure Concept**

One of the key performance objectives of any closure of a waste disposal site is to limit moisture flux through the waste minimizing contamination of surface runoff and underlying groundwater. Because the SDF is designed as a controlled release facility, proper closure to meet the objective of limiting moisture through the waste will be an integral part of long-term acceptability of the disposal site. Because backfilling around the vaults and final closure of the SDF will be delayed for several years, a detailed closure design has not been fully developed for the SDF. Thus, an integral part of the SDF SA required that a closure concept be described and subsequently tested in models that simulate the performance characteristics of the proposed closure concept.

### **1.2.1 Physical Description of the SDF Closure Concept**

The closure concept developed is illustrated in Figure 1-2. After an individual vault cell is filled with Saltstone, interim closure will be performed which consists of the placement of a 16-inch (0.41 m) clean grout layer between the Saltstone and the overlying concrete roof. Final closure will occur when all Saltstone vaults are filled, and will consist of the placement of a closure cap over all of the vaults. This will be followed by a 100-year period of institutional control, as described in Phifer and Nelson, 2003.

Final closure of the SDF will be accomplished by constructing a drainage system and revegetating the site. The drainage system will consist of a system of rip-rap lined ditches that intercept the gravel layer of the moisture barrier. These ditches will divert surface runoff and water intercepted by the moisture barrier away from the disposal site. The drainage ditches will be constructed between rows of vaults and around the perimeter of the SDF.

The topsoil will be revegetated with bamboo. A study conducted by the USDA Soil Conservation Service (Cook and Salvo 1992) has shown that two species of bamboo (*Phyllostachys bissetii* and *Phyllostachys rubromarginata*) will quickly establish a dense ground cover which will prevent the growth of pine trees, the most deeply rooted naturally occurring plant type at SRS. Bamboo is the shallow-rooted climax species which evapotranspires year-around in the SRS climate removing a large amount of moisture from the soil and decreasing the infiltration into the underlying disposal system.

## **1.3 EXISTING VAULT 4 WASTE INVENTORY**

The current radionuclide inventory in Vault 4 is given in Table 1-1.



**Figure 1-1. Aerial View of Vaults 1 (Rear) and 4 (Foreground)**

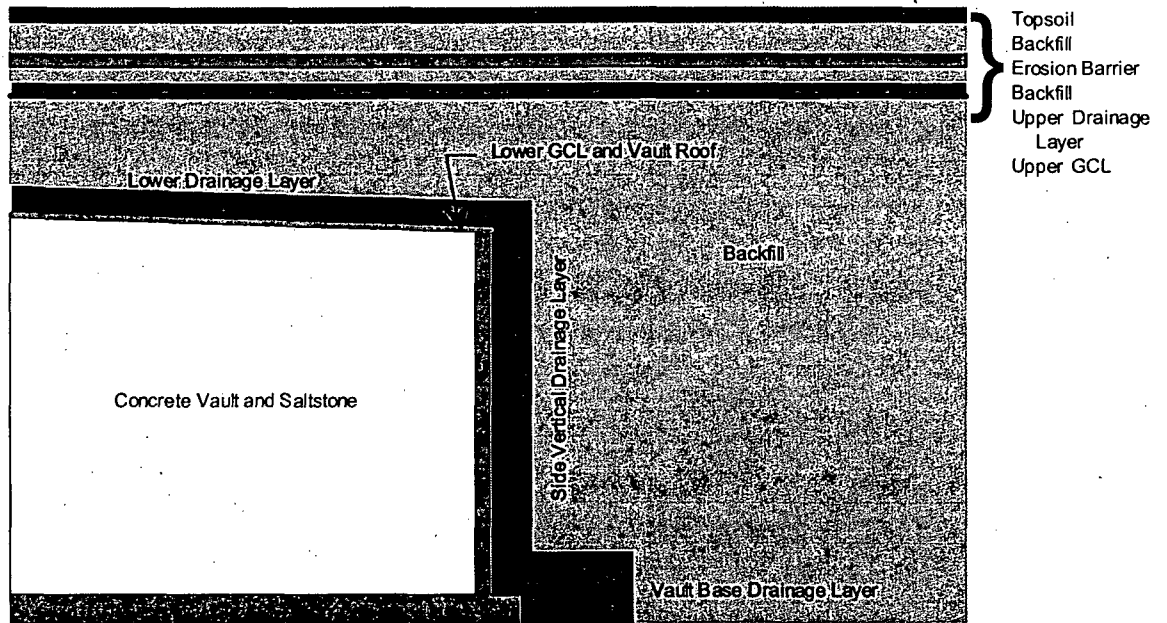


Figure 1-2. SDF Closure Cap Configuration

## A.2 SALTSTONE VAULT NUMBER 4 UNSATURATED ZONE GROUNDWATER MODELING

### A.2.1 Conceptual Model and Modeling Grid

The conceptual model describes the materials, layout, and dimensions of the SDF. Figure A-1 depicts the conceptual model used for the Vault No. 4. The Saltstone monolith is approximately  $200 \times 600 \times 25$  ft<sup>3</sup>. Only half of a vault in the short dimension is modeled, taking advantage of symmetry. The top of the modeling domain is the bottom of the upper geosynthetic clay liner (GCL) layer. Infiltration through this layer as a function of time is calculated by the HELP code (USEPA 1994a, 1994b). The constant infiltration rate is used as a flow boundary condition at the top of the modeling domain. The bottom of the modeling domain is the water table. Capillary pressure at the water table is set to zero to simulate 100% water saturation. The vertical boundary through the center of the vault at the left side of the figure is modeled as a no-flow boundary due to symmetry. The right boundary is also assumed to be a no-flow boundary because it is sufficiently far away from the vault and the predominant contaminant transport mechanism is downward convection.

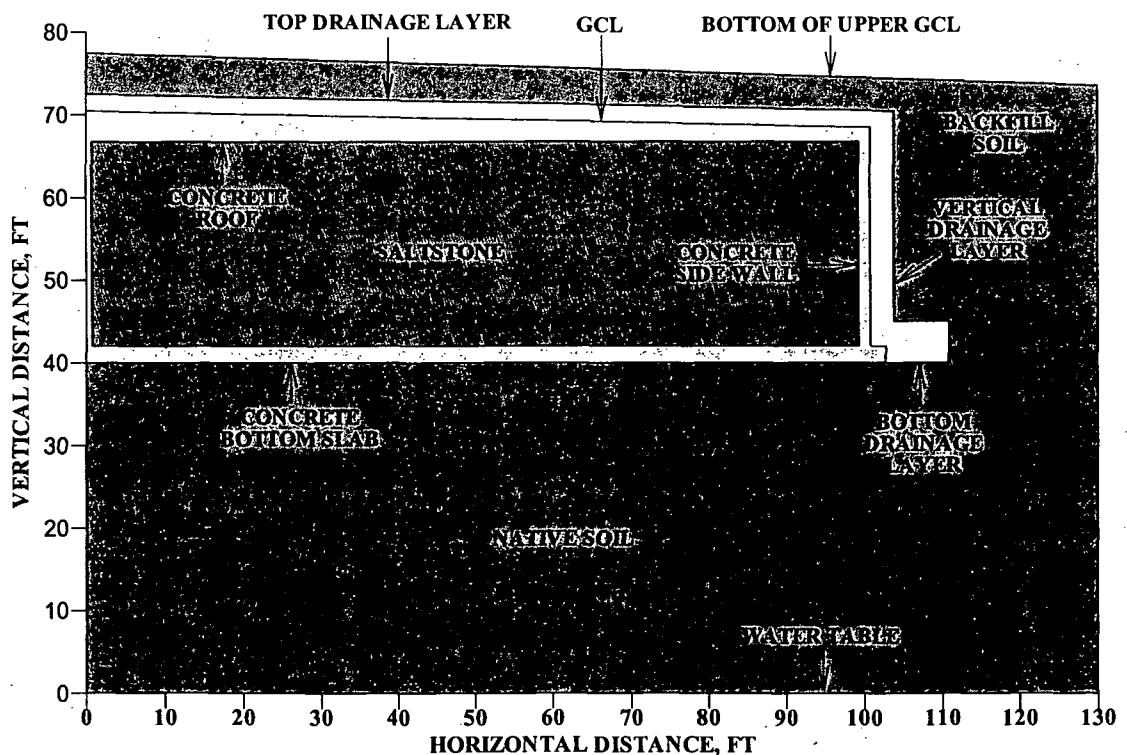


Figure A-1. Conceptual Model for the Saltstone Vault No. 4

The dimensions of the vault and lower portion of the closure are summarized in Table A-2. The “concrete” zone above the Saltstone pour level (at 66.75 ft) includes the top portion of the center and exterior walls and the concrete roof. The drainage layer is a gravel/sand mixture. It is used to reduce water perching above the vault. Test modeling results indicate that perching water can increase water flow rate through the vault, which results in a higher contaminant leaching rate.

The drainage layer is divided into three sections: top, vertical and bottom. The initial hydraulic conductivities in these sections are the same. However, these conductivities degrade at different rates (Phifer 2004) as will be described later. Because the backfill is largely soil excavated during vault construction, it is assumed that the backfill soil has the same properties as the native soil. There is a GCL above the vault roof. Since the conductivity of the Saltstone and the vault is less than or equal to the conductivity of the GCL ( $10^{-9}$  cm/sec), this GCL is ignored in the simulation.

**Table A-2. Dimensions of Saltstone Vault No. 4**

Component	Dimensions of Vertical Distances		
	From (ft)	To (ft)	Thickness (ft)
Native Soil	0.00	40.00	40.00
Bottom Concrete Slab	40.00	42.00	2.00
Saltstone	42.00	66.75	24.75
Concrete at Center <sup>1</sup>	66.75	70.50	3.75
Drainage Layer <sup>2</sup>	70.50	72.50	2.00
Drainage Layer at the Vault Base	40.00	45.00	5.00
Backfill above Drainage Layer <sup>3</sup>	72.50	77.50	5.00
	Dimensions of Horizontal Distances		
Center Slab <sup>4</sup>	0.00	0.75	0.75
Saltstone	0.75	99.25	98.50
Side Slab	99.25	100.75	1.50
Drainage Layer	100.75	103.75	3.00
Drainage Layer at the Vault Base	100.75	110.75	10.00

<sup>1</sup> Concrete includes tip of vault wall, concrete pour and concrete roof.

<sup>2</sup> Slope = 2.0%

<sup>3</sup> Slope = 3.0% at the upper boundary

<sup>4</sup> Actual center slab thickness = 1.50 ft.

The potential impact of cracks on the performance of Vault 4 is discussed in Section A.4. Over 10,000 years, the suction head is great enough that flow through cracks, whether through-wall or not, can be neglected.

The modeling grid used for PORFLOW simulation is shown in Figure A-2. Trapezoidal grid blocks are used for the concrete roof and the backfill to mimic the facility geometry.

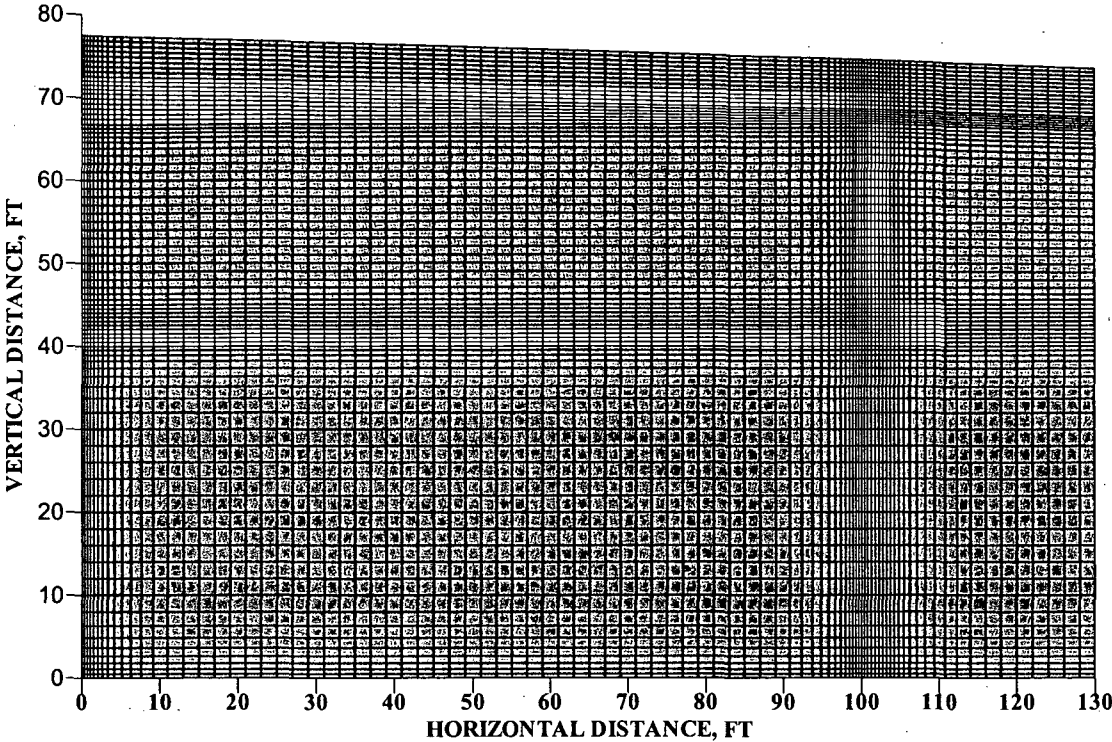


Figure A-2. Modeling Grid



vertical hydraulic conductivities decrease more rapidly than the horizontal conductivities. All of the saturated hydraulic conductivities used for the simulation are summarized in Table A-4. The data, equations, and rationale used to obtain these data are discussed below.

#### NATIVE AND BACKFILL SOIL

The saturated hydraulic conductivity of native and backfill soil is revised from  $10^{-5}$  to  $10^{-4}$  cm/sec to be consistent with the generally accepted value for the SRS General Separations Area. Since soil is a geological material, its conductivity is assumed to be constant.

#### SALTSTONE AND CONCRETE

In the time interval of 0 and 100 years, the hydraulic conductivities of Saltstone and concrete are  $10^{-11}$  and  $10^{-12}$  cm/sec, respectively. Both conductivities degrade to  $10^{-9}$  cm/sec at 10,000 years. The degradation rate for concrete is faster because it is exposed to the environment and is more vulnerable to be attacked by sulfate, chloride and other chemical reactions. The decay rate is calculated by a log-log correlation:

$$\log_{10}(k/k_o) = \alpha \log_{10}(t/t_o) \quad (\text{A-1})$$

where  $k$  = conductivity at time  $t$ , cm/sec

$k_o$  = conductivity at  $t_o = 100$  years, cm/sec

$\alpha$  = degradation rate constant ( $\alpha = 1.0$  for Saltstone and 1.5 for concrete)

Calculated  $k$  values at the end of each time interval are used as PORFLOW input data to generate the steady-state flow field for the time interval. They are summarized in Table A-4.

#### GRAVEL DRAIN LAYERS

The initial hydraulic conductivity of the gravel drain layers is  $10^{-1}$  cm/sec. As time goes on, soil particles carried by the percolation water will plug the drains from the bottom. The plugged-zone thickness will increase with increasing time. Calculated thickness (Phifer 2004) is shown in Table A-5.

**Table A-5. Plugged-Zone Thickness as a Function of Time**

<u>TIME (YEARS)</u>	<u>PLUGGED-ZONE THICKNESS, FT</u>
0	0
100	0.0005
300	0.005
550	0.022
1,000	0.08
1,800	0.21
3,400	0.49
5,600	0.88
10,000	1.66

Plugging results in reduction in effective hydraulic conductivity. Freeze and Cherry (Freeze 1979) suggested equations to calculate horizontal and vertical effective conductivities:

$$k_{h,eff} = [(H-h)k_g + hk_s] / H \quad (\text{A-2})$$

$$k_{v,eff} = H / [(H-h)/k_g + h/k_s] \quad (\text{A-3})$$

where  $H$  = total thickness (2 ft for top drainage layer and 5 ft for bottom drainage layer)

$h$  = plugged-zone thickness, ft .

$k_g$  =conductivity of gravel ( $10^{-1}$  cm/sec)

$k_s$  =conductivity of soil ( $10^{-4}$  cm/sec)

Calculated horizontal and vertical effective hydraulic conductivities for the top and the bottom drainage layers are summarized in Table A-4. The plugged zone thickness used for the calculation is the average for the time interval. For the vertical drainage layer, conductivity remains constant at  $10^{-1}$  cm/sec.

These assumptions on the changes in hydraulic properties over time are based on professional judgment, since actual data over the time periods of interest do not exist. They were discussed during meetings of the performance assessment team and the team agreed to use these values in this analysis.

Because the SDF is constructed in the unsaturated zone, water saturation in the modeling domain is expected to be below 100%. Fluid flow is affected by the capillary pressure (or suction pressure) and relative permeability (or conductivity). Capillary pressure decreases with increasing water saturation, whereas relative permeability increases with increasing water saturation. Saturation dependence of these two parameters is often depicted as characteristic curves. The characteristic curves for Saltstone are illustrated in Figure A-3. Figures A-4 through A-6 show the same curves for the other porous media. In the unsaturated-zone flow model, the capillary pressure and relative permeability are entered as table input.

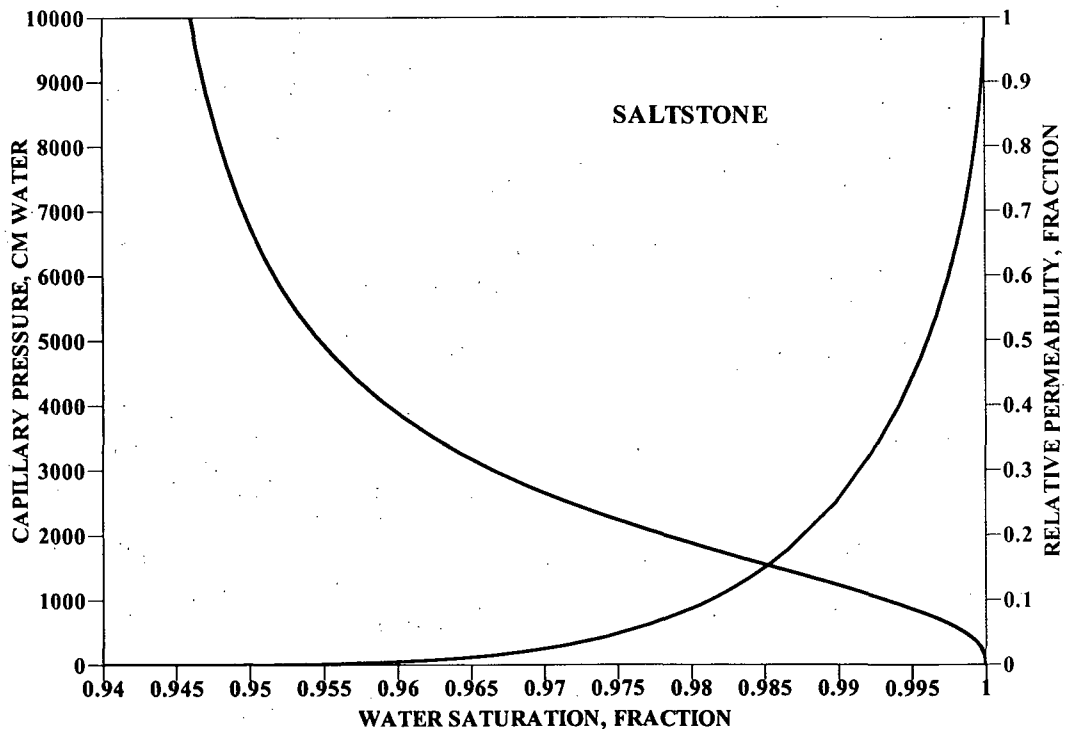


Figure A-3. Characteristic Curves for Saltstone

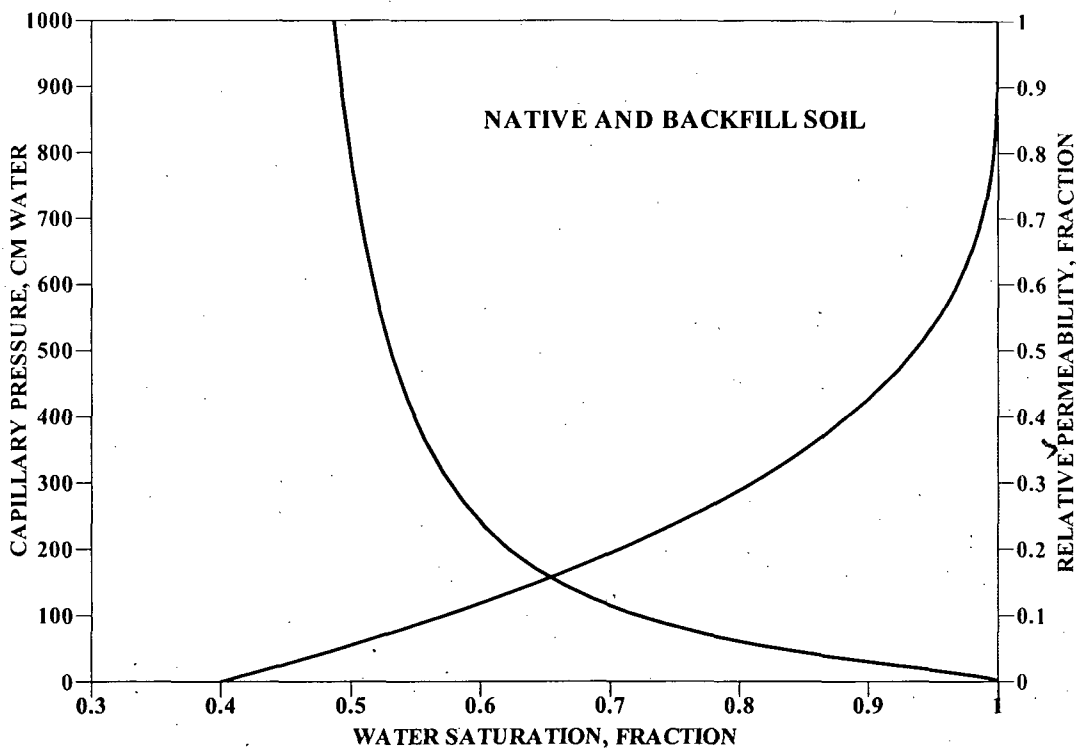


Figure A-4. Characteristic Curves for Native and Backfill Soil

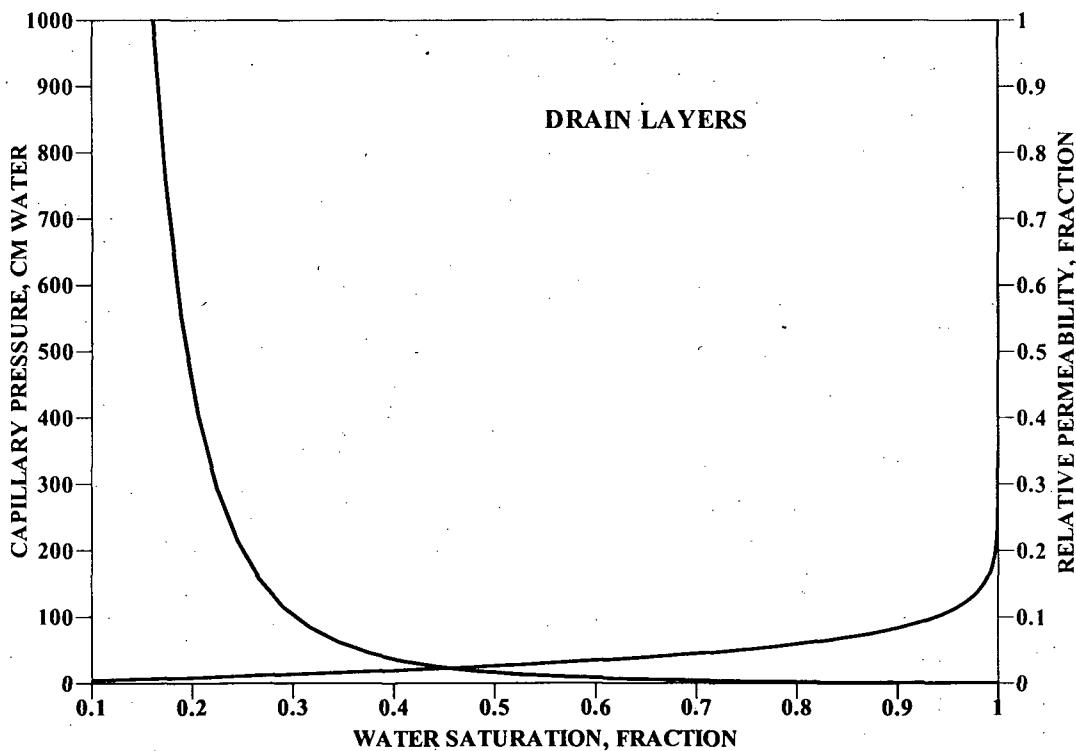


Figure A-5. Characteristic Curves for Drain Layers

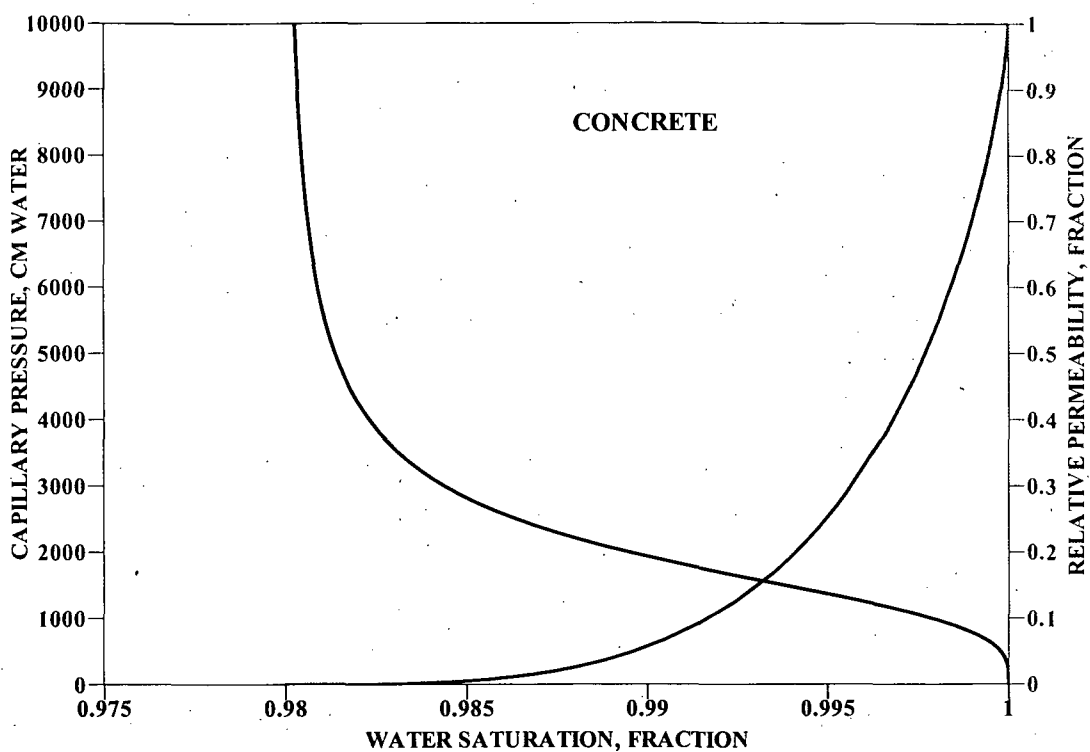


Figure A-6. Characteristic Curves for Concrete

**A.2.3.2 Infiltration Rates**

The infiltration rates (in inches/year) through the lower GCL (Phifer 2004) used for this study are summarized in Table A-6 and shown in Figure A-7.

**Table A-6. Infiltration Rates Used as Upper Boundary Conditions**

Time Interval	Infiltration Rate (in/yr)
0 to 100	0.39
100 to 300	1.73
300 to 550	5.48
550 to 1,000	9.97
1,000 to 1,800	12.90
1,800 to 3,400	13.90
3,400 to 5,600	14.06
5,600 to 10,000	14.09

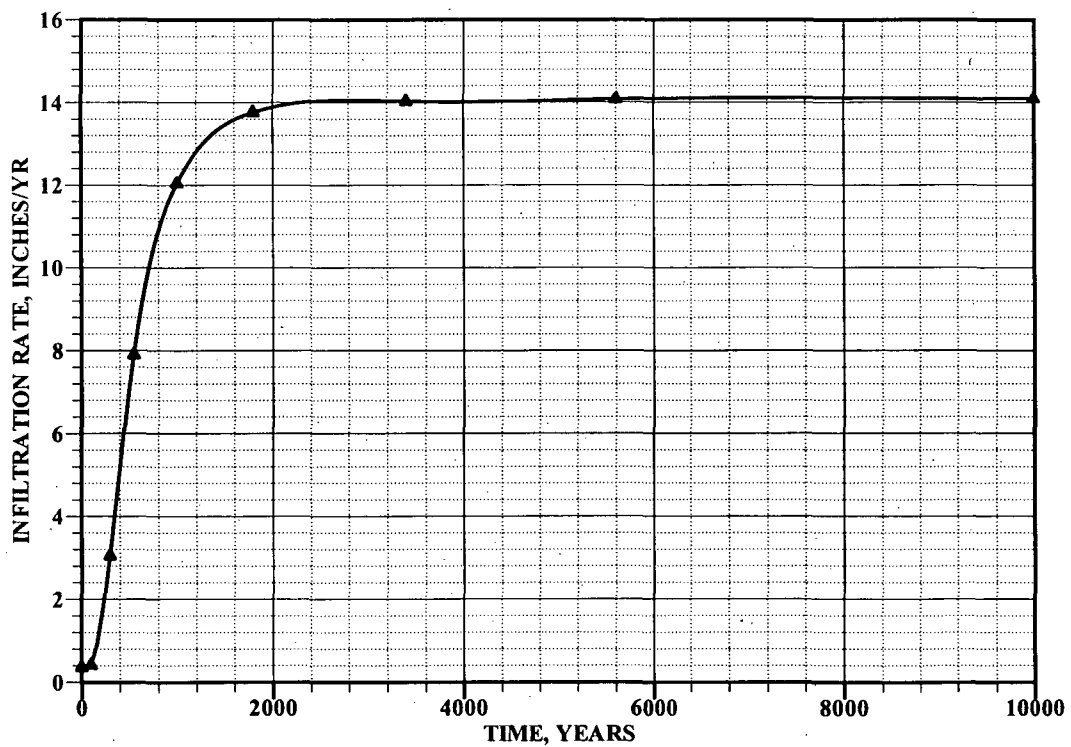


**Figure A-7. Infiltration Rate Through the Lower GCL**

# *Introduction to Soil Physics*

*DANIEL HILLEL*

*Department of Plant and Soil Sciences  
University of Massachusetts  
Amherst, Massachusetts*



ACADEMIC PRESS 1982

*A Subsidiary of Harcourt Brace Jovanovich, Publishers*

New York London

Paris San Diego San Francisco São Paulo Sydney Tokyo Toronto

S  
592.3  
455

357-55282  
CORE.64982

*This book is o:  
where students  
as they prepar:  
to explore the*

COPYRIGHT © 1980, 1982, BY ACADEMIC PRESS, INC.  
ALL RIGHTS RESERVED.  
NO PART OF THIS PUBLICATION MAY BE REPRODUCED OR  
TRANSMITTED IN ANY FORM OR BY ANY MEANS, ELECTRONIC  
OR MECHANICAL, INCLUDING PHOTOCOPY, RECORDING, OR ANY  
INFORMATION STORAGE AND RETRIEVAL SYSTEM, WITHOUT  
PERMISSION IN WRITING FROM THE PUBLISHER.

ACADEMIC PRESS, INC.  
111 Fifth Avenue, New York, New York 10003

United Kingdom Edition published by  
ACADEMIC PRESS, INC. (LONDON) LTD.  
24/28 Oval Road, London NW1 7DX

Library of Congress Cataloging in Publication Data

AVC → Hillel, Daniel.  
TI → Introduction to soil physics.  
Notes → Based on the author's Applications of soil  
physics and Fundamentals of soil physics.  
Bibliography: p.  
Includes index.  
SJK → 1. Soil physics. I. Title  
Call → S592.3.H55 631.4'3 81-10848  
ISBN 0-12-348520-7 AACR2

PRINTED IN THE UNITED STATES OF AMERICA

82 83 84 85 9 8 7 6 5 4 3 2 1

912082-45850

aggregates. The organization of the solid components of the soil determines the geometric characteristics of the pore spaces in which water and air are transmitted and retained. Finally, soil water and air vary in composition, both in time and in space.

The relative proportions of the three phases in the soil vary continuously, and depend upon such variables as weather, vegetation, and management. To give the reader some general idea of these proportions, we offer the rather simplistic scheme of Fig. 2.1, which represents the volume composition of a medium-textured soil at a condition considered to be approximately optimal for plant growth.

#### D. Volume and Mass Relationships of Soil Constituents

Let us now consider the volume and mass relationships among the three phases, and define some basic parameters which have been found useful in characterizing the physical condition of a soil.

Figure 2.2 is a schematic representation of a hypothetical soil showing the volumes and masses of the three phases in a representative sample. The masses of the phases are indicated on the right-hand side: the mass of air  $M_a$ , which is negligible compared to the masses of solids and water; the mass of water  $M_w$ ; the mass of solids  $M_s$ ; and the total mass  $M_t$ . These masses can also be represented by their weights (the product of the mass and the gravitational acceleration). The volumes of the same components are

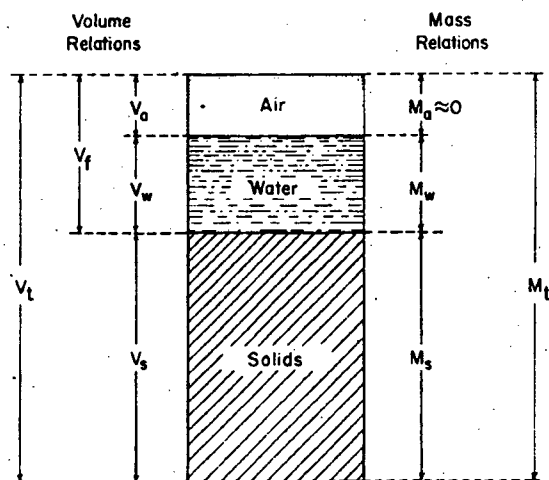


Fig. 2.2. Schematic diagram of the soil as a three-phase system.

#### 2. GENERAL PHYSICAL

indicated on the left-water  $V_w$ , volume of total volume of the r

On the basis of this used to express the constituents.

#### 1. DENSITY OF SOLID

In most mineral soil  $\text{gm/cm}^3$ , and is thus (sandy soils. Aluminum presence of iron oxide value of  $\rho_s$ , whereas the density is expressed density of the material. In the metric system assigned the value of dimensionally) equal

#### 2. DRY BULK DENS

The dry bulk density volume (solids and p and if the pores contain  $\text{gm/cm}^3$ . In sandy soil and in clay soils, it is by the structure of the as by its swelling and water bulk density remain the particles can never body, never complete.

#### 3. POROSITY $f$

The porosity is an generally lies in the less porous than fine pores is greater in the

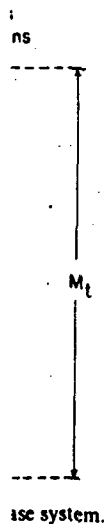
of the soil determines which water and air are vary in composition,

oil vary continuously, on, and management. portions, we offer the e volume composition to be approximately

its

hips among the three been found useful in

tical soil showing the entative sample. The side: the mass of air olids and water; the otal mass  $M_t$ . These product of the mass same components are



indicated on the left-hand side of the diagram: volume of air  $V_a$ , volume of water  $V_w$ , volume of pores  $V_f = V_a + V_w$ , volume of solids  $V_s$ , and the total volume of the representative soil body  $V_t$ .

On the basis of this diagram, we can now define terms which are generally used to express the quantitative interrelations of the three primary soil constituents.

1. DENSITY OF SOLIDS (MEAN PARTICLE DENSITY)  $\rho_s$

$$\rho_s = M_s / V_s \tag{2.1}$$

In most mineral soils, the mean density of the particles is about 2.6–2.7 gm/cm<sup>3</sup>, and is thus close to the density of quartz, which is often prevalent in sandy soils. Aluminosilicate clay minerals have a similar density. The presence of iron oxides, and of various heavy minerals, increases the average value of  $\rho_s$ , whereas the presence of organic matter lowers it. Sometimes the density is expressed in terms of the *specific gravity*, being the ratio of the density of the material to that of water at 4°C and at atmospheric pressure. In the metric system, since the density of water at standard temperature is assigned the value of unity, the specific gravity is numerically (though not dimensionally) equal to the density.

2. DRY BULK DENSITY  $\rho_b$

$$\rho_b = M_s / V_t = M_s / (V_s + V_a + V_w) \tag{2.2}$$

The dry bulk density expresses the ratio of the mass of dried soil to its total volume (solids and pores together). Obviously,  $\rho_b$  is always smaller than  $\rho_s$ , and if the pores constitute half the volume,  $\rho_b$  is half of  $\rho_s$ , namely 1.3–1.35 gm/cm<sup>3</sup>. In sandy soils,  $\rho_b$  can be as high as 1.6, whereas in aggregated loams and in clay soils, it can be as low as 1.1 gm/cm<sup>3</sup>. The bulk density is affected by the structure of the soil, i.e., its looseness or degree of compaction, as well as by its swelling and shrinkage characteristics, which are dependent upon clay content and wetness. Even in extremely compacted soil, however, the bulk density remains appreciably lower than the particle density, since the particles can never interlock perfectly and the soil remains a porous body, never completely impervious.

3. POROSITY  $f$

$$f = V_f / V_t = (V_a + V_w) / (V_s + V_a + V_w) \tag{2.3}$$

The porosity is an index of the relative pore volume in the soil. Its value generally lies in the range 0.3–0.6 (30–60%). Coarse-textured soils tend to be less porous than fine-textured soils, though the mean size of individual pores is greater in the former than in the latter. In clayey soils, the porosity is

highly variable as the soil alternately swells, shrinks, aggregates, disperses, compacts, and cracks. As generally defined, the term porosity refers to the volume fraction of pores, but this value should be equal, on the average, to the areal porosity (the fraction of pores in a representative cross-sectional area) as well as to the average lineal porosity (being the fractional length of pores along a straight line passing through the soil in any direction). The total porosity, in any case, reveals nothing about the *pore size distribution*, which is itself an important property to be discussed in a later section.

#### 4. VOID RATIO $e$

$$e = (V_a + V_w)/V_s = V_t/(V_t - V_s) \quad (2.4)$$

The void ratio is also an index of the fractional volume of soil pores, but it relates that volume to the volume of solids rather than to the total volume of soil. The advantage of this index over the previous one ( $f$ ) is that a change in pore volume changes the numerator alone, whereas a change of pore volume in terms of the porosity will change both the numerator and denominator of the defining equation. Void ratio is the generally preferred index in soil engineering and mechanics, whereas porosity is the more frequently used index in agricultural soil physics. Generally,  $e$  varies between 0.3 and 2.0.

#### 5. SOIL WETNESS

The wetness, or relative water content, of the soil can be expressed in various ways: relative to the mass of solids, relative to the total mass, relative to the volume of solids, relative to the total volume, and relative to the volume of pores. The various indexes are defined as follows (the most commonly used are the first two).

##### a. Mass Wetness $w$

$$w = M_w/M_s \quad (2.5)$$

This is the mass of water relative to the mass of dry soil particles, often referred to as the *gravimetric water content*. The term *dry soil* is generally defined as a soil dried to equilibrium in an oven at 105°C, though clay will often retain appreciable quantities of water at that state of dryness. Mass wetness is sometimes expressed as a decimal fraction but more often as a percentage. Soil dried in "ordinary" air will generally contain several per cent more water than oven-dry soil, a phenomenon due to vapor adsorption and often referred to as soil *hygroscopicity*. In a mineral soil that is saturated,  $w$  can range between 25 and 60% depending on the bulk density. The saturation water content is generally higher in clayey than in sandy soils. In the case of organic soils, such as peat or muck, the saturation water content on the mass basis may exceed 100%.

#### 2. GENERAL PHYSICAL

##### b. Volume Wetness $\theta$

The volume wetness ( $\theta$ ) is the fraction of soil water (volume of soil water) to the total volume of the soil rather than to the volume of solids. In sandy soils, the value of  $\theta$  may approach 60%. In the case of medium-textured soils,  $\theta$  may exceed the porosity of the soil. The use of  $\theta$  rather than of  $f$  is more direct because it is more directly related to the quantities added to soil from the soil by evaporation. The depth ratio of soil water is

##### c. Degree of Saturation

This index expresses the ratio of the volume of soil water to the volume of pores. The index is used in a completely saturated soil, since some air is present in a very wet soil.

#### 6. AIR-FILLED POROSITY

 $f_a$ 

This is a measure of the air-filled porosity, an important criterion of the degree of saturation  $s$  (

#### 7. ADDITIONAL INTERRELATIONS

From the basic definitions, various parameters to be used in useful interrelations.

##### (1) Relation between



- (2) Relation between volume wetness and degree of saturation:

$$\theta = sf \quad (2.11)$$

$$s = \theta/f \quad (2.12)$$

- (3) Relation between porosity and bulk density:

$$f = (\rho_s - \rho_b)/\rho_s = 1 - \rho_b/\rho_s \quad (2.13)$$

$$\rho_b = (1 - f)\rho_s \quad (2.14)$$

- (4) Relation between mass wetness and volume wetness:

$$\theta = w\rho_b/\rho_w \quad (2.15)$$

$$w = \theta\rho_w/\rho_b \quad (2.16)$$

Here  $\rho_w$  is the density of water ( $M_w/V_w$ ), approximately equal to 1 gm/cm<sup>3</sup>. Since the bulk density  $\rho_b$  is generally greater than water density  $\rho_w$ , it follows that volume wetness exceeds mass wetness (the more so in compact soils of higher bulk density).

- (5) Relation between volume wetness, fractional air content, and degree of saturation:

$$f_a = f - \theta = f(1 - s) \quad (2.17)$$

$$\theta = f - f_a \quad (2.18)$$

A number of these relationships are derived or proven at the end of this chapter, and the derivation or proof of the others is left as a useful exercise for students. Of the various parameters defined, the most commonly used in characterizing soil physical properties are the porosity  $f$ , bulk density  $\rho_b$ , volume wetness  $\theta$ , and mass wetness  $w$ .

### E. The Soil Profile

Having defined the soil's components and their proportions, let us now consider a composite soil body as it appears in nature. The most obvious, and very important, part of the soil is its surface zone. An examination of that zone will reveal much about processes taking place through the surface, but will not necessarily reveal the character of the soil as a whole. To get at the latter, we must examine the soil in depth, and we can do this, for instance, by digging a trench and sectioning the soil from the surface downward. The vertical cross section of the soil is called the *soil profile*.

The soil profile is seldom uniform in depth, and typically consists of a succession of more-or-less distinct layers, or strata. Such layers may result from the pattern of deposition, or sedimentation, as can be observed in wind-deposited (aeolian) soils and particularly in water-deposited (alluvial)

soils. If, however, the (genic) processes, they zone of major biological organic matter and comes the *B horizon*, a zone (such as clay or lies the *C horizon*, which soil formed in place from fragmented rock alluvial, aeolian, or g

The A, B, C sequence for example in a typical developed B horizon by an A, C profile. In hardly any profile depends primarily on the vegetation, the to

The typical development summarized as follows or "weathering" of the parent material. Gradation brings about the development of a granular structure and cementation. (This process of weathering (e.g., by reprecipitation may formed tends to migrate soluble salts) down to a intermediate zone (named parent material of the soil) and profile development (washing out of substances emigrate the underlying alluvium) in composition and whole deepens as the until eventually a quiet processes of soil formation. In arid regions, salts dissolved from the upper form a cemented "p depending on local instance, varies from

# Modeling in-situ pine root decomposition using data from a 60-year chronosequence

Kim H. Ludovici, Stanley J. Zarnoch, and Daniel D. Richter

**Abstract:** Because the root system of a mature pine tree typically accounts for 20–30% of the total tree biomass, decomposition of large lateral roots and taproots following forest harvest and re-establishment potentially impact nutrient supply and carbon sequestration in pine systems over several decades. If the relationship between stump diameter and decomposition of taproot and lateral root material, i.e., wood and bark, can be quantified, a better understanding of rates and patterns of sequestration and nutrient release can also be developed. This study estimated decomposition rates from in-situ root systems using a chronosequence approach. Nine stands of 55- to 70-year-old loblolly pine (*Pinus taeda* L.) that had been clear-cut 0, 5, 10, 20, 25, 35, 45, 55, and 60 years ago were identified on well-drained Piedmont soils. Taproot and lateral root systems were excavated, measured, and weighed. Although more than 50% of the total root mass decomposed during the first 10 years after harvest, field excavations recovered portions of large lateral roots (>5 cm diameter) and taproots that persisted for more than 35 and 60 years, respectively. Results indicate that decomposition of total root biomass, and its component parts, from mature, clear-cut loblolly pine stands, can be modeled with good precision as a function of groundline stump diameter and years since harvest.

**Résumé :** Étant donné que le système racinaire d'un pin mature représente normalement 20–30 % de la biomasse totale de l'arbre, la décomposition de la racine pivotante et des grosses racines latérales, à la suite d'une récolte et de la régénération du peuplement, pourrait avoir un impact sur la disponibilité des nutriments et la séquestration du carbone dans les pinèdes pendant plusieurs décades. Si la relation entre le diamètre de la souche et la décomposition des constituants de la racine pivotante et des racines latérales, i.e. le bois et l'écorce, peut être quantifiée, il serait possible d'avoir une meilleure compréhension des taux et des patrons de séquestration et de mise en disponibilité des nutriments. Cette étude a estimé le taux de décomposition de systèmes racinaires in situ en utilisant une approche chronoséquentielle. Neuf peuplements de pin à encens (*Pinus taeda* L.) âgés de 55–70 ans coupés à blanc il y a 0, 5, 10, 20, 25, 35, 45, 55 et 60 ans ont été identifiés sur des sols bien drainés du Piedmont. La racine pivotante et les racines latérales ont été déterrées, mesurées et pesées. Bien que plus de 50 % de la masse totale de racines ait été décomposée au cours des 10 premières années suivant la récolte, les travaux d'excavation ont permis de récupérer des portions de grosse racine latérale (diamètre > 5 cm) et de racine pivotante qui persistaient après plus de 35 et 60 ans respectivement. Les résultats indiquent que la décomposition de la biomasse racinaire totale et de ses composantes, dans les peuplements matures de pin à encens coupés à blanc, peut être modélisée avec une bonne précision en fonction du diamètre de la souche au niveau du sol et du nombre d'années écoulées depuis la récolte.

[Traduit par la Rédaction]

## Introduction

The uptake of soil nutrients and water by tree roots and the subsequent release of nutrients through decomposition are important processes contributing to long-term forest productivity. Roots are the principle source of organic matter in the deeper soil layers, and their decomposition rates impact release rates of forest soil nutrients. Estimates of organic matter inputs and turnover in soil are based in part on as-

sumptions that are not well quantified. The mean annual increase in the mass of the feeding roots in many forests, for example, are estimated to be equal to the quantity of feeding roots that die off (Cox et al. 1978; Joslin and Henderson 1987; Raich and Nadelhoffer 1989; Nadelhoffer and Raich 1992). However, decomposition dynamics of larger roots are likely to be much different from fine roots and are almost entirely unquantified. Because root dynamics control rates of nutrient release to soil pools, current estimates of site resource requirements for sustaining forest productivity have considerable uncertainty. Increased understanding of large root decomposition would enhance the ability to predict nutrient and carbon cycles in the forest ecosystem and contribute to a better understanding of site productivity.

A mature pine tree root system typically accounts for 20–30% of the total tree biomass (Wells et al. 1975; Pehl et al. 1984; Van Lear et al. 2000). Large primary lateral roots are commonly the same or similar in age to the tree itself (Vogt and Persson 1988) and represent a large pool of stored resources. Studies of fine roots of several tree species indicate

Received 14 November 2001. Accepted 10 April 2002.  
Published on the NRC Research Press Web site at  
<http://cjfr.nrc.ca> on 10 September 2002.

K.H. Ludovici.<sup>1</sup> USDA Forest Service, Southern Research Station, Research Triangle Park, NC 27709, U.S.A.  
S.J. Zarnoch. USDA Forest Service, Southern Research Station, Asheville, NC 27708, U.S.A.  
D.D. Richter. Nicholas School of the Environment, Duke University, Durham, NC 28804, U.S.A.

<sup>1</sup>Corresponding author (e-mail: [kludovici@fs.fed.us](mailto:kludovici@fs.fed.us)).

that decomposition rate decreases as a function of increasing root diameter (Fahey et al. 1988; King et al. 1997; Chen et al. 2001). Thus, decomposition of large lateral roots and taproots can potentially impact nutrient release over several decades (Olsen 1963; Jenny 1980; Vogt et al. 1991; Chen et al. 2001). The frequency and temporal dynamics of this input are dependent of tree mortality and site disturbance.

Loblolly pine (*Pinus taeda* L.) occupies 21 x 10<sup>6</sup> ha of forestland in the southeastern United States and accounts for 56% of all planted tree acres in the region (USDA 2000). Sustainability of this forest resource is of increasing importance as land-use patterns change and intensity of management increases site productivity. Most forest soils in the U.S. Southeast have low native fertility. Previous agricultural land uses have greatly altered soil nutrient status and eroded many of the region's clayey soils. The Georgeville series represents 8% of the total land base in the Piedmont and nearly 25% of forested lands in the region. These, and related soils, have relatively small contents of soil organic matter, and nutrient availability is likely to be highly dependent on the turnover and decomposition of large-root systems (Van Lear et al. 2000).

The objective of this study was to quantify decomposition rates of large lateral roots and taproots in situ, over time scales of decades. In this study, management records of the Duke Forest in central North Carolina were used to identify old-field loblolly pine stands that had been clear-cut over a 60-year period (1939-2000). Nine stands of natural regeneration pine, supported by Georgeville series soils, were identified to locate loblolly pine stumps that were subject to decomposition for up to 60 years. A model was developed to predict the mass of lateral and taproots as a function of stump diameter and time since harvest. Decomposition rates for various root components were obtained from parameters of the models.

## Materials and methods

### Study sites

A chronosequence of nine clear-cut stands of old-field loblolly pine (55-70 years old) was identified at the Duke Forest, Durham County, North Carolina. This type of harvest and sequence of stand ages represent an important condition for carbon loading and decomposition on the Piedmont upland landscape (Richter and Markewitz 2001). Stands were selected for uniformity in soil series, species, landform, regeneration, land management, and current overstory. Management records and ground truthing revealed that the stands were clear-cut 5, 10, 20, 25, 35, 45, 55, and 60 years ago. One 55-year-old, intact stand was also selected for comparison and three live trees felled. Most were in the Korstian Division of the Duke Forest, near the intersection of Mount Sinai Road with Turkey Farm Road. Soils were of the Georgeville series with very deep, well-drained, moderately permeable soil that has formed in material weathered from Carolina slate (fine, kaolinitic, thermic Typic Kanhapludults). Slopes ranged from 2 to 10%, and the current stand vegetation is predominantly naturally regenerated loblolly pine of 0-60 years of age. Annual precipitation averages about 123 cm, mean annual temperature is 16°C, and the frost-free season ranges from 190 to 240 days (Albaugh et al. 1998).

### Sample collection and measurements

In June 2000, three tree stumps were randomly selected in each of the nine stands and excavated to recover large lateral roots within 1 m of the stump edge, and taproots within 1 m of the soil surface (Fig. 1). Two additional decomposing root systems that had grafted lateral roots were excluded because grafting allows root systems to continue to live after harvest. Three live trees were selected for representative size and were felled to serve as time 0. Roots were separated into consolidated solid and unconsolidated soft decomposing taproot material, and lateral roots by depths of 0-50 and 50-100 cm. Bark was composited from the taproots and lateral roots. All samples were transported to the USDA Forestry Sciences Laboratory in Research Triangle Park, N.C.

After a tree stump was identified, the forest floor was cleared within a 1-m distance from stump circumference, and all aboveground material was removed. Diameter at ground level was measured at two points inside the bark and averaged. In stands harvested at 0, 5, and 10 years in the past, a ditch witch was used to sever lateral roots 1 m away from the tree stumps. All taproots were excavated to a depth of 1 m and the diameter at the bottom of the root hole, or at the taproot fork, was recorded. Picks, shovels, and scrapers were used to remove soil from crevices and exteriors of each intact stump. Diameter and length of each taproot was measured to estimate total root volume. Slices of solid taproot tissues were collected to estimate root density. Root systems from plots harvested within the previous 15 years required a backhoe for complete excavation. Those harvested 20 and 25 years in the past were extracted with the aid of a heavy-duty winch, and all others were hand excavated. Taproots from 12 of the 27 stumps extended deeper than 1 m, and that mass was also excavated (mean 6.6 kg) but was not included in the model.

Lateral roots were located by hand excavation around each stump and were carefully unearthed to a 1 m distance from stump circumference. Diameter was measured for each lateral where it originated along the taproot surface. Stumps were first excavated to a depth of 0.5 m, ensuring that all laterals were measured and noted for depth of origination (at 0-20 or 20-50 cm soil depth), and then excavated from the full 1 m depth. Finally, lateral root and bark materials were recovered from root channels to a maximum distance of 1 m from the stump edge. All root material was oven-dried to a constant mass at 65°C and weighed. Every sample was chipped, ground, and had loss on ignition performed to correct total biomass calculations for mineral soil contamination. Soil contamination was more evident in lateral root samples than in taproot samples, as lateral root diameters were small and even careful hand excavation often disturbed root channels less than 5 cm. Soil contamination was rarely problematic in decomposed taproot samples, as soil compaction around the taproot was so extreme as to withstand hand shovels and determined removal of bark from the root hole.

### Statistical analysis

Initially an exponential function was used to estimate the decomposition rate of root materials (Yavitt and Fahey 1982; Bloomfield et al. 1993). It was defined as

$$(1) \quad WT_t = a e^{-c(YSH)}$$

Fig. 1. Photograph of recovered root material from 55- to 70-year-old loblolly pine stumps that had been decomposing for (A) 5 years, (B) 20 years, (C) 10 years, and (D) 55 years on a Kanhapluduli in the Piedmont region of North Carolina.

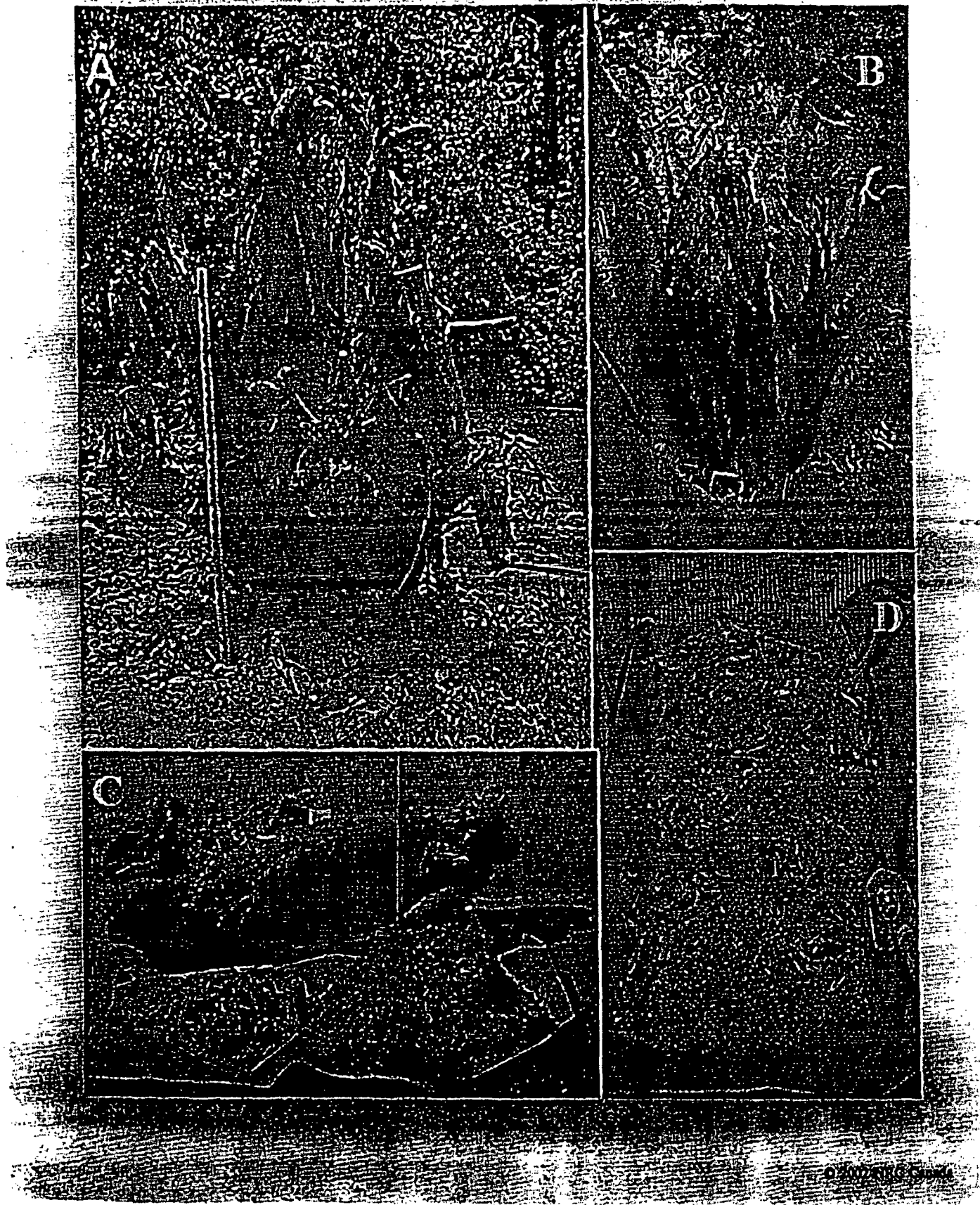
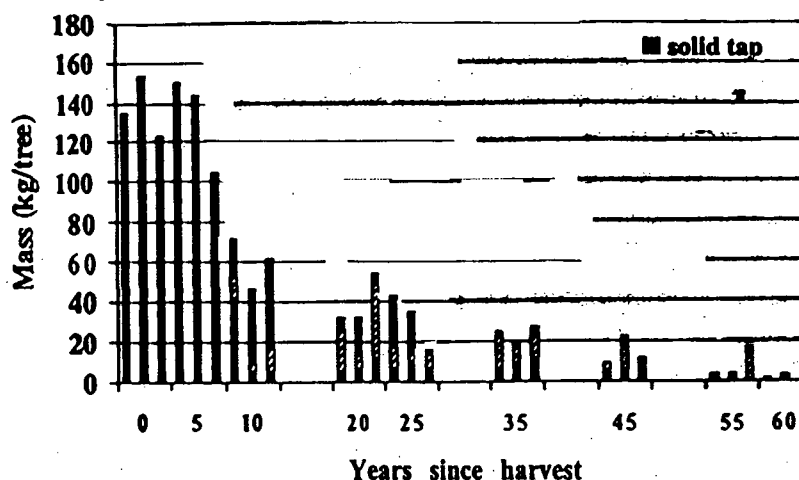


Fig. 2. Actual biomass of each component of recovered loblolly pine root systems, Durham, N.C., June 2000.



where  $WT_t$  is the mass remaining at time  $t$ ,  $a$  is the initial mass,  $c$  is the decomposition rate, and  $YSH$  is years since harvest. This model assumes that decomposition is proportional to the amount of material remaining. The utility of this model is that root mass could be predicted merely as a function of years since harvest. The exponential function was then modified to allow the intercept and decomposition rate to be linear functions of stump diameter, yielding

$$(2) \quad WT_t = [a + b(\text{DIAM})]e^{-(c+d(\text{DIAM}))YSH}$$

where  $\text{DIAM}$  is the average stump diameter and  $a$ ,  $b$ ,  $c$ , and  $d$  are parameters to be estimated. It was hypothesized that predictability of root mass would be increased if information on stump diameter was included. To investigate the effect of soil depth, models were fit to data from the 0-50 cm depth and the 50-100 cm depth separately.

These nonlinear models were fit using the PROC NLIN procedure with the GAUSS option (SAS Institute Inc. 1985). Separate mass models were fit to the lateral root wood, soft taproot wood, solid taproot wood, total taproot wood, bark component, and total roots (lateral, total tap, and bark combined). The models were evaluated based on the mean square error (MSE) criterion and the correlation of the observed with the predicted. The residuals were examined by plotting them over the predicted and dependent variables for each model.

Half width of the confidence interval on the predicted mean was also used as a criterion for predictability. The criteria used to evaluate this was the absolute error defined as

$$(3) \quad AE = \frac{\hat{y}_U - \hat{y}_L}{2}$$

and the percent error defined as

$$(4) \quad PE = 100 \frac{(\hat{y}_U - \hat{y}_L)/2}{\hat{y}}$$

where  $\hat{y}$  is the predicted mean from the regression model,  $\hat{y}_L$  is the lower 95% confidence interval limit on the predicted mean, and  $\hat{y}_U$  is the upper 95% confidence interval limit on the predicted mean

The absolute error is the half width of the 95% confidence interval on the predicted mean and the percent error is the absolute error expressed as a percent of the predicted mean. As variability of the predicted mean increases, the width of the confidence interval increases and, consequently, these two criteria become larger.

The total root mass consists of the lateral wood, tap wood and bark mass components, and thus, this set of models could be considered a system of nonlinear, dependent equations. Parresol (2001) presented methods to fit such a system that has the property of additivity of components. However, in our research it was desired to obtain the best equations for each component without imposing restrictions for additivity.

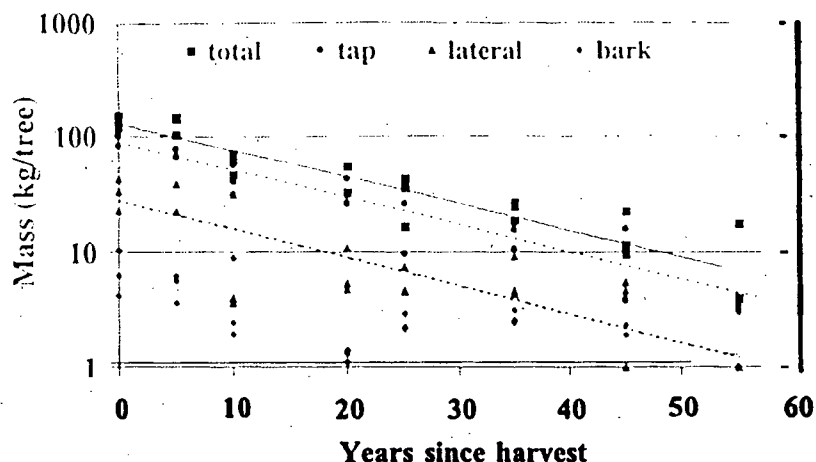
## Results

### Root biomass

The absolute amount of each root component decreased with time since harvest, and total root mass had decreased by more than 50% at 10 YSH (Fig. 2). On average, taproots contributed 71% of the root mass excavated within 1 m of a stump, while lateral roots contributed 25% (Fig. 2). Solid taproot mass decreased approximately 15% during the first 5 years and approximately 65% during the first 10 years, had almost 20% remaining after 25 years, and was still measurable at 60 YSH. Soft taproot tissue was recovered from stumps decomposing 10 years or more. The percentage of root mass composed of decomposing or soft taproot tissue increased with time, but these data were variable. The mass of soft taproot tissue increased through 20 years post-harvest and then decreased (Fig. 2). Lateral roots contributed between 17 and 30% of the excavated root mass, with a mean of 40% of all lateral root mass remaining 10 years after harvest and small but measurable quantities recoverable at 60 years. Contribution of bark to large root mass ranged from 3 to 24%, increasing through the first 45 years before declining sharply thereafter.

The pattern of increasing bark percentage contributions to total remaining mass, with the percent taproot and lateral root contribution relatively constant indicates different rates of decomposition for the taproot wood, lateral

Fig. 3. Actual biomass of recovered loblolly pine root components expressed on a log scale to quantify decomposition rates, Durham, N.C., 2000.



root wood, and bark tissues. To quantify this, individual root component mass was displayed on a log scale (Fig. 3) and decomposition rates ( $k$ ) were estimated (Table 1). Decomposition rates were  $-0.055$  for taproot wood,  $-0.057$  for lateral root wood material, and  $-0.053$  for the root system in total. Decomposition rates for bark ( $-0.023$ ) were less than one-half of other root tissues.

#### Modeling of root biomass

Prediction equations of remaining total large root mass lose robustness by 20 years since harvest, as indicated by increasing percent errors around the predicted mean (Fig. 4A). This deviation from actual values is an indication of differences between lateral root and taproot material, as individual components of taproots and lateral roots decreased at different rates. Decomposition model parameters and fit statistics for individual root components and several component combinations are shown in Table 2. Regression analyses to predict biomass of different combinations of root material (Fig. 5) were compared with results from regression analyses of the total large root model. The weakest relationship was for soft taproot wood mass, which had a MSE of 59.9 and a correlation coefficient of 0.53 (Table 2). Regression analysis of the solid taproot wood was not different from that for the combined solid and soft taproot measure.

Fitting a system of nonlinear equations using PROC SYNLIN confirmed that no additional improvement in the total root model was achieved compared with individual component models. The relationship between total root biomass, time in YSH, and stump diameter was the strongest with MSE of 202.9 and a correlation coefficient of 0.96 (Table 2).

Strength of the models is displayed in the graphs of predicted against actual biomass values. The variability of these relationships is depicted in Figs. 6A–6C, with actual masses of individual root components, bark, lateral wood, soft wood, and solid taproot wood plotted against their predicted values. Evaluation of predicted stump masses against actual masses supported the strength of the models for total root mass (Fig. 6A), total taproot mass (Fig. 6B) and solid tap-

Table 1. Decomposition rates ( $k$ ) of each mature loblolly pine root component, Durham, N.C., Jun 2000.

Root component	Intercept	$k$	$R^2$
Total taproot		0.0546	
Lateral root		0.0568	
Root bark		0.0233	
Total root		0.0534	

root mass (Fig. 6B), as correlation coefficients ( $r$ ) were greater than 90% for each (Table 2). Soft taproot tissue mass was unrelated to YSH and stump diameter (Fig. 6B). The ability to predict lateral root mass was adequate with an  $r$  of 0.756 (Fig. 6C). Bark mass was significantly described by the model but could only be adequately predicted by these models at the 75% confidence level (Fig. 6C). Predictability of solid taproot wood through time was strong with an  $r$  of 0.916 and a probability of  $<0.0001$ , and combining both soft and solid taproot wood components altered the equation for biomass prediction, without changing its strength (Table 2).

Inclusion of depth, as a factor in decomposition, suggested that individual root components at different depths decompose at different rates. The ability to predict total, solid taproot wood mass, or a combined solid and soft taproot wood mass within a depth decreased with increasing depth (Table 3). Strength of the relationship between stump diameter, YSH, and remaining mass was strongest for total stump, total taproot wood, and soft taproot wood, in the 0–50 cm depth, and strongest for total stump, total taproot wood, and lateral root mass prediction in the 50–100 cm depth (Table 3).

#### Prediction evaluation

An evaluation of the models to predict biomass components was based on a measure of precision obtained from confidence intervals constructed on the predicted mean value. Percent errors were defined as the half width of 95%

Fig. 4. (A) Percent error of the predicted mean using the regression model for root component decomposition and (B) the absolute error is the half width of the 95% confidence interval on the predicted mean, Durham, N.C., 2000.

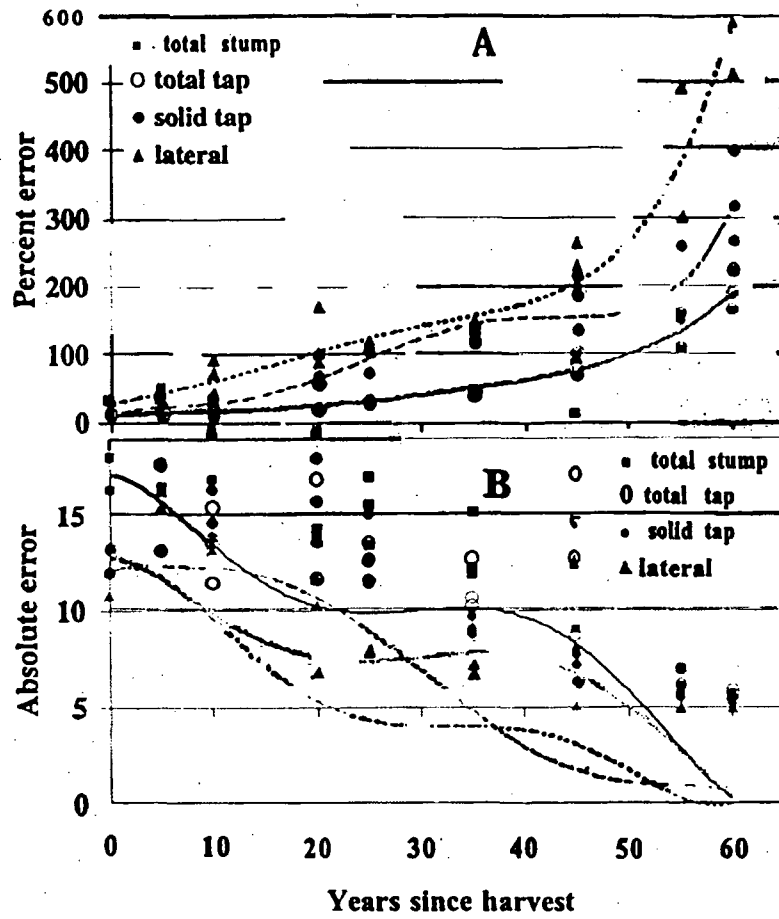
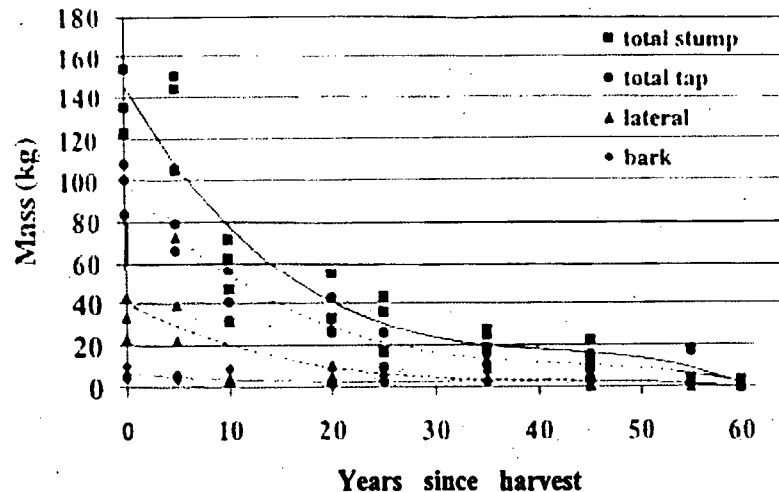


Table 2. Parameters and fit statistics for the initial exponential model 1 and the modified model 2 that allows the intercept and decomposition rate to be linear functions of stump diameter.

Root component	Sample size	Model <sup>a</sup>	a <sup>b</sup>	b	c	d	MSE <sup>c</sup>	r <sup>d</sup>
Soft taproot	21	1		1.44		-0.0052		
		2		0.72		0.0006		
Solid taproot	24	1		.30		-0.0000		
		2		-0.11		-0.0016		
Total taproot	27	1				-0.0016		
		2				-0.0016		

correlation

Fig. 5 Biomass of mature loblolly pine root systems recovered along a time chronosequence, with fitted equations for regression of each root component against time and stump diameter, Durham, N.C., 2000.



confidence intervals and presented as a percentage of the predicted mean (Fig. 4A). In general, error remained less than 20% through 10 YSH for total stump and total taproot wood components and was less than 30% through 25 YSH. Although percent errors generally increased with increasing YSH, absolute values decreased (Fig. 4B). The equation of total stump mass (Fig. 7) produced the smallest percent error, ranging from 10 to 221% (Fig. 4A). Percent error ranged from 10 to 58% for the first 35 years post-harvest, increasing to values of 100% after 55 years, and 200% after 60 years. This error around the predicted mean of total mass appears large on a percentage basis; however, absolute error ranged from 0.0 to 1.4 kg at 55 and 60 YSH.

### Discussion and conclusions

Loblolly pine root systems persist for a long time on southern sites. Stump holes and lateral root channels could be easily identified even 60 YSH, as we observed that soil compaction around the root systems was obvious and long lasting. Root systems thus provided multiple long-term benefits to the site. Before 10 YSH, a developing space between decomposing roots and the mineral soil matrix, created a favorable environment for new elongating roots (Van Lear et al. 2000). The high water content of decomposing roots was obvious when water spurted from the 5 YSH roots as they were excavated. Van Lear et al. (2000) demonstrated that after 10 YSH, established root channels provided a favorable rooting environment for growth of new roots. In that study, fine roots proliferated through old root channels where resources were concentrated and impedance was minimal. The established root channels likewise created favorable environments for insects, herpetofauna, and small mammals.

On average, taproots of these mature pines initially contributed 71% of the excavated root mass, while the lateral roots contributed 25%. This distribution is somewhat different from the taproot contributions of 50–55% and lateral root contributions ranging from 21 to 45%, reported for younger pine trees (Wells et al. 1975; Harris et al. 1977; Van

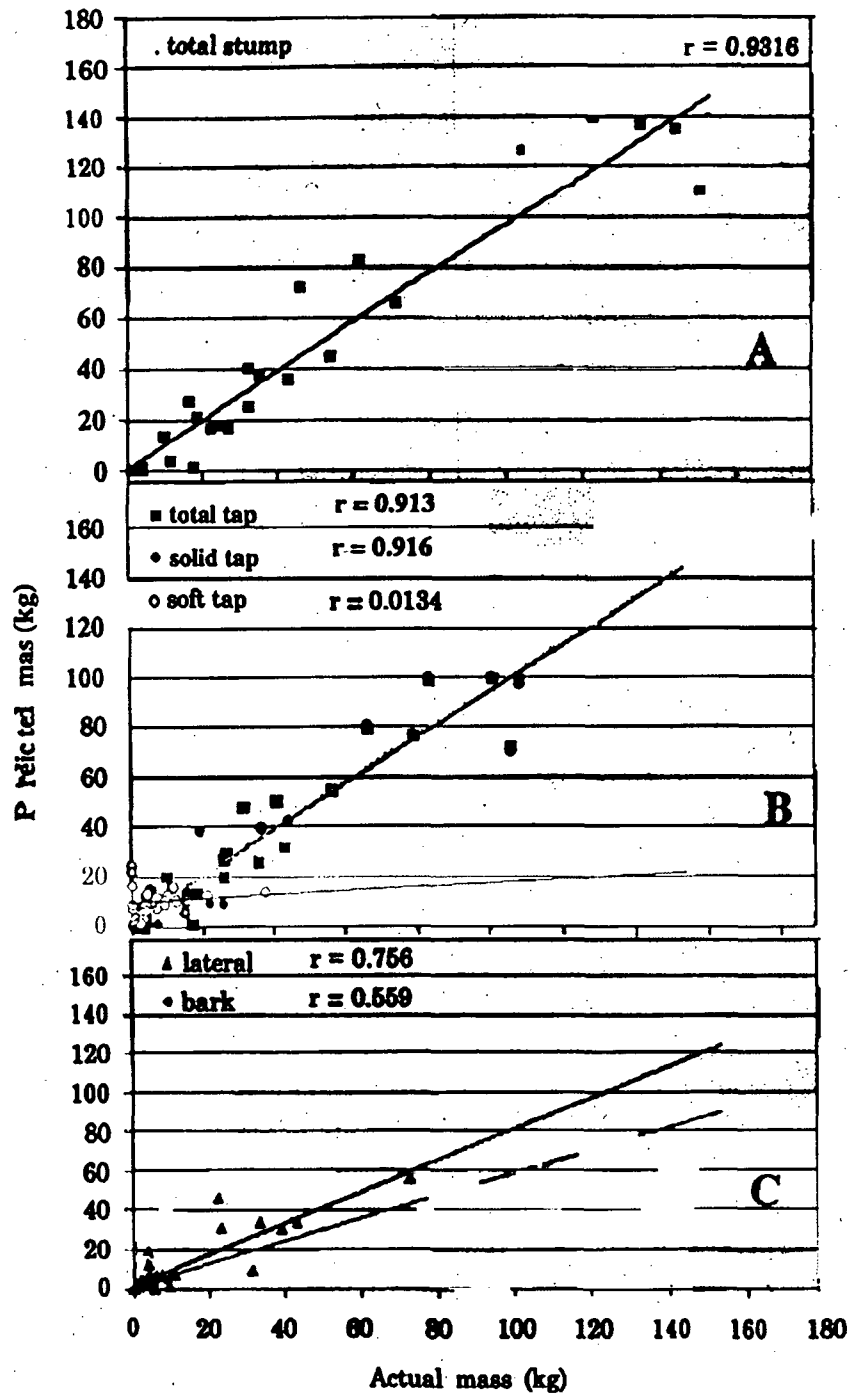
Lear and Kapeluck 1995). Such differences in distribution could be expected because of the different soil volumes explored by trees of different ages. A young tree is likely to distribute the majority of belowground biomass near the surface and within a 1-m distance from the stem. A mature pine tree is expected to have a taproot longer than 120 cm, with lateral roots extending beyond the canopy. As a tree ages, we would expect increasing proportions of the total root biomass to be taproot wood, when excavation is confined to a 1-m distance of the stem.

The pattern of decreasing lateral-root and increasing bark contributions, while relative taproot contribution remained similar through time, indicated different rates of decomposition for the taproot wood, lateral root wood, and bark tissues. The calculated decomposition rate for bark (0.023) was less than one-half the rate for lateral root wood (0.057) or taproot wood (0.055).

Individual root components decompose at different rates at different depths. We expected that these clear-cut sites would have high rates of decomposition because temperature and soil water availability were high and microbial populations were clustered at existing root sites. Our decomposition rates were generally faster than those reported by Chen et al. (2001) for western tree species on northwestern U.S. locations. Comparison of decomposition rates for different species and in different latitudes indicates that (with the exception of lodgepole pine, (Chen et al. 2001)) loblolly pine roots decompose at faster rates.

The ability to quantify belowground biomass is critical to our ability to model carbon fluxes in forests. Yavitt and Fahey (1982) suggested that decomposition of sapwood and heartwood of woody roots should be examined separately to allow more accurate estimation of long-term root mass loss. Chen et al. (2001) also reported that a double-exponential model, which accounts for sapwood and heartwood components separately, provides a better fit than the single-exponential model for woody roots. However, our study did not confirm the need to evaluate various structural components separately in estimating long-term decomposition.

Fig. 6. Predicted and actual mass data for recovered decomposing pine root systems (A) total stump mass, (B) taproot wood components, and (C) lateral wood and bark tissues, Durham, N.C., 2000.



The strength of this decomposition model opens possibilities for improved estimates of the total resource pool and availability of carbon and other nutrients. It also provides researchers with a tool for quantifying carbon fluxes and spatial patterns of carbon cycling and nutrient pools in pine forests of the southeastern United States. The ability to re-

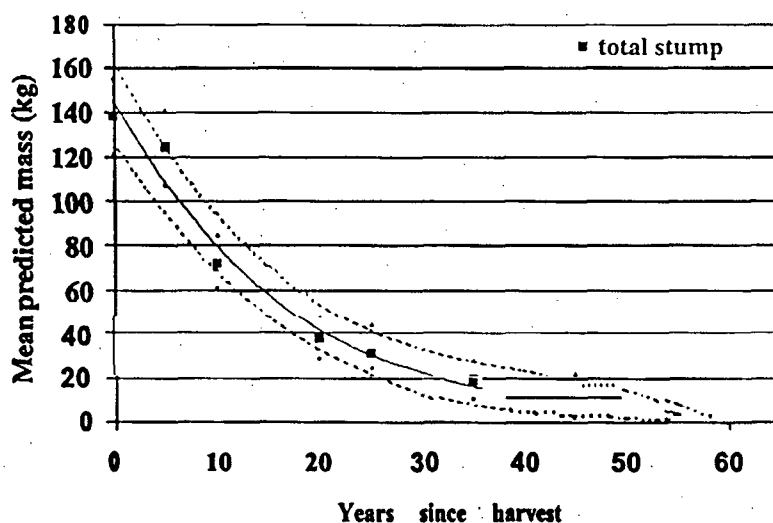
late lateral root diameters to an aboveground measure will further enhance our ability to predict spatial patterns of resource availability. These data support the important contribution of root systems to long-term resource availability. Evaluation of the relationship between stump diameters, years since harvest and decomposition should be tested un-

Table 3. Models for loblolly pine root decomposition by soil depth through 60 years since harvest.

Material	<i>a</i>	<i>b</i>	<i>c</i>	<i>d</i>	<i>P</i>	<i>&gt;F</i>
<b>0-50 cm depth</b>						
Total stump	78.409	0.327	0.164	-0.002	0.933	0.011
Total taproot	56.458	0.240	0.201	-0.002	0.946	0.009
Solid taproot	186.960	6.065	-0.090	0.005	0.967	0.009
Soft taproot	-21.314	0.713	-0.001	0.0005	0.515	0.149
Lateral root	14.807	0.139	0.077	-0.000	0.688	0.085
Root bark	8.162	-0.071	0.113	-0.002	0.625	0.065
<b>50-100 cm depth</b>						
Total stump	-125.443	3.708	-0.157	0.006	0.852	0.045
Total taproot	24.895	-0.133	0.090	-0.001	0.654	0.074
Solid taproot	12.669	0.146	-0.086	0.002	0.651	0.115
Soft taproot	2583.923	-42.281	1.603	-0.026	0.814	0.217
Lateral root	-45.248	1.357	0.267	-0.003	0.879	0.081
Root bark	-7.795	0.201	-0.717	0.016	0.659	0.132

Note: The following model was used: total remaining mass (kg) =  $(a + b(\text{DIAM}))e^{(c + d(\text{DIAM}))YSH}$

Fig. 7. Confidence limits (95%) around the predicted mean of total loblolly pine stump biomass through 60 years, regressed against YSH and stump diameter, Durham, N.C., 2000.



der different management plans and on different soil drainage classes.

### Acknowledgements

The USDA Forest Service provided funding for this study. The authors thank Judson Edeburn, Duke Forest Manager, and the Nicholas School of the Environment at Duke University. We also thank USDA Forest Service personnel Tom Christensen and Bob Eaton for work on plot identification and root recovery and J. Glover, L. Hawkins, C. King, L. Kress, T. Price, K. Sarsony, and D. Sherling for processing root materials. A special thank you is extended to Dr. Lawrence Greenberg. We thank Barb Conklin and Kurt Johnsen for review of an earlier version and two anonymous reviewers for their helpful suggestions.

### References

- Albaugh, T.J., Allen, H.L., Dougherty, P.M., Kress, L.W., and King, J.S. 1998. Leaf area and above- and belowground growth responses of loblolly pine to nutrient and water additions. *For. Sci.* 44: 317-328.
- Bloomfield, J., Vogt, K.A., and Vogt, D.J. 1993. Decomposition rate and substrate quality and foliage of two tropical tree species in the Luquillo Experimental Forest, Puerto Rico. *Plant Soil*, 150: 233-245.
- Chen, H., Harmon, M.E., and Griffiths, R.P. 2001. Decomposition and nitrogen release from decomposing woody roots in coniferous forests of the Pacific Northwest: a chronosequence approach. *Can. J. For. Res.* 31: 246-260.
- Cox, T.L., Harris, W.F., Ausmus, B.S., and Edwards, N.T. 1978. The role of roots in biogeochemical cycles in an eastern deciduous forest. *Pedobiologia*, 18: 264-271.

- Fahey, T.J., Hughes, J.W., Mou, P., and Arthur, M.A. 1988. Root decomposition and nutrient flux following whole-tree harvest of northern hardwood forest. *For. Sci.* 34: 744-768.
- Harris, W.F., Kinerson, R.S., and Edwards, N.T. 1977. Comparison of belowground biomass of natural deciduous forests and loblolly pine plantations. *Pedobiologia*, 17: 369-381.
- Jenny, H. 1980. *The soil resource*. Springer-Verlag, New York.
- Joslin, J.D., and Henderson, G.S. 1987. Organic matter and nutrients associated with fine root turnover in a white oak stand. *For. Sci.* 33: 330-346.
- King, J.S., Allen, H.L., Dougherty, P.M., and Strain, B.R. 1997. Decomposition of roots in loblolly pine: effects of nutrient and water availability and root size class on mass loss and nutrient dynamics. *Plant Soil*, 195: 171-184.
- Nadelhoffer, K., and Raich, J.W. 1992. Fine root production estimates and belowground carbon allocation in forest ecosystems. *Ecology*, 73: 1139-1147.
- Olsen, J.S. 1963. Energy storage and the balance of producers and decomposers in ecological systems. *Ecology*, 44: 322-331.
- Parresol, B.R. 2001. Additivity of nonlinear biomass equations. *Can. J. For. Res.* 31: 865-878.
- Pehl, C.E., Tuttle, C.L., Houser, J.N., and Moehring, D.M. 1984. Total biomass and nutrients of 25-year-old loblolly pine (*Pinus taeda* L.). *For. Ecol. Manage.* 9: 155-160.
- Raich, J.W., and Nadelhoffer, K.J. 1989. Belowground carbon allocation in forest ecosystems: global trends. *Ecology*, 70: 1345-1354.
- Richter, D.D., and Markewitz, D. 2001. *Understanding soil change*. Cambridge University Press, Cambridge, U.K.
- SAS Institute Inc. 1985. *SAS/STAT™ guide for personal computers*, version 6 ed. SAS Institute Inc., Cary, N.C.
- U.S. Department of Agriculture (USDA). 2000. The 2000 RPA timber assessment update. USDA For. Serv. Gen. Tech. Rep. RM-259.
- Van Lear, D.H., and Kapeluck, P.R. 1995. Above- and below-stump biomass and nutrient content of a mature loblolly pine plantation. *Can. J. For. Res.* 25: 361-367.
- Van Lear, D.H., Kapeluck, P.R., and Carroll, W.D. 2000. Productivity of loblolly pine as affected by decomposing root systems. *For. Ecol. Manage.* 138: 435-443.
- Vogt, K.A., and Persson, H. 1988. Root methods. In *Ecophysiology of forest trees*. Vol. 1. Techniques and methodologies. Edited by J.P. Lassoie and T.M. Hinckley. CRC Press, Boca Raton, Fla.
- Vogt, K.A., Vogt D.J., and Bloomfield, J. 1991. Input of organic matter to the soil by tree roots. In *Plant roots and their environment*. Edited by B.L. McMichael and H. Persson. Development in Agriculture and Managed-Forest Ecology, Elsevier, Amsterdam. pp. 171-190.
- Wells, C.G., Jorgensen, J.R., and Burnette, C.E. 1975. Biomass and mineral elements in a thinned loblolly pine plantation. USDA For. Serv. Res. Pap. SE-126.
- Yavitt, J.B., and Fahey, T.J. 1982. Loss of mass and nutrient changes of decaying woody roots in lodgepole pine forests, southeastern Wyoming. *Can. J. For. Res.* 12: 745-752.



Home Publications Work Units **Employees** Search About SRS Site Index Contacts

### Employee Information



Kim Ludovici

Name: **Kim Ludovici**  
Title: **Soil Scientist**  
Unit: **Biological Foundations of Southern Forest Productivity and Sustainability (4154)**  
Phone: **919-549-4044**  
Fax: **919-549-4047 - Location Fax**  
E-Mail: **kludovici@fs.fed.us**

### Location Information

Mailing Address: **USDA-Forest Service  
Southern Research Station  
Forestry Sciences Laboratory  
P.O. Box 12254  
  
Research Triangle Park, NC 27709**

Shipping Address: **3041 E. Cornwallis Road  
Research Triangle Park NC 27709**

Location Phone:

### Research Information

#### Education:

**B.S., Cornell University, Agronomy- Soils, 1984; M.S. North Carolina State University, Forest Soils, 1990; Ph.D., University of Georgia, Forest Soils, 1995**

#### Current Research:

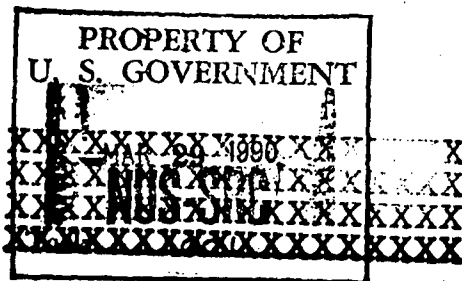
**Long-term effects of soil compaction, organic matter removal and competition on nutrient cycling and biomass allocation in a loblolly pine stand. Specific projects deal with quantifying and modeling root growth and decomposition across soil types and under various silvicultural and anthropogenic conditions; nutrient budgets at the LTSP site, litter decomposition rates; and carbohydrate dynamics of pine root and shoot extension.**

#### Collaborative Research:

**Responses of southern forest systems to silvicultural and anthropogenic stresses and competition (especially as these relate to root and soil carbon pools, and root and soil chemistry).**

**Search for on-line publications by:  
Kim Ludovici:**

SRC-80046



ed J. W. MURRAY,

heffield, and E. E.

on

Director of the State

# PRACTICAL PEDOLOGY Studying Soils in the Field

STUART G. McRAE, BSc, PhD  
Lecturer in Land Resources Science  
Wye College, University of London

kings & Partners

ES

OTHER MARINE

, British Geological

Geology, University

M. D. BRASIER,

ON, Department of  
vices International,

TIN, Department of

Geological Studies,



ELLIS HORWOOD LIMITED  
Publishers · Chichester

Halsted Press: a division of  
**JOHN WILEY & SONS**  
New York · Chichester · Brisbane · Toronto

akm

First published in 1988 by  
**ELLIS HORWOOD LIMITED**  
Market Cross House, Cooper Street,  
Chichester, West Sussex, PO19 1EB, England

*The publisher's colophon is reproduced from James Gillison's drawing of the ancient Market Cross, Chichester.*

**Distributors:**

*Australia and New Zealand:*  
JACARANDA WILEY LIMITED  
GPO Box 859, Brisbane, Queensland 4001, Australia

*Canada:*  
JOHN WILEY & SONS CANADA LIMITED  
22 Worcester Road, Rexdale, Ontario, Canada

*Europe and Africa:*  
JOHN WILEY & SONS LIMITED  
Baffins Lane, Chichester, West Sussex, England

*North and South America and the rest of the world:*  
Halsted Press: a division of  
JOHN WILEY & SONS  
605 Third Avenue, New York, NY 10158, USA

*South-East Asia*  
JOHN WILEY & SONS (SEA) PTE LIMITED  
37 Jalan Pemimpin # 05-04  
Block B, Union Industrial Building, Singapore 2057

*Indian Subcontinent*  
WILEY EASTERN LIMITED  
4835/24 Ansari Road  
Daryaganj, New Delhi 110002, India

© 1988 S.G. McRae/Ellis Horwood Limited

British Library Cataloguing in Publication Data  
McRae, S.G. (Stuart Gordon), 1942-  
Practical pedology  
I. Soil science. Methodology  
I. Title  
631.4'01'8

Library of Congress Card No. 87-37930

ISBN 0-85312-918-5 (Ellis Horwood Limited)  
ISBN 0-470-21062-1 (Halsted Press)

Phototypeset in Times by Ellis Horwood Limited  
Printed in Great Britain by Butler & Tanner, Frome, Somerset

**COPYRIGHT NOTICE**

All Rights Reserved. No part of this publication may be reproduced, stored in a retrieval system, or transmitted, in any form or by any means, electronic, mechanical, photocopying, recording or otherwise, without the permission of Ellis Horwood Limited, Market Cross House, Cooper Street, Chichester, West Sussex, England.

## Table of Contents

### Preface . . . .

<b>1</b>	<b>Understanding</b>
1.1	Introduction
1.2	The soil
1.3	Soil science
1.4	The soil profile
1.5	Soil texture
1.6	Water in the soil
1.7	The soil atmosphere
1.8	Soil temperature
1.9	Soil fertility
1.10	Soil erosion
1.11	Soil conservation

<b>2</b>	<b>Describing the soil</b>
2.1	Introduction
2.2	Soil classification
2.3	Soil mapping
2.4	Stone lines
2.5	Soil profiles
2.6	Cartography
2.7	Addendum
2.8	Porosity
2.9	Soil moisture
2.10	Handbook
2.11	Root systems
2.12	Plant growth
2.13	Soil fertility
2.14	Feeding the soil
2.15	The soil

28/388

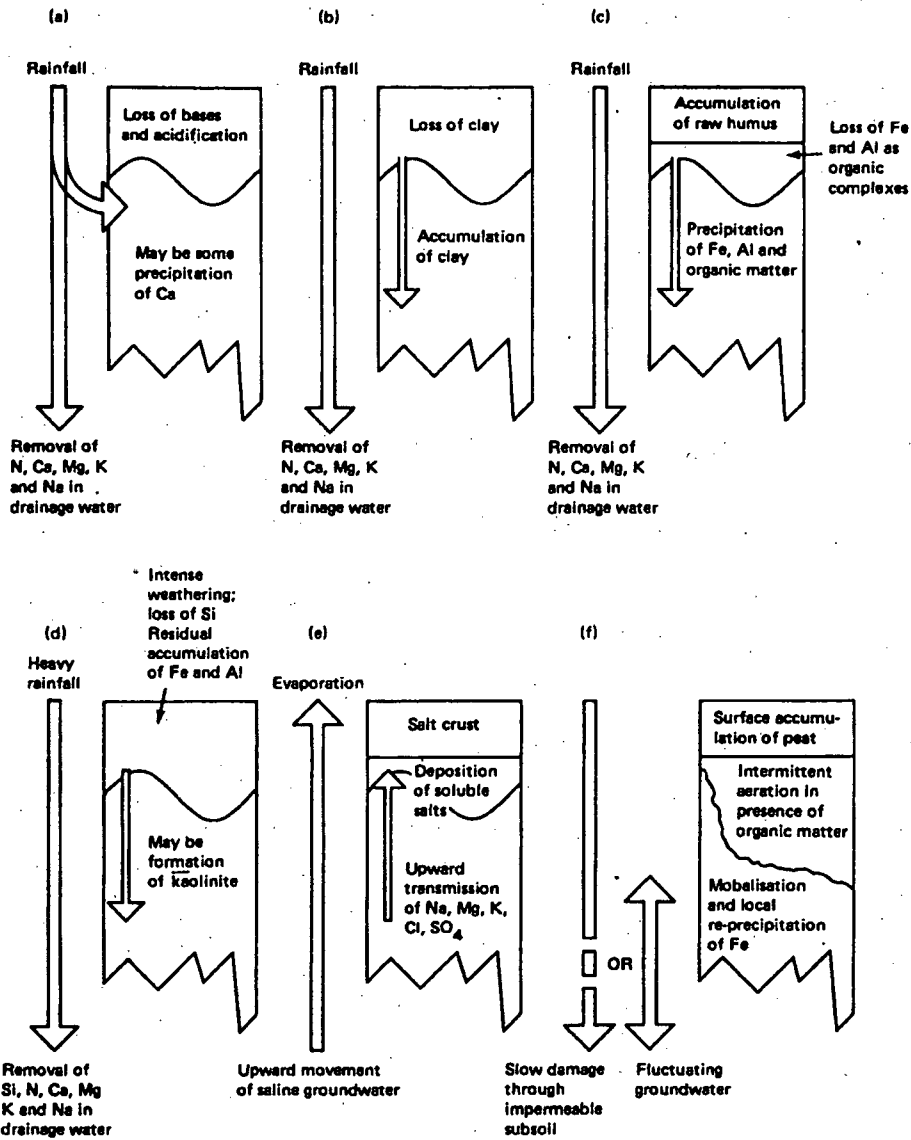


Fig. 1.6— The soil forming processes of (a) leaching (b) clay translocation (c) podzolisation (d) ferallitisation, (e) salinisation and (f) gleying.

#### 1.11.4 Clay translocation

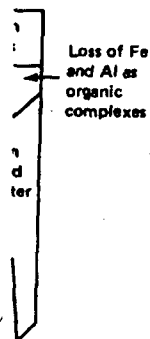
This very slow process involves the washing out of discrete clay particles in slightly acid conditions and their eventual deposition lower in the profile (Fig. 1.6(b)). The zone from which the clay is washed is called an eluvial horizon which becomes lighter

in texture (sometimes called clay usually used and/or below the parent intense weathering depth. Ped the micros called cuta the naked property of thus produced 'anisotropic' e.g. argillite.

1.11.5 Podzolisation  
Russian people call their soils this black soil. They therefore explain the phenolic color of acid soils on the surface, the dark subsoil (Ferralsol) which gives the black (and because of this). The process of accumulation is preferential.

1.11.6 Ferallitisation  
Intense leaching gives soil horizons (Fig. 1.6(d)). Soil Taxonomy calls some local horizons associated with this process called plinthite. The term is used in tropical soils to describe plinthite.

in texture compared with the zone where the clay is deposited, the illuvial horizon, sometimes referred to as a textural B (i.e. subsoil) horizon. The process is sometimes called clay illuviation or lessivage (a French word meaning literally only leaching but usually used specifically for this process). Horizons richer in clay than those above and/or below can arise for reasons other than clay translocation, such as variations in the parent material, superficial deposits of lighter textured materials, and more intense weathering leading to clay destruction nearer the surface of the profile than at depth. Pedologists sometimes have to resort to looking at thin sections of soils under the microscope to prove the process. The clay tends to be deposited in thin skins, called cutans, in cracks and on the faces of structural aggregates, sometimes visible to the naked eye. With a special petrographic microscope these cutans exhibit the property of birefringence because the clay particles are laid down in parallel layers thus producing references to 'birefringent clay' as opposed to the more normal 'anisotropic clays'. Soils exhibiting this process are frequently described as 'argillic' e.g. argillic brown earths.



**1.11.5 Podzolisation**

Russian peasants in the coniferous forest zone noticed that below the surface litter of their soils there was a white horizon, followed at depth by a black one. They thought this black layer was charcoal from past forest fires and that the white layer was ash. They therefore called the soils podzols, literally ash soils. This is, of course, not the explanation for the appearance of the profile. What happens is that organic acids and phenolic compounds from the vegetation and surface organic matter of these very acid soils can form complexes with iron and aluminium and so remove them from the surface, transport them downwards in migrating water and deposit them in the subsoil (Fig. 1.6(c)). The leached eluvial horizon becomes white because the iron which gives most soils their brown colour is removed, while the subsoil becomes black (and brown since there are usually two recognisable zones of deposition) because of the additions of iron and organic matter to the illuvial horizons below. The process removes iron and aluminium preferentially and so silica tends to accumulate in the surface (compare with ferallitisation in which silica is removed preferentially leaving a residue richer in iron and aluminium).



**1.11.6 Ferallitisation**

Intense leaching and weathering, almost always under humid tropical conditions, give soil horizons depleted of silica and thus high in the relatively silica-poor clay mineral kaolinite and often rich in hydrous iron and aluminium oxides and hydroxides (Fig. 1.6(d)). These are the so-called oxic horizons of the American system of Soil Taxonomy and the FAO-UNESCO classification (see Chapter 4). There may be some localised solution, movement and deposition of these hydrous oxides associated with ground-water fluctuations producing a characteristic mottled horizon called plinthite. When this becomes dry it hardens irreversibly and is called laterite. The term laterite and/or latosol is widely and erroneously used for any red-coloured tropical soil irrespective of whether or not it contains horizons of true laterite or plinthite.

ation (d)

is in slightly  
.6(b)). The  
mes lighter

WSRC-TR-2003-00436

Revision 0

APPROVED for Release for  
Unlimited (Release to Public)  
3/19/2004

**KEY WORDS:**

Saltstone Disposal Facility

Performance Assessment

Closure Cap

**SALTSTONE DISPOSAL FACILITY  
CLOSURE CAP CONFIGURATION AND DEGRADATION  
BASE CASE:  
INSTITUTIONAL CONTROL TO PINE FOREST SCENARIO (U)**

**SEPTEMBER 22, 2003**

**PREPARED BY:**

Mark A. Phifer<sup>a</sup>

Eric A. Nelson<sup>a</sup>

Westinghouse Savannah River Company LLC<sup>a</sup>

Westinghouse Savannah River Company LLC

Savannah River Site

Aiken, SC 29808



---

Prepared for the U.S. Department of Energy under Contract No. DE-AC09-96SR18500

## 2.0 INTRODUCTION

The current Saltstone Disposal Facility (SDF) operational and final closure concepts are outlined in detail within the following documents:

- Radiological Performance Assessment for the Z-Area Saltstone Disposal Facility (MMES 1992),
- Closure Plan for the Z-Area Saltstone Disposal Facility (Cook et al. 2000), and
- Special Analysis: Reevaluation of the Inadvertent Intruder, Groundwater, Air, and Radon Analyses for the Saltstone Disposal Facility (Cook et al. 2002a)

The SDF operational and final closure concepts outlined in the above documents involve mixing low-level radioactive salt solution with blast furnace slag, flyash, and cement to form a grout, which is pumped into above grade reinforced concrete vaults. Within the vaults the grout solidifies to form a dense, microporous, monolithic, low-level radioactive waste called saltstone. This concept anticipates that active saltstone disposal operations will last for approximately 30 years. During the operations period the roofed, saltstone-filled vaults remain above grade (interim closure). This concept assumes that the vaults consist of the following from top to bottom:

- 0.1 m (4 inches) thick concrete vault roof,
- 0.4 m (16 inches) thick clean grout layer,
- 7.3 m (288 inches) thick saltstone layer, and
- 0.76 m (30 inches) thick concrete vault floor.

Figure 2.0-1 provides the current projected SDF vault layout based upon this concept. Only vaults 1 and 4 have been constructed based upon this concept. Vault 1 is approximately 600 ft long by 100 ft wide, the apex of the vault roof runs lengthwise (i.e. 600 ft) down its center, and the roof is sloped at 2 percent from the apex to the vault side. This results in a slope length of 50 ft over the vault itself. Vault 4 is approximately 600 ft long by 200 ft wide, the apex of the vault roof runs lengthwise (i.e. 600 ft) down its center, and the roof is sloped at 2 percent from the apex to the vault side. This results in a slope length of 100 ft over the vault itself. Based upon this concept the remaining vaults will be constructed similarly to vault 4 with an approximate footprint of 600 ft by 200 ft and similar roof construction.

Final closure of all the filled vaults is not anticipated until near or at the end of the operational period. This concept assumes that the final closure cap will consist of the following major components from the ground surface to the top of the vault roof (i.e., top to bottom):

- Bamboo vegetative cover
- 0.15 m (6 inches) of vegetative soil (i.e., topsoil),
- 0.76 m (30 inches) of backfill (i.e., structural fill),
- 0.3 m (12 inches) of a gravel drainage layer
- 0.76 m (30 inches) of controlled compacted clay (kaolin),
- 0.3 m (12 inches) of backfill,
- 0.15 m (6 inches) of a gravel drainage layer
- 0.5 m (19.68 inches) of controlled compacted clay (kaolin), and
- 1.0 m (39.37 inches) of grout directly on top of the vault roof.

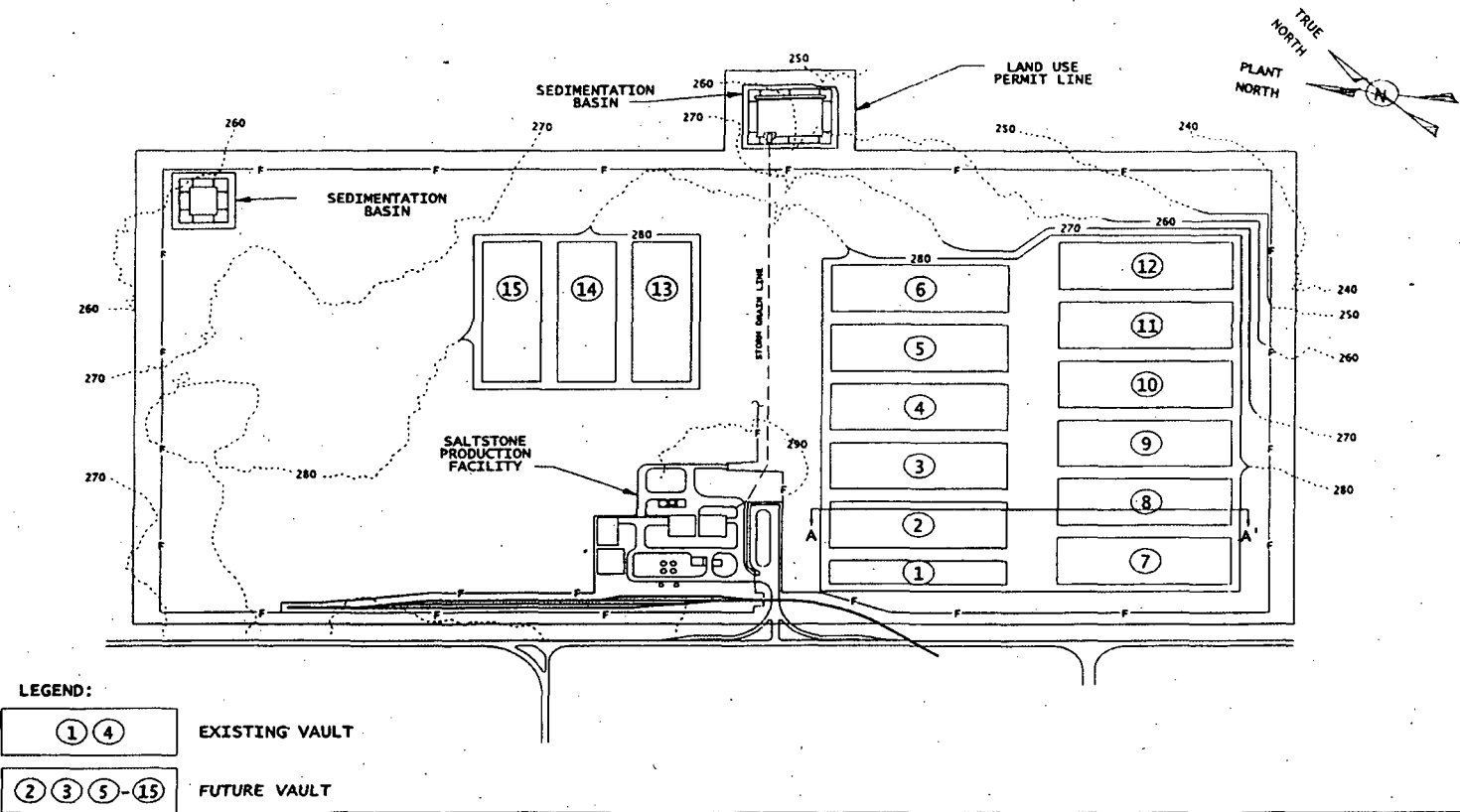


Figure 2.0-1. Current Saltstone Disposal Facility Vault Layout  
(reproduced from Cook et al. 2000)

The required thickness of the closure cap is driven by the resident scenario intruder analysis. This scenario assumes that the resident excavates 3 meters deep for construction of a basement. In order to maintain acceptable exposure results for this scenario the following closure cap assumptions have been made:

- The upper vegetative soil and backfill (0.91 m (36 inches)) erodes away by 1,000 years,
- The upper gravel drainage layer prevents further erosion, and
- A material thickness of 3 meters (119 inches) is maintained above the vault roof,

For this concept at closure, the vault roof slope and slope length will propagate upward from the vault roof to the first backfill layer overlaying the roof. This backfill layer will be used to change the direction of slope by 90 degrees, to increase the slope length to 600 ft, and to increase the slope to 3 percent over the vault itself. The slope and slope length of this backfill layer will propagate upward to the ground surface. Runoff and lateral drainage out of the upper gravel drainage layer will be directed to rip rap filled drainage ditches located along the perimeter of the final cover. Lateral drainage out of the lower gravel drainage layer will be directed to subsurface rip rap filled drainage ditches, located between vaults in each row, which discharge into the perimeter to rip rap filled drainage ditches. The perimeter riprap filled drainage ditches will transport the collected water to a surface discharge point downhill from the SDF and final cover.

The Performance Assessment (PA) for the SDF is currently under revision. As part of the PA revision and as documented herein, the closure cap configuration has been reevaluated and closure cap degradation mechanisms and their impact upon infiltration through the closure cap have been evaluated for the institutional control to pine forest, land use scenario. This land use scenario is considered the base case land use scenario. This scenario assumes a 100-year institutional control period following final SDF closure during which the closure cap is maintained. At the end of institutional control, it is assumed that a pine forest succeeds the cap's original bamboo cover. Infiltration through the upper hydraulic barrier layer of the closure cap as determined by this evaluation will be utilized as the infiltration input to subsequent PORFLOW vadose zone contaminant transport modeling, which will also be performed as part of the PA revision.

## 4.0 CLOSURE CAP CONFIGURATION

Sections 4.1 through 4.6 provide a progressive reevaluation of the closure cap configuration previously presented in Section 2.0. The changes made in a previous section are carried over into the evaluation of subsequent sections, until all changes have been discussed and made. The final revised closure cap configuration is summarized in Section 4.7, Figure 4.7-1 and Table 4.7-1.

### 4.1 Hydraulic Barrier

As outlined in section 2.0, the current SDF PA (MMES 1992) and closure plan (Cook et al. 2000) assume that controlled compacted kaolin is utilized as the closure cap hydraulic barrier layer. However the previously planned controlled compacted kaolin layer for the E-Area Low-Level Waste Facility closure cap was replaced with a geosynthetic clay liner (GCL) as the hydraulic barrier layer within revision 2 of the 'Closure Plan for the E-Area Low-Level Waste Facility' (Cook et al. 2002b). The applicability of also replacing the kaolin layers in the SDF closure cap with GCLs is investigated herein. The acceptability of this change in the hydraulic barrier layer for E-Area was documented within 'Unreviewed Disposal Question Evaluation: Closure Cap Design Change from Compacted Kaolin to Geosynthetic Clay Liner' (Jones and Phifer 2003). An overview of the reasoning for the E-Area change is presented below (Cook et al. 2002a; Cook et al. 2003; Jones and Phifer 2003).

A GCL consists of "bentonite sandwiched between two geotextiles" (USEPA 2001). Bentonite, the hydraulically functional portion of a GCL, is the general term given to a swelling-type montmorillonite clay which formed as the stable alteration product of volcanic ash (Worrall 1975; Jones and Phifer 2003). Therefore bentonite is expected to remain mineralogically and chemically stable. The following is the definition of a Geotextile GCL as defined by the Environmental Protection Agency (USEPA 2001):

A Geotextile GCL "is a relatively thin layer of processed" bentonite ... "fixed between two sheets of geotextile. ... A geotextile is a woven or nonwoven sheet material ... resistant to penetration." ... "Adhesives, stitchbonding, needlepunching, or a combination of the three" are used to affix the bentonite to the geotextile. "Although stitchbonding and needlepunching create small holes in the geotextile, these holes are sealed when the installed GCL's clay layer hydrates."

The following are some of the typical advantages of a Geotextile GCL over compacted clay layers, which led to the replacement of the compacted kaolin with a GCL:

- A GCL has a lower hydraulic conductivity than compacted kaolin (i.e.  $< 5.0 \times 10^{-9}$  cm/s for a GCL versus  $< 1.0 \times 10^{-7}$  cm/s for a compacted kaolin layer) (Phifer 1991; USEPA 2001; GSE 2002)
- Infiltration through a GCL closure cap is generally lower than infiltration through a compacted kaolin closure cap (Cook et al. 2002a; Jones and Phifer 2003).
- A GCL is faster and easier to install than an equivalent compacted kaolin layer (USEPA 2001). Installation of a GCL essentially consists of unrolling the dry GCL like a carpet, overlapping adjacent GCL panels, and covering the GCL with at least a foot of soil. Whereas compacted kaolin must be installed wet of optimum to tight moisture and density controls in multiple lifts with heavy equipment. (Jones and Phifer 2003)
- The bulk of the required Quality Assurance / Quality Control (QA/QC) associated with a GCL is factory based whereas that of compacted kaolin is entirely field based. Factory based QA/QC generally provides a higher degree of QA/QC, and it is included in the cost of the material. (Phifer 1991; GSE 2002; Jones and Phifer 2003)
- Installation of a GCL hydraulic barrier generally costs less than installation of an equivalent compacted kaolin layer (USEPA 2001; Jones and Phifer 2003).

- Installation of a GCL is generally safer than installation of an equivalent compacted kaolin layer, since less heavy equipment use is required (Jones and Phifer 2003).
- A GCL has the ability to self-heal rips or holes, whereas compacted kaolin does not. Additionally a GCL can undergo repeated cycles of dehydration and hydrate without negative impacts to the GCL's saturated hydraulic conductivity, whereas compacted kaolin may irreversibly shrink, crack, and incur increases in its saturated hydraulic conductivity (Phifer 1991; Phifer et al. 1995; Rumer and Ryan 1995; USEPA 2001).
- A GCL incurs less negative impact "due to differential settlement, freezing-thawing cycles, and wetting-drying cycles" than a compacted kaolin layer (Rumer and Mitchell 1995).
- A GCL is not as thick as a compacted kaolin layer (USEPA 2001).
- Hydraulic barriers consisting of compacted clay are 1970's and 1980's technology whereas GCLs are 1990's technology (Jones and Phifer 2003).

The same reasoning for the E-Area change is applicable to the SDF. In order to confirm that replacement of the SDF closure cap compacted kaolin hydraulic barrier with a GCL is appropriate, HELP modeling has been performed. The modeling has been performed to demonstrate that a GCL closure cap is equivalent to or better than the current kaolin closure cap in terms of percolation through the cap and out the facility bottom. Table 4.1-1 provides a comparison of the two configurations from top to bottom. Both configurations consist of 119 inches of material from the top of the upper gravel drainage layer to the bottom of the clean grout on top of the concrete vault roof as required by the PA resident scenario intruder analysis.

**Table 4.1-1. Closure Cap Configuration Comparison**

Current Kaolin Closure Cap		Replacement GCL Closure Cap	
Layer	Thickness (inches)	Layer	Thickness (inches)
Topsoil	6	Topsoil	6
Backfill	30	Backfill	30
Gravel Drainage	12	Drainage Layer	12
Kaolin	30	GCL	0.2
Backfill	12	Backfill	61.28
Gravel Drainage	6	Drainage Layer	6
Kaolin	19.68	GCL	0.2
Clean Grout	39.37 (1 m)	Clean Grout	39.37 (1 m)
Concrete Vault Roof	4	Concrete Vault Roof	4
Clean Grout	16	Clean Grout	16
Saltstone	288	Saltstone	288
Concrete Vault Floor	30	Concrete Vault Floor	30

Several required HELP model input parameters are common to both configurations. Table 4.1-2 provides a listing of these generic input parameters (i.e., HELP model query) and the associated values selected. Use of selected fixed values for these HELP model queries provides compatibility between the different HELP model runs. The landfill area is based upon the length (600 feet) and width (200 feet) of vault 4, which results in a surface area of 120,000 feet squared or 2.75 acres. It has been assumed that the final covers are appropriately sloped so that 100 percent of the covers allow runoff to occur (i.e., there are no depressions). A yes response has been provided to the HELP model

query, which asks, "Do you want to specify initial moisture storage? (Y/N)." The amount of water or snow on the surface of the covers was assumed to be zero as the initial model condition.

**Table 4.1-2. Generic Input Parameter Values**

Input Parameter (HELP Model Query)	Generic Input Parameter Value
Landfill area =	2.75 acres
Percent of area where runoff is possible =	100%
Do you want to specify initial moisture storage? (Y/N)	Y
Amount of water or snow on surface =	0 in.

As stated the initial moisture storage has been specified for all soil layers. While the initial moisture storage is not a fixed value for all runs, a fixed method of selecting the initial moisture storage value has been utilized for consistency. The initial, soil moisture storage value has been selected as follows:

- The initial moisture storage of soil layers designated as either a vertical percolation layer or a lateral drainage layer was set at the field capacity of the soil.
- The initial moisture storage of soil layers designated as a barrier soil liner was set at the porosity of the soil.

The Soil Conservation Service (SCS) runoff curve number (CN) is another required HELP model input parameter that has been made consistent. The HELP model provides three options to specify the CN. The option that produces a HELP model computed curve number, based on surface slope and slope length, soil texture of the top layer, and vegetation, was utilized. Table 4.1-3 provides the input values of surface slope and slope length, soil texture of the top layer, and vegetation that were utilized to produce the HELP model computed curve number. The 3 percent slope is that specified for the top surface of the Saltstone final cover within the Saltstone closure plan (Cook et al. 2000). The 600-foot slope length is the length of an individual Saltstone vault (Cook et al. 2000). The soil texture selected as an input for calculation of the CN is a loamy fine sand per the United States Department of Agriculture (USDA) and a silty sand per Unified Soil Classification System (USCS), since it closely represents the typical vegetative soil layers utilized at SRS. The corresponding number in the HELP default soil texture list is 5. Based upon these input parameter values the HELP model computed a CN of 53.40.

**Table 4.1-3. Input Parameters for HELP Model Computed Curve Number**

CN Input Parameter (HELP Model Query)	CN Input Parameter Value
Slope =	3%
Slope length =	600 ft
Soil Texture =	5 (HELP model default soil texture)
Vegetation =	4 (i.e., a good stand of grass)
HELP Model Computed Curve Number = 53.40	

Table 4.1-4 provides a comparison of the HELP model results for both configurations. The HELP model estimate for the average annual percolation through the upper kaolin hydraulic barrier layer was approximately 0.90 inches/year, while that through the upper GCL hydraulic barrier layer was approximately 0.47 inches/year, approximately half that through the kaolin. The HELP model estimate for the average annual percolation through the lower kaolin hydraulic barrier layer was approximately 0.84 inches/year, while that through the lower GCL hydraulic barrier layer was

approximately 0.055 inches/year, approximately fifteen times less than that through the kaolin. For both configurations the average annual percolation through the vault floor was estimated to be 0.00001 inches/year, however this percolation is controlled by the very low saturated hydraulic conductivity of the vault roof and floor (see Table 3.0-2) rather than by the closure cap hydraulic barrier layers. The results clearly show that replacement of the kaolin layers with GCLs produces a closure cap that is equivalent to or better than the current kaolin closure cap in terms of percolation. See the following appendices for the detailed HELP model input data and output files for both configurations:

- Appendix E, Current Kaolin Closure Cap: HELP Model Input Data and Output File (output file name: ZKAOout.OUT)
- Appendix F, Replacement GCL Closure Cap: HELP Model Input Data and Output File (output file name: ZGCLout.OUT)

**Table 4.1-4. Comparison of Closure Cap Configurations HELP Model Results**

HELP Model Output Parameter	Current Kaolin Closure Cap	Replacement GCL Closure Cap	Replacement GCL Closure Cap w/o Vault
Percolation through upper hydraulic barrier layer	0.90 inches/year	0.47 inches/year	0.47 inches/year
Percolation through lower hydraulic barrier layer	0.84 inches/year	0.055 inches/year	0.055 inches/year
Percolation out vault floor	0.00001 inches/year	0.00001 inches/year	Not applicable

A separate HELP model run was made for the GCL closure cap without inclusion of the vault layers (i.e. the last four layers in Table 4.1-1). This was done to determine whether or not inclusion of the vault layers was necessary to determine the percolation rate through the upper GCL hydraulic barrier. Percolation through the upper GCL hydraulic barrier is to be utilized as input to the subsequent PORFLOW vadose zone flow and contaminant transport modeling. The PORFLOW model will be utilized to model flow and contaminant transport through the vault. The vault is assumed to degrade over time, particularly through settlement- and earthquake-induced cracking. The HELP model can not take into account such cracking degradation directly. The cracking would have to be converted into an equivalent saturated hydraulic conductivity for use in the HELP model. Therefore, if inclusion of the vault layers is not necessary, the HELP modeling could be significantly simplified by their exclusion. As indicated by Table 4.1-4 elimination of the vault layer from the replacement GCL closure cap configuration HELP modeling did not affect the estimated percolation through the upper GCL, therefore these layer will be deleted from further HELP modeling associated with this evaluation. See the following appendix for the detailed HELP model input data and output file:

- Appendix G, Replacement GCL Closure Cap without Vault Layers: HELP Model Input Data and Output File (output file name: ZGCLAout.OUT)

## 4.2 Drainage System Configuration

Three conceptual SDF closure cap drainage system configurations have been evaluated versus percolation through the upper GCL, soil fill volume, ditch length, and relative long-term maintenance requirements. The relationship of each of these parameters to configuration preference is as follows:

- The configuration with the least amount of percolation through the upper GCL is preferable in order to minimize contaminant transport. The configuration determines the maximum slope length over a vault, which in turn impacts the quantity of percolation.
- The configuration that requires the least amount of soil fill volume is preferable in order to minimize construction costs.
- The configuration that requires the least ditch length is preferable in order to minimize construction costs and long-term maintenance. The ditches must be specialized ditches that not only accommodate surface runoff but also intersect and accommodate flow from the subsurface drainage layers. These ditches are expensive to construct and will require substantial long-term maintenance in order to maintain their functionality.

Vaults 1 through 12 are considered representative of all the vaults, therefore vaults 13 through 15 are not considered specifically here (see Figure 2.0-1). The 600-foot slope length configuration shown in Figure 4.2-1 is essentially the configuration presented in the current Performance Assessment (MMES 1992) and Closure Plan (Cook et al. 2000). The closure cap crest is between the two rows of vaults (i.e. between vaults 1 through 6 and vaults 7 through 12) and drainage is directed to the perimeter of the entire disposal area in this configuration. The 300-foot slope length configuration shown in Figure 4.2-2 has a crest down the centerline of each row of vaults and drainage is directed to the perimeter of the entire disposal area and between the two rows of vaults. The 100-foot slope length configuration shown in Figure 4.2-3 has a separate crest down the centerline of each individual vault and drainage is directed between vaults and then to the perimeter of the entire disposal facility.

Table 4.2-1 provides a comparison of the percolation, soil fill volume, ditch length, and relative long-term maintenance requirements relative to the three drainage system configurations. The percolation through the upper GCL associated with the Figure 4.2-1 drainage configuration is the same as that presented in Table 4.1-4 for the GCL closure cap without vault layers. See the following appendices for the detailed HELP model input data and output files associated with the Figures 4.2-2 and 4.2-3 drainage system configurations, respectively:

- Appendix H, Replacement GCL Closure Cap with 300-foot Slope Lengths: HELP Model Input Data and Output File (output file name: ZGCLBout.OUT)
- Appendix I, Replacement GCL Closure Cap with 100-foot Slope Lengths: HELP Model Input Data and Output File (output file name: ZGCLCout.OUT)

See Appendix J for the calculations associated with the fill volume and ditch lengths associated with each drainage system configuration.

Based upon this evaluation the 300-foot, slope length drainage system configuration (Figure 4.2-2) has been selected. It substantially reduces percolation through the upper GCL and required soil fill volume over the current PA (MMES 1992) and closure plan (Cook et al. 2000) configuration, while minimizing the increase in ditch lengths and resultant relative long-term maintenance over the 100-foot, slope length drainage system configuration.

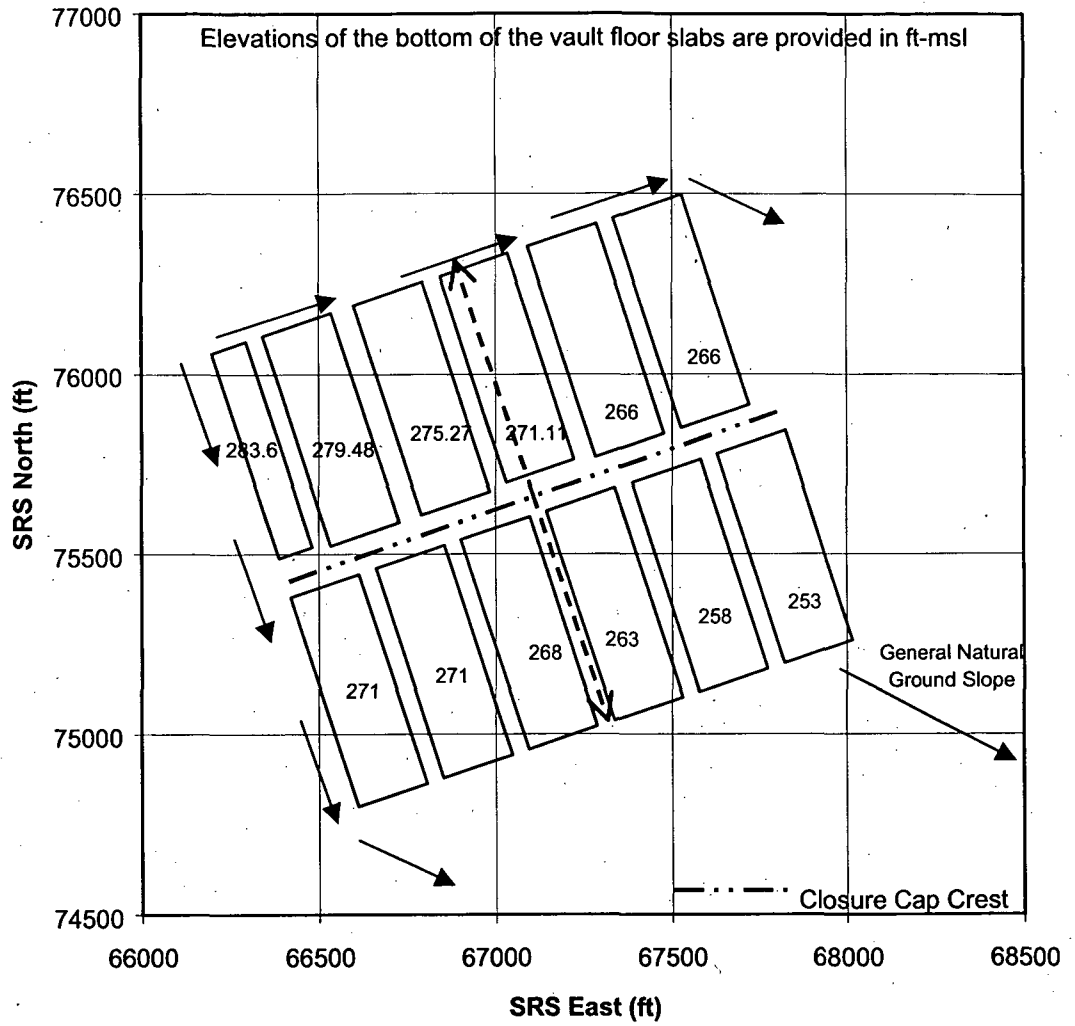


Figure 4.2-1. Current PA and Closure Plan 600-foot Slope Length Drainage System Configuration

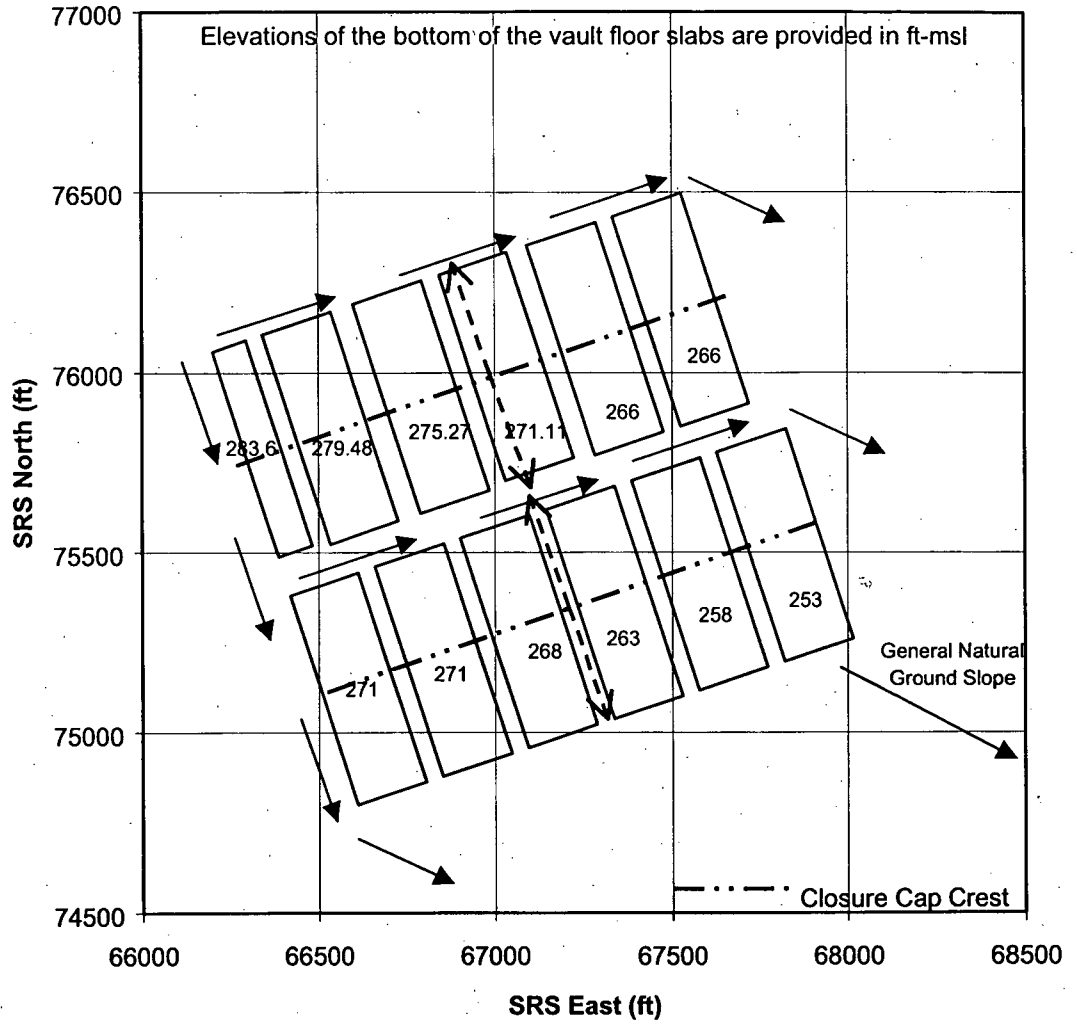


Figure 4.2-2. 300-Foot Slope Length Drainage System Configuration

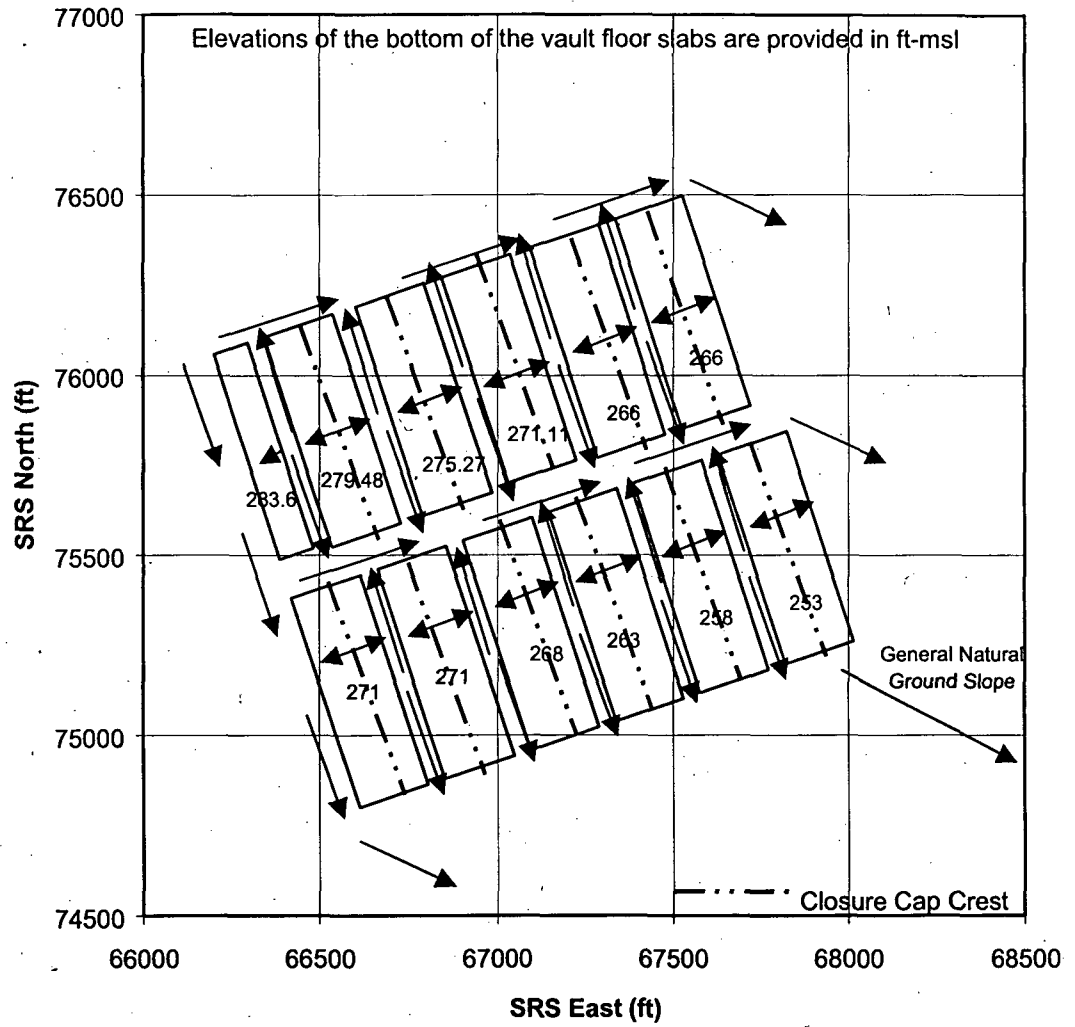


Figure 4.2-3. 100-Foot Slope Length Drainage System Configuration

**Table 4.2-1. Drainage System Configuration Comparison**

Parameter	Drainage System Configuration		
	Figure 4.2-1 <sup>1</sup>	Figure 4.2-2 <sup>2</sup>	Figure 4.2-3 <sup>3</sup>
Maximum Slope Length over a Vault, ft	600	300	100
Percent Slope Length Reduction		50%	83%
Percolation through Upper GCL, in/yr	0.467	0.254	0.110
Percent Percolation Reduction		46%	76%
Soil Fill Volume, cu yd	1,588,300	1,197,600	987,600
Percent Fill Reduction		25%	38%
Ditch Lengths, ft	4,200	5,650	13,450
Percent Ditch Increase		134%	320%
Relative Long-term Maintenance Requirements	Least	Slightly More	Significantly More

<sup>1</sup> Current PA (MMES 1992) and closure plan (Cook et al. 2000) 600-foot slope length drainage system configuration.

<sup>2</sup> 300-foot slope length drainage system configuration

<sup>3</sup> 100-foot slope length drainage system configuration

### 4.3 Erosion Barrier And Upper Drainage Layer

To produce acceptable exposure results associated with the resident scenario intruder analysis, the current PA and closure plan assume that the upper gravel drainage layer functions as both a drainage layer and an erosion barrier to maintain the required material thickness of 3 meters (119 inches) above the vault roof. To function as a drainage layer the grain size of the material needs to be balanced between the need for a fairly high saturated hydraulic conductivity and the need to minimize the infiltration of overlying fines. Such an infiltration of fines would negatively impact the saturated hydraulic conductivity. To function as an erosion barrier the grain size of the material needs to be large enough to prevent material transport by erosion. These two functions can not be readily reconciled therefore an erosion control barrier separate from and overlying the drainage layer will be utilized.

The erosion barrier has been sized based upon the maximum precipitation event for a 10,000-year return period. The maximum precipitation event for a 10,000-year return period is 3.3 inches over a 15-minute accumulation period (Table XIX from Weber et al. 1998). Based upon this precipitation event a one foot thick layer of 2-inch to 6-inch granite stone with a  $d_{50}$  (i.e. median size) of 4 inches has been selected for use as the erosion barrier (sizing based upon Logan 1977; Goldman et al. 1986; NCSU 1991). See Appendix K for the calculations associated with this selection.

In order to prevent the loss of overlying material into the erosion barrier and to reduce the saturated hydraulic conductivity of the erosion barrier layer, the granite stone will be filled with a Controlled Low Strength Material (CLSM) or Flowable Fill. This results in a combined material with the soil properties listed in Table 4.3-1. See Appendix K for the calculations associated with the soil properties for this combined material.

**Table 4.3-1. Erosion Barrier Combined Material Soil Properties**

Property	Property Value
Saturated hydraulic conductivity	3.97E-04 cm/s
Porosity	0.06
Field Capacity	0.056
Wilting Point	0.052

#### 4.4 Erosion Impact upon Evapotranspiration Zone

Table 4.4-1 presents the revised GCL closure cap configuration based upon the changes outlined in Sections 4.1 through 4.3. HELP modeling of this configuration with and without the layers above the erosion barrier (i.e. topsoil and underlying backfill layers) has been performed to evaluate the potential impact of complete erosion of these layers on the hydraulic performance. See the following appendices for the detailed HELP model input data and output files associated with the configurations with and without the layers above the erosion barrier, respectively:

- Appendix L, Replacement GCL Closure Cap with Erosion Barrier: HELP Model Input Data and Output File (output file name: ZGCLDout.OUT)
- Appendix M, Replacement GCL Closure Cap with Erosion Barrier without Overlying Layers: HELP Model Input Data and Output File (output file name: ZGCLEout.OUT)

**Table 4.4-1. Replacement GCL Closure Cap Configuration**

Layer	Thickness (inches)
Topsoil	6
Upper Backfill	30
Erosion Barrier	12
Geotextile Filter Fabric <sup>1</sup>	-
Upper Drainage Layer	12
Upper GCL	0.2
Lower Backfill	49.28
Geotextile Filter Fabric <sup>1</sup>	-
Lower Drainage Layer	6
Lower GCL	0.2
Clean Grout	39.37 (1 m)

<sup>1</sup> It is assumed that a geotextile filter fabric will be placed above the drainage layers to minimize the infiltration of fines from the overlying layers into the drainage layer. However it is not necessary to include the filter fabric in the HELP models.

Table 4.4-2 presents a comparison of the pertinent HELP model results for this configuration with and without the layers above the erosion barrier. As seen in Table 4.4-2 elimination of the layer above the erosion barrier result in significantly less evapotranspiration and significantly more water flux into the upper drainage layer. This increased water flux to the upper drainage layer would require the drainage system to handle additional water volumes and would result in increased infiltration through the upper GCL particularly with any degradation of the GCL. The decrease in evapotranspiration is due the intersection of the evapotranspiration zone with the drainage layer. The evapotranspiration

zone is assumed to extend 22 inches deep from the ground surface (USEPA 1994a; USEPA 1994b). It intersects the top 10 inches of the upper drainage layer with elimination of the layers above the erosion barrier. The drainage layer does not provide effective water storage for evapotranspiration but quickly removes water from the evapotranspiration zone, and therefore decreases the overall evapotranspiration. In order to increase evapotranspiration for the case where the soil layers above the erosion barrier have eroded away, a twelve-inch backfill layer will be placed between the erosion barrier and the upper drainage layer. HELP modeling of this configuration without the layers above the erosion barrier but with the backfill layer between the erosion barrier and upper drainage layer has been performed. See the following appendix for the detailed HELP model input data and output file associated with this configuration:

- Appendix N, Replacement GCL Closure Cap with Erosion Barrier without Overlying Layers Plus Middle Backfill Layer: HELP Model Input Data and Output File (output file name: ZGCLFout.OUT)

A comparison of the HELP model results for this configuration with the other two is also provided in Table 4.4-2. As seen the addition of this backfill layer between the erosion barrier and upper drainage layer, the evapotranspiration greatly improves.

**Table 4.4-2. HELP Model Results for Replacement GCL Closure Cap Configurations with and without Upper Topsoil and Backfill Layers**

HELP Model Output Parameter	Configuration with Upper Topsoil and Backfill Layers	Configuration without Upper Topsoil and Backfill Layers	Deviation	Configuration without Upper Topsoil and Backfill Layers Plus Middle Backfill Layer
Runoff, inches/year	0.16	0.19	Increase of 0.03	0.24
Evapotranspiration, inches/year	34.6	23.7	Decrease of 10.9	29.7
Lateral Drainage from Upper Drainage Layer, inches/year	13.8	24.5	Increase of 10.7	18.6
Percolation / Leakage through Upper GCL, inches/year	0.25	0.43	Increase of 0.18	0.33

#### 4.5 Grout Layer over Vault Roof

The 2002 Saltstone Intruder Special Analysis (Cook et al. 2002a) assumed in the resident scenario intruder analysis that the resident excavates 3 meters deep for construction of a basement. This lead to the requirement for 3 meters of material between the vault top and the top of the erosion barrier in order to prevent the resident from excavating into the Saltstone waste itself. In the Special Analysis, a 1-meter-thick grout layer above the vault roof was added to achieve the requirement for 3 meters of material. According to the Special Analysis the only reason for adding the grout layer was to increase the material thickness between the vault top and the top of the erosion barrier. Typical soil materials would perform the required function as well as grout. Therefore the 1-meter-thick grout layer will be replaced with 1 meter of soil materials.

#### 4.6 Lower Drainage Layer

Previous undocumented PORFLOW modeling has indicated that water could build up on top of the vault, due to the low permeability of the vault roof and the inadequate thickness of the overlying drainage layer particularly as the drainage layer silts-in over time (see Section 5.3). Such a build up increases the hydraulic head, which is the driving force for flow of water through the vault. To minimize build up of water on top of the vault the following changes to the closure cap configuration were made:

- The lower drainage layer thickness was increased from 6 inches to 2 feet,
- A 3-foot wide vertical drainage layer was added along the sides of the vaults, and
- A 5-foot-thick by 10-foot-long drainage layer was added at the base of the vaults.

All three of these layers are interconnected in order to route water off the vault top along the vault sides to the soil layer below the vaults.

#### 4.7 Closure Cap Configuration Summary and Intact Infiltration

The following are the changes that have been made to the closure cap configuration from that described within the current PA, Closure Plan, and PA Intruder Special Analysis (MMES 1992; Cook et al. 2000; Cook et al. 2002a) as outlined in Section 2.0:

- The kaolin hydraulic barriers have been replaced with GCLs (see Section 4.1).
- The drainage system configuration has been revised from that depicted in Figure 4.2-1 to that of Figure 4.2-2. This decreases the slope lengths from a maximum of 600 feet to 300 feet over the vaults. The Figure 4.2-2 configuration has a crest down the centerline of each row of vaults and drainage is directed to the perimeter of the entire disposal area and between the two rows of vaults. (see Section 4.2)
- An erosion barrier separate from and above the upper drainage layer has been added. The erosion barrier is one-foot thick and consists of 2-inch to 6-inch granite stone with a  $d_{50}$  (i.e. median size) of 4 inches. (see Section 4.3)
- A twelve-inch-thick backfill layer has been added between the erosion barrier and the upper drainage layer.
- The 3-meter-thick grout layer has been replaced with 3 meters of soil materials.
- The lower drainage layer thickness has been increased from 6 inches to 2 feet, a 3-foot wide vertical drainage layer has been added along the sides of the vaults, and a 5-foot-thick by 10-foot-long drainage layer has been added at the base of the vaults.

Figure 4.7-1 and Table 4.7-1 present the resulting SDF GCL closure cap configuration. Table 4.7-1 also includes the associated HELP Model soil input data. Additional HELP model input change from the previous modeling include:

- The landfill area modeled has been modified to conform to the Figure 4.2-2 drainage layer configuration as shown in Figure 4.7-1. The area modeled has been changed 350-foot by 250-foot, which results in a surface area of 87,500 feet squared or 2.009 acres.
- The surface slope length has been changed to 350 feet as shown in Figure 4.7-1. This change results in a HELP model computed curve number of 55.20.
- The slope length of the upper drainage layer has been changed to 350 feet.
- The slope length of the lower drainage layer has been changed to 250 feet.

The initial moisture storage has been specified as done in Section 4.1.

HELP modeling of the Table 4.7-1 intact SDF GCL closure cap configuration has been performed as outlined above. Based upon this modeling the infiltration through the upper GCL has been estimated to be 0.29 inches per year for intact conditions. The following appendix provides the detailed HELP model, input data and output file for the intact condition:

- Appendix O, Intact SDF GCL Closure Cap (0 Years): HELP Model Input Data and Output File (output file name: ZGCLout.OUT)

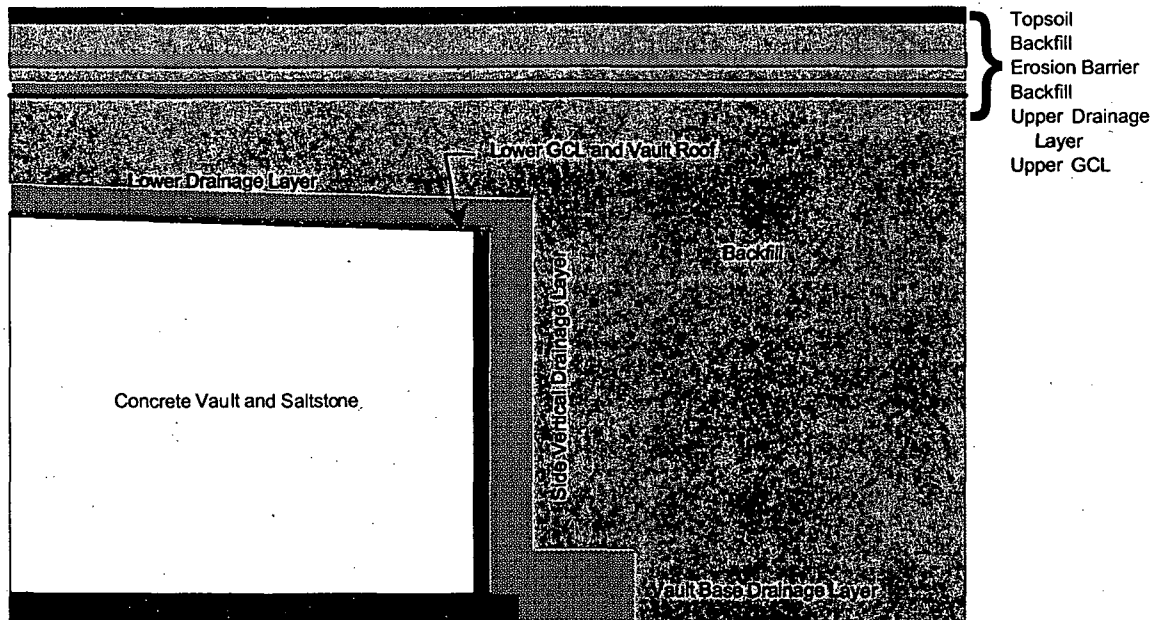
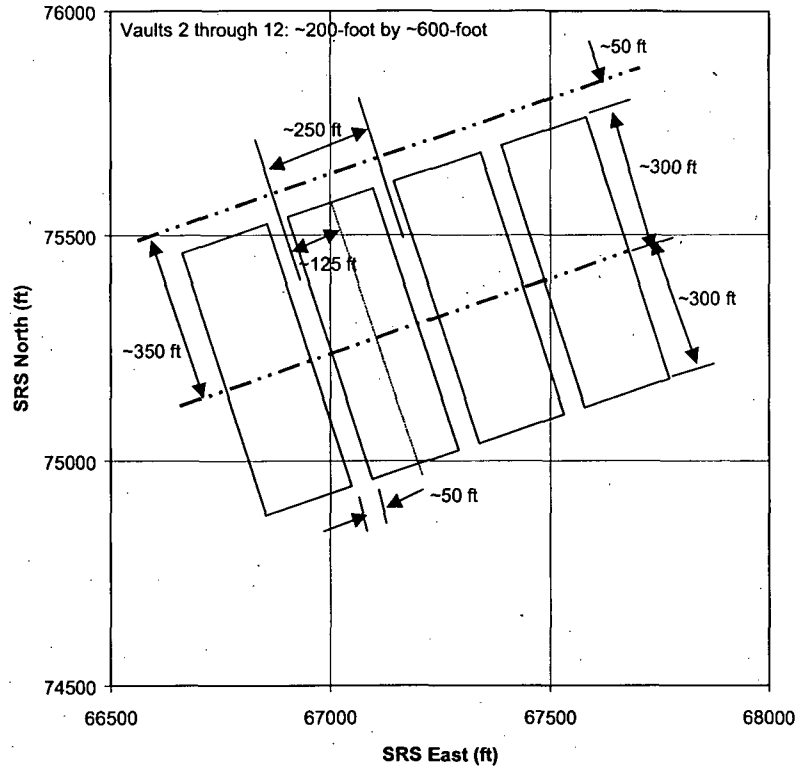


Figure 4.7-1. SDF GCL Closure Cap Configuration

**Table 4.7-1. Intact SDF GCL Closure Cap Configuration and HELP Model Required Soil Property Data**

Layer	Thickness (inches)	Saturated Hydraulic Conductivity (cm/sec)	Total Porosity (Vol/Vol)	Field Capacity (Vol/Vol)	Wilting Point (Vol/Vol)
Topsoil <sup>1</sup>	6	1.00E-03	0.4	0.11	0.058
Upper Backfill <sup>1</sup>	30	1.00E-04	0.37	0.24	0.136
Erosion Barrier <sup>2</sup>	12	3.97E-04	0.06	0.056	0.052
Middle Backfill <sup>1</sup>	12 <sup>6</sup>	1.00E-04	0.37	0.24	0.136
Geotextile Filter Fabric <sup>5</sup>	-	-	-	-	-
Upper Drainage Layer <sup>1</sup>	12	1.00E-01	0.38	0.08	0.013
Upper GCL	0.2	5.00E-09 <sup>3</sup>	0.75 <sup>4</sup>	0.747 <sup>4</sup>	0.40 <sup>4</sup>
Lower Backfill <sup>1</sup>	58.65 <sup>6</sup>	1.00E-04	0.37	0.24	0.136
Geotextile Filter Fabric <sup>5</sup>	-	-	-	-	-
Lower Drainage Layer <sup>1</sup>	24 <sup>6</sup>	1.00E-01	0.38	0.08	0.013
Lower GCL	0.2	5.00E-09 <sup>2</sup>	0.75 <sup>3</sup>	0.747 <sup>3</sup>	0.40 <sup>3</sup>

<sup>1</sup> WSRC 2002.<sup>2</sup> See Section 4.3<sup>3</sup> GSE 2002<sup>4</sup> USEPA 1994a and USEPA 1994b<sup>5</sup> It is assumed that a geotextile filter fabric will be placed above the drainage layers to minimize the infiltration of fines from the overlying layers into the drainage layer. However it is not necessary to include the filter fabric in the HELP models.<sup>6</sup> The 39.37 inches (1 m) of clean grout immediately above the vault roof was replaced with 12 inches of Middle Backfill, 9.37 inches of Lower Backfill, and 18 inches of lower drainage layer.

**THIS PAGE INTENTIONALLY LEFT BLANK**

## 5.0 CLOSURE CAP DEGRADATION

The following three primary closure cap degradation mechanisms have been assumed to significantly impact the infiltration through the closure cap over time:

- Pine forest succession
- Erosion
- Colloidal clay migration

Each of these degradation mechanisms is discussed in detail below.

### 5.1 Pine Forest Succession

According to the PA and Closure Plan the SDF closure cap will be vegetated with bamboo. Bamboo is a shallow-rooted species that quickly establishes a dense ground cover and evapotranspires year-round in the SRS climate. Pine trees are the most deeply rooted naturally occurring plants at SRS. (MMES 1992; Cook et al. 2000). The institutional control to pine forest, land use scenario evaluated herein assumes a 100-year institutional control period following final SDF closure during which the closure cap is maintained. It is assumed that a pine forest begins to encroach upon the bamboo at the end of institutional control, when the approximately 43-acre closure cap (approximate area (~1300 foot by ~1450 foot) over vaults 1 through 12 in Figure 2.0-1) is no longer maintained.

The following discussion of the assumed successional transition from bamboo to pine trees is derived from the following references: Bohm (1979), Burns and Hondala (1990), Ludovici et al. (2002), Taylor (1974), Ulrich et al. (1981), Walkinshaw (1999), and Wilcox (1968).

After institutional control, it is assumed that it will take approximately 100 years for loblolly pine to be established around the closure cap perimeter and for some breakup of the bamboo to begin to occur. Within 10 years of pine tree establishment around the perimeter, the pines begin shading the bamboo located along the perimeter, which allows the establishment of pine tree seedlings 50 feet in from the perimeter of the closure cap. The process of pine tree growth and bamboo shading followed by further seedling encroachment in 50-foot increments toward the cap center continues to occur on a 10-year cycle until the entire closure cap is established with pine trees. 200 years after the end of institutional control it is assumed that the entire cap is covered with pine trees, with the oldest trees near the perimeter and the youngest in the center (i.e. an uneven age distribution).

Because of the age structure difference from edge to center, the second generation, and subsequent ones, will also probably be variable across the cap. Decline of loblolly will begin around 100 years of age. After the second establishment, the new seedlings will be established as "gaps" occur in the overstory, either through the decline or death of a dominant tree, or through abiotic occurrences (wind throw, lightning strikes, fire, insect outbreak, tornado, etc.). This will tend towards making the entire acreage an uneven age, constantly re-establishing forest. In this region, fire may be quite important in the long-term ecology of the cap. Fire will reduce the smaller understory individuals and seedlings, but will have minimal impact on the dominant individuals. It may affect the age structure over long periods of time and make the 43-acre cap closer in age distribution than the original establishment period would indicate.

It is anticipated that tree density will remain fairly constant. For a natural regeneration stand, the tree density is assumed to be approximately 550 dominant and co-dominant trees per acre with approximately 400 mature (i.e. 70 to 125 years old) trees per acre. Smaller trees will be suppressed and die.

It is assumed that mature pine will have 5 deep roots, mainly near the center of the tree spread (i.e., concentrated near main trunk). Of these 5 deep roots, four go to a depth of 6 feet and one to 12 feet.

Deep roots have a diameter of 3 inches in the top foot of soil and taper with depth to 0.25 inches at depth. These roots will be maintained over the life of the tree and exhibit little turnover prior to death. They will enlarge with yearly growth, similar to branches, although anatomically different and at a slower rate. Smaller trees, which are suppressed and die, will not establish deep roots in excess of 4 to 5 feet, and primarily only 1 or 2 such roots. Hard layers and water-saturated layers will slow root penetration. A continuous water surface will stop elongation. Hard layers will eventually be penetrated.

Decomposition of roots near the ground surface should occur fairly quickly due to better microclimate for microbial populations than at depth. Decomposition of roots at depth will be fairly slow, depending on the soil environment and aeration. It is assumed that it will take 25 years for the decomposition of intermediate depth roots and 30 years at depth due to the soil environment. Some shrinkage of the deep roots may occur at depth and provide a channel for water or sediment movement along the surface. Very rapid yearly turnover of fine roots and feeder roots occurs in the soil, although these are primarily in the top 18 inches of soil and will not go vertically with any intensity or longevity.

Based upon this discussion the following assumptions are made relative to the succession of bamboo by a pine forest for this evaluation:

- 200 years after the end of institutional control it is assumed that the entire cap is dominated by pine.
- Complete turnover of the 400 mature trees per acre occurs every 100 years (in a staggered manner).
- There are 400 mature trees per acre with 4 roots to 6 feet and 1 root to 12 feet. The roots are 3 inches in diameter at a depth of 1 foot and 0.25 inches in diameter at either 6 or 12 feet, whichever is applicable.

## 5.2 Erosion

The topsoil and upper backfill layers, which are located above the erosion barrier, are subject to erosion. For the institutional control to pine forest land use scenario, it is assumed that the closure cap will be vegetated with bamboo during the institutional control period, with a combination of bamboo and pine trees for 200 years immediately following the institutional control period, and with a pine forest thereafter. The projected erosion rate for both the topsoil and upper backfill layers has been determined utilizing the Universal Soil Loss Equation (Horton and Wilhite 1978; Goldman et al. 1986). The Universal Soil Loss Equation is expressed as:

$$A = R \times K \times LS \times C \times P \quad (\text{Eq. 5.2-1})$$

where

A = soil loss (tons/acre/year)

R = rainfall erosion index (100 ft·ton/acre per in/hr)

K = soil erodibility factor, tons/acre per unit of R

LS = slope length and steepness factor, dimensionless

C = vegetative cover factor, dimensionless

P = erosion control practice factor, dimensionless

The erosion rate for the SRP Burial Grounds (i.e. current SRS E-Area) was previously estimated and documented by Horton and Wilhite (1978) as provided in Table 5.2-1.

**Table 5.2-1. Previous SRP Burial Grounds Estimated Erosion Rate (Horton and Wilhite 1978)**

Parameter	Value Utilized	Comment
R	260	-
K	0.28	Dothan subsoil
LS	0.67	1000 foot long 2% slope
C	0.001	Natural successional forest
P	1	No supporting practices
A (soil loss)	0.05 tons/acre/year	-
A (soil loss)	0.0007 cm/year	Assuming dry bulk density of 1.6 g/cm <sup>3</sup>

The following are estimated parameter values based upon Horton and Wilhite 1978 and Goldman et al. 1986:

- From Figure 5.2 of Goldman et al. (1986), R is slightly greater than 250 but significantly less than 300 100 ft-ton/acre per in/hr. Therefore will utilize the Horton and Wilhite 1978 R value of 260 100 ft-ton/acre per in/hr
- From Figure 5.6 of Goldman et al. (1986):
  - If topsoil is assumed to consist of 70% sand, 25% silt, and 5% clay, K equals 0.28 tons/acre per unit of R.
  - If backfill is assumed to consist of 70% sand, 20% silt, and 10% clay, K equals 0.20 tons/acre per unit of R.
- With a slope length of 350 feet (see Figure 4.2-2) and a slope of 3% the LS value equals 0.40 as determined from Table 5.5 of Goldman et al. (1986).
- Will assume that both bamboo and a pine forest, have C values of a natural successional forest, therefore the C value equals 0.001 as utilized by Horton and Wilhite (1978).
- No supporting practices are associated with the closure cap therefore P equals 1.

Based upon the Universal Soil Loss Equation and the parameter values listed above the following are the estimated soil losses:

- Topsoil with a natural successional forest has an estimated soil loss of 0.0291 tons/acre/year ( $A = 260 \times 0.28 \times 0.40 \times 0.001 \times 1$ ). Based upon the dry bulk density the estimated soil loss can be converted to a loss in terms of depth of loss per year. From Jones and Phifer (2002), the dry bulk density of topsoil was taken as 90 lbs/ft<sup>3</sup>. Topsoil with a natural successional forest has an estimated depth of soil loss of approximately 1.8E-04 inches/year ( $Loss = \frac{0.0291 \text{ tons / acre / year} \times 2000 \text{ lbs / ton} \times 12 \text{ inches / foot}}{43560 \text{ ft}^2 / \text{acre} \times 90 \text{ lbs / ft}^3}$ ).
- Backfill with a natural successional forest has an estimated soil loss of 0.0208 tons/acre/year ( $A = 260 \times 0.20 \times 0.40 \times 0.001 \times 1$ ). Based upon the dry bulk density the estimated soil loss can be converted to a loss in terms of depth of loss per year. From Jones and Phifer (2002), the dry bulk density of backfill was taken as 104 lbs/ft<sup>3</sup>. Backfill with a natural successional forest has an

estimated depth of soil loss of approximately 1.1E-04 inches/year  
 (Loss =  $\frac{0.0208 \text{ tons / acre / year} \times 2000 \text{ lbs / ton} \times 12 \text{ inches / foot}}{43560 \text{ ft}^2 \text{ / acre} \times 104 \text{ lbs / ft}^3}$ ).

The previous estimated erosion rate of 0.0007 cm/year (2.8E-04 inches/year) for the SRP Burial Grounds (Horton and Wilhite 1978) compares well with the current estimates for the SDF closure cap of 1.8E-04 and 1.1E-04 inches/year for topsoil and backfill, respectively. The primary difference in input between the two estimates is associated with the site-specific slopes and slope lengths.

### 5.3 Colloidal Clay Migration

It is assumed that colloidal clay migrates from overlying backfill layers and accumulates in the drainage layers reducing the saturated hydraulic conductivity of the drainage layers over time. The clay minerals (in order of predominance) at SRS are shown in Table 5.3-1 along with the percentage range of the clay mineral fraction and typical range in particle size for each. Colloids can be mineral grains such as clays, which have particle sizes between 0.01 and 10  $\mu\text{m}$  (Looney and Falta 2000). Colloidal clay can exist in groundwater in concentrations up to 63 mg/L as measured by suspended solids (Puls and Powell 1991). Based upon this information and the previous assumption, it will be assumed that water flux driven colloidal clay migration at a concentration of 63 mg/L occurs from overlying backfill layers to the drainage layers. It will be further assumed that the colloidal clay accumulates in the drainage layer from the bottom up filling the void space of the drainage layer with clay at a density of 1.1 g/cm<sup>3</sup> (Hillel 1982). These assumptions are analogous to the formation of the B soil horizon as documented in the soil science literature. Clay translocation is a very slow process where discrete clay particles are washed out in slightly acidic conditions and deposited lower in the soil profile (McRae 1988). Evidence has been found that the B-horizon where the translocated clay is deposited may form at a rate of 10 inches per 5,000 years (Buol et al. 1973).

Table 5.3-1. SRS Clay Minerals

Clay Mineral	Percentage Range of the Clay Mineral Fraction <sup>1</sup> (%)	Typical Particle Size Range <sup>2</sup> ( $\mu\text{m}$ )
Kaolinite	62.6 to 98.8	0.1 to 4
Vermiculite	0.7 to 34.3	0.1 to 2
Illite	0 to 7.1	0.1 to 2

<sup>1</sup> Looney et al. (1990), Table 6.31

<sup>2</sup> Mitchell (1993)

### 5.4 Closure Cap Degradation Summary

Base upon the assumed closure cap degradation mechanisms, pine forest succession, erosion, and colloidal clay migration, an assumed degradation scenario has been assumed for each layer as outlined in Table 5.4-1. These degradation scenarios form the basis for modifying the thickness and hydraulic properties of each layer over time. This information will be utilized in section 6.0 to determine infiltration through the upper GCL over time.

**Table 5.4-1. SDF GCL Closure Cap Layer Degradation Scenarios**

Layer	Degradation Scenario
Vegetation	Bamboo is maintained during the 100-year institutional control period, pine trees begin to encroach upon the bamboo at the end of institutional control, and a pine forest covers the cap 200 years after the end of institutional control.
Topsoil	Topsoil erosion occurs at 1.8E-04 inches per year.
Upper Backfill	Backfill erosion occurs at 1.1E-04 inches per years, after the topsoil layer has been depleted.
Erosion Control Barrier	Maintenance during institutional control period prevents degradation of the erosion control barrier. However pine forest succession and associated root penetration results in holes through the erosion control barrier. This does not impact its ability to function as an erosion barrier, however it allows the overlying backfill to fill the holes left after the roots decompose.
Middle Backfill	Colloidal clay migration from the 1-foot-thick middle backfill to the underlying 1-foot-thick upper drainage layer causes the saturated hydraulic conductivity to increase over time.
Geotextile Filter Fabric	For purposes of colloidal clay migration into the underlying drainage layer the geotextile filter fabric is assumed to be ineffective over the time period under consideration.
Upper Drainage Layer	Colloidal clay migration from the overlying 1-foot-thick backfill into the 1-foot-thick upper drainage layer causes the saturated hydraulic conductivity to decrease over time.
Upper GCL	Maintenance during institutional control period prevents degradation of the upper GCL. However pine forest succession and associated root penetration results in holes through the GCL. This allows the overlying drainage layer to fill the holes after the roots decompose.
Lower Backfill	None. While it is assumed that colloidal clay migration from this layer to the underlying lower drainage layer occurs, it is also assumed that the thickness of the lower backfill layer (almost 5-foot) relative to the lower drainage layer (2-foot) prevents the quantity of clay loss necessary to change the hydraulic properties of the lower backfill.
Geotextile Filter Fabric	For purposes of colloidal clay migration into the underlying drainage layer the geotextile filter fabric is assumed to be ineffective over the time period under consideration.
Lower Drainage Layer	Colloidal clay migration from the overlying ~5-foot-thick lower backfill into the 1-foot-thick lower drainage layer reduces its saturated hydraulic conductivity over time.
Lower GCL	None. Pine tree roots do not penetration to a sufficient enough depth to impact this layer. Additionally the underlying concrete vault roof along with the GCL produces a hard layer and continuous water saturation within and above these layers so that root elongation is stopped.
Side Vertical Drainage Layer <sup>1</sup>	None, until the vault base drainage layer has been filled with colloidal clay.
Vault Base Drainage Layer <sup>1</sup>	Colloidal clay migrates from the overlying ~30-foot-thick backfill into the 5-foot-thick drainage layer reduces its saturated hydraulic conductivity over time.

<sup>1</sup> These layers are not included in the HELP model for determination of the infiltration through the upper GCL. However their degradation properties will be included in the subsequent PORFLOW vadose zone modeling.

**THIS PAGE INTENTIONALLY LEFT BLANK**

## 6.0 CLOSURE CAP INFILTRATION

### 6.1 Degraded Layer Properties over Time

The SDF GCL closure cap initial (0 year) intact layer thickness and hydraulic property values from top to bottom are provided in Table 4.7-1. The degradation scenarios for each layer are provided in Table 5.4-1. Based upon the Table 5.4-1 degradation scenarios, the Table 4.7-1 initial SDF closure cap layer thickness and hydraulic property values have been modified to account for degradation at 100, 300, 550, 1,000, 1,800, 3,400, 5,600 and 10,000 years after closure of the SDF. The following discussions provide additional detail associated with determination of the degraded properties for the erosion barrier, upper GCL, middle backfill, upper drainage layer, lower drainage layer, and vault base drainage layer.

#### 6.1.1 Erosion Barrier

Maintenance during the institutional control period prevents degradation of the erosion barrier. However pine forest succession and associated root penetration results in holes through the erosion control barrier. This does not impact its ability to function as an erosion barrier, however it allows the overlying backfill to fill the holes after the roots decompose. It is assumed that the hydraulic conductivity of the infiltrating backfill increases one order of magnitude (i.e. from  $1.0E-04$  to  $1.0E-03$  cm/s) when it fills the hole since it will not be mechanically compacted at that time. The equivalent hydraulic properties of the overall erosion barrier change as the area of holes filled with backfill material increases with time. The equivalent hydraulic properties have been estimated over time by area proportioning the properties between that of the intact erosion barrier and infiltrating backfill.

#### 6.1.2 Upper GCL

Maintenance during the institutional control period prevents degradation of the upper GCL. However pine forest succession and associated root penetration results in holes through the erosion barrier. This allows the overlying drainage layer to fill the holes after the roots decompose. The holes in the GCL essentially act as direct conduits from the upper drainage layer to the lower backfill layer. When saturated conditions occur in the drainage layer after major precipitation events, cones of depression are created around the holes in the GCL with a radius of influence much greater than the radius of the hole. This means that a small area of GCL holes can greatly reduce the lateral flow of water in the drainage layer and increase the vertical flow into the lower backfill. Due to the significant influence of holes in the GCL to the quantity of infiltration, the use of equivalent hydraulic properties is not appropriate, since it does not consider the radius of influence associated with holes. Therefore, within the HELP model the degraded GCL has been modeled as a geomembrane liner with leakage through holes. The HELP model considers both water flux through intact portions of the geomembrane using an "equivalent geomembrane hydraulic conductivity" and water flux through holes in the geomembrane. The HELP model does not assign a porosity, field capacity, or wilting point to geomembranes, however this is not considered essential to the GCL, since it is assumed that the GCL will remain fully saturated and it is below the depth where evapotranspiration is assumed to occur. The HELP model allows the input of up to 999,999 one square centimeter installation defects for a geomembrane liner. Therefore the calculated area of holes created by root penetration has been converted into an equivalent number of one square centimeter installation defects for input to the HELP model. Excellent contact is assumed between the GCL and underlying backfill layer as a HELP model input, since the GCL is put in dry and swells into the surrounding soil as it hydrates.

### 6.1.3 Middle Backfill and Upper Drainage Layer

It is assumed that water flux driven colloidal-clay migration from the 1-foot-thick middle backfill to the underlying 1-foot-thick upper drainage layer causes the middle backfill saturated hydraulic conductivity to increase over time and that of the upper drainage layer to decrease over time. It has been assumed that clay migration occurs out of the backfill into the drainage layer with the water flux containing 63 mg/L of colloidal clay. Since both layers are of the same thickness and the middle backfill layer has limited clay content, it has been assumed that half the clay content of the backfill will migrate into the drainage layer. At which point the two layers essentially become the same material and material property changes cease. Based upon this it will be assumed that the endpoint saturated hydraulic conductivity of the layers will become that of the log mid-point between the initial backfill and upper drainage layer conditions. It will also be assumed that the endpoint porosity, field capacity, and wilting point will become the arithmetic average of the backfill and upper drainage layer. The hydraulic properties at times prior to the endpoint have been proportioned between that of the endpoint properties and the initial properties based upon the fraction of clay that has migrated out of the backfill.

### 6.1.4 Lower Drainage Layer

It is assumed that colloidal clay migration from the approximately 5-foot-thick overlying backfill into the 2-foot-thick lower drainage layer is driven by the water flux through the upper GCL. This water flux driven clay migration enters into the lower drainage layer and fills the lower drainage layer from the bottom up. This reduces the saturated hydraulic conductivity of the clay-filled portion from 1.0E-01 to 1.0E-04 cm/s (i.e. to the saturated hydraulic conductivity of the overlying backfill), while the conductivity of the clean portion remains at 1.0E-01 cm/s. As the thickness of the lower drainage layer filled with clay increases, the equivalent hydraulic conductivity of the entire layer decreases. The equivalent horizontal hydraulic conductivity for this layer has been determined from the following equation (Freeze and Cherry 1979):

$$K_h = \sum_{i=1}^n \frac{K_i d_i}{d} \quad (\text{Eq. 6.1-1})$$

where

- $K_h$  = equivalent horizontal saturated hydraulic conductivity,
- $K_i$  = horizontal saturated hydraulic conductivity of  $i^{\text{th}}$  layer,
- $d_i$  = thickness of  $i^{\text{th}}$  layer,
- $d$  = total thickness

This is different from that assumed for the upper drainage layer, since the lower drainage layer has significantly more backfill overlying it.

### 6.1.5 Vault Base Drainage Layer

It is assumed that colloidal clay migration, from the overlying backfill (approximately 30 feet) into the 5-foot-thick vault base drainage layer, is driven by the water flux through the upper GCL. This water-flux-driven clay migration enters into the vault base drainage layer and fills the lower drainage layer from the bottom up. The saturated hydraulic conductivity of the clay-filled portion is reduced from 1.0E-01 to 1.0E-04 cm/s (i.e. the saturated hydraulic conductivity of the overlying backfill layer), while the conductivity of the clean portion remains at 1.0E-01 cm/s. The thickness of the clay-

filled portion increases with time, while the thickness of the clean portion decreases with time. This is essentially the same process as that described above for the lower drainage layer.

The calculations associated with determination of the layer thicknesses and hydraulic property values over time are provided in Appendix P. Table 6.1-1 provides the primary Appendix P, material property results (thickness, saturated hydraulic conductivity, and holes in the upper GCL), for layers which change with time and were utilized in subsequent HELP modeling. The porosity, field capacity, and wilting points are not provided in Table 6.1-1. Values for these parameters are provided in Appendix P.

**Table 6.1-1. Material Property Summary Results for HELP Modeling from Appendix P**

Year	Vegetation	Topsoil Layer Thickness (inches)	Erosion Barrier Saturated Hydraulic Conductivity (cm/s)	Middle Backfill Layer Saturated Hydraulic Conductivity (cm/s)
0	Bamboo	6	3.97E-04	1.00E-04
100	Bamboo	5.982	3.97E-04	1.20E-04
300	Pine Forest	5.946	3.98E-04	1.60E-04
550	Pine Forest	5.901	3.99E-04	2.30E-04
1,000	Pine Forest	5.82	4.01E-04	4.60E-04
1,800	Pine Forest	5.676	4.06E-04	1.60E-03
3,400	Pine Forest	5.388	4.15E-04	3.20E-03
5,600	Pine Forest	4.992	4.27E-04	3.20E-03
10,000	Pine Forest	4.2	4.51E-04	3.20E-03
Year	Upper Drainage Layer Saturated Hydraulic Conductivity (cm/s)	One Square Centimeter Holes in Upper GCL <sup>1</sup> (#/acre)	Lower Drainage Layer Saturated Hydraulic Conductivity (cm/s)	
0	1.00E-01	0	1.00E-01	
100	8.60E-02	0	1.00E-01	
300	6.30E-02	7,432	9.98E-02	
550	4.30E-02	26,013	9.91E-02	
1,000	2.10E-02	59,458	9.64E-02	
1,800	6.30E-03	118,916	9.01E-02	
3,400	3.20E-03	237,832	7.62E-02	
5,600	3.20E-03	401,341	5.68E-02	
10,000	3.20E-03	728,360	1.81E-02	

<sup>1</sup> Number of HELP model installation defects

## 6.2 Degraded Closure Cap Infiltration over Time

Table 6.1-1 and Appendix P data were utilized as input to the HELP model (USEPA 1994a and USEPA 1994b) in order to determine infiltration through the upper GCL at each degraded time step. The following appendices provide the detailed HELP model, input data and output files for each time step:

- Appendix Q, Degraded SDF GCL Closure Cap (100 Years): HELP Model Input Data and Output File (output file name: ZGCLD1ou.OUT)
- Appendix R, Degraded SDF GCL Closure Cap (300 Years): HELP Model Input Data and Output File (output file name: ZGCLD2ou.OUT)
- Appendix S, Degraded SDF GCL Closure Cap (550 Years): HELP Model Input Data and Output File (output file name: ZGCLD3ou.OUT)
- Appendix T, Degraded SDF GCL Closure Cap (1,000 Years): HELP Model Input Data and Output File (output file name: ZGCLD4ou.OUT)
- Appendix U, Degraded SDF GCL Closure Cap (1,800 Years): HELP Model Input Data and Output File (output file name: ZGCLD5ou.OUT)
- Appendix V, Degraded SDF GCL Closure Cap (3,400 Years): HELP Model Input Data and Output File (output file name: ZGCLD6ou.OUT)
- Appendix W, Degraded SDF GCL Closure Cap (5,600 Years): HELP Model Input Data and Output File (output file name: ZGCLD7ou.OUT)
- Appendix X, Degraded SDF GCL Closure Cap (10,000 Years): HELP Model Input Data and Output File (output file name: ZGCLD8ou.OUT)

The following outputs from this evaluation are necessary inputs to the subsequent PORFLOW vadose zone modeling:

- Infiltration through the upper GCL
- Saturated hydraulic conductivity of the 2-foot-thick lower Drainage Layer
- Saturated hydraulic conductivity of the 3-foot-thick Side Vertical Drainage Layer
- Saturated hydraulic conductivity of the 5-foot-thick Vault Base Drainage Layer

Table 6.2-1 provides a summary of these parameter values. The 3-foot Side Vertical Drainage Layer is assumed to have no degradation within the 10,000-year time frame. Rather than denoting the degradation of the Vault Base Drainage Layer with a single saturated hydraulic conductivity value, its degradation has been denoted as an upper thickness with a saturated hydraulic conductivity of 0.1 cm/s and a lower thickness with a saturated hydraulic conductivity of 0.0001 cm/s. Figure 6.2-1 additionally provides the infiltration through the upper GCL over time in graphical format.

**Table 6.2-1. Inputs for PORFLOW Vadose Zone Modeling**

Year	Infiltration through Upper GCL (in/yr)	Lower Drainage Layer Saturated Hydraulic Conductivity (cm/s)	Side Vertical Drainage Layer Saturated Hydraulic Conductivity (cm/s)	Thickness of Upper Portion of the Vault Base Drainage Layer with a K of 0.1 cm/s (feet)	Thickness of Lower Portion of the Vault Base Drainage Layer with a K of 0.0001 cm/s (feet)
0	0.29165	1.00E-01	1.00E-01	5	0
100	0.33135	1.00E-01	1.00E-01	4.9996	0.0004
300	2.48161	9.98E-02	1.00E-01	4.996	0.004
550	7.01335	9.91E-02	1.00E-01	4.98	0.02
1,000	11.55066	9.64E-02	1.00E-01	4.93	0.07
1,800	13.65308	9.01E-02	1.00E-01	4.8	0.2
3,400	14.00566	7.62E-02	1.00E-01	4.52	0.48
5,600	14.05202	5.68E-02	1.00E-01	4.14	0.86
10,000	14.09426	1.81E-02	1.00E-01	3.36	1.64

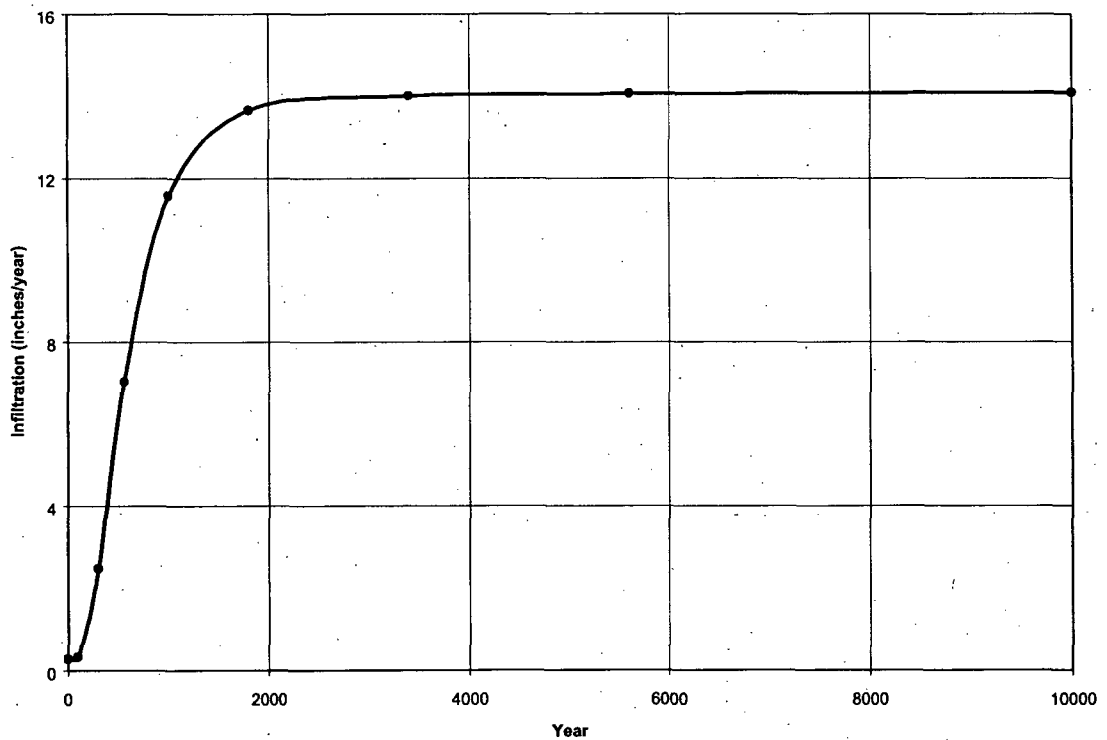
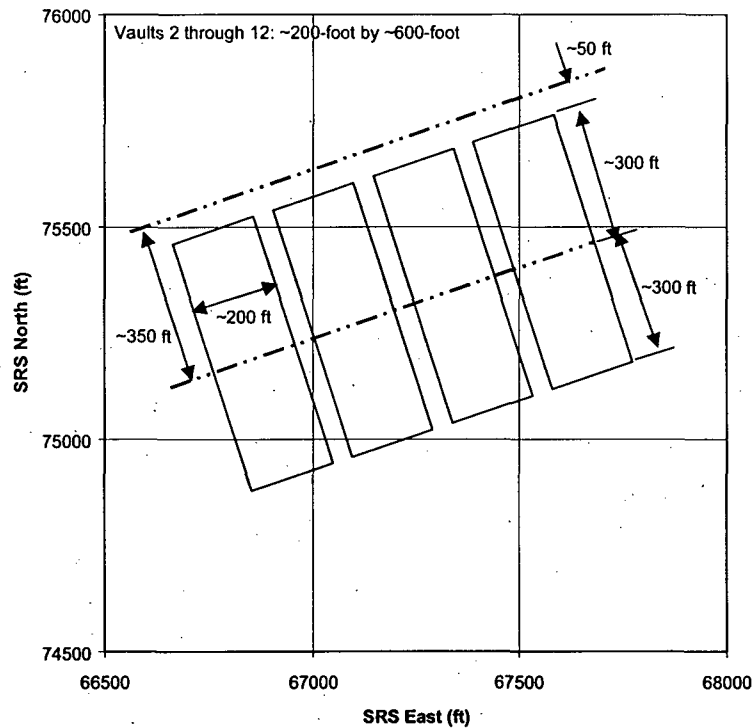


**Figure 6.2-1. Infiltration through Upper GCL**

**THIS PAGE INTENTIONALLY LEFT BLANK**

## Appendix K, Erosion Barrier Sizing and Material Properties

The erosion barrier has been sized based upon the maximum precipitation event for a 10,000-year return period. The maximum precipitation event for a 10,000-year return period is 3.3 inches over a 15-minute accumulation period (Table XIX from Weber et al. (1998)). The figure below shows that the maximum drainage length is 350 feet over a 200-foot wide vault.



Determine the maximum flow ( $Q$  in  $\text{ft}^3/\text{s}$ ) resulting from the 3.3-inch over a 15-minute accumulation period rainfall event:

To be conservative it has been assumed that all rainfall results in runoff and that there is no lag period due to the 350-foot flow path (that is all the rainfall over the entire area immediately becomes discharge out the end of the area).

$$Q = \frac{(P/12 \text{ in/ft}) \times (350' \times 200')}{D \times 60 \text{ min/hr} \times 60 \text{ s/min}}, \text{ where } P = \text{precipitation in inches and } D = \text{duration in hours}$$

$$Q = 1.62 \frac{P}{D}, \text{ where } P = 3.3 \text{ inches and } D = 15 \text{ minutes} = 0.25 \text{ hours}$$

$$Q = 1.62 \frac{3.3}{0.25} \text{ ft}^3/\text{s}, \text{ over a 200-foot width}$$

$$Q = 21.4 \text{ ft}^3/\text{s}, \text{ over a 200-foot width}$$

Determine the approximate depth of flow using Manning's equation (Clark et al. 1977):

$$V = \frac{1.49}{n} R^{2/3} S^{1/2}, \text{ where } V = \text{velocity, fps; } n = \text{coefficient of roughness;}$$

$R$  = hydraulic radius, ft; and  $S$  = slope

$$V = \frac{Q}{A}, \text{ where } V = \text{velocity, ft/s; } Q = \text{flow, ft}^3/\text{s; } A = \text{area, ft}^2$$

$$Q = 21.4 \text{ ft}^3/\text{s}, \text{ over a 200-foot width (i.e. } b)$$

$$A = bd, \text{ where } b = \text{width, ft; } d = \text{depth, ft}$$

$$A = 200d \text{ ft}^2$$

insert values:

$$V = \frac{21.4 \text{ ft}^3/\text{s}}{200d \text{ ft}^2}$$

Assume the use of 2-inch to 6-inch granite stone with a  $d_{50}$  (i.e. median size) of 4 inches. From Figure 7.29 of Goldman (1986):  $n = 0.033$

$$R = A/\text{wetted perimeter} = A/(b + 2d)$$

$$R = 200d/(200 + 2d)$$

$$3\% \text{ slope (see Section 2.0): } S = 0.03$$

insert values:

$$\frac{21.4}{200d} = \frac{1.49}{0.033} \left( \frac{200d}{200 + 2d} \right)^{2/3} (0.03)^{1/2}$$

$$0.0137 = d \left( \frac{200d}{200 + 2d} \right)^{2/3}$$

Given d	0.0137
0.1	0.0215
0.08	0.0148
0.075	0.0133
0.076	0.0136

$$d \approx 0.076$$

Determine if the use of a 2-inch to 6-inch granite stone with a  $d_{50}$  (i.e. median size) of 4 inches is satisfactory to perform as an erosion barrier for a 10,000-year return period, maximum precipitation event:

$$b/d = 200'/0.076' = 2632, \text{ therefore } b/d > 50.$$

From Figure 7.30 of Goldman (1986): Since the  $b/d > 50$  then the P/R is greater than 60.

From Figure 7.31 of Goldman (1986): With a slope (S) of 0.03, a flow (Q) of 21.4 ft<sup>3</sup>/s, and a P/R > 60, the minimum d<sub>50</sub> of the stone must be approximately 3 inches.

Therefore the use of a 2-inch to 6-inch granite stone with a d<sub>50</sub> (i.e. median size) of 4 inches is satisfactory to perform as an erosion barrier for a 10,000-year return period, maximum precipitation event.

The selection of the 2-inch to 6-inch granite stone as an erosion barrier is also satisfactory versus Figure C-3 of Logan 1997.

Based upon NCSU 1991 the 2-inch to 6-inch granite stone is a common sized erosion control stone. NCSU 1991 also indicates the minimum thickness of the erosion control stone must be 1.5 times the maximum stone diameter. That is the thickness must be at least 9 inches for a maximum 6-inch stone. A 12-inch thickness of 2-inch to 6-inch granite stone with a d<sub>50</sub> (i.e. median size) of 4 inches will be utilized as the erosion barrier.

Determine the combined soil material properties for the 2-inch to 6-inch granite stone filled with CLSM or Flowable Fill:

The porosity of the 2-inch to 6-inch granite stone with a d<sub>50</sub> (i.e. median size) of 4 inches is taken as 0.397 based upon the porosity of poorly graded gravel from USEPA 1994a and USEPA 1994b.

Typical CLSM or Flowable Fill properties based upon a May 8, 2003 personal conversation with Christine A. Langton:

Typical CLSM consists of sand with a porosity of 30%, with the pore space filled with 50% porosity binder and has a saturated hydraulic conductivity of 1.0E-03 cm/s.

Based upon this information the following are the assumed properties of the CLSM:

Property	Property Value
Saturated Hydraulic Conductivity	1.0E-03 cm/s
Porosity	$0.30 \times 0.50 = 0.15$
Field Capacity <sup>1</sup>	0.14
Wilting Point <sup>1</sup>	0.13

<sup>1</sup> Field capacity is assumed to be 0.01 less than the porosity, and the wilting point is assumed to be 0.01 less than the field capacity based upon the porosity-wilting point-field capacity relationship of the clean grout and concrete vault roof and floor, which like the CLSM uses cement as the binder.

The matrix of an individual granite stone itself is considered impermeable and non-porous. The porosity of a layer of granite stone is considered to be 0.397. When the granite stone porosity is filled with CLSM, the resultant hydraulic properties, which are area or volume based, become that of the CLSM times the granite stone porosity. The resultant hydraulic properties are shown below:

Property	Property Value
Saturated Hydraulic Conductivity	$1.0E-03 \text{ cm/s} \times 0.397 = 3.97E-04 \text{ cm/s}$
Porosity	$0.15 \times 0.397 = 0.06$
Field Capacity <sup>1</sup>	$0.14 \times 0.397 = 0.056$
Wilting Point <sup>1</sup>	$0.13 \times 0.397 = 0.052$

Taylor, H.M. 1974

# The Plant Root and Its Environment

*Proceedings of an institute  
sponsored by the Southern Regional Education Board,  
held at Virginia Polytechnic Institute and State University,  
July 5-16, 1971*

*edited by E. W. Carson*

Virginia Polytechnic Institute  
and State University

University Press of Virginia

Charlottesville

# 11. Root Behavior as Affected by Soil Structure and Strength

*Howard M. Taylor*

AGRICULTURAL workers have long known that soil physical properties affect agricultural usage. For example, Xenophon (about 400 B.C.) recommended spring plowing because the land is more friable at that time. Virgil (70-19 B.C.) described a method for determining soil bulk density and stated that "loose soils provide bounteous vines but dense soils provide reluctant clods and stiff ridges" (Tisdale and Nelson, 1966).

Today's agricultural workers often discuss effects of soil structure on crop growth or tillage energy requirements. However, the term *soil structure* means different soil properties to different people. Some people have considered part or all of the research in soil tilth, consistence, strength, friability, bulk density, aggregation, porosity, fabric, matric, plasma, pedality, and texture to be part of soil structure research. In this discussion, *soil structure* is defined as "the physical constitution of a soil material as expressed by the size, shape and arrangement of the solid particles and voids, including both the primary particles to form compound particles and the compound particles themselves" (Brewer, 1964). *Soil strength* is defined as "the ability or capacity of a particular soil in a particular condition to resist or endure an applied force" (Gill and Vanden Berg, 1967). This article describes effects of both soil structure and soil strength on root behavior.

## I. MECHANICS OF ROOT ELONGATION

### *A. Elongation through Resisting Systems*

A particular root increases in length during primary growth when cells of the meristematic region divide, elongate, and push the root tip forward

Contribution from the Soil and Water Conservation Research Division, Agricultural Research Service, U.S. Department of Agriculture, in cooperation with the Department of Agronomy and Soils, Alabama Agricultural Experiment Station, Auburn University, Auburn, Alabama 36830.

through the surrounding material. Turgor pressure in the elongating cells is the driving force and must be sufficient to overcome the cell wall constraints and any additional constraints imposed by the external material (Lockhart, 1965). Thus, cellular turgor pressure, resistance of the cell walls to strain, and resistance of the external medium to deformation are important in evaluating root growth through resisting systems. Soil physical conditions, directly or indirectly, will affect the magnitudes of all three factors.

### B. Root Growth Pressure

The pressure available for a root to accomplish work against an external constraint has been termed *root growth pressure* (Gill and Bolt, 1955). Mathematically, root growth pressure is defined as

$$(\Sigma F_t - \Sigma F_{cw})/A,$$

where  $\Sigma F_t$  is the summation of the longitudinal forces in the root that arise as a result of cellular turgor pressure (dynes),  $\Sigma F_{cw}$  is the summation of those longitudinal forces that arise in the cell walls and tend to resist cellular elongation (dynes), and  $A$  is the cross-sectional area of the root at the plane where force is determined ( $\text{cm}^2$ ).

It is extremely difficult to measure directly either turgor pressure or cell wall constraint. However, several investigations have determined the longitudinal force that a plant root can exert across a nonencased zone between two sections of encased root. For the first 2 or 3 hours, the force transmitted across this zone was small. Presumably, turgor forces are almost balanced by cell wall forces. After 12 to 18 hours, the force exerted across the nonencased zone reaches a maximum, and the force per unit area of root is about equal to the average osmotic pressure of the cellular contents (Taylor and Ratliff, 1969a). At that time, it appears that the cell wall forces must be small because a force almost equal to the turgor pressure is transmitted to an external sensor (or external media).

#### 1. Magnitudes

When the root was exerting its maximum force, root growth pressures usually ranged from 9 to 13 bars (Fig. 11.1) (Pfeffer, 1893; Stolzy and Barley, 1968; Taylor and Ratliff, 1969a; Eavis *et al.*, 1969).

#### 2. Effects of Environmental Factors

Root growth pressure of cotton (*Gossypium hirsutum* L.) was reduced from 11 bars to 5 bars when air surrounding the roots was reduced in

oxygen content from 21% to 3% (Eavis *et al.*, 1969). This reduced oxygen supply could affect root growth pressure either by reducing the turgor pressure or by increasing the cell wall constraint. For turgor pressure to decrease, water would have to be transferred longitudinally in the root, or the osmotic concentration in that portion of root would have to be shifted substantially. Huck (1970) showed that a reduced oxygen supply stopped root elongation almost instantaneously. Therefore, it seems somewhat more probable that lack of oxygen decreases root growth pressure by increasing the cell wall constraint. However, definitive measurements have not been used to check this hypothesis.

3. Research Needed

No known investigations have determined variation in growth pressure among the roots on the same plant. In addition, it is not known how

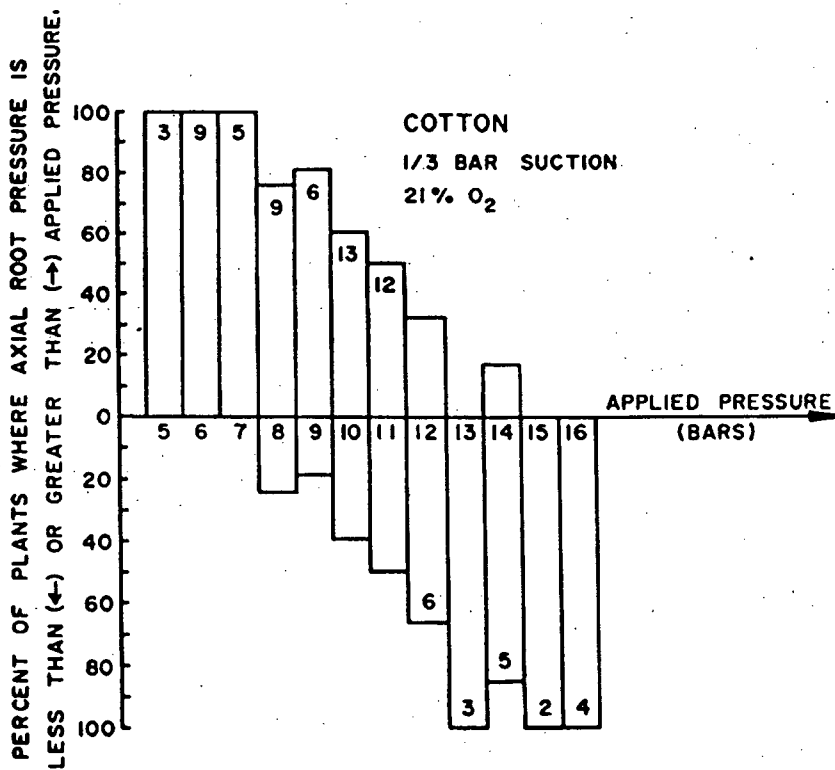


Fig. 11.1. Percentage of cotton (*Gossypium hirsutum* L.) plants with root growth pressure sufficient (*above line*) or insufficient (*below line*) to lift the pressure applied by a dead load. The number of plants used in the test is indicated within each applied pressure interval. (Eavis *et al.*, 1969)

growth pressure of a particular root varies from one time to another, or how growth pressure is affected by hormonal activity, soil chemical environment, or temperature.

## II. ROOT ELONGATION THROUGH A SOIL WITH UNIFORM FABRIC

Soil fabric, which is "the physical constitution of a soil material as expressed by the spatial arrangement of the solid particles and voids" (Brewer, 1964), is extremely important in root growth. Soil fabric determines physical behavior and controls water, heat, aeration, and strength relations important in root growth.

### A. Soil Strength Effects

If the soil has no continuous pores that are large in relation to the root tip, elongation rates will depend on the magnitude of the external constraint. As an example, Barley (1962) examined the ability of corn (*Zea mays* L.) roots to overcome external constraints by using an apparatus which enabled measurement of length as the roots grew. When cells differentiated and elongated while the apex was compressed, root length increased continuously, but at a rate that declined with increased mechanical stress. Taylor and Ratliff (1969b) showed that the rate of peanut (*Arachis hypogaea* L.) root elongation decreased as soil strength (measured by penetrometer resistance) around the root increased (Fig. 11.2). The elongation rate was 2.7 mm/hr when penetrometer resistance was near zero bars. At a penetrometer resistance of 15 bars, the elongation rate was about 1.5 mm/hr, and it was about 0.8 mm/hr at 30 bars. Soil water potentials between  $-0.19$  and  $-12.5$  bars (water contents between 7.0% and 3.8% by weight) did not affect the root elongation-soil strength relationship. The compaction process used by Taylor and Ratliff left few continuous voids that were larger than the diameter of the peanut root tip; so soil strength controlled elongation rate.

### B. Soil Porosity Effects

If enough large vesicles (defined by Brewer, 1964, as voids with walls that consist of smooth, simple curves) or other large pores exist, roots can grow through high-strength material. Aubertin and Kardos (1965a, 1965b) illustrated this point by growing corn in a container

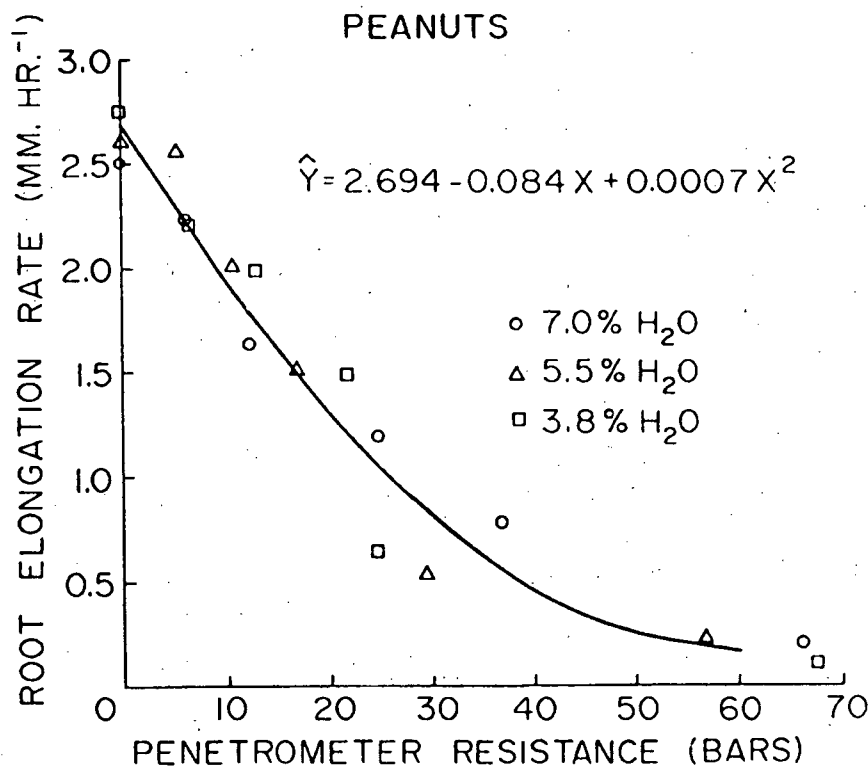


Fig. 11.2. Effect of soil water content and soil strength as measured by penetrometer resistance on peanut (*Arachis hypogaea* L.) root elongation for 40 to 80 hours after radicle emergence. (Reprinted by permission from H. M. Taylor and L. F. Ratliff, *Soil Sci.* 108: 113-19, © 1969, The Williams & Wilkins Co., Baltimore, Md. 21202, U.S.A.)

where a clamping device could alter rigidity of the glass bead matrix. Systems were used whose modal pore sizes ranged from  $46\mu$  to  $412\mu$  in diameter. In the nonrigid system, roots could grow equally well at  $46\mu$  as at  $278\mu$  (Fig. 11.3A), but corn roots did not grow into the rigid systems where pore diameters were less than  $138\mu$  (Fig. 11.3B). Any reduction in pore diameter below  $412\mu$  reduced root growth in the rigid systems.

The diameters of plant roots near the root tips vary greatly. Plants whose roots have small diameters near the tips can penetrate rigid soil volumes that roots with larger tips cannot. On the same plant, tertiary roots often act differently from tap, or seminal, roots. Sometimes their reaction is different because the tertiary roots are smaller; however, the main exploring roots also may have encountered a particular soil volume at a time when its soil water was different from that encountered by the tertiary roots.

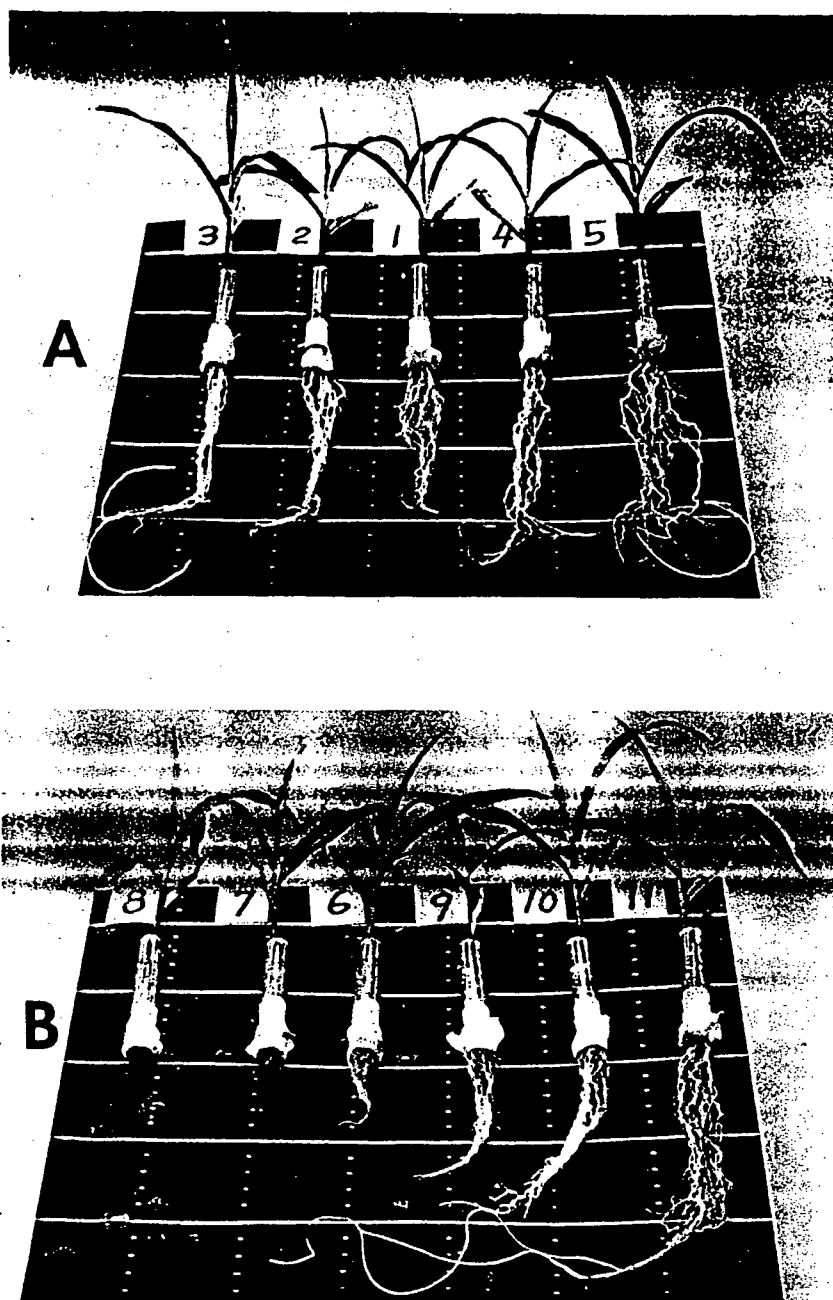


Fig. 11.3. Corn (*Zea mays* L.) seedlings grown in nonrigid (A) and rigid (B) glass bead systems with modal pore diameters of:  $46\mu$  (3, 8),  $87\mu$  (2, 6),  $138\mu$  (1, 9),  $240\mu$  (4, 10), and  $278\mu$  (5, 11). (Data of Aubertin and Kardos, 1965)

*C. Systems with Both Soil Strength  
and Soil Porosity Effects*

In most soils, roots penetrate partly by growing through existing voids and partly by moving aside soil particles (Wiersum, 1957; Aubertin and Kardos, 1965a, 1965b). When a soil is compacted, the modal pore size is reduced, soil strength is increased, and soil aeration is reduced. In a classic early experiment, Veihmeyer and Hendrickson (1948) investigated the effects on root growth of increases in soil bulk density (defined as the mass of oven-dry material per unit volume of soil). They showed that root growth decreased as soil bulk density increased, but their data did not delineate the various factors that might have caused the reduced root growth.

Taylor and Gardner (1963) found that root penetration at a particular soil water potential decreased as bulk density increased (Fig. 11.4). At a specific bulk density, root penetration decreased as soil water potential or water content decreased. They concluded that in their experiment root penetration was reduced as soil strength increased. Taylor *et al.* (1966)

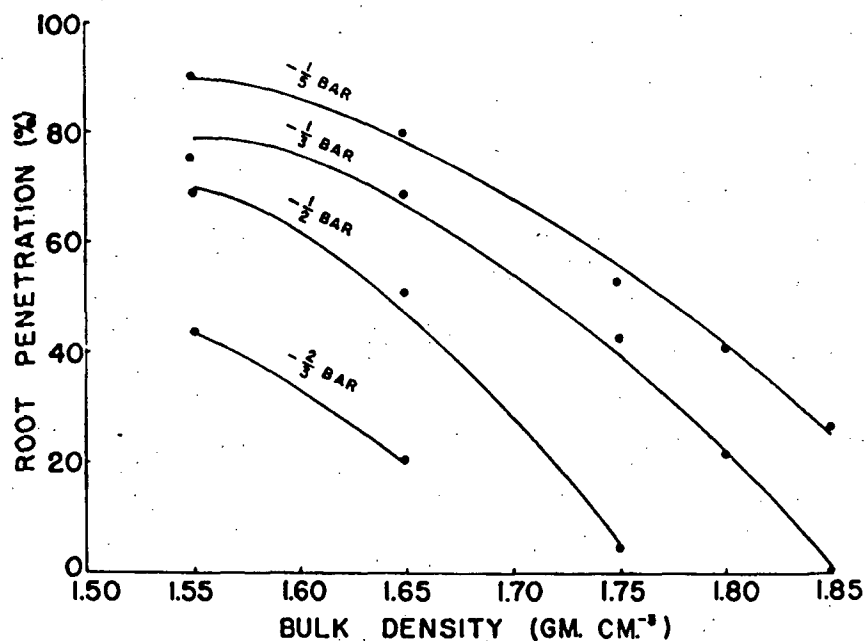


Fig. 11.4. Penetration of cotton (*Gossypium hirsutum* L.) seedling roots through 2.5-cm layers of Amarillo fine sandy loam soil as affected by bulk density and water potential. Each point represents 80 planted seeds. (Reprinted by permission from Taylor and Gardner, *Soil Sci.* 96:153-56, © 1963, The Williams & Wilkins Co., Baltimore, Md. 21202, U.S.A.)

altered penetrometer resistance of four soils by changing water contents or bulk densities and found that root penetration through the four soils was inversely related to penetrometer resistance (Fig. 11.5). Independently, Barley (1963) found that soil strength was a controlling factor in root growth. Barley and Taylor and Gardner (1963) concluded that soil aeration was not a major factor in their experiments.

Hopkins and Patrick (1970) investigated relations among soil compaction, soil oxygen, and root growth. At low compaction levels, root growth increased with oxygen concentration. At high compactions, root growth was only slightly affected by oxygen level, probably because growth was controlled by soil strength.

Pearson *et al.* (1970) grew cotton seedlings in glass-fronted boxes with varying soil temperature, pH, and strength levels. Root elongation rate increased as temperature increased to 32C, then fell sharply as temperature was increased further. The effect of temperature was greatest at low levels of strength and a pH of 6.2. Similarly, the effect of increased soil strength was greatest at 32C and a pH of 6.2.

These experiments of Hopkins and Patrick and Pearson *et al.* probably indicate the general pattern of strength effects on root growth through

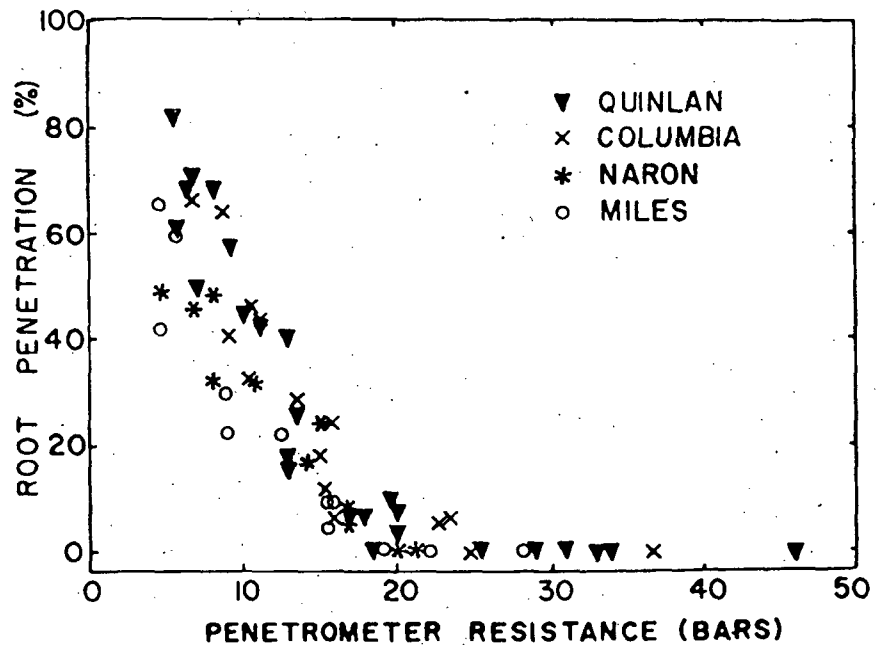


Fig. 11.5. Relations among root penetration and the penetrometer resistance of four soil materials. (Reprinted by permission from H. M. Taylor, G. M. Roberson, and J. J. Parker, Jr., *Soil Sci.* 102: 18-22, © 1966, The Williams & Wilkins Co., Baltimore, Md. 21202, U.S.A.)

soil with uniform fabric. When other growth factors are satisfactory, root growth decreases as soil strength increases. However, when other factors limit root growth, soil strength probably exerts little or no effect.

#### *D. Measurement of Soil Strength*

Soil strength is affected not only by changes in water content and soil bulk density but also by changes in types and amounts of saturating cations (Gerard, 1965), the number of particle-to-particle contacts (Lotspeich, 1964), the type of clay mineral (Grim, 1962), and the amount and type of organic materials (Jamison, 1954). Consequently, there is no simple way to predict soil strength from measurement of soil texture, organic matter, pH, or other common parameters. The American Society of Agricultural Engineers has published a standard for the design and use of penetrometers in estimating soil strength (American Society of Agricultural Engineers, 1970, ASAE Recommendation R313 Soil Cone Penetrometer, *ASAE Yearbook*, pp. 296-98). In root penetration studies the penetrometer technique is probably as useful as any other technique for assessing soil strength. However, it is emphasized that the various techniques provide different quantitative values when used on the same soil sample. These values, although quantitatively different, often are highly correlated (Taylor and Burnett, 1964).

### III. ROOT ELONGATION INTO SOILS WITH WELL-DEVELOPED STRUCTURAL DISCONTINUITIES

Much of the research evaluating effects of soil fabric and soil strength on root elongation has been conducted using unusual methods to achieve uniformity, but nearly all field soils contain some structural development. Where this development has occurred, soil porosities and soil strengths vary from one volume of soil to another. As a result, physical conditions important to root growth will vary from one location to another within the soil profile.

#### *A. Vertical Cracking Pattern Effects*

E. Burnett (private communication) investigated the pattern of soil shear planes and plant rooting in Houston Black clay, a Udic Pellustert occurring in the Texas Blacklands. The soil has long continuous planes (sometimes greater than 2 m in length) where one block of soil has moved in

relation to its neighbor. These shear planes persist from year to year at the same location. This plane of structural weakness provided a recurring path for root penetration, and roots tended to be concentrated along these shear planes (Fig. 11.6).

V. L. Hauser (private communication) found that vertical shrinkage cracks penetrated at least 5 m in Pullman silty clay loam soil at Bushland, Texas. He found living plant roots, tentatively identified as blueweed (*Helianthus ciliaris* DC), penetrating to a 9-m depth at this site. For most of this depth, the roots tended to follow the shrinkage cracks. Since blueweed is perennial, Hauser could not estimate the time required for root penetration to the 9-m depth.

### B. Strong Ped Development Effects

#### 1. Distortion of Rooting Patterns

Many soils contain a three-dimensional network of structural discontinuities. These networks separate soil volumes into peds, defined as "the individual natural aggregates consisting of clusters of primary particles, and separated from adjoining peds by surfaces of weakness which are recognizable as voids or natural surfaces" (Sleeman, 1963).

Edwards *et al.* (1964) studied corn root penetration through Weir silt loam, a Typic Ochraqualf found in Illinois. They found that large corn roots were confined to the larger spaces between peds but that many medium and small roots penetrated about one-half of the discrete peds in the claypan B horizon. Corn roots did not penetrate peds with a bulk density greater than 1.80 g/cm<sup>3</sup>.

Fehrenbacher *et al.* (1965) compared the penetration of corn roots with those of alfalfa (*Medicago sativa* L.) through four soils derived from shale. Alfalfa roots penetrated deeper than corn roots. Most of the alfalfa roots followed cracks and cleavage planes in the shale. They cautioned that the deeper alfalfa root penetration could have occurred in the fall when the corn had completed growth.

Growing root hairs can deform clay soils (Champion and Barley, 1969). When pea (*Pisum* sp.) radicles were grown on or in a saturated molded clay, root hairs penetrated the clay mass when the initial voids ratio exceeded 1:1 (bulk density less than 1.3 g/cm<sup>3</sup>). The pea radicles penetrated soil materials where root hairs failed to develop. Where ped surfaces are covered with "skins," root hairs must deform the peds to obtain potassium (Soileau *et al.*, 1964) and other nutrients.

Sutton (1969) found that roots of young white spruce (*Picea glauca* Voss) readily penetrated a highly structured Lucas silt loam, but the roots



*Fig. 11.6.* Plant roots located in a vertical shrinkage crack of Houston Black clay. Note that the roots apparently were unable to readily penetrate the vertical face of the crack. (Photograph courtesy of E. Burnett)



*Fig. 11.7.* Roots of white spruce (*Picea glauca*) conforming to structural ped surfaces in a Lucas silt loam at Ithaca, N.Y. (Reprinted by permission from R. F. Sutton, *Form and Development of Conifer Root Systems*, © 1969, Commonwealth Forestry Bureau)

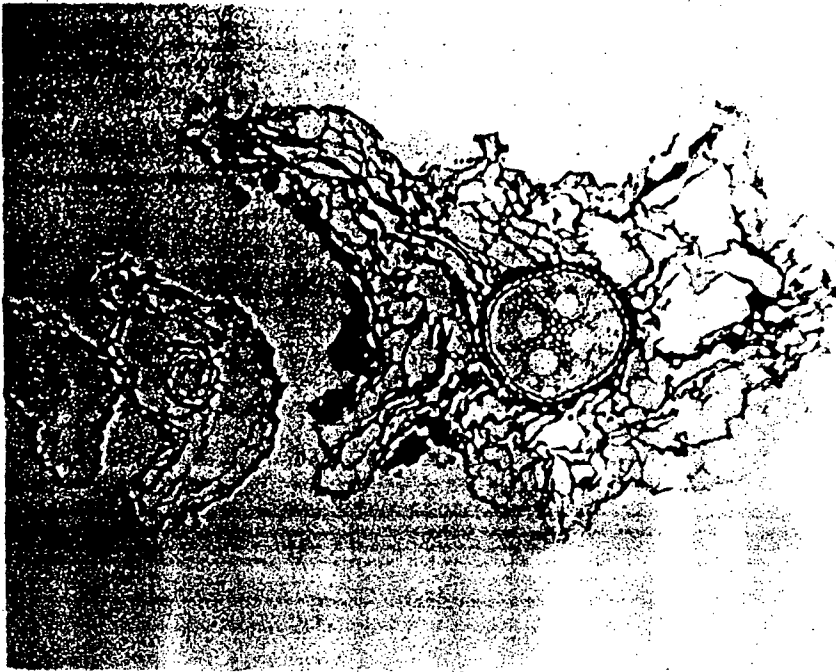


Fig. 11.8. A cross-sectional segment of three sugarcane (*Saccharum officinarum*) roots showing a badly distorted cortex. The stele shows slight distortion. Roots showing this amount of distortion are physiologically active. (Reprinted by permission from A. C. Trowse, Jr., pp. 137-52 in *12th Congr. Int. Sugar Cane Technol. Proc.* © 1965, Elsevier Publishing Company)

occurred only between structural elements. The roots were flattened in cross section, and they zigzagged, conforming with the structural element surfaces (Fig. 11.7). Misshapen roots are common in soils high in clay content (Stephenson and Schuster, 1939; Trowse, 1965). Nevertheless, these deformed roots (Fig. 11.8) are physiologically active (Trowse, 1965).

## 2. Difference in Growth Conditions between Ped Surfaces and Interiors

A word of caution is necessary here. Currie (1962) has emphasized that ped interiors and ped surfaces have different aeration relations. Therefore, one should not assume that excessive soil strength of the ped interior is the only cause of high concentration of roots at the surface. Also, water, temperature, nutrition, and pH may differ between ped surface and interior. The effects of ped size or shape on total root growth or crop yield are not known.

In structured soils, there is considerable difficulty in actually assessing the soil strength that a root must overcome to penetrate. First, most penetrometers are larger in diameter than the elongating portions of roots. Second, the root tips often have mucigel layers (Leiser, 1968), which may reduce the coefficient of friction between root surface and soil particles below that which occurs between the penetrometer tip and soil particles. Third, the root is easily deformed (Camp and Lund, 1964), but the penetrometer tip is rigid. Fourth, different types of penetrometers used in root penetration studies give different values of soil strength. Thus, measurements of media constraints with penetrometers are, at best, empirical. Measurements of soil strength and other root growth parameters should be made on a scale about equal to the diameter of the root.

### C. Horizontal Pan Effects

#### 1. Rooting Patterns on Pans

Most of the highly structured soils are fine textured. However, fabric discontinuities also exist in loams or sandier soils. Some of these horizontal layers, variously called hardpans, plowpans, tillage pans, plow soles, or tillage soles, divert roots and reduce rooting intensity below the pans. Initially, young roots grow downward through soil loosened by tillage. When they encounter a soil pan, part of the roots enter the pan and part are diverted horizontally. Roots that penetrate the pan at least 1 cm exhibit a reduced elongation rate as the soil strength increases. The roots that are diverted laterally may later encounter a vertical crack through which they can penetrate the pan (Taylor and Burnett, 1964). If no crack is encountered, the roots continue to grow horizontally along the pan surface until growth conditions change.

Soil pans sometimes restrict plant rooting to the few centimeters of soil near the surface (Fig. 11.9). As a result, the plants are subjected to extreme drought conditions in semiarid sandy soils. If soils containing pans are chiseled deep enough to disrupt the pans, plants will grow into the chisel slots but not where the soil pan still remains (Fig. 11.10). These soil pans, by reducing the depth of rooting, will reduce the quantity of water available for plant growth (Lowry *et al.*, 1970).

#### 2. Transitory Effects of Pans

Effects of soil pans on root growth often are transitory and depend largely on water content of the soil pan. Taylor *et al.* (1964a) investigated



Fig. 11.9. Root system of a pigweed (*Amaranthus retroflexus*) that grew on soil with a horizontal soil pan of excessive strength. (Reprinted by permission from H. M. Taylor and E. Burnett, *Soil Sci.* 98: 174-80, © 1964, The Williams & Wilkins Co., Baltimore, Md. 21202, U.S.A.)

17 root-restricting pans in the Southern Great Plains. They concluded that excessive soil strength caused by drying in the cohesive pan layer was the principal reason for distorted rooting patterns. If pan layers were at water contents near field capacity, most of the roots penetrated the pans. However, few roots penetrated pans that had dried below  $-1$  or  $-2$  bars

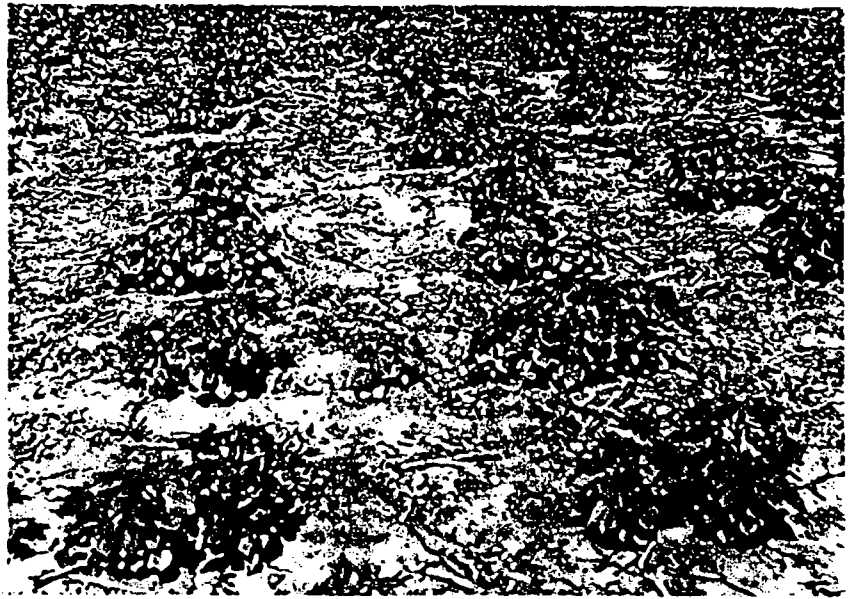


Fig. 11.10. On a compacted soil, cotton (*Gossypium hirsutum* L.) plants were established only where the planted row crossed a soil pan fracture created by chiseling to a 30-cm depth. (Taylor and Burnett, 1963)

water potential. Thus, rain or irrigation could change a root-restricting pan to a nonrestricting one. Sometimes, cotton roots penetrated pan layers that later dried sufficiently to girdle plants. If the girdling persisted long enough, the plants died (Mathers and Welch, 1964), probably as a result of reduced transport efficiency for water and nutrients (Taubenhaus *et al.*, 1931). When the pan layer was rewet, the roots again expanded radially (Taylor *et al.*, 1964a).

### 3. Crop Growth Effects

The root and shoot systems of a plant are dependent on and competitive with each other. Roots absorb water and minerals; leaves provide photosynthates and growth compounds. The proportion of the total supply of water, minerals, photosynthates, and growth compounds used by a particular organ changes with the environment. Therefore, the effect of a given level of soil strength will vary from environment to environment.

Consider a soil pan at a 15-cm depth which is rigid and has no pores larger than the rootcap. If the 15-cm depth above the pan can readily supply the plant's demand for water and nutrients without altering the heat or osmotic balance, yield should not be reduced below that of a nearby soil containing no pan. Similarly, soil pan strength or porosity

would show no effect if some other factor, such as high aluminum ion activity, is prohibiting root growth.

#### 4. Crop Yield Effects

Several experiments have shown that yield of cotton can be increased by disrupting high-strength pans. In California's Central Valley, Carter *et al.* (1965) and Carter and Tavernetti (1968) found that seed cotton yield was negatively correlated with penetrometer resistance of a sandy soil. Yields increased when the soil pan immediately below the cotton rows was disrupted in sandy soils (soils whose field capacity water content was below 12% by weight), but they did not increase in finer-textured soils. Presumably, sufficient vertical cracking occurred for adequate rooting through the pans in the fine-textured soils.

Lowry *et al.* (1970) found that cotton yield was reduced as depth to a soil pan decreased, or as strength of the pan increased (Fig. 11.11). Deep plowing or chiseling of compacted soils increased cotton yields in experiments of Grissom *et al.* (1955), Bruce (1960), and Burleson *et al.* (1957).

Yields of corn (Phillips and Kirkham, 1962), four species of grass (Barton *et al.*, 1966), grain sorghum (*Sorghum bicolor*) (Taylor *et al.*, 1964b), and sugar beets (*Beta vulgaris*) (Taylor and Bruce, 1968) were reduced as soil strength increased. It seems probable that high-strength pans will reduce yields of nearly all crops if, and probably only if, the pans substantially increase water stress, mineral deficiencies, or toxicities.

### IV. CONCLUDING DISCUSSION

Roots penetrate most soils partly by growing through existing voids and partly by moving soil particles from the path of the root. When no pores larger than the rootcap exist, roots must move substantial quantities of soil from their paths. In this case, increased soil strength will reduce the exploitation of water and nutrients within the soil mass. If large, continuous voids exist, roots can often follow these voids through the soil mass, even in very rigid systems. Size and frequency of the voids will control utilization of water and nutrients in these porous but rigid systems.

The term *soil structure* has been used loosely in contemporary literature on soils. It is suggested that this term be used only when one refers to the arrangement of primary particles into compound natural units and their arrangement within the profile. If force, displacement, or strain is the important consideration, *soil strength* is probably the correct term to be used.

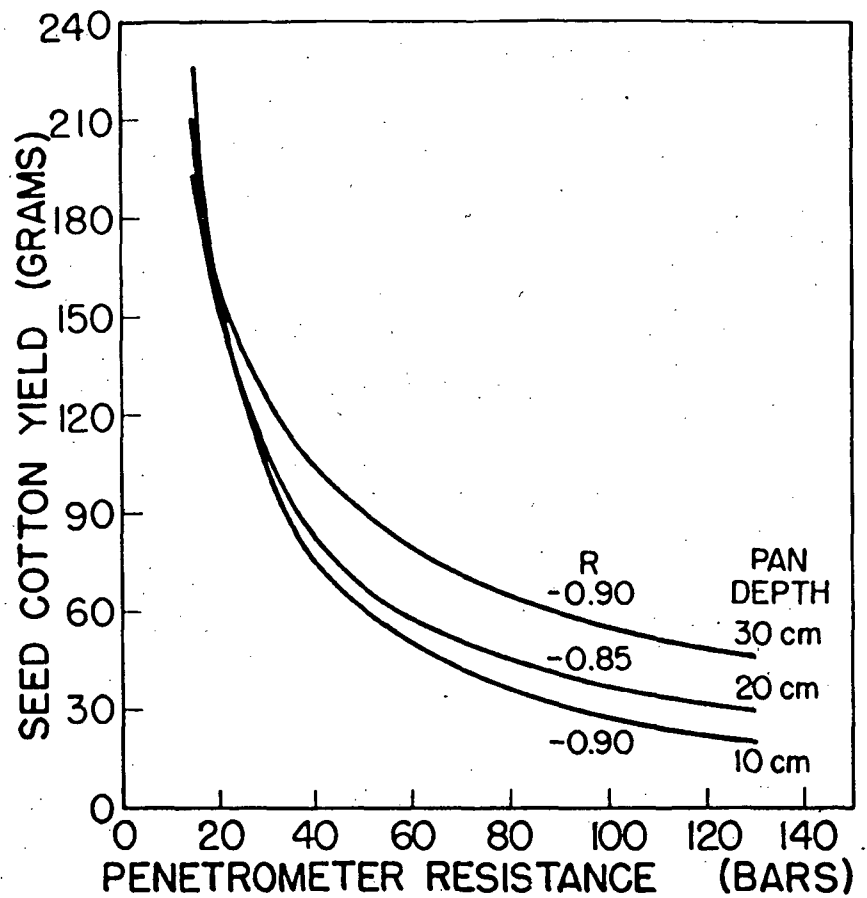


Fig. 11.11. Relations among soil pan depth, penetrometer resistance of the soil pan 48 hours after wilting, and seed cotton (*Gossypium hirsutum* L.) yield. (Lowry et al., 1970)

Soil structure can be extremely important to root growth in fine-textured soils, but soil strength usually is more important than soil structure in sandy soils. If roots encounter zones of high soil strength, elongation will be reduced. However, there is no direct, simple relationship between root growth and top growth. In many cases, a small proportion of the plant top is harvested and marketed, so there may not be even a simple, direct relationship between plant tops and yield of marketable product. Excessive soil strength usually reduces yield of marketable product by causing plants to undergo additional stress for water or nutrients at critical times. Effects on yield of the various types of structural discontinuities found in fine-textured soils have not been studied extensively.

## References

- Aubertin, G. M., and L. T. Kardos. 1965a. Root growth through porous media under controlled conditions. I. Effect of pore size and rigidity. *Soil Sci. Soc. Amer. Proc.* 29: 290-93.
- . 1965b. Root growth through porous media under controlled conditions. II. Effects of aeration levels and rigidity. *Soil Sci. Soc. Amer. Proc.* 29: 363-65.
- Barley, K. P. 1962. The effects of mechanical stress on the growth of roots. *J. Exp. Bot.* 13: 95-110.
- . 1963. Influence of soil strength on growth of roots. *Soil Sci.* 96: 175-80.
- Barton, Howard, W. G. McCully, H. M. Taylor, and J. E. Box, Jr. 1966. Influence of soil compaction on emergence and first-year growth of seeded grasses. *J. Range Manage.* 19: 118-21.
- Brewer, R. 1964. Structure and mineral analysis of soils. In *Soil Clay Mineralogy: A Symposium*, ed. C. I. Rich and G. W. Kunze. Chapel Hill, N.C.: University of North Carolina Press.
- Bruce, R. R. 1960. Deep tillage of dry soils gives better returns. *Mississippi Farm Res.* 23: 1, 6.
- Burleson, C. A., M. E. Bloodworth, and J. W. Biggar. 1957. *Effect of Subsoiling and Deep Fertilization on the Growth, Root Distribution and Yield of Cotton*. Texas Agr. Exp. Sta. Progress Rep. 1992.
- Camp, C. R., and Z. F. Lund. 1964. Effect of soil compaction on cotton roots. *Crops and Soils* 17: 13-14.
- Carter, L. M., J. R. Stockton, J. R. Tavernetti, and R. F. Colwick. 1965. Precision tillage for cotton production. *Trans. Amer. Soc. Agr. Eng.* 8: 177-79.
- Carter, L. M., and J. R. Tavernetti. 1968. Influence of precision tillage and soil compaction on cotton yields. *Trans. Amer. Soc. Agr. Eng.* 11: 65-67, 73.
- Champion, R. A., and K. P. Barley. 1969. Penetration of clay by root hairs. *Soil. Sci.* 108: 402-7.
- Currie, J. A. 1962. The importance of aeration in providing the right conditions for plant growth. *J. Sci. Food Agr.* 13: 380-85.
- Eavis, B. W., L. F. Ratliff, and H. M. Taylor. 1969. Use of a dead-load technique to determine axial root growth pressure. *Agron. J.* 61: 640-43.
- Edwards, W. M., J. B. Fehrenbacher, and J. P. Varva. 1964. The effect of discrete ped density on corn root penetration in a planasol. *Soil Sci. Soc. Amer. Proc.* 28: 560-64.
- Fehrenbacher, J. B., B. W. Ray, and W. M. Edwards. 1965. Rooting volume

- of corn and alfalfa in shale-influenced soils in Northwestern Illinois. *Soil Sci. Soc. Amer. Proc.* 29: 591-94.
- Gerard, C. J. 1965. The influence of soil moisture, soil texture, drying conditions and exchangeable cations on soil strength. *Soil Sci. Soc. Amer. Proc.* 29: 641-45.
- Gill, W. R., and G. H. Bolt. 1955. Pfeffer's studies of the root growth pressures exerted by plants. *Agron. J.* 47: 166-68.
- Gill, W. R., and G. E. Vanden Berg. 1967. *Soil Dynamics in Tillage and Traction*. U.S. Dept. Agr. Handbook no. 316.
- Grim, R. E. 1962. *Applied Clay Mineralogy*. New York: McGraw-Hill.
- Grissom, P., E. B. Williamson, O. B. Wooten, F. E. Fulgham, and W. A. Raney. 1955. Cotton yields doubled by deep tillage in 1954 tests on hardpan soils in Delta. *Miss. Farm Res.* 18: 1, 2.
- Hopkins, R. M., and W. H. Patrick, Jr. 1970. Combined effects of oxygen concentration and soil compaction on root penetration. *Soil Sci.* 108: 408-13.
- Huck, M. G. 1970. Variation in taproot elongation rate as influenced by composition of the soil air. *Agron. J.* 62: 815-18.
- Jamison, V. C. 1954. Effect of some soil conditioners on friability and compactibility of soils. *Soil Sci. Soc. Amer. Proc.* 18: 391-94.
- Leiser, A. T. 1968. A mucilaginous root sheath in *Ericaceae*. *Amer. J. Bot.* 55: 391-98.
- Lockhart, J. A. 1965. Cell extension. In *Plant Biochemistry*, ed. J. Bonner and J. E. Varner, pp. 826-49. New York: Academic Press.
- Lotspeich, F. B. 1964. Strength and bulk density of compacted mixtures of kaolinite and glass beads. *Soil Sci. Soc. Amer. Proc.* 28: 737-43.
- Lowry, F. E., H. M. Taylor, and M. G. Huck. 1970. Growth rate and yield of cotton as influenced by depth and bulk density of soil pans. *Soil Sci. Soc. Amer. Proc.* 34: 306-9.
- Mathers, A. C., and N. H. Welch. 1964. Pans in Southern Great Plains soils. II. Effect of duration of radial root restriction on cotton growth and yield. *Agron. J.* 56: 313-15.
- Pearson, R. W., L. F. Ratliff, and H. M. Taylor. 1970. Effect of soil temperature, strength and pH on cotton seedling root elongation. *Agron. J.* 62: 243-46.
- Pfeffer, W. 1893. Druck-und Arbeit-leistung durch wachsende Pflanzen. *Abhandl. Sachs. Ges. (Akad.) Wiss.* 33: 235-474.
- Phillips, R. E., and Don Kirkham. 1962. Soil compaction in the field and corn growth. *Agron. J.* 54: 29-34.
- Sleeman, J. R. 1963. Cracks, peds and their surfaces in some soils of the Riverine Plain, N.S.W. *Aust. J. Soil Res.* 1: 91-102.
- Soileau, J. M., W. A. Jackson, and R. J. McCracken. 1964. Cutans (clay films) and potassium availability to plants. *Soil Sci.* 15: 117-23.
- Stephenson, R. E., and C. E. Schuster. 1939. Physical properties of soils

- that affect plant nutrition. *Soil Sci.* 44: 22-36.
- Stolzy, L. H., and K. P. Barley. 1968. Mechanical resistance encountered by roots entering compact soils. *Soil Sci.* 105: 297-301.
- Sutton, R. F. 1969. *Form and Development of Conifer Root Systems*. Commonwealth Forest. Bur. Tech. Commun. no. 7.
- Taubenhaus, J. J., W. N. Ezekial, and H. E. Rea. 1931. Strangulation of cotton roots. *Plant Physiol.* 6: 161-66.
- Taylor, H. M., and R. R. Bruce. 1968. Effect of soil strength on root growth and crop yield in the Southern United States. *Trans. 9th Int. Congr. Soil Sci.* 1: 803-11.
- Taylor, H. M., and E. Burnett. 1963. Some effects of compacted soil pans on plant growth in the Southern Great Plains. *J. Soil Water Conserv.* 18: 235-36.
- . 1964. Influence of soil strength on the root growth habit of plants. *Soil Sci.* 98: 174-80.
- Taylor, H. M., and H. R. Gardner. 1963. Penetration of cotton seedling taproots as influenced by bulk density, moisture content and strength of soil. *Soil Sci.* 96: 153-56.
- Taylor, H. M., A. C. Mathers, and F. B. Lotspeich. 1964a. Pans in Southern Great Plains soils I. Why root-restricting pans occur. *Agron. J.* 56: 328-32.
- Taylor, H. M., L. F. Locke, and J. E. Box, Jr. 1964b. Pans in Southern Great Plains soils III. Their effects on yield of cotton and grain sorghum. *Agron. J.* 56: 542-45.
- Taylor, H. M., and L. F. Ratliff. 1969a. Root growth pressures of cotton, peas, and peanuts. *Agron. J.* 61: 398-402.
- . 1969b. Root elongation rates of cotton and peanuts as a function of soil strength and soil water content. *Soil Sci.* 108: 113-19.
- Taylor, H. M., G. M. Roberson, and J. J. Parker, Jr. 1966. Soil strength-root penetration relations for medium- to coarse-textured soil materials. *Soil Sci.* 102: 18-22.
- Tisdale, S. L., and W. L. Nelson. 1966. *Soil Fertility and Fertilizers*, p. 9. 2nd ed. New York: Macmillan.
- Trouse, A. C., Jr. 1965. Effects of soil compression on the development of sugar-cane roots. *12th Congr. Int. Sugar Cane Technol. Proc.*, pp. 137-52.
- Veihmeyer, F. J., and A. H. Hendrickson. 1948. Soil density and root penetration. *Soil Sci.* 65: 487-93.
- Wiersum, L. K. 1957. The relationship of the size and structural rigidity of pores to their penetration by roots. *Plant Soil* 9: 75-78.

## 5. Soil processes

B. ULRICH, P. BENECKE, W. F. HARRIS, P. K. KHANNA &  
R. MAYER

1981

### Contents

Dynamics of water. <i>P. Benecke</i>	265
Driving forces	266
Internal processes	283
Simulation of evapotranspiration and percolation	288
Dynamics of chemical elements. <i>R. Mayer, P. K. Khanna &amp; B. Ulrich</i>	293
Pathways of chemical input	293
Internal processes	303
Ways of output	316
Root dynamics. <i>W. F. Harris</i>	318
Seasonal accumulation and turnover of root organic matter	320
Root organic accumulation during stand development	323
The significance of root dynamics to element inputs to soil and element cycling	325
The significance of root sloughing to the forest energy balance	327
References	328

### Dynamics of water

Dynamics of water in this context means considering a section of the water cycle (Fig. 5.1), namely the fate of precipitation water that happens to fall on some kind of an ecosystem. This section deals with the processes the water is subjected to during its passage from the canopy to the bottom of the soil profile from where it may seep deeper to some aquifer thus recharging the ground water. As such it may be pumped by water plants or re-emerge in wells and contribute to rivers and streams.

The scope of this section is represented in Fig. 5.2, which shows a model of a forest ecosystem. This model, furthermore, is helpful in explaining and visualizing the processes that are essential for the water turnover in ecosystems. The dashed line represents interfaces between an ecosystem and neighboring systems: the atmosphere, the underground and possibly adjacent ecosystems. Arrows crossing this line are termed as input or output, arrows between the subdivisions (or compartments) of the ecosystem are interactions, normally fluxes of water, matter or energy, within the ecosystem.

Input and output variables act as driving forces because they trigger flow processes by changing the hydraulic potential at the boundary. Evaporation lowers the potential, thus establishing a hydraulic gradient that causes the

### *Dynamic properties of forest ecosystems*

supply of decomposable organic matter, when temperatures are not too low. Losses of gaseous ammonia,  $\text{NH}_3$ , occur only in soils of  $\text{pH} > 7$ , especially at periods of rapid nitrogen mineralization. As in the case of gaseous adsorption by soils, the gaseous losses are very difficult to measure. From the conditions described under which losses may occur it becomes obvious that they are probably negligible for a great number of forest soils in steady state.

#### *Leaching from root zone*

The flux of elements in percolation water at a soil depth below the rooting zone from which no upward water fluxes take place is considered as an output from the forest ecosystem. Considerable changes in the element load of the drainage water may occur before it appears as a surface water body. Therefore, the output data from a watershed must not be identical with leaching from the root zone.

#### *Other pathways of output*

Erosion output of elements by subsurface and ground water flow, as opposed to sedimentation, is governed by the same principles which applied in the previous discussion on other ways of input. Export is of main importance in managed forests. Since in most cases the amount of the product taken out of a forest are exactly determined, the assessment of the element output connected with the export should pose no difficulties.

#### **Root dynamics**

Knowledge of the dynamics of forest ecosystems is extensive. Our knowledge base has progressed rapidly, especially during the period 1968–78, to the point where we can begin to describe the forest ecosystem with some success as a system of mathematical equations representing underlying physiological processes, structural relationships and their interactions with external driving variables of climate. The one exception to this understanding is the below-ground ecosystem, especially roots. Roots comprise the primary interface between the plant and the soil for uptake of water and nutrients. A great deal is known about the biochemistry, cell physiology and membrane physics associated with these important processes (see, for example, Devlin (1966), Larcher (1975) and Pitman (1976)), but it is neither possible nor within the scope of this work to review this important area of physiology.

The question addressed here is the role of the below-ground ecosystem, especially the autotrophic root component, in the structure and function of

the forest ecosystem. Beyond the role of anchoring the terrestrial plants and uptake of water and nutrients, this component of the forest ecosystem has been largely neglected.

Forest biomass below-ground is large. Bazilevich & Rodin (1968), in summarizing the reserve of below-ground organic matter in terrestrial ecosystems, indicated that the broad-leaved and subtropical forest types are characterized by a maximum of from 70 000 to 100 000 kg/ha dry weight of root organic matter (here defined as the total of living and recently dead root structure) which constitutes 15% to 33% of the total accumulated biomass. This below-ground organic matter is surpassed only by tropical forests; however, the proportion of the total biomass represented by roots is lowest for forests and ranges up to 90% for tundra and certain steppe vegetation types. Bazilevich & Rodin (1968) conclude from their review that, in general, the root biomass is proportional to the *total* accumulated biomass, and as 'site quality' decreases the proportion of total biomass as roots increases. Estimates of below-ground biomass have been obtained by soil monolith analysis (Karizumi, 1968), allometric analysis (Kira & Ogawa, 1968), and only rarely by whole tree excavation. Besides the extensive reviews by Rodin & Bazilevich (1967) and Bazilevich & Rodin (1968), extant data on root biomass have been summarized by Ovington (1967), Whittaker (1962), Bray (1963) and Santantonio, Hermann & Overton (1977).

Such a large amount of organic matter, accumulated at considerable expense of carbohydrates, clearly could serve several purposes, such as storage of plant sugar and essential nutrients. The following discussion reviews briefly some of the recent findings on the behavior of the below-ground ecosystem and suggests some additional questions yet to be resolved. In particular, the seasonal production and turnover of root biomass, the role of root processes in nutrient turnover and the significance of below-ground dynamics to the energy balance of the forest ecosystem are considered.

Before proceeding further, some discussion of why understanding the below-ground ecosystem is in order. Our concept of forest root dynamics incorporates several reasonable but generally untested assumptions. These assumptions have arisen primarily because of the extreme methodological problems and labor intensive requirements for research on forest tree roots (Newbould, 1967; Lieth, 1968). Recent progress in this area of study is related to two factors. First, much of the work emanates from the large integrated studies of forest ecosystems such as those initiated as part of the IBP. These studies supported the pool of skilled and dedicated technicians necessary to obtain the requisite data. Second, as more became known about the metabolism of forest ecosystems, the potential role of roots in ecosystem function and their energy demands associated with the accumulation and turnover of carbon and other essential elements, surfaced as a

### *Dynamic properties of forest ecosystems*

central link coupling physiological processes and their environmental constraints with ecosystem behavior. As a result some interesting findings are now available. By no means do we know enough to generalize, but these initial findings are exciting and counter to what had been the common wisdom. The next several years should see considerable addition to the few examples which follow.

#### *Seasonal accumulation and turnover of root organic matter*

The root biomass of forests is not static. It changes annually and represents a varying proportion of the total biomass during stand development. By far the most dynamic component of root biomass is the fraction defined as 'fine roots'. No standard definition exists for fine roots; the distinction between fine and large roots is usually based on an arbitrarily chosen diameter limit which has ranged mainly from 0.2 to 1.0 cm. It has long been known that a seasonal periodicity of root growth is common in woody plants (see reviews by Lyr & Hoffmann, (1967) and Kozłowski (1971)). For example, radial growth of woody roots (with secondary xylem thickening) can closely follow the pattern of radial increment growth above-ground (Fayle, 1968). Studies concerned with seasonal periodicity of root elongation, initiation of laterals and subsequent elongation have not clarified whether periods of inactivity reflect physiological or environmentally-mediated dormancy (Santantonio, unpublished observations). Sutton (1969) concluded that evidence for autonomous control is not convincing and that primary growth of roots is probably dominated by environmental conditions. In fact, the real basis for control probably lies with the interaction of endogenous and environmental mechanisms, but this remains to be satisfactorily demonstrated.

While there is considerable information on the phenology of root growth, there is an insufficient basis for making estimates of root production and turnover. The earliest studies of root production are probably those of Heikurainen (1957) and Kalela (1957). Both studies involved Scots pine (*Pinus sylvestris* L.) and both reported a modal pattern of rapid growth to peak root biomass in the spring and a gradual decline during the summer to a low of about 50% of the peak level. A bimodal peak in root biomass has been reported for an oak woodland in central Minnesota, USA (Ovington, Heitkamp & Lawrence, 1963) and a stand of European beech (*Fagus sylvatica* L.) in the Solling area of West Germany (Göttsche, 1972). In both instances, biomass peaked in spring with a second but lower peak in the fall. Investigations by Harris, Kinerson & Edwards (1978) in a yellow poplar (*Liriodendron tulipifera* L.) stand in east Tennessee also revealed a spring-fall bimodal peak, while for loblolly pine (*Pinus taeda* L.) in North Carolina the modality was less clear with peaks observed in late fall, late winter and

possibly late spring. As with root elongation, the correlations of periods of peak biomass with environmental patterns are inconclusive. The year-to-year consistency observed by Harris *et al.* (1978) for yellow poplar suggest a strong measure of endogenous control.

The surprising result of recent studies on the seasonal dynamics of fine roots is the large flux of organic matter which is involved - large in an absolute sense as well as relative to the other organic matter fluxes of the forest ecosystem (Harris *et al.*, 1978). Using a coring device consisting of a masonry hole saw blade attached to a steel cylinder with the shaft adapted to a gasoline powered auger assembly, Harris *et al.* (1978) sampled a yellow poplar forest stand intensively over a two-year period. The lateral root biomass of yellow poplar showed considerable variation in the smaller root size classes (Fig. 5.19). Small roots within this forest were characterized by a peak in late winter (1 March), a minimum in mid-May, a second peak in

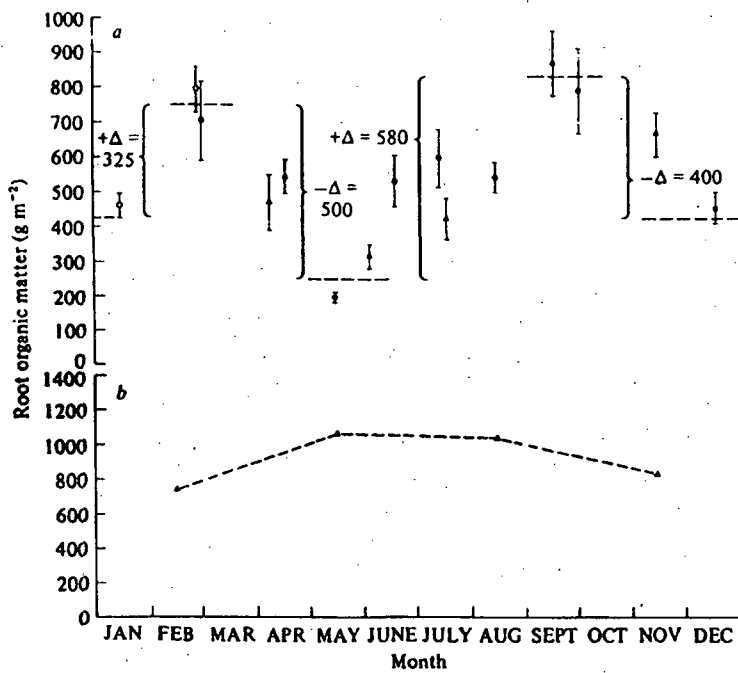


Fig. 5.19. Seasonal distribution of lateral root biomass in a *Liriodendron* forest for (a) roots less than 0.5 cm diameter and (b) roots of 0.5 cm diameter or greater ( $\bar{X} \pm 1$  SE). Net biomass production and turnover were calculated from differences in pool size through the year. Based on monthly summary of core data, no consistent pattern of biomass dynamics could be detected for roots greater than 0.5 cm in diameter.  $\blacktriangle$ , 1971;  $\bullet$ , 1972;  $\circ$ , 1973;  $\triangle$ , pooled data.

### *Dynamic properties of forest ecosystems*

mid-September, and a minimum in early winter (December to January). This pattern appears to be consistent among successive years. Based on summation of positive seasonal differences between minimum and subsequent peak biomass estimates, net root biomass production was 9000 kg/ha, with a net annual turnover (translocation and sloughing) of equal magnitude. This value of net annual small root production is 2.8 times larger than mean annual above-ground wood production determined for the study area from allometric equations and periodic (1965 to 1970) dbh inventory (Sollins *et al.* 1973).

Other experimental data on ecosystem carbon metabolism for the *Liriodendron* forest study area corroborate the existence of a large, annual below-ground allocation of carbon. Estimated net photosynthetic influx and soil-litter carbon efflux yield an amount of unaccounted carbon input to soil equivalent to 7500 kg organic matter per ha (Harris *et al.*, 1975; Edwards & Harris, 1977). For the dominant species in this study site, *Liriodendron tulipifera*, <sup>14</sup>C-sucrose tracer field studies indicate a vernal allocation of root-associated labile carbon above-ground of approximately 1500 kg/ha organic matter (H. H. Shugart & W. F. Harris, unpublished data). For temperate deciduous forests, the assumption that below-ground primary production is a fraction of above-ground primary production proportional to biomass pool size as is commonly assumed would lead to an underestimate of total annual root production. The results from yellow poplar are not an extreme example. While the number of studies is limited, a sufficient range of forest ecosystem types is represented to suggest that the large flux of organic matter below-ground is a general property of forest ecosystems. For example, McGinty (1976) found primary production of fine roots in an oak-hickory forest to be 6000 kg/ha. Persson (1978) reports root production of 3500 kg/ha in a young Scots pine stand in central Sweden, while Santantonio (unpublished data) has found root production in Douglas fir (*Pseudotsuga menziesii* Franco) of 6000–9000 kg/ha.

The large accumulation of root organic matter is a seasonal phenomenon. The net annual accumulation of root organic matter is much smaller and can best be described as a ratio of total above- to below-ground biomass multiplied by the net annual aboveground production. What then is the fate of the seasonal fluxes of organic matter below-ground? Most of this material is promptly metabolized by the soil heterotrophs (Edwards & Harris, 1977). Analysis of the total and proportional efflux of carbon dioxide from the soil surface (Edwards & Harris, 1977) and experimental measurements of root decay rate (W. F. Harris, unpublished data) all corroborate the prompt metabolism of root detritus. Again, similar findings by McGinty (1976), Persson (1978) and Santantonio (unpublished data) all point to the prompt disappearance of fine root organic matter. We are thus left with the following generalization: the soil of temperate coniferous and

### Soil processes

deciduous forest ecosystems annually receives an input of root organic matter equal to or much greater than from any other source; this organic matter is promptly metabolized by heterotrophs.

Before leaving the subject of root organic matter dynamics, some mention should be made about the dynamics of larger structural roots ( $\geq 0.5$  cm diameter). Generally, this organic matter component is much more stable, certainly not exhibiting significant seasonal or even annual dynamics. However, it would be a mistaken impression to consider this a static pool. Again, the evidence is sparse, but Kolesnikov (1968) has reported the interesting observation that during the development of a forest stand there is a cyclic renewal of large structural roots. One cannot escape making the analogy of such renewal to the individual forest tree adjusting this main structural component to exploit with its fine root structure 'new' areas of its soil habitat. Whether this generalization will withstand closer observation, and what the controlling factors and mechanisms might be, remain to be answered.

#### *Root organic accumulation during stand development*

During forest stand development, the amount of root organic matter increases on an absolute basis, but the proportion of the total biomass as root organic matter decreases. As reviewed by Rodin & Bazilevich (1967), the patterns of root/shoot ratio between deciduous and coniferous forests vary. Generally, coniferous forests reach an equilibrium root/shoot ratio earlier in stand development (i.e., at a lower total biomass) than is the case for deciduous forests. The trend for root organic accumulation in a mixed deciduous forest in east Tennessee (Walker Branch Watershed) is shown in Fig. 5.20.

Total below-ground biomass has ranged from 32 000 to 47 000 kg/ha for the deciduous and mixed coniferous-deciduous forest stands examined which has total above-ground biomass that ranged from 110 000 to 185 000 kg/ha (Fig. 5.20). Above-ground biomass have been estimated allometrically from dbh data and allometric equations reported elsewhere (Harris, Goldstein & Henderson, 1973). The more mesic *Liriodendron* forest followed a pattern of biomass distribution similar to upland hardwood stands with a total above-ground biomass of 130 000 kg/ha and a below-ground biomass of 36 000 kg/ha. A loblolly pine forest in North Carolina deviated considerably from the pattern observed in deciduous forests. The total above-ground estimate was 90 000 kg/ha while below-ground biomass amounted to 21 500 kg/ha (C. W. Ralston, Duke University, unpublished data).

For both plantation and deciduous forest ecosystems, the ratio of below- to above-ground biomass (Fig. 5.19) followed trends similar to those

## Dynamic properties of forest ecosystems

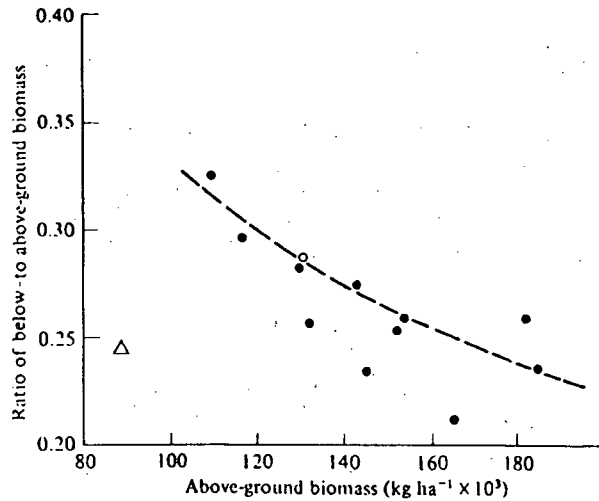


Fig. 5.20. Distribution of below- to above-ground biomass ratios over a range of above-ground biomass pool sizes on Walker Branch Watershed (●). The dashed line is a hand-fitted approximation of the trend noted by Rodin & Bazilevich (1967) for broad-leaved deciduous forests (○, *Liriodendron*). The displacement of the loblolly pine ratio (Δ, Saxapahaw area) appears to follow the trend for coniferous forests where ratios typically are lower.

reported by Rodin & Bazilevich (1967). They report that the percentage contribution of roots to total forest biomass of coniferous forest ecosystems approaches a constant value of 22.5% as total biomass exceeds 75 000 kg/ha. Roots comprised 19% of the total loblolly pine biomass. The proportion of biomass contributed by roots in deciduous forests approaches a constant value more slowly (Rodin & Bazilevich, 1967). The proportion tends to stabilize at about 20% as total biomass approaches 300 000 kg/ha. The root:shoot ratios of hardwood forests on Walker Branch Watershed follow the trend (dashed line, Fig. 5.19) suggested by the geographically more extensive data summary of Rodin & Bazilevich (1967). The pattern of below- to above-ground biomass distribution, which appears to be consistent over a wide range of forest types, describe (1) the size of the below-ground biomass pool and (2) the net annual biomass production over some interval when estimates of above-ground biomass pool and accumulation are known. While useful as a means of indirectly estimating below-ground biomass pool size and net annual production, this approach cannot be used to determine total annual root production.

On an annual basis, root core analysis and other harvest techniques lack the precision to detect readily net annual below-ground accumulation of biomass. However, applying the rather consistent values of below- to above-ground biomass ratios to stand data on biomass of tops would

suggest that total below-ground biomass pool should increase about 3% to 7% each year over the range of stand development examined.

*The significance of root dynamics to element inputs to soil and element cycling*

If our knowledge of root organic matter dynamics is limited, our knowledge of the role of root production/turnover (sloughing) to element cycling is vanishingly small. Of course, some idea or assumptions about root element content can be used to estimate the flux of elements to the soil. McGinty's work (1976) begins to place the contribution of roots in perspective. In the oak-hickory and eastern white pine forests of Coweeta, North Carolina, roots comprised 28% of the forest biomass but contain 40% of the plant nutrients in hardwoods and 65% of the plant nutrients in pines. Thus, this dynamic root component is a nutrient-rich substrate.

Roots can return nutrients to the soil in several ways, by death and decay, by exudation and leaching and indirectly after consumption. There are no known studies which consider total herbivory on roots. Certainly root feeding nematodes and various larval stages (e.g., cicada) might be principal consumers as described by Ausmus *et al.* (1978).

Studies of leaching and exudation from roots are likewise limited. In a northern hardwood forest ecosystem, Smith (1970) has found root exudation (growing season) to account for 4 kg/ha of carbon, 8 kg/ha of potassium and 34.2 kg/ha of sodium for three principal tree species (*Betula alleghaniensis*, *Fagus grandifolia* and *Acer saccharum*). Although the techniques employed (modified axenic culture) risk introducing artifacts, there is nonetheless a considerable potential for contribution of elements to the soil via exudation.

Radiotracer studies with  $^{134}\text{Cs}$  have shown that over 50% of the  $^{134}\text{Cs}$  in roots of tagged yellow poplar seedlings was transferred to culture solutions in less than seven days (Cox, 1972). Sandberg, Olson & Clebsch (1969) estimated that during one growing season 75% of  $^{137}\text{Cs}$  transfers by yellow poplar seedlings grown in sand was due to exudation-leaching. In their analysis of a cesium-tagged yellow poplar forest, Waller & Olson (1967) considered root exudation leaching processes as important pathways of cesium transfer to the soil based on concentration of  $^{137}\text{Cs}$  in soil at various depths. If *in situ* processes of cesium are comparable to those of the chemical analog, potassium, large quantities of potassium could be transferred to the soil annually by leaching exudation processes.

There are very few data which compare the return of elements to the soil via above-ground and below-ground processes. Table 5.7 summarizes a comparison for an extensively studied yellow poplar forest at Oak Ridge, Tennessee (Cox *et al.*, 1978). In this analysis, consumption was assumed to be 10% of the root detritus. Root detritus turnover was estimated by the

*Dynamic properties of forest ecosystems*

Table 5.7. Annual above- and below-ground organic matter and element returns (kg/ha) to soil in a yellow poplar (*Liriodendron tulipifera* L.) stand. From Cox et al. 1978

	Biomass	Nitrogen	Potassium
Above-ground <sup>a</sup>			
Dryfall/wetfall		7.2	3.6
Canopy leaching		2.3	29.4
Litterfall	3310	42.2	10.0
Total Above-ground return	3310	51.7	43.0
Below-ground <sup>b</sup>			
Root transfer processes			
Death and decay	6750	76	128
Consumption	750	9	14
Exudation-leaching <sup>c</sup>	—	—	128
Total Below-ground return	7500	85.0	270
Total return to soil	10810	136.7	313

<sup>a</sup> Above-ground data from Edwards & Shanks (unpublished data); chemical determinations were made on downed (fallen) material.

<sup>b</sup> Root biomass estimates from a *Liriodendron* stand (>80% *Liriodendron*).

<sup>c</sup> Exudation-leaching data are extrapolated from seedling studies of Cox (1975) assuming equivalent behavior of cesium and potassium. Element losses via root sloughing are based on (amount of sloughed biomass) times (mean root nitrogen content); element flux via consumption assumed to 10% of total below-ground return.

large residual carbon dioxide efflux from the soil unaccounted for after litter decomposition and autotrophic root respiration were subtracted from the total soil carbon dioxide efflux.

In the example illustrated in Table 5.7 annual return of elements to the soil by root processes was three times the combined above-ground inputs (including atmospheric) for potassium and at least 1.5 times above-ground inputs for nitrogen. Of the total (above- and below-ground) return to the soil, root processes accounted for turnover of 70% of the organic matter, 62% of the nitrogen and 86% of potassium. Some additional fraction (here assumed about 10% of the total estimated detrital flux) was transferred to soil consumer pools.

Only with caution can these results be generalized to other forests. However, given the large production/turnover of root material in diverse forests (as discussed above), there is some indirect basis for viewing these results more generally. As this volume is written, there are new studies underway (e.g., by D. Santantonio, Oregon, and H. Persson, Sweden) which should add to these results. However, despite the limited comparative data, the notion that element return to the forest soil occurs principally above-ground is short-lived.

*The significance of root sloughing to the forest energy balance*

Odum (1969) suggested a strategy of increasing conservation of nutrients in the element cycle during forest ecosystem development. In temperate forest systems, the mechanism leading to a closed cycle for nitrogen could be root sloughing and subsequent microbial mineralization. Biomass and nitrogen accumulate in roots during periods favorable for growth (summer) or just preceding growth (late winter); the winter growth occurs largely at the expense of stored photosynthate. During periods unfavorable for growth (fall-winter) or when above-ground energy demands are high (spring-early summer canopy development), root biomass is sloughed, thus reducing the total energy demand on the temperate forest system at a time when reserves are seasonally depleted and/or plant requirements for carbon are high elsewhere (e.g., canopy development). Nitrogen contained in the sloughed organic matter is conserved as part of the soil detritus by those microbial processes which immobilize it.

The cyclic pattern of photosynthate accumulation in a deciduous forest and the sustained productivity, which is in part dependent on available nitrogen, are closely coupled through the activities of soil microbes on a large systematically replenished substrate rich in nitrogen. In this respect, continuous maintenance of living roots in temperate forests would impose energy limitations on detritores by reducing the periodic influx of nitrogen-rich root organic matter, because this flux represents 70% of the total detrital input. While data from other deciduous systems are scarce, we hypothesize that evolution of temperate forest species has favored mechanisms which contribute to the systematic return of elements and organic matter through below-ground sloughing. Sloughing, therefore, stabilizes biogeochemical cycles of potentially limiting elements in an environment typified by seasonally limited photosynthate availability.

The energy expenditure to forest ecosystems represented by root sloughing is high. In the yellow poplar forest at Oak Ridge (Harris *et al.*, 1975; Edwards & Harris, 1977), Edwards (in Auerbach, Nelson & Struxness, 1974) estimated that lateral root growth, sloughing and maintenance respiration accounts for 44.8% of the total energy fixed annually in photosynthesis ( $1.88 \times 10^4$  kcal/m<sup>2</sup>). As discussed above, root sloughing with subsequent microbial immobilization offers a particularly attractive mechanism to explain retention of essential elements in the uptake zone. In another context, however, it can be argued that maintenance and development of a fertile soil require significant input of energy stored in soil organic matter. For the yellow poplar forest, the energy requirements for maintenance of soil are on the order of 66% of the energy fixed annually by photosynthesis (roots + 21% allocation to leaves). It is thus easily seen that many of man's activities which reduce both the energy fixed photosynthetically and/or the energy input to the soil are most severely manifested by

## Dynamic properties of forest ecosystems

Table 5.8. Comparison of turnover times for carbon, nitrogen and calcium in temperate deciduous forests (Tennessee). From O'Neill *et al.* 1975

Component	Turnover time (yr)		
	Carbon <sup>a</sup>	Nitrogen <sup>b</sup>	Calcium <sup>c</sup>
Soil	107	109	32 <sup>d</sup>
Forest Biomass <sup>e</sup>	155	88	8
Litter (01 + 02)	1.12	< 5	< 5
Total <sup>f</sup>	54	1815	445
Decomposers	0.01	0.02	?

<sup>a</sup> Data based on carbon metabolism of yellow poplar forest (Reichle *et al.*, 1973a; Harris *et al.*, 1975).

<sup>b</sup> Data based on nitrogen budget for mixed deciduous forest (Henderson & Harris, 1975).

<sup>c</sup> Data based on calcium budget from a *Liriodendron tulipifera* forest (Shugart *et al.*, in press).

<sup>d</sup> Turnover time based on available calcium and assumes all losses of calcium from soil are from the pool of available calcium.

<sup>e</sup> Considers above-ground biomass pool. Cyclic renewal of structural roots (Kolesnikov, 1968) would lower turnover time. Tree mortality estimated from permanent plot resurvey (three-year interval) and probably underestimates the mortality rate over the duration of a forest generation.

<sup>f</sup> Total calculated as sum of elements in living and dead components of the ecosystem; element loss based on sum of all losses from ecosystem.

degradation of the soil with respect to humified soil organic matter and fertility. The role of energy inputs to the soil (dominated in temperate forests by root sloughing) is to maintain the fertility of the soil components. As illustrated in Table 5.8, carbon (energy) is rapidly metabolized within the ecosystem and lost (as carbon dioxide). Essential elements, on the other hand, because of the interactions of autotrophs and decomposers are retained effectively.

### References

- Allison, F. E. (1965). Evaluation of incoming and outgoing processes that affect nitrogen. In *Soil nitrogen*, ed. W. V. Bartholomew & F. E. Clark. Agronomy No. 10, Madison.
- Ando, M. (1970). Litter fall and decomposition in some evergreen coniferous forests in Japan. *J. Ecol.* 20, 171-81.
- Auerbach, S. I., Nelson, D. J. & Struxness, E. G. (1974). Environmental Science Division Annual Progress Report. Period ending 30 September 1973. Oak Ridge National Laboratory Report ORNL-4935. Oak Ridge, Tennessee.
- Ausmus, B. S., Ferris, J. M., Reichle, D. E. & Williams, E. C. (1978). The role

- belowground herbivores in mesic forest root dynamics. *Pedobiologia*, 18, 289-95.
- Baldwin, J. P. & Nye, P. H. (1974). A model to calculate the uptake by a developing root system or root hair system of solutes with concentration variable diffusion coefficients. *Plant and Soil*, 40, 703-6.
- Barber, S. A. (1966). The role of root interception, mass flow and diffusion in regulating the uptake of ions by plants from soil, pp. 45-56. In *Limiting steps in ion uptake by plants from soil*. Technical Report Series No. 65. FAO/IAEA, Vienna.
- Baum, U. (1975). Stickstoff-Mineralisation und Stickstoff-Fraktionen von Humusformen unterschiedlicher Wald-Ökosysteme. *Göttinger Bodenkundliche Berichte*, 38, 1-96.
- Bazilevich, N. I. & Rodin, L. E. (1968). Reserves of organic matter in the underground sphere of terrestrial phytocoenoses, pp. 4-8. In *International Symposium, USSR, Methods of Productivity Studies in Root Systems and Rhizosphere Organisms*. Reprinted for the International Biological Programme by Biddles, Ltd., Guildford, U.K.
- Beckett, P. (1964). Studies on soil potassium. I. Confirmation of the ratio law: Measurement of potassium potential. *J. soil Sci.* 15, 1-8.
- Beese, F. & van der Ploeg, R. R. (1976). Influence of hysteresis on moisture flow in an undisturbed soil monolith. *Proc. Soil. Sci. Soc. America*, 40, 480-4.
- Benecke, P. (1959). Kinetik des Ionaustausches bei Phosphaten. *Dissertation der Landwirtschaftlichen Fakultät, Universität Göttingen*.
- Benecke, P. (1976). Soil water relations and water exchange of forest ecosystems. In *Ecological studies*, 19, ed. O. C. Lange, L. Kappen & E. D. Schulze, Springer-Verlag, Berlin-Heidelberg-New York.
- Benecke, P. & Mayer, R. (1971). Aspects of soil water behaviour as related to beech and spruce stands - some results of the water balance investigations, pp. 153-63. In *Integrated Experimental Ecology, Ecological Studies*, 2, ed. H. Ellenberg. Springer-Verlag, Berlin-Heidelberg-New York.
- Benecke, P. & van der Ploeg, R. R. (1976). Quantifizierung des zeitlichen Verhaltens der Wasserhaushaltskomponenten eines Buchen- und eines Fichtenaltholzbestandes im Solling mit bodenhydrologischen Methoden. *Verhandlungen der Gesellschaft für Ökologie*, Göttingen 1976. Dr W. Junk B. V. - The Hague (in Vorbereitung).
- Bernhard-Reversat, F. (1975). Nutrients in throughfall and their quantitative importance in rain forest mineral cycles, pp. 153-9. In *Tropical Ecological Systems, Ecological Studies*, 11, ed. F. B. Golley & E. Medina. Springer-Verlag, Berlin-Heidelberg-New York.
- Blume, H. P., Munnich, K.-O. & Zimmermann, U. (1966). Das Verhalten des Wassers in einer Loess-Parabraunerde unter Laubwald. *Zeitschrift fuer Pflanzenernahrung, Dungung, Bodenkunde*, 112, 156-68.
- Blume, H. P. & Schlichting, E. (1965). The relationships between historical and experimental pedology, pp. 340-53. In *Experimental Pedology*, ed. E. G. Hallsworth & D. V. Crawford. Butterworths, London.
- Bolin, B. & Persson, Ch. (1975). Regional dispersion of atmospheric pollutants with particular application to sulfur pollution over Western Europe. *Tellus* 27, 281-310.
- Bolt, G. H. (1967). Cation-exchange equations used in soil science - a review. *Netherlands J. agric. Sci.* 15, 81-103.
- Bormann, F. H. & Likens, G. E. (1967). Nutrient cycling. *Science*, Washington, 155, 424-9.

### *Dynamic properties of forest ecosystems*

- Bosse, I. (1964). Verwitterungsbilanzen von charakteristischen Bodentypen aus Flugsanden der nordwestdeutschen Geest (Mittelweser-Gebiet). *Dissertation Universität Göttingen*.
- Bray, J. R. (1963). Root production and the estimation of net productivity. *Can. J. Bot.* 41, 65-72.
- Brechtel, H. M. (1970). Schneecansammlung und Schneeschmelze im Wald und ihre wasserwirtschaftliche Bedeutung. *gwf-wasser und abwasser*, 111. Jg., H. 7, S. 377-9.
- Brechtel, H. M. (1971). Einfluss des Waldes auf Hochwasserabflüsse bei Schneeschmelzen. *Wasser und Boden*, 23. Jg., H. 3, S. 60-3.
- Brechtel, H. M. & Zahorka, H. (1971). Beeinträchtigt die Umwandlung von Buchen- und Fichtenbeständen die wasserwirtschaftliche Funktion des Waldes. *Allgemeine Forstzeitschrift*, 8.
- Campbell, N. E. R. & Lees, H. (1967). The nitrogen cycle. In *Soil biochemistry*, ed. A. D. McLaren & G. H. Paterson, New York.
- Carlisle, A., Brown, A. H. F. & White, E. J. (1966). The organic matter and nutrient elements in the precipitation beneath a sessile oak (*Quercus petraea*) canopy. *J. Ecol.* 54, 87-98.
- Chamberlain, A. C. (1960). Aspects of the deposition of radioactive and other gases and particles. *Int. J. Air Pollution* 3, 63-88.
- Chang, S. C. & Jackson, M. L. (1957). Fractionation of soil phosphorus. *Soil Sci.* 84, 133-44.
- Cole, D. W. & Gessel, S. P. (1965). Movement of elements through a forest soil as influenced by tree removal and fertilizer additions, pp. 95-104. In *Forest-Soil Relationship in North America*. Ed. C. T. Youngberg.
- Cole, D. W., Gessel, S. P. & Held, E. E. (1961). Tension lysimeter studies of ion and moisture movements in glacial till and coral atoll soils. *Proc. Soil Sci. Soc. America*, 25, 321-5.
- Cox, T. L. (1972). Production, mortality and nutrient cycling in root systems of *Liriodendron* seedlings. Ph.D. thesis, University of Tennessee, Knoxville.
- Cox, T. L. (1975). Accumulation and mobility of cesium in roots of tulip poplar seedlings, pp. 482-488. In *Mineral cycling in southeastern ecosystems*, ed. F. G. Howell, J. B. Gentry & M. H. Smith. ERDA Symposium Series (CONF-740513).
- Cox, T. L., Harris, W. F., Ausmus, B. S. & Edwards, N. T. (1978). The role of roots in biogeochemical cycles in an eastern deciduous forest. *Pedobiologia*, 18, 264-71.
- Coulter, B. C. & Talibudeen, O. (1968). Calcium: aluminum exchange equilibria in clay minerals and acid soils. *J. soil Sci.* 19, 237-50.
- Delfs, J., Friedrich, W., Kiesekamp, H. & Wagenhoff, A. (1958). Der Einfluss des Waldes und des Kahlschlages auf den Abflussvorgang, den Wasserhaushalt und den Bodenabtrag. - Ergebnisse der ersten 5 Jahre der forstlich-hydrologischen Untersuchungen im Oberharz (1948-53). H. Hannover.
- Denaeayer-de Smet, S. (1962). Contribution à l'étude du pluviollessivage du couvert forestier. *Bulletin de la Société Royale de Botanique de Belgique*, 94, 285-308.
- Denaeayer-de Smet, S. (1969). Apports d'éléments minéraux par les eaux de précipitation, d'égouttement sous couvert forestier et d'écoulement le long des troncs (1965, 1966, 1967). *Bulletin de la Société Royale de Botanique de Belgique* 102, 355-72.
- Devlin, R. M. (1966). *Plant Physiology*. Reinhold Publishing Corp. New York.
- Dickinson, C. H. & Pugh, G. J. F. (1974). *Biology of Plant Litter Decomposition*. Academic Press, London and New York.

- Duvigneaud, P. & Denacyer-de Smet (1969). Cycle des éléments biogènes dans les écosystèmes forestiers d'Europe (principalement forêts caducifoliées). *Unesco 1971. Productivité des écosystèmes forestiers, Actes Coll. Bruxelles 4*, 527-42.
- Duvigneaud, P. & Denacyer-de Smet (1970). Biological cycling of minerals in temperate deciduous forests, pp. 198-225. In *Analysis of Temperate Forest Ecosystems*, Ecological studies, 1, ed. D. E. Reichle. Springer-verlag, Berlin-Heidelberg-New York.
- Duvigneaud, P., Denacyer-de Smet, S. & Marbaise, J. L. (1969). Litière totale annuelle et restitution au sol des polyéléments biogènes. *Bulletin de la Société Royale de Botanique de Belgique*, 102, 339-54.
- Edwards, N. T. & Harris, W. F. (1977). Carbon cycling in a mixed deciduous forest floor. *Ecology*, 58, 431-7.
- Ehlers, W. (1966). Beiträge zum Kaliumaustausch des Bodens. Dissertation der Universität Göttingen, Göttingen, Germany.
- Elwood, J. W. & Henderson, G. S. (1975). Hydrologic and chemical budgets at Oak Ridge, Tennessee, pp. 30-51. In *Coupling of Land and Water Systems*, Ecological Studies, 10, ed. A. D. Hasler. Springer-Verlag, Berlin-Heidelberg-New York.
- Eriksson, E. (1952). Composition of atmospheric precipitation. I. Nitrogen compounds. *Tellus*, 4, 215-32.
- Eriksson, E. (1963). The yearly circulation of sulfur in nature. *J. geophys. Res.* 68, 4001-8.
- Ernst, W. (1972). Zink- und Cadmium-Immissionen auf Böden und Pflanzen in der Umgebung einer Zinkhütte. *Berichte der Deutschen Botanischen Gesellschaft*, 85, 295-300.
- Eschner, A. R. (1967). Interception and soil moisture distribution. In *International Symposium on Forest Hydrology*, ed. W. E. Sopper & H. W. Lull. Pergamon Press Ltd., Oxford.
- Fayle, D. C. F. (1968). *Radial growth in tree roots*. Univ. of Toronto, Fac. For. Tech. Report No. 9.
- Feddes, R. A. & Rijtema, P. E. (1972). Water withdrawal by plant roots. *Technical Bull.* 83. Institute of Land and Water Management Research, Wageningen, The Netherlands.
- Friedrich, W., Liebscher, H., Rudolph, R. & Wagenhoff, A. (1968). Forstlich-hydrologische Untersuchungen in bewaldeten Versuchsgebieten im Oberharz - Ergebnisse aus den Abflussjahren 1951-65. *Aus dem Walde H.* 7, Hannover.
- Frissel, M. J. & Reiniger, P. (1974). Simulation of accumulation and leaching in soils. *Wageningen*.
- Froment, A. & Mommaerts-Billiet, F. (1969). La respiration du sol, l'azote minéral et la décomposition des feuilles de chêne et de hêtre en relation avec les facteurs de l'environnement. *Bulletin de la Société Royale de Botanique de Belgique*, 102, 317-410.
- Froment, A. & Tanghe, M. (1972). L'utilisation du Facteur Azote dans la Caractérisation des Groupes Ecologiques le long d'un Transect de la Région d'Eprave-Rochefort. *Bulletin de la Société Royale de Botanique de Belgique*, 105, 157-68.
- Gapon, E. N. (1933). On the theory of exchange adsorption in soils. *J. Gen. Chemistry U.S.S.R.* 3, 144.
- Gardner, W. R. (1960). Dynamic aspects of water availability to plants. *Soil Sci.* 89, 63-73.
- Garg, R. K. & Vyas, L. N. (1975). Litter production in deciduous forest near Udaipur (South Rajasthan), India, pp. 131-5. In *Tropical ecological systems*, Ecological Studies, 11, ed. F. B. Golley & E. Medina, Springer-Verlag, Berlin-Heidelberg-New York.

### Dynamic properties of forest ecosystems

- Garrels, R. M. & Christ, C. L. (1965). *Solutions, Minerals and Equilibria*. Harper & Row Publishers, New York.
- Garstka, W. U. (1964). Snow and snow survey, pp. 10-1 to 10-57. In *Handbook of Applied Hydrology*, ed. Ven Te Chow. McGraw-Hill, Inc., New York.
- Gebhardt, H. & Coleman, N. T. (1974). Anion adsorption by allophanic tropical soils: II. Sulfate adsorption. *Proc. Soil Sci. Soc. America*, 38, 259-62.
- Giesel, W., Renger, M. & Strebel, O. (1971). Berechnung des kapillaren Aufstiegs aus dem Grundwasser in den Wurzelraum unter stationären Bedingungen. *Zeitschrift fuer Pflanzenernährung und Bodenkunde* 132, 17-29.
- Giesel, W., Renger, M. & Strebel, O. (1973). Numerical treatment of the unsaturated water flow equation: comparison of experimental and computed results. *Water Resources Res.* 9, 174-7.
- Gloaguen, J. C. & Touffet, J. (1974). Production de litière et apport au sol d'éléments minéraux dans un hêtraie atlantique. *Oecologia Plantarum*, 9, 11-28.
- Göttsche, D. (1972). *Verteilung von Feinwurzeln und Mykorrhizen in Bodenprofileines Buchen- und Fichtenbestandes in Solling*. Kommissionsverlag Buchhandlung Max Wiedebusch, Hamburg.
- Granat, L. (1972). On the relation between pH and the chemical composition in atmospheric precipitation. *Tellus* 24, 550-60.
- Granat, L. (1974). On the deposition of chemical substances by precipitation (as observed with the aid of the atmospheric chemistry network in Scandinavia). *Department of Meteorology, University of Stockholm, International Meteorological Institute, Report AC 27*.
- Granat, L. (1975). On the variability of rain water composition and errors in estimates of areal wet deposition. *Institute of Meteorology, University of Stockholm, International Institute of Meteorology, Report AC 30*.
- Granat, L. & Söderlund, R. (1975). Atmospheric deposition due to long and short distance sources - with special reference to wet and dry deposition of sulfur compounds around an oil-fired power plant. *Department of Meteorology, University of Stockholm, International Meteorological Institute, Report AC 32*.
- Grunert, F. (1964). Der biologische Stoffkreislauf in Kiefern-Buchen-Mischbeständen und Kiefernbeständen. *Albrecht-Thaer-Archiv*, 8, 435-51.
- Gunary, D. (1970). A new adsorption isotherm for phosphate in soils. *J. Soil Sci.* 21, 72-7.
- Harris, W. F., Goldstein, R. A. & Henderson, G. S. (1973). Analysis of forest biomass pools, annual primary production and turnover of biomass for a mixed deciduous forest watershed, pp. 41-64. In *Proceedings IUFRO conference on forest biomass studies*, ed. H. Young. Univ. Maine Press, Orono.
- Harris, W. F., Sollins, P., Edwards, N. T., Dinger, B. E. & Shugart, H. H. (1975). Analysis of carbon flow and productivity, pp. 116-122. In *Productivity of World Ecosystems, Proc. IBP V General Assembly*. Ed. D. E. Reichle & J. Franklin. National Academy of Science, Washington, 166 p.
- Harris, W. F., Kinerson, R. S. & Edwards, N. T. (1978). Comparisons of below-ground biomass of natural deciduous forest and loblolly pine plantations. *Pedobiologia*, 17, 369-81.
- Heikurainen, L. (1957). Über Veränderungen in der Wurzelverhältnissen der Kiefernbestände auf Moorböden in Laufe des Jahres. *Act. for. fenn.* 62, 1-54.
- Heiseke, D. (1974). Schneedecke und Wasserhaushalt der Steilen Bramke im Oberharz 1962/63. *Aus dem Walde* H. 22, S. 140-71.
- Henderson, G. S. & Harris, W. F. (1975). An ecosystem approach to characterization of the nitrogen cycle in a deciduous forest watershed, pp. 179-193. In

- Forest Soils and Forest Land Management*, ed. B. Bernier & C. H. Winget, pp. 179-93. Laval University Press, Quebec, Canada.
- Henderson, G. S. *et al.* (1971). Walker Branch Watershed: a study of terrestrial and aquatic system interaction, pp. 30-48. In *Ecological Sciences Division Annual Progress Report*, ORNL-4759, Oak Ridge National Laboratory, Oak Ridge, Tennessee.
- Henin, S. & Pedro, G. (1965). The laboratory weathering of rocks. In *Experimental pedology*, ed E. G. Hallsworth & D. V. Crawford, Butterworth, London.
- Hillel, D. (1971). *Soil and water*. Academic Press, Inc., New York & London.
- Hingston, F. J., Atkinson, R. J., Posner, A. M. & Quirk, J. P. (1967). Specific adsorption of anions. *Nature, Lond.* **215**, 1459-61.
- Holl, W. & Hampp, R. (1975). Lead and plants. *Residue Rev.* **54**, 97-111.
- Jenny, H., Gessel, S. & Bingham, F. T. (1949). Comparative study of decomposition rates of organic matter in temperate and tropical regions. *Soil Sci.* **68**, 419-32.
- Jensen, H. L. (1965). Nonsymbiotic nitrogen fixation. In *Soil Nitrogen*, ed. W. V. Bartholomew & F. E. Clark, Agronomy No. 10, Madison, Wisconsin.
- Johnson, P. L. & Swank, W. T. (1973). Studies of cation budgets in the southern Appalachians on four experimental watersheds with contrasting vegetation. *Ecology*, **54**, 70-80.
- Jost, D. (1969). Survey of the distribution of trace substances in pure and polluted atmospheres, pp. 643-53. In *Air pollution*, International Symposium, Cortina d'Ampezzo.
- Junge, Ch.E. (1963). *Air chemistry and radioactivity*, International Geophysics Series 4, Academic Press, New York & London.
- Kalela, E. K. (1957). Manniköiden ja Kunsiköiden juurisuiteista. I. *Acta for. fem.* **57**, 1-79 (English summary).
- Karizumi, N. (1968). Estimation of root biomass in forests by soil block sampling, pp. 79-86. In: *International Symposium, USSR Methods of Productivity Studies in Root Systems and Rhizosphere Organisms*. Reprinted for the International Biological Programme by Biddles, Ltd., Guildford, U.K.
- Khanna, P. K. (1975). Saisonalität der Flüsse von Stickstoffformen in einem Buchen- und einem Fichtenwald-Ökosystem. *Mitteilungen der Deutschen Bodenkundlichen Gesellschaft*, **22**, 359-64.
- Khanna, P. K. & Ulrich, B. (1967). Phosphatfraktionierung im Boden und isotopisch austauschbares Phosphat verschiedener Phosphatfraktionen. *Zeitschrift für Pflanzenernährung und Bodenkunde*, **117**, 53-65.
- Khanna, P. K. & Ulrich, B. (1973). Ion exchange equilibria in an acid soil. *Göttinger Bodenkundliche Berichte*, **29**, 211-30.
- Khanna, P. K. & Ulrich B. (1974). Gaponkoeffizienten als Mass für die Kationenselektivität der Bodenaustauscher. *Mitteilungen der Deutschen Bodenkundlichen Gesellschaft*, **18**, 218-78.
- Kirkham, D. & Powers, W. L. (1972). *Advanced soil physics*. John Wiley & Sons, Inc.
- Kittredge, J. (1948). *Forest influences*. McGraw-Hill Book Company, Inc., New York.
- Kira, T. & Ogawa, H. (1968). Indirect estimation of root biomass increment in trees, pp. 96-101. In *International Symposium, USSR, Methods of Productivity Studies in Root Systems and Rhizosphere Organisms*. Reprinted for the International Biological Programme by Biddles, Ltd., Guildford, UK.
- Koenigs, F. F. R. (1973). Bedingungen für die Verwendung der Tensiometerplatte als Lysimeter. *Zeitschrift für Pflanzenernährung und Bodenkunde*, **133**, 1-4.
- Kolesnikov, V. A. (1968). Cyclic renewal of roots in fruit plants, pp. 102-106. In *International Symposium, USSR, Methods of Productivity Studies in Root*

## Dynamic properties of forest ecosystems

- Systems and Rhizosphere Organisms*. Reprinted for the International Biological Programme by Biddles, Ltd., Guildford, UK.
- Kozłowski, T. T. (1971). *Growth and development of trees. Vol. II*. Academic Press, New York.
- Kundler, P. (1959). Zur Methodik der Bilanzierung der Ergebnisse von Bodenbildungsprozessen (Profilbilanzierung), dargestellt am Beispiel eines Texturprofils auf Geschiebemergel in Norddeutschland. *Zeitschrift für Pflanzenernährung, Düngung und Bodenkunde*, 86, 215-22.
- Lagerwerff, J. V. (1972). Lead, mercury and cadmium as environmental contaminants, pp. 593-636. In *Micronutrients in agriculture*. Madison, Wisconsin, USA.
- Larcher, W. (1975). (As translated by M. A. Brederman-Thorson). *Physiological Plant Ecology*. Springer-Verlag, New York.
- Lemée, G. (1967). Investigations sur la minéralisation de l'azote et son évolution annuelle dans des humus forestiers in situ. *Oecologia Plantarum*, 2, 285-324.
- Lieth, H. (1968). The determination of plant dry-matter production with special emphasis on the underground parts, pp. 179-86. In *Functioning of terrestrial ecosystems at the primary production level. Proc. of the Copenhagen Symposium. Vol. V*, ed. F. E. Eckhardt. UNESCO, Paris.
- Likens, G. E. & Bormann, F. H. (1975). An experimental approach to New England landscapes, pp. 7-29. In *Coupling of land and water systems*, Ecological Studies, 10, ed. A. D. Hasler, Springer-Verlag, Berlin-Heidelberg-New York.
- Little, P. (1973). A study of heavy metal contamination of leaf surfaces. *Environmental Pollution*, 5, 159-72.
- Loughnan, F. C. (1969). *Chemical weathering of the silicate minerals*. American Elsevier Publishing Company, New York.
- Luttge, U. & Pitman, M. G., ed. (1976). Transport in plants. II, Part B, Tissues and organs. In *Encyclopedia of plant physiology, new series*, ed. A. Pirson & M. H. Zimmermann, Springer-Verlag, Berlin-Heidelberg-New York.
- Lyr, H. & Hoffmann, G. (1967). Growth rates and growth periodicity of tree roots, pp. 181-236. In *International review of Forestry Research. Vol. 2*, ed. X. Y. Romberger & X. Y. Mikola. Academic Press, New York.
- McCull, J. C. (1973). Environmental factors influencing ion transport in a Douglas-fir forest soil in western Washington. *J. Ecol.* 61, 71-83.
- McGinty, D. T. (1976). Comparative root and soil dynamics on a white pine watershed and in the hardwood forest in the Coweeta basin. Unpublished Ph.D. Dissertation, Univ. of Georgia, Athens.
- Madgwick, H. A. I. & Ovington, J. D. (1959). The chemical composition in adjacent forest and open plots. *Forestry* 32, 1-22.
- Malaisse, F., Freson, R., Goffinet, G. & Malaisse-Mousset, M. (1975). Litter fall and litter breakdown in Miombo, pp. 137-52. In *Tropical ecological systems*, Ecological Studies, 11, ed. F. B. Golley & E. Medina, Springer-Verlag, Berlin-Heidelberg-New York.
- Malkonen, E. (1974). Annual primary production and nutrient cycle in some Scots pine stands. *Communicationes Instituti Forestalis Fenniae*, 84.5, 87 pp.
- Mayer, R. (1971). Bioelement-Transport im Niederschlagswasser und in der Bodenlösung eines Wald-Ökosystems, *Göttinger Bodenkundliche Berichte*, 19, 1-119.
- Mayer, R. (1972a). Untersuchungen über die Freisetzung der Bioelemente aus der organischen Substanz der Humusaufgabe in einem Buchenbestand. *Zeitschrift für Pflanzenernährung und Bodenkunde*, 131, 261-73.
- Mayer, R. (1972b). Bioelementflüsse im Wurzelraum saurer Waldböden, *Mitteilungen der Deutschen Bodenkundlichen Gesellschaft*, 16, 136-45.

- Mayer, R. (1974). Ermittlung des Stoffaustauschs aus Boden mit dem Versickerungswasser. *Mitteilungen der Deutschen Bodenkundlichen Gesellschaft*, **20**, 292-9.
- Mayer, R. & Ulrich, B. (1974). Conclusion on the filtering action of forests from ecosystem analysis. *Oecologia Plantarum*, **9**, 157-68.
- Mecklenburg, R. A., Tukey, H. B., Jr. & Morgan, J. V. (1966). A mechanism for the leaching of calcium from foliage. *Plant Physiol.* **41**, 610-13.
- Miller, R. B. (1963). Plant nutrients in hard beech. *New Zealand J. Sci.* **6**, 365-413.
- Mitscherlich, G. (1971). *Wald, Wachstum und Umwelt. Zweiter Band: Waldklima und Wasserhaushalt*. J. P. Sauerlanders Verlag, Frankfurt am Main.
- Munn, R. E. & Bolin, B. (1971). Global air pollution meteorological aspects a survey. *Atmospheric Environment*, **5**, 363-402.
- Nakayama, F. S. (1968). Calcium activity, complex and ion-pair in saturated  $\text{CaCO}_3$  solutions. *Soil Sci.* **106**, 429-34.
- Neuberger, H., Hosler, C. L. & Kocmond, W. C. (1967). Vegetation as aerosol filter. *Biometeorology*, **2**, 693-702.
- Newbould, D. J. (1967). *Methods for estimating the primary production of forests*. IBP Handbook No. 2. Blackwell Scientific Pub., Oxford.
- Nielsen, D. R., Biggar, J. W. & Erh, K. T. (1973). Spatial variability of field-measured soil-water properties. *Hilgardia*, **42**, 215-60.
- Nihlgard, B. (1970). Precipitation, its chemical composition and effect on soil water in a beech and a spruce forest in south Sweden. *Oikos, Copenhagen*, **21**, 208-17.
- Nimah, M. N. & Hanks, R. J. (1973a). Model for estimating soil water, plant, and atmospheric interrelations: I. Description and sensitivity. *Proc. Soil Sci. Soc. Amer.* **37**, 522-7.
- Nimah, M. N. & Hanks, R. J. (1973b). Model for estimating soil water, plant, and atmospheric interrelations: II. Field test of model. *Proc. Soil Sci. Soc. Amer.* **37**, 528-32.
- Nutman, P. S. (1965). Symbiotic nitrogen fixation, pp. 00-00. In *Soil nitrogen*, ed. W. V. Bartholomew & F. E. Clark, Agronomy No. 10, Madison.
- Odum, E. P. 1969. The strategy of ecosystem development. *Science*, Washington. **164**, 262-70.
- Olsen, S. R. & Watanabe, F. S. (1957). A method to determine a phosphate adsorption maximum of soils as measured by the Langmuir isotherm. *Proc. Soil Sci. Soc. Amer.* **21**, 144-9.
- Olson, J. S. (1963). Energy storage and the balance of producers and decomposers in ecological systems. *Ecology*, **44**, 322-31.
- O'Neill, R. V., Harris, W. F., Ausmus, B. S. & Reichle, D. E. (1975). A theoretical basis for ecosystem analysis with particular reference to element cycling, pp. 28-40. In *Mineral Cycling in Southeastern Ecosystems*, ed. F. G. Howell, J. B. Gentry & M. H. Smith. ERDA Symposium Series (CONF-740513).
- Ovington, J. D. (1962). Quantitative ecology and woodland ecosystem concept, pp. 103-92. In *Advances in ecological research*, **1**, ed. J. B. Cragg. Academic Press, New York.
- Ovington, J. D. (1967). Quantitative ecology and the woodland ecosystem concept. *Adv. Ecol. Res.* **1**, 103-92.
- Ovington, J. D., Heitkamp, D. & Lawrence, D. B. (1963). Plant biomass of prairie, savanna, oakwood and maize field ecosystems in central Minnesota. *Ecology*, **44**, 52-63.
- Pavlov, M. (1972). Bioelement-Inventur von Buchen- und Fichtenbeständen im Solling. *Göttinger Bodenkundliche Berichte*, **25**, 1-174.
- Penman, H. L. (1963). Vegetation and hydrology. *Technical Column*. **53**. Commonwealth Agriculture Bureaux, Harpenden, England.

### *Dynamic properties of forest ecosystems*

- Persson, H. (1978). Root dynamics in a young Scots pine stand in Central Sweden. *Oikos*, 30, 508-19.
- Pitman, M. G. (1976). Nutrient uptake by roots and transport to the xylem, pp. 85-100. In *Transport and Transfer Processes in plants*, ed. I. F. Wardlaw & J. B. Passioura. Academic Press, New York.
- Poulovassilis, A. (1973). The hysteresis of pore water in presence of non-independent water elements, pp. 161-79. In *Physics of soil water and salts, Ecological studies*, 4, ed. A. Hadas, D. Schwartzendruber, P. E. Rijtema, M. Fuchs & B. Yaron. Springer-Verlag, Berlin-Heidelberg-New York.
- Prather, R. J., Miyamoto, S. & Bohn, H. L. (1973). Nitric oxide sorption by calcareous soils. *Proc. Soil Sci. Soc. Amer.* 37, 877-9.
- Prince, R. & Ross, F. F. (1972). Sulphur in air and soil. *Water, Air and Soil Pollution*, 1, 286-302.
- Quervain, M. R. de & Gand, H. R. (1967). Distribution of snow deposit in a test area for alpine reforestation, pp. 233-9. In *Forest Hydrology*, ed. W. E. Sopper & H. W. Lull. Pergamon Press Ltd., Oxford.
- Rapp, M. (1971). Cycle de la matière organique et des éléments minéraux dans quelques écosystèmes méditerranéens. *Editions du Centre Nationale de la Recherche Scientifique, Paris*, Recherche Coopérative sur programme du CNRS, No. 40, 184 pp.
- Reichle, D. E., Dinger, B. E., Edwards, N. T., Harris, W. F. & Sollins, P. (1973). Carbon flow and storage in a Forest Ecosystem, pp. 345-365. In *Carbon and the Biosphere*, ed. G. M. Woodwell & E. V. Pecan, pp. 345-65. Proceedings of the 24th Brookhaven Symposium in Biology. AEC-CONF-720510. NTIS, Springfield, Virginia.
- Rijtema, P. E. (1965). An analysis of actual evapotranspiration. *Agricultural Research Reports No 659*. Centre for Agricultural Publications and Documentation, Wageningen, Netherlands.
- Roberts, B. R. (1974). Foliar sorption of atmospheric sulphur dioxide by woody plants. *Environmental Pollution*, 7, 133-40.
- Rodhe, H. (1972). A study of the sulfur budget for the atmosphere over Northern Europe. *Tellus*, 34, 128-38.
- Rodin, L. E. & Bazilevich, N. I. (1967). *Production and Mineral Cycling in Terrestrial Vegetation*. Oliver & Boyd, Edinburgh & London.
- Rose, C. W. (1966). *Agricultural Physics*. Pergamon Press Ltd., Oxford.
- Ruhling, A. & Tyler, G. (1973). Heavy metal deposition in Scandinavia. *Water, Air and Soil Pollution*, 2, 445-55.
- Runge, M. (1971). Investigation of the content and the production of mineral nitrogen in soils, pp. 191-202. In *Integrated Experimental Ecology, Ecological Studies*, 2, ed. H. Ellenberg, Springer-Verlag, Berlin-Heidelberg-New York.
- Russell, E. W. (1973). *Soil conditions and plant growth*. Longman, London & New York.
- Saito, H. & Shidei, T. (1972). Studies on estimation of leaf fall under model canopy. *Bulletin of the Kyoto University Forests*, No 43, 162-85.
- Salmon, R. C. (1964). Cation exchange reactions. *J. Soil Sci.* 15, 273-83.
- Sandberg, G. R., Olson, J. S. & Clebsch, E. E. C. (1969). *Internal distribution and loss from roots by leaching of cesium-137 inoculated into Liriodendron tulipifera L. seedlings grown in sand culture*. Oak Ridge National Laboratory Report No. ORNL/TM-2660, Oak Ridge, TN. 68 p.
- Santantonio, D., Hermann, R. K. & Overton, W. S. (1977). Root biomass studies in forest ecosystems. *Pedobiologia*, 17, 1-31.

- Schlesinger, W. H., Reiners, W. A. & Knopman, D. S. (1974). Heavy metal concentrations and deposition in bulk precipitation in montane ecosystems of New Hampshire, USA. *Environmental Pollution*, 6, 39-47.
- Schlichting, E. & Schwertmann, U. (1973). *Pseudogley and Gley*, Transactions of Commissions V and VI of the International Society of Soil Science, Verlag Chemie GmbH, Weinheim/Bergstr.
- Schofield, R. K. (1947). A ratio law governing the equilibrium of cations in the soil solution. *Proceedings of XIth International Congress on Pure and Applied Chemistry*, 3, 257-61.
- Schofield, R. K. (1955). Can a precise meaning be given to 'available' soils phosphorus? *Soils and Fertilizers*, 18, 373-5.
- Schofield, R. K. & Taylor, A. W. (1955a). The measurement of soil pH. *Proc. Soil Sci. Soc. Amer.* 19, 164-7.
- Schofield, R. K. & Taylor, A. W. (1955b). Measurements of activities of bases in soils. *J. Soil Sci.* 6, 137-46.
- Schouwenberg, J. Ch. von & Schuffelen, A. C. (1963). Potassium exchange behaviour of an illite. *Netherlands J. Agric. Sci.* 11, 13-22.
- Singer, S. F., ed. (1970). Global effects of environmental pollution. *Dordrecht*.
- Slatyer, R. O. (1967). *Plant-Water Relationships*. Academic Press, London & New York.
- Smith, W. H. (1970). Technique for collection of root exudation from mature trees. *Plant and Soil*, 32, 238-41.
- Sollins, P., Reichle, D. E. & Olson, J. S. (1973). Organic matter budget and model for a southern Appalachian *Liriodendron* forest. EDPB-IBP-73-2. Oak Ridge National Laboratory, Oak Ridge, Tennessee.
- Stafford, R. G. & Ettinger, H. J. (1971). Comparison of filter media against liquid and solid aerosols. *American Industrial Hygiene Association J.* 31, 319-26.
- Stenlid, G. (1958). Salt losses and restitution of salts in higher plants, pp. 615-37. In *Encyclopedia of plant physiology*, ed. W. Ruhland, 4, Springer-Verlag, Berlin-Göttingen-Heidelberg.
- Sutton, R. F. (1969). *Form and development of conifer root systems*. Tech. Commun. 7. Commonwealth For. Bull., Oxford, England.
- Taylor, A. W. (1958). Some equilibrium solution studies on Rothamsted soils. *Proc. Soil Sci. Soc. Amer.* 22, 511-13.
- Thomas, W. A. (1969). Accumulation and cycling of calcium by dogwood trees. *Ecological Monographs*, 39, 101-20.
- Thomas, W. A. (1970). Weight and calcium losses from decomposing tree leaves on land and in water. *J. appl. Ecol.* 7, 237-41.
- Tukey, H. B. Jr. (1970). The leaching of substances from plants. *Annu. Rev. Plant Physiol.* 21, 305-24.
- Ulrich, B. (1961). Die Wechselbeziehungen von Boden und Pflanze in physikalisch-chemischer Betrachtung. *Ferdinand Enke Verlag*, Stuttgart, 114 pp.
- Ulrich, B. (1969). Investigations on cycling of bioelements in forests of central Europe, pp. 501-7. In *Unesco 1971, Productivity of Forest Ecosystems, Proceedings of the Brussels Symposium 1969*.
- Ulrich, B. (1975). Die Umweltbeeinflussung des Nährstoffhaushaltes eines bodensauren Buchenwaldes. *Forstwissenschaftliches Centralblatt*, 94 Jg., H.6, 280-7.
- Ulrich, B. & Khanna, P. K. (1968). Schofield'sche Potentiale und Phosphatformen in Boden. *Geoderma*, 2, 65-77.
- Ulrich, B. & Khanna, P. K. (1969). Ökologisch bedingte Phosphatumlagerung und Phosphatformenwandel bei der Pedogenese. *Flora, Abteilung B*, 158, 594-622.

### Dynamic properties of forest ecosystems

- Ulrich, B., Ahrens, E. & Ulrich, M. (1971). Soil chemical differences between beech and spruce sites - an example of the methods used, pp. 171-90. In *Integrated Experimental Ecology, Ecological Studies*, 2, ed. H. Ellenberg, Springer-Verlag, Berlin-Heidelberg-New York.
- Ulrich, B., Mayer, R., Khanna, P. K. & Prenzel, J. (1973). Modelling of bioelement cycling in a beech forest of Solling district. *Göttinger Bodenkundliche Berichte*, 29, 1-54.
- Ulrich, B., Mayer, R., Khanna, P. K., Seckamp, G. & Fassbender, H. W. (1976). Input, Output und interner Umsatz von chemischen Elementen in einem Buchen- und einem Fichtenbestand. 6. *Jahrestagung der Gesellschaft für Ökologie im Sept. 1976 in Göttingen* (Congress Proceedings).
- Urone, P. & Schroeder, W. H. (1969). SO<sub>2</sub> in the atmosphere: A wealth of monitoring data, but few reaction rate studies. *Environmental Science and Technology*, 3, 437-45.
- Vachaud, G. & Thony, J. L. (1971). Hysteresis during infiltration and redistribution in a soil column at different initial water contents. *Water Resources Res.* 7, 111-27.
- Van der Ploeg, R. R. (1974). Simulation of moisture transfer in soils: One-dimensional infiltration. *Soil Sci.* 118, 349-57.
- Van der Ploeg, R. R. & Beese, F. (1976). Model calculations for the extraction of soil water by ceramic cups and plates. *Proc. Soil Soc. Amer.*
- Van der Ploeg, R. R. & Benecke, P. (1974a). Simulation of one dimensional moisture transfer in unsaturated, layered field soils. *Göttinger Bodenk. Ber.* 30, 150-69.
- Van der Ploeg, R. R. & Benecke, P. (1974b). Unsteady, unsaturated, n-dimensional moisture flow in soil: A computer simulation program. *Proc. Soil Sci. Soc. Amer.* 38, 881-5.
- Van der Ploeg, R. R., Ulrich, B., Prenzel, J. & Benecke, P. (1975). Modeling the mass balance of forest ecosystems, pp. 793-802. In *Proceedings of the 1975 Summer Computer Simulation Conference*, Simulation Councils Inc., LaJolla, California.
- Walker, T. W. (1965). The significance of phosphorus in pedogenesis. In *Experimental pedology*, ed. E. G. Hallsworth & D. V. Crawford, Butterworth, London.
- Waller, H. D. & Olson, J. S. (1967). Prompt transfers of cesium-137 to the soils of a tagged *Liriodendron* forest. *Ecology*, 48, 15-25.
- Weihe, J. (1968). Zurückhaltung von Regenniederschlägen durch Buchen und Fichten. *AFZ* 86-90.
- White, E. J. & Turner, F. (1970). A method of estimating income of nutrient in a catch of airborne particles by a woodland canopy. *J. appl. Ecol.* 7, 441-61.
- Whittaker, R. H. (1962). Net production relations of shrubs in the Great Smoky Mountains. *Ecology*, 43, 357-77.
- Wit, C. T. de & Keulen, H. van (1972). Simulation of transport processes in soils, *Wageningen*, 108 pp.
- Wit, de C. T. & Arnold, G. W. (1976). Some speculation on simulation, pp. 00-00. In *Critical Evaluation of Systems Analysis in Ecosystems Research and Management*, ed. G. W. Arnold & C. T. de Wit, PUDOC, Wageningen, Centre for Agricultural Publishing and Documentation.
- Witherspoon, J. P. (1964). Cycling of cesium-134 in white oak trees. *Ecological Monographs*, 34, 403-20.
- Witkamp, M. (1969). Environmental effects on microbial turnover of some mineral elements. *Soil Biology and Biochemistry*, 1, 167-84.
- Witkamp, M. (1971). Forest soil microflora and mineral cycling, pp. 413-24. In *Productivity of Forest Ecosystems*, Proceedings of the Brussels Symposium, Vol. 4, UNESCO.

### Soil processes

- Witkamp, M. & Frank, M. L. (1964). First year of movement, distribution and availability of  $Cs^{137}$  in the forest floor under tagged tulip poplars. *Radiation Botany*, 4, 485-95.
- Witter, S. H. & Bukovac, M. J. (1969). The uptake of nutrients through leaf surfaces, pp. 235-300. In *Handbuch der Pflanzenernährung und Düngung*, I, 1, ed. Hg. H. Linsler, Wien, New York.
- Witter, S. H. & Teubner, F. G. (1959). Foliar absorption of mineral nutrients. *Annu. Rev. Plant Physiol.* 10, 13-27.
- Wittich, W. (1942). Natur und Ertragsfähigkeit der Sandboden im Gebiet des norddeutschen Diluviums. *Zeitschrift für das Forst- und Jagdwesen*, 74, 1-42.
- Yamada, Y., Rasmussen, H. P., Bukovac, M. J. & Witter, S. H. (1966). Binding sites for inorganic ions and urea on isolated cuticular membrane surfaces. *Amer. J. Bot.* 53, 170-2.
- Ziemer, R. R. (1968). Soil moisture depletion patterns around scattered trees. *US Forest Service Research Note PSW-166*, US Department of Agriculture.

was established by the  
in 1964 as a counterpart  
The subject of the IBP  
productivity and Human  
ent was recognition that  
alled for a better under-  
he rational management  
ved only on the basis of  
of biology and in many  
At the same time it was  
ating rapid and compre-  
in terms of human wel-  
tion of basic knowledge

which biologists through-  
ther for a common cause.  
mination of a wide range  
ated through a series of  
object areas of research.  
h the study of biological  
the seas, together with  
gen fixation. Three sec-  
of human populations,  
biological resources.  
terminated in June 1974  
in the form of syntheses,  
tivities.

# Dynamic properties of forest ecosystems

Edited by

D. E. REICHLE

Environmental Sciences Division, Oak Ridge National Laboratory  
Oak Ridge, Tennessee, U.S.

RETURN TO:

SAVANNAH RIVER LABORATORY

E.I. DUPONT de NEMOURS & CO.

**CAMBRIDGE UNIVERSITY PRESS**

CAMBRIDGE

LONDON NEW YORK NEW ROCHELLE

MELBOURNE SYDNEY

PB87-227518

VERIFICATION OF THE HYDROLOGIC EVALUATION  
OF LANDFILL PERFORMANCE (HELP)  
MODEL USING FIELD DATA

(U.S.) Army Engineer Waterways Experiment  
Station, Vicksburg, MS

NOTICE: This material may be reproduced by  
any person for individual or internal use only.

Jul 87

U.S. DEPARTMENT OF COMMERCE  
National Technical Information Service

**NTIS**

Savannah River Lab  
Technical Library  
U S Property

EPA/600/2-37/050  
July 1987

VERIFICATION OF THE HYDROLOGIC EVALUATION  
OF LANDFILL PERFORMANCE (HELP) MODEL  
USING FIELD DATA

PB87-22751d

by

P. R. Schroeder and R. L. Peyton  
U.S. Army Engineer Waterways Experiment Station  
Vicksburg, MS 39180-0631

Interagency Agreement Number DW96930236-01-1

Project Officer

D. C. Ammon  
Landfill Pollution Control Division  
Hazardous Waste Engineering Research Laboratory  
Cincinnati, OH 45268

NOTICE: This material may be protected by  
copyright law (Title 17, U. S. Code)

HAZARDOUS WASTE ENGINEERING RESEARCH LABORATORY  
OFFICE OF RESEARCH AND DEVELOPMENT  
U.S. ENVIRONMENTAL PROTECTION AGENCY  
CINCINNATI, OH 45268

Savannah River Lab  
Technical Library  
U S Property

REPRODUCED BY  
U.S. DEPARTMENT OF COMMERCE  
NATIONAL TECHNICAL  
INFORMATION SERVICE  
SPRINGFIELD, VA 22161

TECHNICAL REPORT DATA		
<i>(Please read instructions on the reverse before completing)</i>		
1. REPORT NO. EPA/600/2-87/050	2.	3. RECIPIENT'S ACCESSION NO. PB87-227518A3
4. TITLE AND SUBTITLE Verification of the Hydrologic Evaluation of Landfill Performance (HELP) Model Using Field Data	5. REPORT DATE July 1987	
	6. PERFORMING ORGANIZATION CODE	
7. AUTHOR(S) P.R. Schroeder and R. L. Peyton	8. PERFORMING ORGANIZATION REPORT NO.	
9. PERFORMING ORGANIZATION NAME AND ADDRESS U.S. Army Engineer Waterways Experiment Station Vicksburg, Mississippi 39180	10. PROGRAM ELEMENT NO.	
	11. CONTRACT/GRANT NO. DW-96930236	
12. SPONSORING AGENCY NAME AND ADDRESS Hazardous Waste Engineering Research Laboratory Office of Research and Development U.S. Environmental Protection Agency Cincinnati, Ohio 45268	13. TYPE OF REPORT AND PERIOD COVERED	
	14. SPONSORING AGENCY CODE EPA/600/12	
15. SUPPLEMENTARY NOTES Project Officer: Douglas C. Ammon		
16. ABSTRACT  This report describes a study conducted to verify the Hydrologic Evaluation of Landfill Performance (HELP) computer model using existing field data from a total of 20 landfill cells at 7 sites in the United States. Simulations using the HELP model were run to compare the predicted water balance with the measured water balance. Comparisons were made for runoff, evapotranspiration, lateral drainage to collection systems and percolation through liners. The report also presents a sensitivity analysis of the HELP model input parameters.		
17. KEY WORDS AND DOCUMENT ANALYSIS		
a. DESCRIPTORS	b. IDENTIFIERS/OPEN ENDED TERMS	c. COSATI Field/Group
18. DISTRIBUTION STATEMENT Release to Public	19. SECURITY CLASS (This Report) Unclassified	21. NO. OF PAGES 180
	20. SECURITY CLASS (This page) Unclassified	22. PRICE

## ABSTRACT

Simulations of 20 landfill cells from seven sites were performed using the Hydrologic Evaluation of Landfill Performance (HELP) model. Results were compared with field data to verify the model and to identify shortcomings. Sites were located in California, Kentucky, New York, and Wisconsin and included a wide variety of climates and landfill designs. Landfill descriptions and soil properties were loosely defined, requiring much judgment in selecting model input values and allowing significant variance in the simulation results. The field measurements of the various water budget components varied greatly from cell to cell despite some having identical designs. Consequently, the precision of the verification effort is fairly low, but the study demonstrates that the HELP model is a useful tool for realistically estimating landfill water budgets. Simulation results generally fell within the range of field observations. The results indicated that two modifications in the HELP model may be warranted. Specifically, the computation of daily temperatures for estimating snowmelt and the estimation of unsaturated hydraulic conductivity for vertical drainage should be changed. Further study is needed for verification of lateral drainage and percolation when the infiltration rate is small.

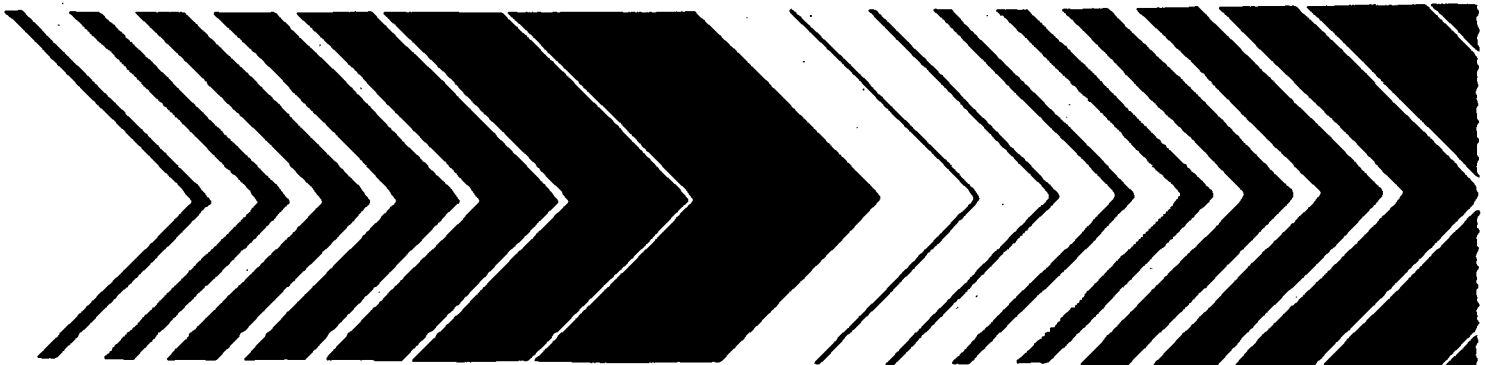
A sensitivity analysis of the HELP model was performed to examine the effects of the major design parameters on components of the water budget for landfills. Hydraulic conductivity values for the topsoil, lateral drainage layers, and clay liners are the most important parameters in determining the water budget components. These parameters are particularly important in estimating the percolation through the landfill. Other design parameters tend to affect the apportionment among runoff, evapotranspiration, and lateral drainage from the cover. This information, along with the verification results, was used to evaluate RCRA landfill design guidance and regulation.

This report was submitted in partial fulfillment of Interagency Agreement DW96930236-01-1 between the U.S. Environmental Protection Agency and the U.S. Army Engineer Waterways Experiment Station. This report covers a period from October 1984 to September 1986, and work was completed as of September 1986.



# The Hydrologic Evaluation of Landfill Performance (HELP) Model

User's Guide for  
Version 3



**THE HYDROLOGIC EVALUATION OF LANDFILL  
PERFORMANCE (HELP) MODEL**

***USER'S GUIDE FOR VERSION 3***

by

Paul R. Schroeder, Cheryl M. Lloyd, and Paul A. Zappi  
Environmental Laboratory  
U.S. Army Corps of Engineers  
Waterways Experiment Station  
Vicksburg, Mississippi 39180-6199

and

Nadim M. Aziz  
Department of Civil Engineering  
Clemson University  
Clemson, South Carolina 29634-0911

Interagency Agreement No. DW21931425

Project Officer

Robert E. Landreth  
Waste Minimization, Destruction and Disposal Research Division  
Risk Reduction Engineering Laboratory  
Cincinnati, Ohio 45268

**RISK REDUCTION ENGINEERING LABORATORY  
OFFICE OF RESEARCH AND DEVELOPMENT  
U.S. ENVIRONMENTAL PROTECTION AGENCY  
CINCINNATI, OHIO 45268**

## SECTION 1

### INTRODUCTION

The Hydrologic Evaluation of Landfill Performance (HELP) computer program is a quasi-two-dimensional hydrologic model of water movement across, into, through and out of landfills. The model accepts weather, soil and design data, and uses solution techniques that account for the effects of surface storage, snowmelt, runoff, infiltration, evapotranspiration, vegetative growth, soil moisture storage, lateral subsurface drainage, leachate recirculation, unsaturated vertical drainage, and leakage through soil, geomembrane or composite liners. Landfill systems including various combinations of vegetation, cover soils, waste cells, lateral drain layers, low permeability barrier soils, and synthetic geomembrane liners may be modeled. The program was developed to conduct water balance analysis of landfills, cover systems and solid waste disposal and containment facilities. As such, the model facilitates rapid estimation of the amounts of runoff, evapotranspiration, drainage, leachate collection and liner leakage that may be expected to result from the operation of a wide variety of landfill designs. The primary purpose of the model is to assist in the comparison of design alternatives as judged by their water balances. The model, applicable to open, partially closed, and fully closed sites, is a tool for both designers and permit writers.

#### 1.1 BACKGROUND

The HELP program, Versions 1, 2 and 3, was developed by the U.S. Army Engineer Waterways Experiment Station (WES), Vicksburg, MS, for the U.S. Environmental Protection Agency (EPA), Risk Reduction Engineering Laboratory, Cincinnati, OH, in response to needs in the Resource Conservation and Recovery Act (RCRA) and the Comprehensive Environmental Response, Compensation and Liability Act (CERCLA, better known as Superfund) as identified by the EPA Office of Solid Waste, Washington, DC.

HELP Version 1 (Schroeder et al., 1984) represented a major advance beyond the Hydrologic Simulation on Solid Waste Disposal Sites (HSSWDS) program (Perrier and Gibson, 1980; Schroeder and Gibson, 1982), which was also developed at WES. The HSSWDS model simulated only the cover system, did not model lateral flow through drainage layers, and handled vertical drainage only in a rudimentary manner. The infiltration, percolation and evapotranspiration routines were almost identical to those used in the Chemicals, Runoff, and Erosion from Agricultural Management Systems (CREAMS) model, which was developed by Knisel (1980) for the U.S. Department of Agriculture (USDA). The runoff and infiltration routines relied heavily on the Hydrology Section of the National Engineering Handbook (USDA, Soil Conservation Service, 1985). Version 1 of the HELP model incorporated a lateral subsurface drainage model and improved unsaturated drainage and liner leakage models into the HSSWDS model. In

addition, the HELP model provided simulation of the entire landfill including leachate collection and liner systems.

Version 2 (Schroeder et al., 1988) represented a great enhancement of the capabilities of the HELP model. The WGEN synthetic weather generator developed by the USDA Agricultural Research Service (ARS) (Richardson and Wright, 1984) was added to the model to yield daily values of precipitation, temperature and solar radiation. This replaced the use of normal mean monthly temperature and solar radiation values and improved the modeling of snow and evapotranspiration. Also, a vegetative growth model from the Simulator for Water Resources in Rural Basins (SWRRB) model developed by the ARS (Arnold et al., 1989) was merged into the HELP model to calculate daily leaf area indices. Modeling of unsaturated hydraulic conductivity and flow and lateral drainage computations were improved. Accuracy was increased with the use of double precision. Default soil data were improved, and the model permitted use of more layers and initialization of soil moisture content. Input and editing were simplified. Output was clarified, and standard deviations were reported.

In Version 3, the HELP model has been greatly enhanced beyond Version 2. The number of layers that can be modeled has been increased. The default soil/material texture list has been expanded to contain additional waste materials, geomembranes, geosynthetic drainage nets and compacted soils. The model also permits the use of a user-built library of soil textures. Computation of leachate recirculation between soil layers and groundwater drainage into the landfill have been added. Moreover, HELP Version 3 accounts for leakage through geomembranes due to manufacturing defects (pinholes) and installation defects (punctures, tears and seaming flaws) and by vapor diffusion through the liner. The estimation of runoff from the surface of the landfill has been improved to account for large landfill surface slopes and slope lengths. The snowmelt model has been replaced with an energy-based model; the Priestly-Taylor potential evapotranspiration model has been replaced with a Penman method, incorporating wind and humidity effects as well as long wave radiation losses (heat loss at night). A frozen soil model has been added to improve infiltration and runoff predictions in cold regions. The unsaturated vertical drainage model has also been improved to aid in storage computations. Input and editing have been further simplified with interactive, full-screen, menu-driven input techniques.

In addition, the HELP Version 3 model provides a variety of methods for specifying precipitation, temperature and solar radiation data. Now, data from the most commonly available government and commercial sources can be imported easily. Moreover, data used in HELP Version 2 can still be used with minimum user effort. Specifying weather data manually and editing previously entered weather data can be easily done by using built-in spreadsheet facilities.

The use of data files in Version 3 is much simpler and more convenient than HELP Version 2 because data are saved permanently in user defined file names at a user-specified location. Similarly, the user has more flexibility to define units for every type

of data needed to run the HELP model. Finally, Version 3 of the HELP model provides on-line help at every step of the data preparation process.

Although applicable to most landfill applications, the HELP model was developed specifically to perform hazardous and municipal waste disposal landfill evaluations as required by RCRA. Hazardous waste disposal landfills generally should have a liner to prevent migration of waste from the landfill, a final cover to minimize the production of leachate following closure, careful controls of runoff and runoff, and limits on the buildup of leachate head over the liner to no more than 1 ft. The HELP model is useful for predicting the amounts of runoff, drainage, and leachate expected for reasonable designs as well as the buildup of leachate above the liner. However, the model should not be expected to produce credible results from input unrepresentative of landfills.

## **1.2 OVERVIEW**

The principal purpose of this User's Guide is to provide the basic information needed to use the computer program. Thus, while some attention must be given to definitions, descriptions of variables and interpretation of results, only a minimal amount of such information is provided. Detailed documentation providing in-depth coverage of the theory and assumptions on which the model is based and the internal logic of the program is also available (Schroeder et al., 1994). Potential HELP users are strongly encouraged to study the documentation and this User's Guide before attempting to use the program to evaluate a landfill design. Additional documentation concerning the sensitivity of program inputs, application of the model and verification of model predictions are under development.

## **1.3 SYSTEM AND OPERATING DOCUMENTATION**

### **1.3.1 Computer Equipment**

The model entitled "The Hydrologic Evaluation of Landfill Performance" (HELP) was written to run on IBM-compatible personal computers (PC) under the DOS environment.

### **1.3.2 Required Hardware**

The following IBM-compatible CPU (8088, 80286, 80386 or 80486) hardware is required:

1. Monitor, preferably color EGA or better
2. Floppy disk drive (5.25-inch double-sided, double- or high-density; or 3.5-inch

double-sided, double- or high-density)

3. Hard disk drive or a second floppy disk drive
4. 400k bytes or more of available RAM memory
5. 8087, 80287, 80387 or 80486 math co-processor
6. Printer, if a hard copy is desired

### **1.3.3 Software Requirements**

The user must use Microsoft or compatible Disk Operating Systems (MS-DOS) Version 2.10 or a higher version. The user interface executable module was compiled and linked with Microsoft Basic Professional Development System 7.1. Other executable components were compiled with the Ryan-McFarland FORTRAN Version 2.42. The Microsoft Basic Professional Development System and Ryan-McFarland FORTRAN compiler are not needed to run the HELP Model.



# The Hydrologic Evaluation of Landfill Performance (HELP) Model

Engineering  
Documentation for  
Version 3



EPA/600/R-94/168b  
September 1994

**THE HYDROLOGIC EVALUATION OF LANDFILL  
PERFORMANCE (HELP) MODEL**

**ENGINEERING DOCUMENTATION FOR VERSION 3**

by

Paul R. Schroeder, Tamsen S. Dozier, Paul A. Zappi,  
Bruce M. McEnroe, John W. Sjostrom and R. Lee Peyton  
Environmental Laboratory  
U.S. Army Corps of Engineers  
Waterways Experiment Station  
Vicksburg, MS 39180-6199

Interagency Agreement No. DW21931425

Project Officer

Robert E. Landreth  
Waste Minimization, Destruction and Disposal Research Division  
Risk Reduction Engineering Laboratory  
Cincinnati, Ohio 45268

**RISK REDUCTION ENGINEERING LABORATORY  
OFFICE OF RESEARCH AND DEVELOPMENT  
U.S. ENVIRONMENTAL PROTECTION AGENCY  
CINCINNATI, OHIO 45268**



Printed on Recycled Paper

---

## SECTION 1

### PROGRAM IDENTIFICATION

**PROGRAM TITLE:** Hydrologic Evaluation of Landfill Performance (HELP) Model

**WRITERS:** Paul R. Schroeder, Tamsen S. Dozier, John W. Sjostrom and Bruce M. McEnroe

**ORGANIZATION:** U.S. Army Corps of Engineers, Waterways Experiment Station (WES)

**DATE:** September 1994

**UPDATE:** None Version No.: 3.00

**SOURCE LANGUAGE:** The simulation code is written in ANSI FORTRAN 77 using Ryan-McFarland Fortran Version 2.44 with assembly language and Spindrift Library extensions for Ryan-McFarland Fortran to perform system calls, and screen operations. The user interface is written in BASIC using Microsoft Basic Professional Development System Version 7.1. Several of the user interface support routines are written in ANSI FORTRAN 77 using Ryan-McFarland Fortran Version 2.44, including the synthetic weather generator and the ASCII data import utilities.

**HARDWARE:** The model was written to run on IBM-compatible personal computers under the DOS environment. The program requires an IBM-compatible 8088, 80286, 80386 or 80486-based CPU (preferably 80386 or 80486) with an 8087, 80287, 80387 or 80486 math co-processor. The computer system must have a monitor (preferably color EGA or better), a 3.5- or 5.25-inch floppy disk drive (preferably 3.5-inch double-sided, high-density), a hard disk drive with 6 MB of available storage, and 400k bytes or more of available low level RAM. A printer is needed if a hard copy is desired.

**AVAILABILITY:** The source code and executable code for IBM-compatible personal computers are available from the National Technical Information Service (NTIS). Limited distribution immediately following the initial distribution will be available from the USEPA Risk Reduction Engineering Laboratory, the USEPA Center for Environmental Research Information and the USAE Waterways Experiment Station.

**ABSTRACT:** The Hydrologic Evaluation of Landfill Performance (HELP) computer program is a quasi-two-dimensional hydrologic model of water movement across, into, through and out of landfills. The model accepts weather, soil and design data and uses solution techniques that account for surface storage, snowmelt, runoff, infiltration, vegetative growth, evapotranspiration, soil moisture storage, lateral subsurface drainage, leachate recirculation, unsaturated vertical drainage, and leakage through soil, geomembrane or composite liners. Landfill systems including combinations of vegetation, cover soils, waste cells, lateral drain layers, barrier soils, and synthetic geomembrane liners may be modeled. The program was developed to conduct water balance analyses of landfills, cover systems, and solid waste disposal facilities. As such, the model facilitates rapid estimation of the amounts of runoff, evapotranspiration, drainage, leachate collection, and liner leakage that may be expected to result from the operation of a wide variety of landfill designs. The primary purpose of the model is to assist in the comparison of design alternatives as judged by their water balances. The model, applicable to open, partially closed, and fully closed sites, is a tool for both designers and permit writers.

The HELP model uses many process descriptions that were previously developed, reported in the literature, and used in other hydrologic models. The optional synthetic weather generator is the WGEN model of the U.S. Department of Agriculture (USDA) Agricultural Research Service (ARS) (Richardson and Wright, 1984). Runoff modeling is based on the USDA Soil Conservation Service (SCS) curve number method presented in Section 4 of the National Engineering Handbook (USDA, SCS, 1985). Potential evapotranspiration is modeled by a modified Penman method (Penman, 1963). Evaporation from soil is modeled in the manner developed by Ritchie (1972) and used in various ARS models including the Simulator for Water Resources in Rural Basins (SWRRB) (Arnold et al., 1989) and the Chemicals, Runoff, and Erosion from Agricultural Management System (CREAMS) (Knisel, 1980). Plant transpiration is computed by the Ritchie's (1972) method used in SWRRB and CREAMS. The vegetative growth model was extracted from the SWRRB model. Evaporation of interception, snow and surface water is based on an energy balance. Interception is modeled by the method proposed by Horton (1919). Snowmelt modeling is based on the SNOW-17 routine of the National Weather Service River Forecast System (NWSRFS) Snow Accumulation and Ablation Model (Anderson, 1973). The frozen soil submodel is based on a routine used in the CREAMS model (Knisel et al., 1985). Vertical drainage is modeled by Darcy's (1856) law using the Campbell (1974) equation for unsaturated hydraulic conductivity based on the Brooks-Corey (1964) relationship. Saturated lateral drainage is modeled by an analytical approximation to the steady-state solution of the Boussinesq equation employing the Dupuit-Forchheimer (Forchheimer, 1930) assumptions. Leakage through geomembranes is modeled by a series of equations based on the compilations by Giroud et al. (1989, 1992). The processes are linked together in a sequential order starting at the surface with a surface water balance; then evapotranspiration from the soil profile; and finally drainage and water routing, starting at the surface with infiltration and then proceeding downward through the landfill profile to the bottom. The solution procedure is applied repetitively for each day as it simulates the water routing throughout the simulation period.

## SECTION 2

### NARRATIVE DESCRIPTION

The HELP program, Versions 1, 2 and 3, was developed by the U.S. Army Engineer Waterways Experiment Station (WES), Vicksburg, MS, for the U.S. Environmental Protection Agency (EPA), Risk Reduction Engineering Laboratory, Cincinnati, OH, in response to needs in the Resource Conservation and Recovery Act (RCRA) and the Comprehensive Environmental Response, Compensation and Liability Act (CERCLA, better known as Superfund) as identified by the EPA Office of Solid Waste, Washington, DC. The primary purpose of the model is to assist in the comparison of landfill design alternatives as judged by their water balances.

The Hydrologic Evaluation of Landfill Performance (HELP) model was developed to help hazardous waste landfill designers and regulators evaluate the hydrologic performance of proposed landfill designs. The model accepts weather, soil and design data and uses solution techniques that account for the effects of surface storage, snowmelt, runoff, infiltration, evapotranspiration, vegetative growth, soil moisture storage, lateral subsurface drainage, leachate recirculation, unsaturated vertical drainage, and leakage through soil, geomembrane or composite liners. Landfill systems including various combinations of vegetation, cover soils, waste cells, lateral drain layers, low permeability barrier soils, and synthetic geomembrane liners may be modeled. Results are expressed as daily, monthly, annual and long-term average water budgets.

The HELP model is a quasi-two-dimensional, deterministic, water-routing model for determining water balances. The model was adapted from the HSSWDS (Hydrologic Simulation Model for Estimating Percolation at Solid Waste Disposal Sites) model of the U.S. Environmental Protection Agency (Perrier and Gibson, 1980; Schroeder and Gibson, 1982), and various models of the U.S. Agricultural Research Service (ARS), including the CREAMS (Chemical Runoff and Erosion from Agricultural Management Systems) model (Knisel, 1980), the SWRRB (Simulator for Water Resources in Rural Basins) model (Arnold et al., 1989), the SNOW-17 routine of the National Weather Service River Forecast System (NWSRFS) Snow Accumulation and Ablation Model (Anderson, 1973), and the WGEN synthetic weather generator (Richardson and Wright, 1984).

HELP Version 1 (Schroeder et al., 1984a and 1984b) represented a major advance beyond the HSSWDS program (Perrier and Gibson, 1980; Schroeder and Gibson, 1982), which was also developed at WES. The HSSWDS model simulated only the cover system, did not model lateral flow through drainage layers, and handled vertical drainage only in a rudimentary manner. The infiltration, percolation and evapotranspiration routines were almost identical to those used in the Chemicals, Runoff, and Erosion from Agricultural Management Systems (CREAMS) model, which was developed by Knisel (1980) for the U.S. Department of Agriculture (USDA). The runoff and infiltration routines relied heavily on the Hydrology Section of the National Engineering Handbook

(USDA, Soil Conservation Service, 1985). Version 1 of the HELP model incorporated a lateral subsurface drainage model and improved unsaturated drainage and liner leakage models into the HSSWDS model. In addition, the HELP model provided simulation of the entire landfill including leachate collection and liner systems.

Version 1 of the HELP program was tested extensively using both field and laboratory data. HELP Version 1 simulation results were compared to field data for 20 landfill cells from seven sites (Schroeder and Peyton, 1987a). The lateral drainage component of HELP Version 1 was tested against experimental results from two large-scale physical models of landfill liner/drain systems (Schroeder and Peyton, 1987b). The results of these tests provided motivation for some of the improvements incorporated into HELP Version 2.

Version 2 (Schroeder et al., 1988a and 1988b) presented a great enhancement of the capabilities of the HELP model. The WGEN synthetic weather generator developed by the USDA Agricultural Research Service (ARS) (Richardson and Wright, 1984) was added to the model to yield daily values of precipitation, temperature and solar radiation. This replaced the use of normal mean monthly temperature and solar radiation values and improved the modeling of snow and evapotranspiration. Also, a vegetative growth model from the Simulator for Water Resources in Rural Basins (SWRRB) model developed by the ARS (Arnold et al., 1989) was merged into the HELP model to calculate daily leaf area indices. Modeling of unsaturated hydraulic conductivity and flow and lateral drainage computations were improved. Default soil data were improved, and the model permitted use of more layers and initialization of soil moisture content.

In Version 3, the HELP model has been greatly enhanced beyond Version 2. The number of layers that can be modeled has been increased. The default soil/material texture list has been expanded to contain additional waste materials, geomembranes, geosynthetic drainage nets and compacted soils. The model also permits the use of a user-built library of soil textures. Computations of leachate recirculation and groundwater drainage into the landfill have been added. Moreover, HELP Version 3 accounts for leakage through geomembranes due to manufacturing defects (pinholes) and installation defects (punctures, tears and seaming flaws) and by vapor diffusion through the liner based on the equations compiled by Giroud et al. (1989, 1992). The estimation of runoff from the surface of the landfill has been improved to account for large landfill surface slopes and slope lengths. The snowmelt model has been replaced with an energy-based model; the Priestly-Taylor potential evapotranspiration model has been replaced with a Penman method, incorporating wind and humidity effects as well as long wave radiation losses (heat loss at night). A frozen soil model has been added to improve infiltration and runoff predictions in cold regions. The unsaturated vertical drainage model has also been improved to aid in storage computations. Input and editing have been further simplified with interactive, full-screen, menu-driven input techniques.

The HELP model requires daily climatologic data, soil characteristics, and design specifications to perform the analysis. Daily rainfall data may be input by the user,

generated stochastically, or taken from the model's historical data base. The model contains parameters for generating synthetic precipitation for 139 U.S. cities. The historical data base contains five years of daily precipitation data for 102 U.S. cities. Daily temperature and solar radiation data are generated stochastically or may be input by the user. Necessary soil data include porosity, field capacity, wilting point, saturated hydraulic conductivity, and Soil Conservation Service (SCS) runoff curve number for antecedent moisture condition II. The model contains default soil characteristics for 42 material types for use when measurements or site-specific estimates are not available. Design specifications include such things as the slope and maximum drainage distance for lateral drainage layers, layer thicknesses, leachate recirculation procedure, surface cover characteristics and information on any geomembranes.

Figure 1 is a definition sketch for a somewhat typical closed hazardous waste landfill profile. The top portion of the profile (layers 1 through 4) is the cap or cover. The bottom portion of the landfill is a double liner system (layers 6 through 11), in this case composed of a geomembrane liner and a composite liner. Immediately above the bottom composite liner is a leakage detection drainage layer to collect leakage from the primary liner, in this case, a geomembrane. Above the primary liner are a geosynthetic drainage net and a sand layer that serve as drainage layers for leachate collection. The drain layers composed of sand are typically at least 1-ft thick and have suitably spaced perforated or open joint drain pipe embedded below the surface of the liner. The leachate collection drainage layer serves to collect any leachate that may percolate through the waste layers. In this case where the liner is solely a geomembrane, a drainage net may be used to rapidly drain leachate from the liner, avoiding a significant buildup of head and limiting leakage. The liners are sloped to prevent ponding by encouraging leachate to flow toward the drains. The net effects are that very little leachate should leak through the primary liner and virtually no migration of leachate through the bottom composite liner to the natural formations below. Taken as a whole, the drainage layers, geomembrane liners, and barrier soil liners may be referred to as the leachate collection and removal system (drain/liner system) and more specifically a double liner system.

Figure 1 shows eleven layers--four in the cover or cap, one as the waste layers, three in the primary leachate collection and removal system (drain/liner system) and three in the secondary leachate collection and removal system (leakage detection). These eleven layers comprise three subprofiles or modeling units. A subprofile consists of all layers between (and including) the landfill surface and the bottom of the top liner system, between the bottom of one liner system and the bottom of the next lower liner system, or between the bottom of the lowest liner system and the bottom of the lowest soil layer modeled. In the sketch, the top subprofile contains the cover layers, the middle subprofile contains the waste, drain and liner system for leachate collection, and the bottom subprofile contains the drain and liner system for leakage detection. Six subprofiles in a single landfill profile may be simulated by the model.

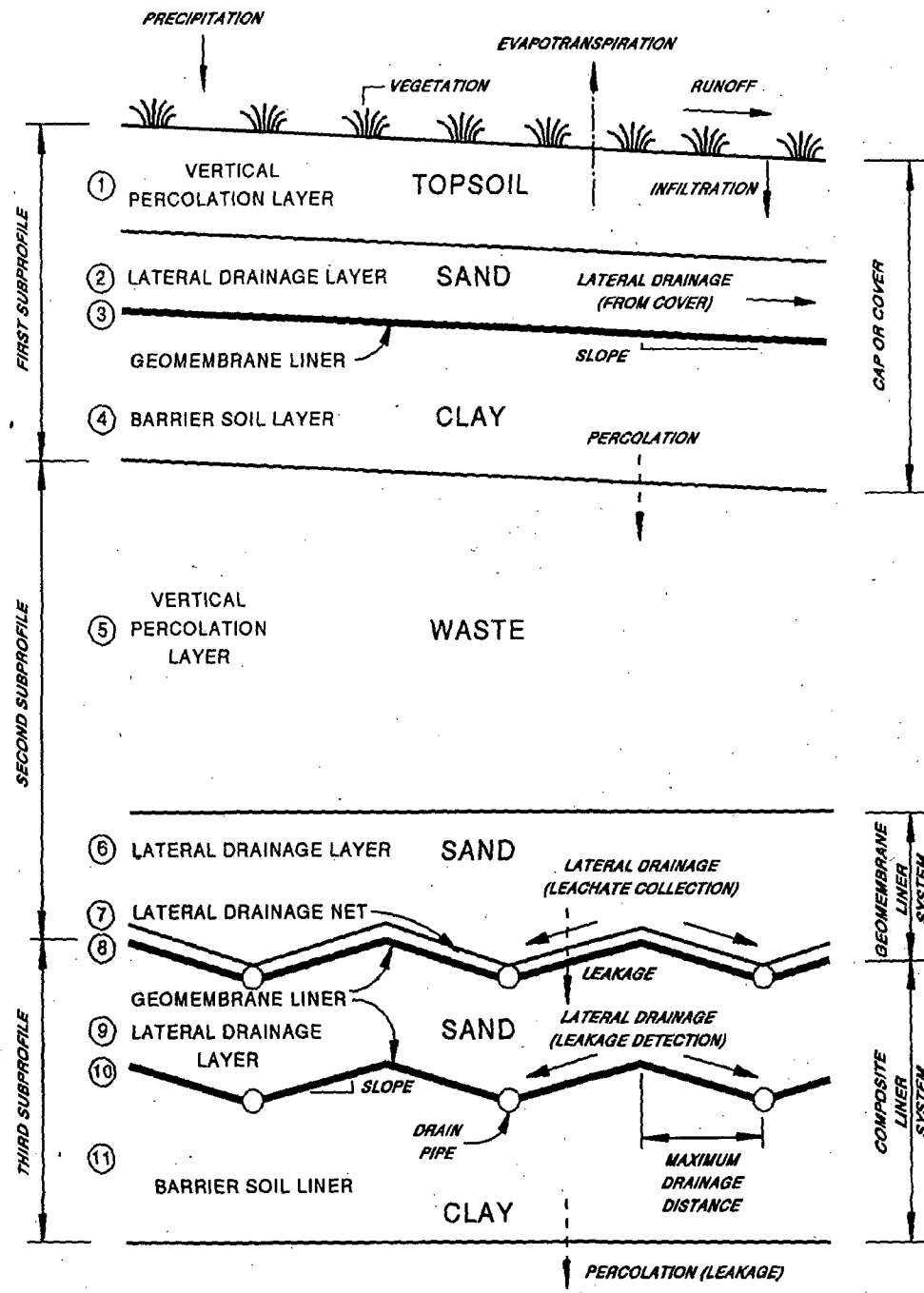


Figure 1. Schematic Profile View of a Typical Hazardous Waste Landfill

The layers in the landfill are typed by the hydraulic function that they perform. Four types of layers are available: vertical percolation layers, lateral drainage layers, barrier soil liners and geomembrane liners. These layer types are illustrated in Figure 1. The topsoil and waste layers are generally vertical percolation layers. Sand layers above liners are typically lateral drainage layers; compacted clay layers are typically barrier soil liners. Geomembranes are typed as geomembrane liners. Composite liners are modeled as two layers. Geotextiles are not considered as layers unless they perform a unique hydraulic function.

Flow in a vertical percolation layer (e.g., layers 1 and 5 in Figure 1) is either downward due to gravity drainage or extracted by evapotranspiration. Unsaturated vertical drainage is assumed to occur by gravity drainage whenever the soil moisture is greater than the field capacity (greater than the wilting point for soils in the evaporative zone) or when the soil suction of the layer below the vertical percolation layer is greater than the soil suction in the vertical percolation layer. The rate of gravity drainage (percolation) in a vertical percolation layer is assumed to be a function of the soil moisture storage and largely independent of conditions in adjacent layers. The rate can be restricted when the layer below is saturated and drains slower than the vertical percolation layer. Layers, whose primary hydraulic function is to provide storage of moisture and detention of drainage, should normally be designated as vertical percolation layers. Waste layers and layers designed to support vegetation should be designated as vertical percolation layers, unless the layers provide lateral drainage to collection systems.

Lateral drainage layers (e.g., layers 2, 6, 7 and 9 in Figure 1) are layers that promote lateral drainage to collection systems at or below the surface of liner systems. Vertical drainage in a lateral drainage layer is modeled in the same manner as for a vertical percolation layer, but saturated lateral drainage is allowed. The saturated hydraulic conductivity of a lateral drainage layer generally should be greater than  $1 \times 10^{-3}$  cm/sec for significant lateral drainage to occur. A lateral drainage layer may be underlain by only a liner or another lateral drainage layer. The slope of the bottom of the layer may vary from 0 to 40 percent.

Barrier soil liners (e.g., layers 4 and 11 in Figure 1) are intended to restrict vertical flow. These layers should have hydraulic conductivities substantially lower than those of the other types of layers, typically below  $1 \times 10^{-6}$  cm/sec. The program allows only downward flow in barrier soil liners. Thus, any water moving into a liner will eventually percolate through it. The leakage (percolation) rate depends upon the depth of water-saturated soil (head) above the base of the layer, the thickness of the liner and the saturated hydraulic conductivity of the barrier soil. Leakage occurs whenever the moisture content of the layer above the liner is greater than the field capacity of the layer. The program assumes that barrier soil liner is permanently saturated and that its properties do not change with time.

Geomembrane liners (e.g., layers 3, 8 and 10 in Figure 1) are layers of nearly

impermeable material that restricts significant leakage to small areas around defects. Leakage (percolation) is computed to be the result from three sources: vapor diffusion, manufacturing flaws (pinholes) and installation defects (punctures, cracks, tears and bad seams). Leakage by vapor diffusion is computed to occur across the entire area of the liner as a function of the head on the surface of the liner, the thickness of the geomembrane and its vapor diffusivity. Leakage through pinholes and installation defects is computed in two steps. First, the area of soil or material contributing to leakage is computed as a function of head on the liner, size of hole and the saturated hydraulic conductivity of the soils or materials adjacent to the geomembrane liner. Second, the rate of leakage in the wetted area is computed as a function of the head, thickness of soil and membrane and the saturated hydraulic conductivity of the soils or materials adjacent to the geomembrane liner.

# DEATH OF ROOT TISSUES IN STANDING [LIVE] AND FELLED LOBLOLLY PINES<sup>1</sup>

Charles H. Walkinshaw<sup>2</sup>

**Abstract**—Recycling tree root components is important in sustaining the productivity of southern pine forests. Death of outer cortical tissues and mortality of short roots is ubiquitous in conifers. Affected tissues lose their starch grains and accumulate secondary products, such as tannins. In this study, 10-year-old loblolly pine trees were cut at the soil surface and sequential samples of roots were collected, fixed, embedded, and sectioned for light microscopy at monthly intervals. Observations showed roots of felled trees were similar to those of standing controls for approximately 5 months. Indicators of cell and tissue death were the disappearance of starch grains, increased tannin accumulation, and decreased staining of nuclei. This pattern of changes was remarkably similar to that of dying cortical cells. The long period (5 months) after felling and before the roots die probably has a significant effect on root microflora and the distribution of nutrients from the decomposition of surface woody debris and root systems.

## INTRODUCTION

Loss of biomass from the crowns of loblolly pines (*Pinus taeda* L.) is easy to measure (Kozlowski and others 1991; Sampson and others 1998); loss of below-ground biomass can be harder to sample and measure (Kozlowski 1971, Ruark 1993). Death and rate of root decay are important on many reforestation sites where nutrient supply is marginal for seedling establishment and early tree growth. Nutrient cycling is influenced by how quickly root turnover occurs. Death of root cells was reviewed by Coulter as early as 1900 (Eames and MacDaniels 1947). I used ease of peeling the root cortex to assess the condition of primary roots. Smith (1935), Eames and MacDaniels (1947) and Esau (1953) detailed the function of the root cortex and its relationship to secondary growth. Those anatomical descriptions emphasize the complexity of below-ground biomass loss. Moreover, they suggest that microscopical examination is essential for classifying cortical cells as dead. Medical investigators routinely use a number of cellular traits to determine cell death (Ellis and others 1991, Robbins 1987). Emphasis is placed on the condition of the nucleus when standardized stain schedules are applied to sections of tissue. I applied such schedules to pine root tissues.

My objective was to devise quantitative measurements of cell traits that would precisely define root cell death. After accomplishing this, cell death was induced by tree felling and studied in detail. These two approaches provided a quantitative method for studying below-ground biomass in loblolly pine roots.

## SITES

Observations to select methods and cellular traits were made on roots from young (5 to 10 years) loblolly pine stands in the Palustris Experimental Forest (Louisiana), the Homochitto National Forest (Mississippi), and in a Forest Service planting near Laurinburg, NC. A total of 5,476 roots were sectioned and stained for light microscopy.

Experiments to induce root-cell death were conducted in the Palustris Experimental Forest. Treatments imposed in a 10-year-old loblolly pine study area included: (1) a control (no treatment), (2) felling in February and May 1994, (3) girdling at breast height, and (4) pruning lower limbs (leaving the top 1/3 of crown). Root anatomy of 10 trees each of the

control and those that were felled in February and May (treatment 2) was evaluated each month for 6 months. Treatments 3 and 4 were applied in May and sampled only 5 months following treatment.

## PROCEDURES

Roots were sampled 1 m from the stem to a 20-cm depth for 6 to 10 trees at each site (Walkinshaw 1995). A cross-section of each root <1 cm in diameter was excised and placed unwashed into formalin-acetic acid-alcohol (FAA) (Sass 1951). After 2 to 4 weeks, roots were rinsed with 70 percent ethyl alcohol. Specimens were cut to 1 to 3 mm, dehydrated in ethyl alcohol series, embedded in paraffin and cut into 7- to 10- $\mu$ m sections. Two or three sections that contained 9 to 18 roots from a single tree were mounted on a slide. Nine slides were prepared for each tree. Several staining schedules were used on root sections during the observation phase: acid fuchsin, Congo red, Giemsa, Groett's methenamine, safranin-aniline blue, toluidine blue, hematoxylin-eosin, Papanicolaou's schedule, and an acid-Schiff schedule (Haas 1980). Only the last three were used during the experimental phase. Root traits were scored as proportions or as real values. Papanicolaou's schedule was read for two slides with two or three sets of roots per slide. I used hematoxylin-eosin stain to verify nuclear viability in cells. Starch and tannin deposits were confirmed using an acid-Schiff schedule (Walkinshaw and Tiaras 1998). Cell traits used as dependent variables in the treatment evaluations are listed in table 1.

## RESULTS

### Initial Observations

Shedding of the root cortex was first indicated in a large number of cells, distributed at random, by the breakdown of starch grains. Nuclei with changed stain affinity were prominent in most parenchyma and cortical ray cells. Cytoplasm became condensed to a small volume in the cortical cell periphery. These cells appeared net-like with primary cell walls held to each other and to the thin residual of living cortical cells. Nuclear staining as a measure of loss of vitality indicated that death of the cortex shed occurs after the loss of starch grains (Greenberg 1997).

The proportion of roots with shedding was high in collections from 5- and 10-year-old trees in the Palustris Experimental

<sup>1</sup> Paper presented at the Tenth Biennial Southern Silvicultural Research Conference, Shreveport, LA, February 16-18, 1999.

<sup>2</sup> Emeritus Scientist, USDA Forest Service, Southern Research Station, Pineville, LA 71360.

**Table 1—Cell traits used to evaluate root viability in loblolly pine**

Trait	Description
Abnormal cambium	Cambial initials reduced in number or out of alignment. Necrotic derivations present.
Cortex shedding	Cortical cells dead and remain attached or are released into the soil.
Dead root	Cells with ruptured membranes. Tannin adheres to cell walls. Chromatin abnormal. Starch grains may or may not be present.
Nuclear stain	Degeneration (pyknosis) of chromatin. Altered staining throughout the tissues.
Number of	Number of starch-containing plastids per cell viewed at a single focus per cell length at 100 to 500 diameters.
Root diameter	Actual measurement of roots less than 3 mm. Estimates for larger roots. Diameter includes attached shed.
Size of	Size of starch grains scored as 1, 2, or 3 for each cell. Range in actual size was 0.5 to 4.0 microns.
Starch use	Starch grains 50 percent or more degraded.
Tannin	Accumulation of tannin-containing cells in the cortex, rays and inner xylem. Number of cells with accumulation <10 to >1000.

Forest (table 2); I collected root samples in the fall on two sites there. The biomass loss in shed material was 65 to 75 percent of the root as determined by light microscopy.

Mycorrhizal short roots died during cortex shedding. Tannin accumulated at their base and sealed the torn end of the dead short root. New lateral roots often emerged from the dead mycorrhizal short roots.

Starch grain degradation varied from 0 to 100 percent in cortical cells of loblolly pine roots (table 3). Values were low for the younger 5-year-old trees and widely different in collections from 10-year-old trees.

**Table 2—Incidence of shedding in roots of plantation-grown loblolly pines on different sites**

Number of roots sectioned	Proportion of roots with cortical shedding
111	0.90 ± 0.06
120	.78 ± .09
126	.80 ± .16
132	.70 ± .12
119	.69 ± .14
112	.73 ± .16

**Table 3—Variation in use of starch grains in the root cortex in loblolly pines<sup>a</sup>**

Number of roots	Proportion of roots with starch utilization
101	0.93
122	.76
079	.41
064	.33
264	.17
258	.01

<sup>a</sup>Largest two samples of roots were taken from 5-year-old trees. Other samples were from 10-year-old trees.

### Experimental

An analysis of variance (ANOVA) procedure using "month after felling" as class gave a probability of  $p = 0.0001$  for each dependent variable. Tukey's studentized range test (Snedecor 1956) indicated significance when comparisons were made of 5-month means and 0-, 1-, 3- and 4-month means, respectively. Means for traits and treatments 5 months after felling are given in table 4. A plot of abnormal nuclei and dead roots 6 months after felling is given in figure 1. Means for other traits from 0 to 6 months after felling are given in figures 2 and 3.

### DISCUSSION

#### Initial Observations

The cortical shedding in roots from felled loblolly pines appears to involve about 75 percent of the primary root biomass. Some of the biomass may be lost with the gradual disappearance of starch grains. Abnormal staining of chromatin in the nucleus indicated depletion of energy and death of the cortical cells. Cell mortality in the formation of shed material was unusual for the low incidence of tannin that accumulated. Wounds in the cortex were unusually few and microbial invasion of cells in the shed material was

Table 4—Cellular traits in sectioned roots sampled five months after installing treatments

Trait	Fell 2/94	Fell 5/94	Girdle	Prune	Control
----- Percent of roots -----					
Nuclei	50.0	40.0	9.0	2.0	0.0
Starch grain (no.)	2.2	2.4	5.2	4.0	10.2
Size of starch	1.0	0.6	1.5	1.2	2.3
Starch use	30.0	10.0	30.0	1.2	76.0
Tannin X 5	70.0	60.0	50.0	20.0	26.0
Cambium dam.	40.0	30.0	0.0	0.0	0.0

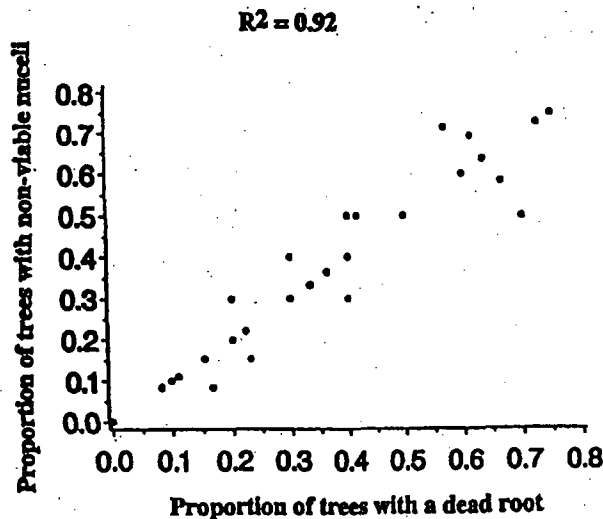


Figure 1—Relationship between nuclear condition and dead roots 5 months after felling.

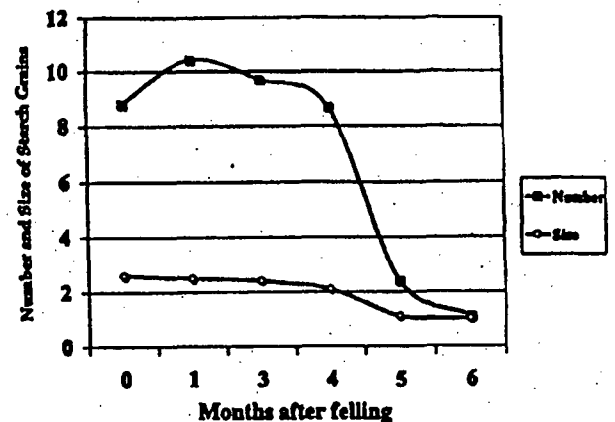


Figure 2—Effect of felling on number and size of starch grains in cortical cells.

Root death was characterized by depletion of starch, abnormal staining of nuclei, and alteration of tannin deposits. Tannin was released from cell vacuoles and increased protein alteration. In roots of felled trees, the appearance of cortical cells after 5 and 6 months was similar to that of cells of cortex shed. Both conditions suggest nutrient starvation. In trees girdled or pruned, root anatomy did not differ from that of the control.

delayed until they were nearly devoid of cytoplasm. These events can be compared to shedding of above-ground plant parts (Kozlowski 1973). Although mycorrhizal root death and shedding occurred simultaneously, considerable tannin accumulated at the base of these short roots. This suggests a more active process than occurred in shed cells. Mycorrhizal roots are not connected to vascular tissue.

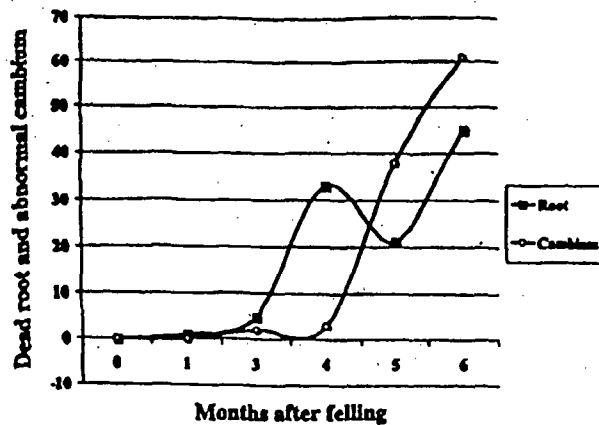


Figure 3—Delayed response of loblolly pine roots to felling.

Lateral roots form only when nuclear division occurs in the vascular zone (Smith and Read 1997); they are, therefore, only temporary structures in the below-ground biomass (Kozlowski 1971).

#### Experimental

Death of root cells in felled trees occurred in a sequence that has been described for other plant and animal cells (Ellis and others 1991, Greenberg 1997, Robbins 1987). Ample evidence shows that nuclear staining is a reliable indicator of cell death. In pine roots, nuclei are relatively large (8  $\mu\text{m}$ ) and easy to classify as active (bright red), quiescent (bluish purple), and dead (gray with black). Abnormal nuclei appeared in large numbers 5 months after felling. This signaled root death.

Microscopical light observations have focused on anatomical details in only a few specimens (Eames and MacDaniels 1947, Esau 1953, Kozlowski and others 1991). This study considered thousands of observations and compared variables and means by standard statistical analysis. When the means of dependent variables were plotted, plot trends were apparent over time. However, the data taken over time are not independent and should be considered with caution. The easiest variable to quantify microscopically was the number of starch grains per cell. However, as cell death approached (5 months after felling), starch grains became so depleted that counts had to be made at 500 diameters. By contrast, nuclei were the same size or had enlarged before death occurred.

Often, silviculturists and pathologists consider below-ground tissue death to occur when trees are felled. However, Bormann (1961) showed that eastern white pine (*Pinus strobus* L.) trees that were not root grafted to intact standing trees were alive one growing season following cutting. Because trees in this study were young, extensive root grafting had not likely occurred (Kozlowski 1971). Three to four months after felling, the roots (small to large) from felled trees were not anatomically different from untreated controls. Pathogenic and saprophytic organisms might increase significantly in roots of freshly felled trees, but

unless there is significant root grafting there should be little effect on standing trees. Stand density and tree age may also affect root interaction with microorganisms and the degree of root deterioration, but we did not measure those variables.

#### CONCLUSIONS

Death of cortical cells and mycorrhizae during the shedding process can cause a loss of 75 percent of the primary root biomass. A lot of starch grains are broken down during shedding, a process that can be reproduced by root starvation resulting from removal of above-ground tissues. Of the variables evaluated, disappearance of starch grains and abnormal nuclei staining are the most reliable when monitoring cell death. Roots of felled trees lived 4 months or longer. The extended life of a felled tree's roots probably will significantly affect microflora. The distribution of nutrients from extended root decay following harvest may affect nutrient availability for forest regeneration.

#### REFERENCES

- Bormann, F.H. 1961. Intraspecific root grafting and the survival of eastern white pine stumps. *Forest Science*. 7: 247-256.
- Eames, A.J.; MacDaniels, L.H. 1947. Introduction to plant anatomy. 2<sup>nd</sup> ed. New York: McGraw-Hill. 427 p.
- Ellis, R.E.; Yuan, J.; Horvitz, H.R. 1991. Mechanisms and functions of cell death. *Annual Review Cell Biology*. 7: 663-698.
- Esau, K. 1953. Plant anatomy. New York: John Wiley. 735 p.
- Greenberg, J.T. 1997. Programmed cell death in plant-pathogen interactions. *Annual Review Plant Physiology Plant Molecular Biology*. 48: 625-645.
- Haas, E. 1980. Fifty diagnostic special stains for surgical pathology. Los Angeles: All-Type Editorial. 86 p.
- Kozlowski, T.T. 1971. Growth and development of trees. New York: Academic Press. 348 p. Vol. 2.
- Kozlowski, T.T. 1973. Shedding of plant parts. New York: Academic Press. 560 p.
- Kozlowski, T.T.; Kramer, P.J.; Pallardy, S.G. 1991. The physiological ecology of woody plants. New York: Academic Press. 657 p.
- Robbins, S.L. 1987. Basic pathology. Philadelphia: W.B. Saunders Company. 787 p.
- Ruark, G.A. 1993. Modeling soil temperature effects on *in situ* decomposition rates for fine roots of loblolly pine. *Forest Science*. 39: 118-129.
- Sass, J.E. 1951. Botanical microtechnique. 2<sup>nd</sup> ed. Ames, IA: Iowa State College Press. 228 p.
- Smith, G.M. 1935. A textbook of general botany. 3<sup>rd</sup> ed. New York: Macmillan. 574 p.
- Smith, S.E.; Read, D.J. 1997. Mycorrhizal symbiosis. 2<sup>nd</sup> ed. New York: Academic Press. 605 p.
- Snedecor, G.W. 1956. Statistical methods. 5<sup>th</sup> ed. Ames, IA: Iowa State University Press. 634 p.

Walkinshaw, C.H. 1995. Vulnerability of loblolly pine roots to environmental and microbial stresses. In: Edwards, M.B., ed. Proceedings of the eighth biennial southern silvicultural research conference; 1994 November 1-3; Auburn, AL. Gen. Tech. Rep. SRS-1. Asheville, NC: U.S. Department of Agriculture, Forest Service, Southern Research Station: 354-356.

Walkinshaw, C.H.; Tarks, A.E. 1998. Effects of soil compaction and organic matter removal on morphology of secondary roots of loblolly pine. In: Waldrop, T.A., ed. Proceedings of the ninth biennial southern silvicultural research conference; 1997 February 25-27; Clemson, SC. Gen. Tech. Rep. SRS-20. Asheville, NC: U.S. Department of Agriculture, Forest Service, Southern Research Station: 418-421.

# MORPHOLOGICAL STUDIES OF THE ROOT OF RED PINE, PINUS RESINOSA I. GROWTH CHARACTERISTICS AND PATTERNS OF BRANCHING<sup>1</sup>

HUGH E. WILCOX

Department of Forest Botany and Pathology, State University College of Forestry, Syracuse, New York

## A B S T R A C T

Observations were made of the seasonal root growth behavior under natural conditions and under controlled conditions in plant observation boxes. Under natural conditions root growth conformed to the commonly reported pattern of a surge of growth in the spring, a mid-summer low, and a renewed burst in the fall. Growth of individual roots was cyclic. Growth patterns ordinarily varied according to root diameter and branching and in the plantations were modified by soil moisture conditions. Observations of roots during periods of constant elongation showed that the distance from the root apex to the first lateral root primordium varied directly with growth rate. Laterals did not arise in strict acropetal succession, and lateral root abortion was common, particularly in large-diameter, fast-growing roots. Observations of root initiation in relation to seasonal growth increments and to dormancy structures showed an increase in numbers of laterals on both the proximal and distal portions of a seasonal increment.

IN AN EARLIER paper (Wilcox, 1964) the root morphology of red pine (*Pinus resinosa* Ait.) and the anatomical variations in dimensions and configurations of primary xylem that accompany differences in diameter and length of individual roots were described. A scheme of root classification was proposed in an effort to relate roots to one another in field investigations. This classification utilized the separation into contrasting long- and short-root branches and further subdivided long roots into classes termed pioneer, mother, and subordinate mother roots. These classes were delimited on the basis of diameter and closeness of branching. The present paper examines the relationship of such differences in branching to various aspects of growth activity in the root. A subsequent paper will consider these features in relation to the seasonal development of mycorrhizae.

**MATERIALS AND METHODS**—The roots examined were from three principal sources: (1) Experiments with 2- and 3-year-old seedlings in root observation boxes; (2) weekly samplings of 2- and 3-year-old seedlings from a nursery throughout two growing seasons; and (3) periodic collections of terminal root portions from 20- to 30-year-old plantation trees on a variety of sites.

In the root observation experiments, red pine seedlings were lifted from a nursery and planted in individual boxes, each made from two panes of glass mounted  $\frac{1}{2}$  inch apart on a rigid wooden frame. The soil in these boxes was collected from the Ap horizon of a Hinckley coarse sand. The

boxes were placed in a growth chamber operating on a 16-hr photoperiod under an illumination of approximately 3000 ft-c from eighteen 100-w cool-white fluorescent lamps supplemented by eight 100-w incandescent lamps. Room temperature was 75 F during the photoperiod and 55 F during the dark period. The boxes were watered regularly and periodically received a complete nutrient solution.

Observations were made of the growth rates and growth periodicity of individual roots and of their patterns of lateral root initiation. Samples for anatomical investigation were selected from roots which had maintained a constant growth rate for at least 10 days prior to sampling. The sampled roots were killed in CRAF III (Sass, 1940), embedded in paraffin, and slides prepared by conventional techniques.

Roots of the 2- and 3-year-old seedlings from the nursery were carefully excavated and the root systems photographed for patterns of development. Terminal root portions of the various branch orders were sampled for investigation of anatomical features associated with seasonal development. Slides were prepared according to the procedures mentioned above. Details of fungal invasion were studied from slides prepared with a chlorazol-Pianese stain combination (Wilcox and Marsh, 1964). Slides stained in an alcoholic solution of *Chelidonium majus* L. (procedure by Elisei, 1941) were used for a study of the developmental stages of the dormant root by fluorescence microscopy. Entire root systems and selected first- and second-order laterals were preserved in FAA for later morphological studies. Some of these were bleached in sodium hypochlorite and cleared in chloral

<sup>1</sup> Received for publication 5 June 1967.  
This research was supported in part by N. S. F. grant G 2093.

hydrate for studies of patterns of root initiation in relation to seasonal increments of root elongation. Others were used for preparation of transverse freehand sections to follow changes in diameter of the primary body.

The roots collected from plantation trees were treated exactly as those from the nursery. In addition, photographs were made of the details of mycorrhizal structure and mycorrhizae were collected for studies of their seasonal ontogeny.

**SEASONAL GROWTH BEHAVIOR OF INDIVIDUAL ROOTS UNDER NATURAL CONDITIONS**—The individual roots of red pine are dormant throughout the winter under natural conditions in the vicinity of Syracuse, N. Y. Many roots have ceased elongation by early November and there is a progressive increase in numbers of non-growing roots throughout this month, with most roots being inactive by mid-December.

In each root the process of metacutization (Wilcox, 1954) proceeds gradually in certain cells of the cortex and root cap following the cessation of elongation. This process culminates in the formation of dormancy layers enclosing the apical region. The metacutized layers develop first in the cells of the root cap and form a thimble-shaped zone of cells surrounding the apex (Fig. 1). The tissues of the root continue their acropetal differentiation and the endodermis becomes suberized to the vicinity of the apical initials. The culminating event in the development of the dormant apex is the formation of a bridge of metacutized cells in the cortex joining the outer metacutized cells of the root cap to the suberized endodermis. Figure 2 is an early stage in the development of this bridge. The bridge develops last in the central region of the cortex with the junction of two arcs of metacutized cells, one extending centrifugally from a position of contact with the suberized endodermis and the other extending centripetally from the outer zone of metacutized cells.

All roots collected on 1 January 1957 and on 1 January 1958 were completely enclosed in dormancy layers. Figure 3 shows the appearance of a completely enclosed root sampled on 21 February 1958. Occasional white tips were encountered throughout the winter, but anatomical examination of such roots revealed dormancy layers completely enclosing the apices. The white appearance resulted from the fact that the metacutization layers surrounding the apices occurred along the surface of the root cap; thus no cells were isolated to become necrotic and brown.

The roots of red pine remain dormant until late April or early May. Periodic collections of nursery seedlings in the spring revealed that root growth commences about a week before separation of the bud scales in the terminal leader of the shoot. The closeness in the onset of root and shoot growth in red pine was in contrast to

the situation in adjacent beds of spruce, fir, and larch in which active root growth occurred for 4 to 6 weeks ahead of visible shoot growth.

The beginning of root growth in red pine is marked by the rupture of the outer metacutization layers and the emergence of a new white apex which contrasts sharply with the brown of the previous seasonal increment. The cells of the closure through the cortex remain intact and can be detected as long as the cortex is retained (Fig. 4).

When a dormant apex starts to grow it elongates gradually and achieves its maximum rate from 1 to 2 weeks later. This delay may result partly from the fact that the previous year's cells have matured, and renewed cell elongation requires an initial period of cell division. Also during this interval there is a significant increase in soil temperature which could contribute to the rate increase.

Dormant apices do not become active simultaneously over the whole root system but resume their activity over a period of several weeks. The pattern of root system activation is complex and is influenced by differences in branching order, root vigor, and soil depth of the individual apices. Roots begin to grow earlier in the upper than in the deeper soil layers. Less explicable is the fact that second-order laterals frequently start their growth before the first-order lateral from which they arise. In some cases, this might be explainable by differences in soil depth, but the same phenomenon was frequently encountered between second- and third-order laterals with the earlier growth of the latter. However the growth period of these higher-order laterals is very short, and many third-order laterals cease elongating by the time the first-order laterals commence to grow.

The peak of the spring root growth activity as indicated by the greatest number of actively growing apices occurs during the month of June. A midsummer lull occurs in July or August with only the apices of the larger roots remaining active. This lull is followed by another surge of activity in late summer or early fall, depending on soil moisture conditions. This second period of root growth may even appear more vigorous than the spring period because of the activity of increasing numbers of new roots initiated during the current season, as well as the renewed vigor of the principal first- and second-order laterals. The formation of mycorrhizae also is greatly stimulated during this period.

Although the above observations refer to root activity in the forest nursery, analagous patterns of development are found in collections from the plantations. Root growth activity is similarly delayed in the spring until about the time for renewed shoot activity. Root growth is first encountered in the renewed growth of the smaller apices in the litter layer. These rootlets include

ce, fir, and  
 occurred for  
 growth.  
 red pine is  
 metacutiza-  
 new white  
 e brown of  
 cells of the  
 ct and can  
 is retained

it elongates  
 rate from  
 sult partly  
 cells have  
 requires an  
 luring this  
 use in soil  
 o the rate

tive simul-  
 out resume  
 ral weeks.  
 is complex  
 branching  
 individual  
 the upper  
 plicable is  
 frequently  
 der lateral  
 this might  
 depth, but  
 ountered  
 erals with  
 wever the  
 rals is very  
 rals cease  
 er laterals

activity as  
 of actively  
 month of  
 or August  
 remaining  
 er surge of  
 depending  
 nd period  
 e vigorous  
 e activity  
 ted during  
 wed vigor  
 er laterals.  
 is greatly

er to root  
 is patterns  
 ions from  
 s similarly  
 e time for  
 h is first  
 he smaller  
 ts include

both mycorrhizae and very thin subordinate  
 mother roots. The period of peak spring activity  
 is characterized by a maximum number of

growing apices in all categories—pioneer, mother,  
 subordinate mother, and short-root branches.  
 Particularly striking is the occurrence of numbers

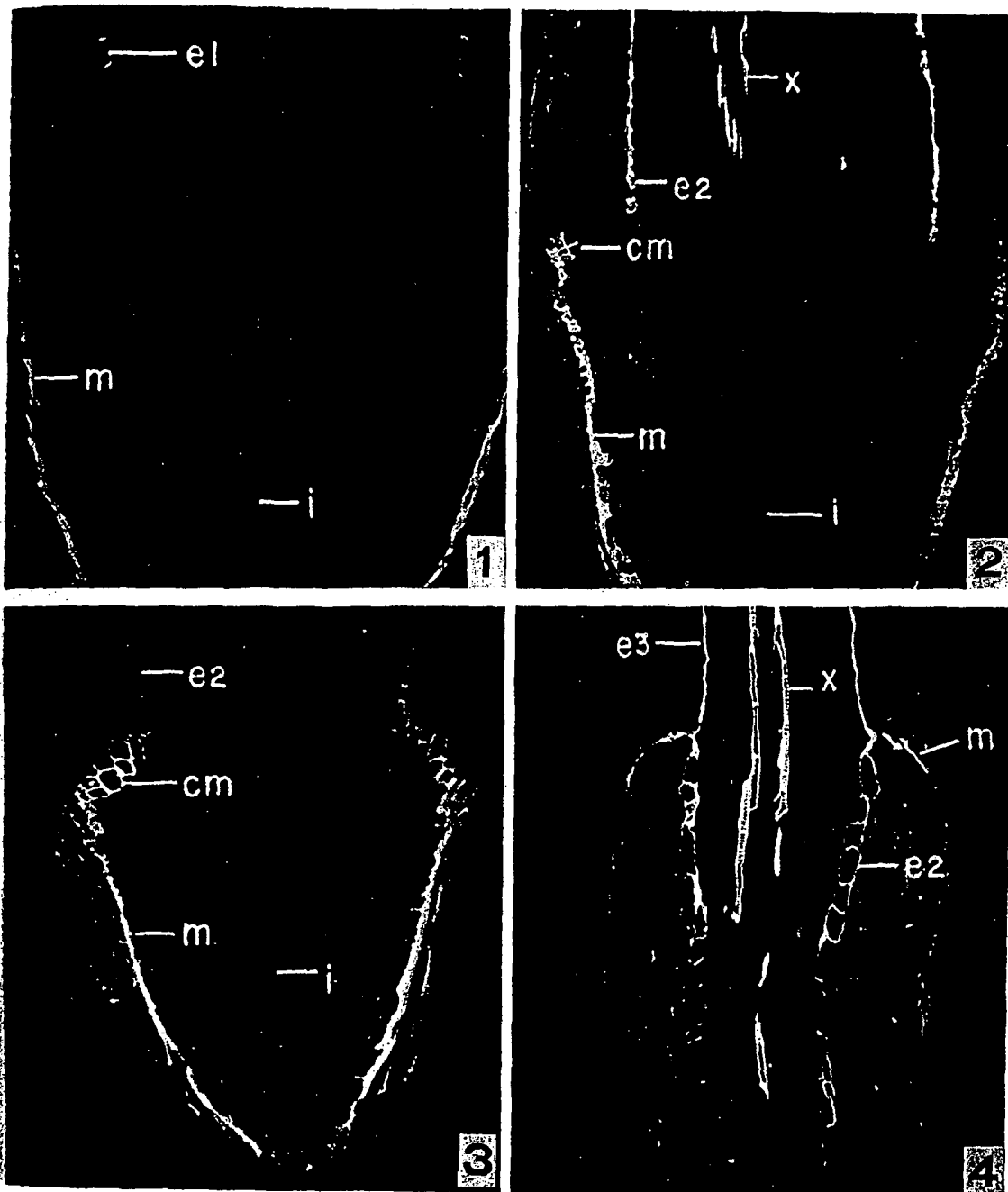


Fig. 1-4. Developmental stages of dormancy structures in red pine root apex. Details are: e1, endodermis with initial Casparian strips; e2, endodermis with suberized walls; e3, collapsed endodermis; i, apical initials; m, metacutization layer; cm, metacutized cortical cells; x, xylem elements.—Fig. 1. Initial appearance of metacutization layer around root apex together with acropetal differentiation of Casparian strips in endodermis; 27 November 1957, X 65.—Fig. 2. Early stage in development of metacutized cortical bridge joining outer metacutization layer to the suberized endodermis; 4 December 1957, X 65.—Fig. 3. Dormant root apex with dormancy structures completely developed; 21 February 1958, X 50.—Fig. 4. Remnants of dormancy structures following resumption of root growth; 29 April 1958, X 80.

of large-diameter pioneer roots with their long white apices and sparse branching. The relative numbers of actively growing roots in the various categories vary with site conditions and stand vigor in a manner which is poorly understood.

A midsummer lull in root growth activity also occurs in the plantations and is similarly followed by a renewed surge of growth in the late summer and early fall. Actively growing pioneer roots are again frequently evident, but mycorrhizal development also is active. These two contrasting types of roots are found in balanced numbers in the healthier stands (Fig. 5), but on sites with "red pine decline" (Stone, Morrow, and Welch, 1954) pioneer roots frequently occur alone during periods of peak root growth activity (Fig. 6). The lack of a finer root system is particularly striking in some of these areas.

It should not be assumed that the growth of individual roots is continuous throughout their season of activity. Many of the roots obtained from the plantations showed evidences of repeated cycles of growth and dormancy. The location and spacing of the metacutized layers strongly indicated intra-seasonal cycles of growth activity. The fact that these roots were usually in the upper soil layers seems to indicate the controlling influence of drought. Photographs of these roots and discussion of their

nature have been published previously (Wilcox, 1964).

**GROWTH BEHAVIOR OF INDIVIDUAL ROOTS UNDER CONTROLLED CONDITIONS**—The seedlings for the root observation experiments were lifted from the nursery during the dormant season, generally in late winter. Root growth commenced within 2 weeks after they were placed in the growth room, and the pattern closely followed that described above for seedlings in the nursery. The elongation of individual roots follows the typical sigmoid curve of growth with the slope or growth rate related to the root order and root diameter. Figure 7 summarizes the average growth rate for roots of various orders in 2-0 seedlings in the observation boxes. The faster growth rate and the longer growth period of the primary root is responsible for the taproot appearance. In general, progressively higher orders of branching show progressively diminishing growth rates and decreasing lengths of growth cycles. The average length in days of the initial growth period for the various root orders is shown in Table 1.

A subsequent growth period was encountered in various roots following the completion of the initial period of sigmoid root growth. In primary roots there was a brief pause or lull in growth

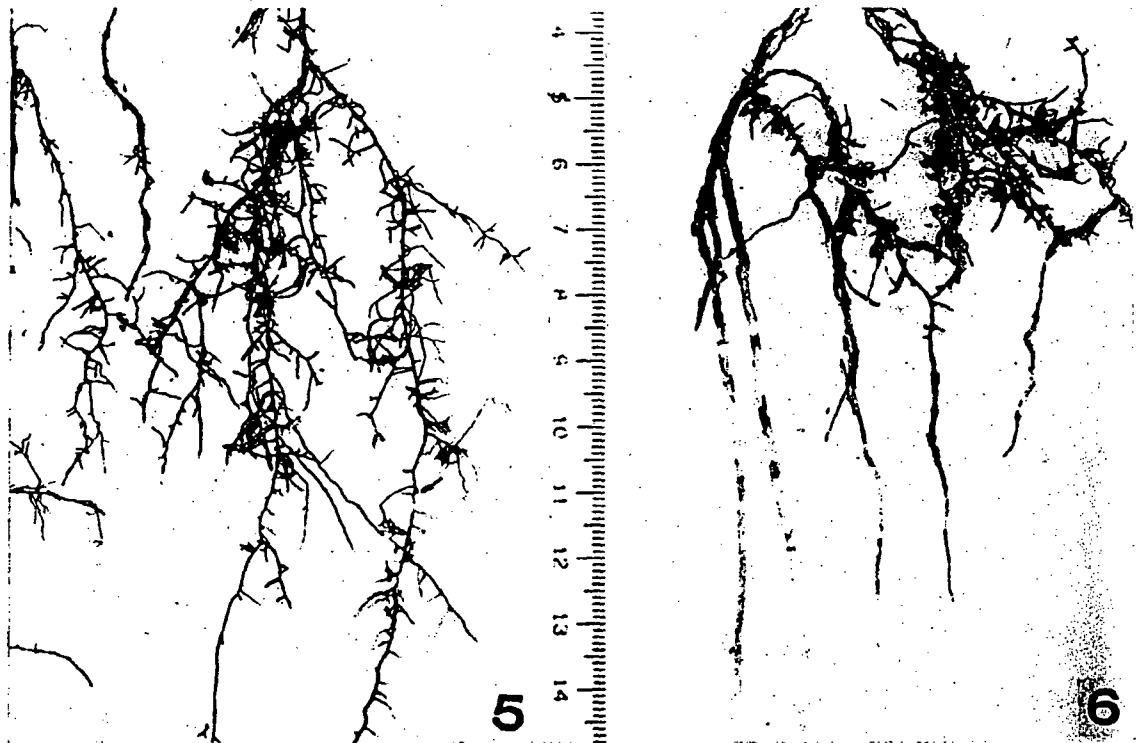


Fig. 5, 6.—Fig. 5. Red pine roots from a healthy plantation showing active root growth in all root classes; 31 July 1958.—Fig. 6. Red pine roots from a plantation in which trees are dying from the so-called "red pine malady" showing active growth of pioneer roots without finer root branches; 31 July 1958.

y (Wilcox,

ROOTS UN-  
seedlings for  
ere lifted  
at season,  
mmenced  
ed in the  
followed  
e nursery.  
ollows the  
the slope  
r and root  
ge growth  
l seedlings  
rowth rate  
e primary  
pearance.  
of branch-  
rowth rates  
cles. The  
al growth  
shown in

countered  
ion of the  
n primary  
in growth



ROOT GROWTH OF RED PINE

7

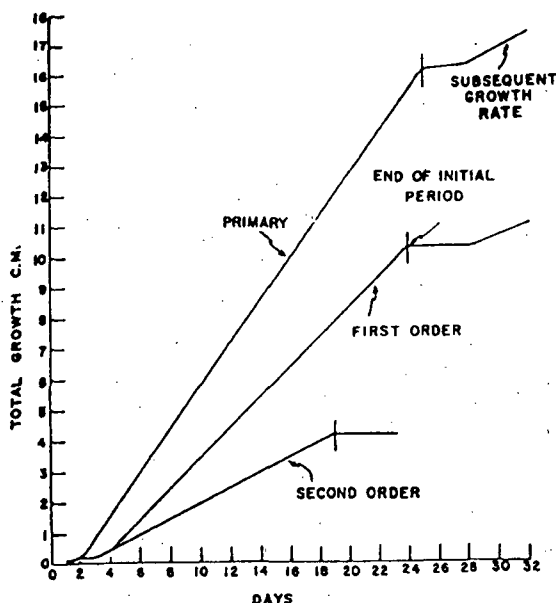


Fig. 7. Average growth rates for roots of various orders of 2-0 red pine seedlings. Seedlings were grown in observation boxes in a growth chamber. Data are taken from an unpublished student's report submitted by George L. Switzer.

followed by an extended period of growth at a reduced rate. The physical limitations of the observation boxes made it impossible to determine the culmination of this root growth, but in one experiment continuous root growth was observed throughout the entire observation period of 186 days.

Beyond the initial period, a first-order lateral followed one of three growth patterns: (1) A pattern similar to that of the primaries but at a reduced rate, (2) a pattern of varying periods of dormancy and activity at a rate slower than the initial period and with periods of dormancy varying from 17 to 30 days and periods of activity from 20 to 40 days, and (3) an extended period of dormancy. The differences in behavior of first-order laterals are difficult to explain but are

TABLE 1. Duration of growth phases in initial root growth period of red pine seedlings\*

Root order.	Phase	
	Acceleration	Grand
Primary	2.0 days	23.5 days
First order	3.5 "	19.7 "
Second order	2.8 "	16.5 "

\* Data are taken from an unpublished student's report submitted by George L. Switzer.

possibly caused by differences in root vigor, position of attachment to the primary, the number of forks and branches basal to their meristems, etc. The older or more frequently branched roots were slower-growing and more often quiescent than those that were younger or less branched.

Second-order laterals had two subsequent patterns of behavior. Approximately two-thirds of the roots observed were characterized by a dormancy from which there was no evidence of recovery. The remaining second-order laterals underwent a protracted period of dormancy of 60-70 days followed by a subsequent period of growth late in the growing season. The failure of many of these roots to renew their growth activity is associated with a high degree of natural pruning which appears to be characteristic of these laterals. Many of the successful second-order laterals are those which had been initiated early in the season during the beginning of the longitudinal increment of the mother root or, alternatively, those that had been initiated near the end of the season. Frequently these late-formed laterals become dormant shortly after emerging from the mother root and resume their growth the following spring. Laterals initiated through the midportion of the season are prone to abort after one cycle of elongation.

PATTERNS OF ROOT BRANCHING IN RELATION TO THE GROWTH ACTIVITY OF THE MOTHER ROOT— Since the cyclic growth behavior of individual roots varies with the season and position of initiation, it was decided to investigate initiation and distribution of lateral root primordia. Figure 8 shows the distribution of lateral roots on individual long roots during periods of constant growth rate. The lower curve shows the distance from the apex to the initial divisions for a lateral root primordium plotted against growth rate. The distance to the first emerging lateral is shown in the upper curve. In both cases the distance varies directly with growth rate. The length of ordinate between the two curves of Fig. 8 represents the length of root with unemerged laterals. The divergence of the two curves indicates that with increasing growth rate there is a progressive increase in length of root with unemerged laterals. A count of the number of unemerged laterals in cleared roots disclosed an increasing number in the longer distances represented by the greater ordinate distances on the right of Fig. 8. However, although the total number was greater, the number per unit length of root was less than for the shorter ordinate distances on the left of the figure. This indicates that there is a possible apical dominance over lateral root formation in the larger roots.

It is possible to derive additional curves from Fig. 8 showing linear increases with increase in growth rate for the number of laterals emerging

6

es; 31 July  
y" showing

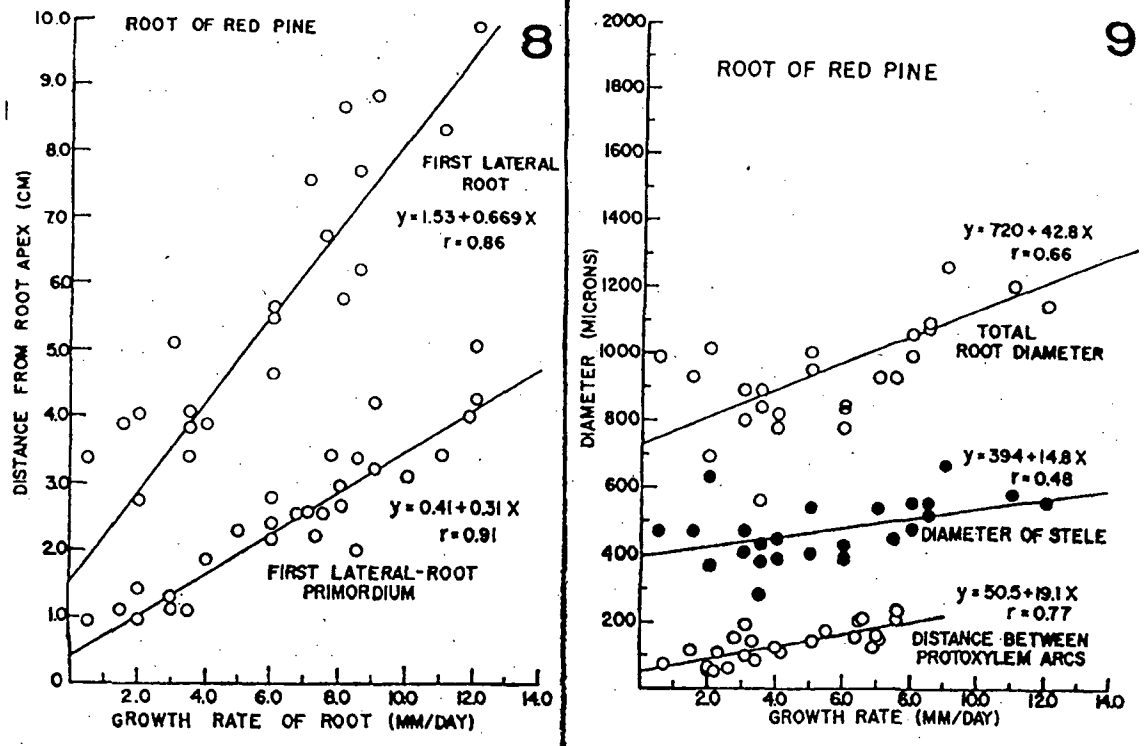


Fig. 8, 9.—Fig. 8. Distances from the root apex of red pine to the first lateral root primordium and to the first emerging lateral in relation to growth rate. Data were obtained from roots which had maintained a constant growth rate for at least 10 days prior to sampling. Correlation coefficients significant at the 5% level.—Fig. 9. Graphs showing relation of various parameters of diameter to rate of growth in roots of red pine. Data were obtained from roots which had maintained a constant growth as in Fig. 8. Correlation coefficients significant at the 5% level.

per day and for the average rate of growth of primordia through the cortex. The last would appear to occur despite the progressively wider cortex of the faster-growing mother roots which can be deduced from the data shown in Fig. 9.

Most of the lateral root primordia initiated by the first- and second-order laterals in the growth room ultimately emerged but not in strict acropetal sequence. Those larger primordia which seemed destined to become long-root branches emerged earlier than many of the slower-growing short-root primordia. Lateral root primordia frequently became dormant before emergence from mother roots which were entering dormancy, but study of root segments from older increments of actively growing roots failed to show any unemerged laterals which had remained permanently arrested, so the arrest must be temporary. However, many lateral root primordia either ceased to grow soon after emergence and became recognizable short-root branches or aborted immediately after emergence and left little evidence of their earlier existence.

The patterns of root initiation and emergence are still more complex in the roots from the nursery or plantation. The relationships shown

in Fig. 8 for roots growing at a constant rate are probably obscured by fluctuations in growth rate caused by varying environmental conditions. Also, in the plantations the pioneer roots are considerably larger than the largest roots studied in the growth room and may consequently deviate in their behavior. The number of lateral roots initiated appears to correspond to the number expected from an extrapolation of the graphs of diameter/growth rate and lateral root primordia/growth rate, but the numbers of laterals developing are few. A high percentage of lateral root primordia die before emerging from the cortex while others abort immediately after emergence. It is possible that some of the unemerged lateral root primordia which appear dead may emerge at a later date, but examination of older pioneer roots showed that this could not be very common since no newer lateral roots were found.

In subordinate mother roots delayed lateral root development occurs under some circumstances, because new short-root branches arise in juxtaposition to older inactive short roots. Since no arrested primordia were found in these roots, it is reasonable to assume that these newly appearing roots are adventitious.

Patterns of root initiation and emergence are profoundly affected, as already indicated, by periods of dormancy of the mother root. The fact that lateral root primordia are found in close proximity to the apical meristem of the dormant mother root indicates that the process of lateral root initiation may continue after cessation of growth of the long root. Also the spacing of un-emerged dormant laterals is closer at the end of the seasonal increment, which indicates either that roots form closer together as root elongation slows or that primordia continue to form after the main meristem becomes dormant and presumably loses its antagonizing effect toward lateral meristem initiation.

Root primordia may be spaced close together on the distal side as well as on the proximal side of a zone of stoppage of the mother root. The greater number of lateral root primordia per length formed during periods at the onset and breaking of dormancy may have a significant effect on the morphological appearance of the root system. In vigorous mother roots a large proportion of these closely spaced primordia develop into long-root branches, and the root system appears to possess a definite seasonal branching pattern. In less vigorous mother roots and in subordinate mother roots, the greater proportion become short-roots. These are especially conspicuous when they become mycorrhizal and the seasonal junctures become marked by clusters of mycorrhizal short-roots. However, mycorrhizal structures are generally ephemeral, so this line of demarcation between the seasonal increments of mother roots is not persistent.

**DISCUSSION**—The cyclic growth behavior of red pine roots under the uniform conditions in the growth room indicates that root dormancy is a naturally occurring phenomenon and is not merely the result of adverse growing conditions. Although the rhythmicity represents an inherent phenomenon, its expressions are manifold among the individual roots. This complexity makes it necessary to distinguish between the behavior of individual roots and the patterns of activity of the root system as a whole. The growth cycles of individual roots vary in duration, intensity, and periodicity depending on stage of development, branching order, position, immediate environment, and many other internal and external factors difficult to elucidate. The activity of the root system as an entity can be seen as the integral expression of the growth of all the individual roots growing at any one time.

During periods of maximum root system activity, a comparatively large number of the individual roots may be growing at one time. On the other hand, there are seasonal lulls in root system activity in which only a few individual roots may be growing but with rapidity. This is a complication which has not always been

recognized by investigators of root growth, and may account for the disagreements on the occurrence of root dormancy (Ladefoged, 1939). Investigators searching for evidence of root activity have frequently been able to find it even during periods of relative quiescence and have thereupon denied the existence of root dormancy. Conversely, investigators focusing their attention on the behavior of individual roots have found dormant roots even during periods of maximum root system activity.

The disagreement regarding the occurrence of root dormancy may also have been fostered by the use of white root tips as a criterion of root growth. As indicated, dormant roots of red pine possess white tips when the metacuticized dormancy layers are formed in the outer layers of the root cap.

From what has been said, it is obviously necessary to establish criteria for assessing growth activity of roots in investigations. For example, in the evaluation of root activity in a particular forest stand, adequate samples of roots should be obtained to permit the estimation of relative numbers of root apices active in each of the several long-root classes and the approximate numbers of functional short roots on each. This is a laborious procedure, but it would involve less labor than many of the whole tree excavations and root-mapping experiments which have been performed.

Several features of the growth behavior of individual roots of red pine merit discussion because of their possible importance in solving various plantation problems. One of these is the extreme sensitivity of root growth to soil moisture. This has already been referred to in a previous paper (Wilcox, 1964), but it deserves greater emphasis. Roots were frequently encountered with a banded appearance caused by the repeated dormancy layers, and one extreme example exhibited 14 growth stoppages in a relatively short distance. The occurrence of such roots in the upper litter layers of dry sites is a strong indication of moisture stress. This is corroborated by the work of Merritt (1959), who was able to cause repeated cycling of red pine roots in observation boxes by regulation of watering procedures.

Many of the sites which are susceptible to summer droughts paradoxically also exhibit impeded internal drainage and are water-logged during the period of usual maximum root growth activity in the spring. Red pine is adversely affected by these conditions and makes little root growth under conditions of excessive moisture. If a wet spring is followed by a summer drought there will frequently be an extreme depression in total tree growth. The trees may survive such conditions for a few years, but they will die when the crowns reach a size too large for the meager root system to support. Similar delayed mortality has been described in *Pinus sylvestris* under soil conditions which have permitted only

a shallow root system to develop and have hindered the progressive formation of a deep root system necessary for later tree success (Liese, 1926; Laitakari, 1927).

One of the features of seasonal root growth which is notable in the red pine seedlings is their need for some stimulus from the growing shoot. This is in contrast to the relative independence of root and shoot growth in *Abies procera* Rehd. grown in root observation boxes (Wilcox, 1954). It is also in contrast to the growth behavior of various species of *Abies*, *Tsuga*, and *Larix* in seed beds adjacent to the red pine. Although shoot growth occurred in these species at about the same time as in the red pine, root growth occurred from a month to 6 weeks earlier, apparently independent of shoot growth. If this greater dependence of red pine on events occurring in the shoot is substantiated by closer studies, it might explain one of the reasons for the succession to spruce-fir and hemlock in the northern part of its range.

An interesting question raised by this study is the cause of lateral root abortion and sparse branching of pioneer roots. This failure of pioneer roots to branch is apparently a widespread phenomenon in the pines (Noelle, 1910; Aldrich-Blake, 1930). It is not caused by a failure of laterals to emerge through the voluminous cortex of the pioneer root, because it is very common for abortion to occur following emergence. It is not the result of inadequate size of lateral root meristems, because many of these are relatively large. It probably does not indicate a failure of laterals to receive adequate nutrients, because there appear to be food reserves in the vicinity of the primordia. It might possibly be caused by some internal hormonal correlative mechanism, but little is yet known of centers of hormonal production in roots. It is also not clear under what circumstances pioneer roots arise in the first place, and it might be that the two problems are related.

Growth studies with pioneer roots should be rewarding. It is not known at what age they first appear nor how long individual pioneer roots can persist. There is some evidence that they are undergoing continual appearance and disappearance, thus they should provide a dynamic system for developmental studies.

## LITERATURE CITED

- ALDRICH-BLAKE, R. N. 1930. The plasticity of the root system of Corsican pine in early life. Oxford Forest. Mem. 12: 1-60.
- ELISEI, F. G. 1941. Ricerche microfluoroscopiche sui punti di Caspary. Pavia Univ. Ist. Bot. Atti 13: 1-64.
- LADEFOGED, K. 1930. Untersuchungen über die Periodizität im Ausbruch und Längenwachstum der Wurzeln. Andr. Fred. Høst and Søn, Copenhagen.
- LAITAKARI, E. 1927. The root system of pine (*Pinus sylvestris*). A morphological investigation. Acta Forst. Fennica 33: 306-330.
- LIESE, J. 1926. Beiträge zur Kenntnis des Wurzelsystems der Kiefer (*Pinus sylvestris*). Z. Forst-Jagdwesen 58: 129-181.
- MERRITT, C. 1959. Studies on the root growth of red pine (*Pinus resinosa* Ait.). Ph.D. thesis, Univ. Michigan.
- NOELLE, W. 1910. Studien zur vergleichenden Anatomie und Morphologie der Koniferenwurzeln mit Rücksicht auf die Systematik. Bot. Zeit. 68: 169-266.
- SASS, J. E. 1940. Elements of botanical microtechnique. 1st ed. McGraw-Hill, New York.
- STONE, E. L., R. R. MORROW, AND D. S. WELCH. 1954. A malady of red pine on poorly drained sites. J. For. 52: 104-114.
- WILCOX, H. 1954. Primary organization of active and dormant roots of noble fir, *Abies procera*. Amer. J. Bot. 41: 812-821.
- . 1964. Xylem in roots of *Pinus resinosa* Ait. in relation to heterorhizy and growth activity, p. 459-478. In M. Zimmerman [ed.], Formation of wood in forest trees. Academic Press, Inc., New York.
- , AND L. C. MARSH. 1964. Staining plant tissues with chlorazol black E and Pianese III-B. Stain Tech. 39: 81-86.

**RESPONSE TO RAI COMMENT 29  
ROADMAP TO REFERENCES**

<b>REFERENCED DOCUMENT</b>	<b>*EXCERPT LOCATION</b>	<b>REMARK</b>
Cook et al. 2005	Excerpt enclosed following response.	Section 2.1.
Phifer and Nelson. 2003	Excerpt enclosed following response.	Section 5.1.
Salvo and Cook 1992		General reference, no excerpt included with this response.

**\*Excerpt Locations:**

1. Excerpt included in response: The excerpt is included within the text of the response or is appended to the response.
2. Excerpt enclosed following response: The excerpt is enclosed on a separate sheet or sheets following the response.
3. Representative excerpt(s) enclosed following response: Representative excerpts from a document that is wholly or largely applicable are enclosed following the response.
4. Other

**APPROVED** for Release for  
Unlimited (Release to Public)

7/14/2005

**APPROVED** for Release for  
Unlimited (Release to Public)  
6/6/2005

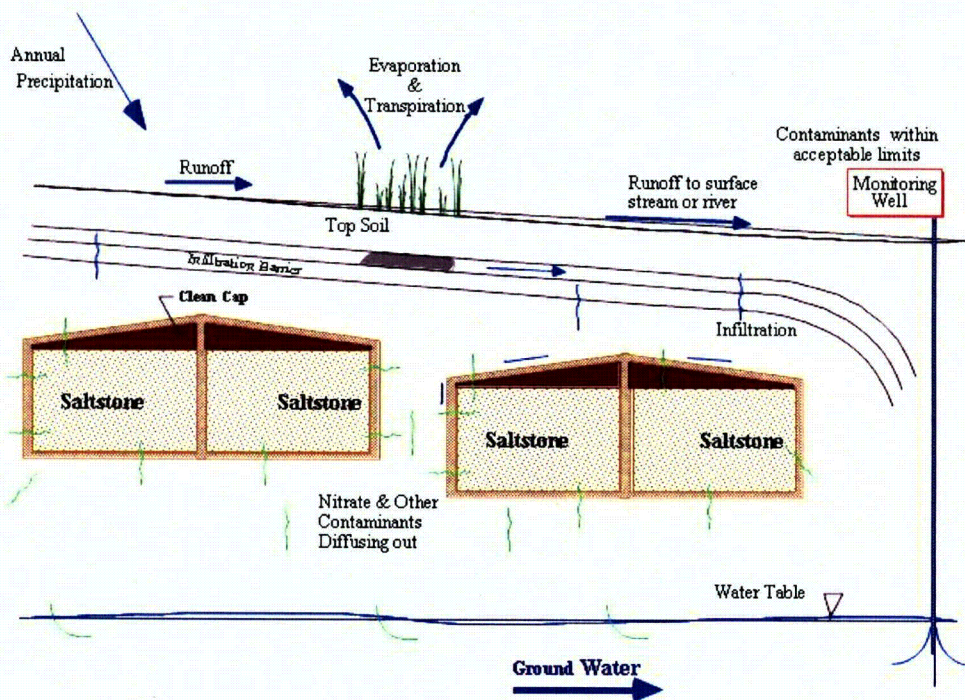
WSRC-TR-2005-00074  
Revision 0

**KEY WORDS:** Performance Assessment  
Low-level Radioactive Waste Disposal

**SPECIAL ANALYSIS:  
REVISION OF SALTSTONE VAULT 4 DISPOSAL LIMITS (U)**

**PREPARED BY:**  
**James R. Cook**  
**Elmer L. Wilhite**  
**Robert A. Hiergesell**  
**Gregory P. Flach**

**MAY 26, 2005**



Westinghouse Savannah River Company  
Savannah River Site  
Aiken, SC 29808

Prepared for the U.S. Department of Energy Under  
Contract Number DE-AC09-96SR18500



## 2.0 GROUNDWATER ANALYSIS

### 2.1 Methodology

The groundwater pathway analysis for each radionuclide involves two steps. First a vadose zone flow and transport simulation is done to estimate flux to the water table for a disposed radionuclide parent and any subsequent progeny. Then saturated zone flow and transport modeling is used to estimate the groundwater concentration(s) at a hypothetical well placed 100 meters down-gradient from the disposal unit.

The vadose zone flow model was developed to reflect the current Z-Area closure concept (Phifer and Nelson 2003), which calls for a geosynthetic cover system instead of a kaolin cap as assumed in the 1992 PA. After completion of the institutional control period, infiltration is predicted to gradually increase over time as the closure system degrades due to phenomena such as intrusion of deep-rooted plants (e.g., trees) and silting of drainage layers (Phifer 2004). While it is assumed that tree root penetration will contribute to closure system degradation, tree roots should not penetrate into the Saltstone, itself, and uptake radionuclides for the following reasons:

- Several layers of the multi-layered cover system above the vault roof are frequently at or near saturation. Since tree roots are opportunistic and seek sources of water, the roots will concentrate in these layers above the vault roof, which contain significant water.
- While roots might penetrate to the vault roof, the concrete roof presents a hardened surface over which roots are more likely to extend along rather than penetrate.
- The pore fluid within Saltstone is essentially a salt solution (brackish water) which the trees could not utilize.
- It is unlikely that roots would be able to extract water from Saltstone due to the matrix potential within Saltstone.

The purpose of the deeper roots of pine trees is to seek sources of water. The multi-layered cover system will produce local zones of saturated water in the drainage layers overlying the barrier layers. The pine tree roots will tend to follow these layers rather than attempt to penetrate to deeper levels since it is much easier for the roots to extract water from saturated soil than unsaturated soil. Therefore, pine tree roots are not expected to penetrate the vault roof.

A potential PA concern is the effects of cracks developing in the Saltstone monolith over time. A structural analysis (Peregoy 2003) predicts that cracks will develop and their aperture will increase with increasing time. However, the analysis shows that the cracks will open either at the top or at the bottom and will be pinched closed at the opposite end. Therefore, no through-wall cracks will develop. A separate modeling study (Yu and Cook 2004) concluded that cracks of this nature have very little effect on contaminant transport rate. Based on this finding cracks are not considered in this SA.

The conceptual model describes the materials, layout, and dimensions of the SDF. Figure 2-1 depicts the conceptual model used for the Vault No. 4. The Saltstone monolith is approximately 200×600×25 ft. Only half of a vault in the short dimension is modeled, taking advantage of symmetry. The top of the modeling domain is the bottom of the upper GCL layer. Infiltration through this layer as a function of time is calculated by the HELP code (USEPA 1994a, 1994b). The constant infiltration rate is used as a flow boundary condition at the top of the modeling domain. The bottom of the modeling domain is the water table. Capillary pressure at the water table is set to zero to simulate 100% water saturation. The vertical boundary through the center of the vault is modeled as a no-flow boundary due to symmetry. The right boundary is also assumed to be a no-flow boundary because it is sufficiently far away from the vault and the predominant

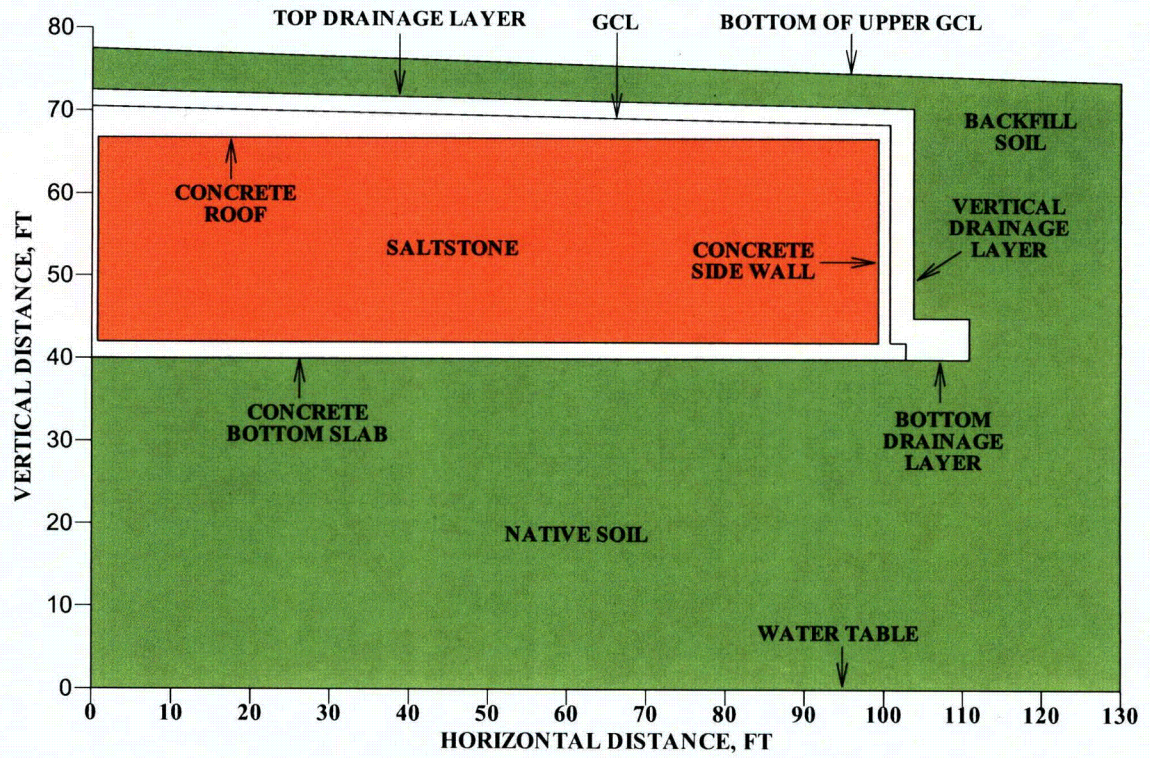


Figure 2-1. Conceptual Model for the Saltstone Vault No. 4

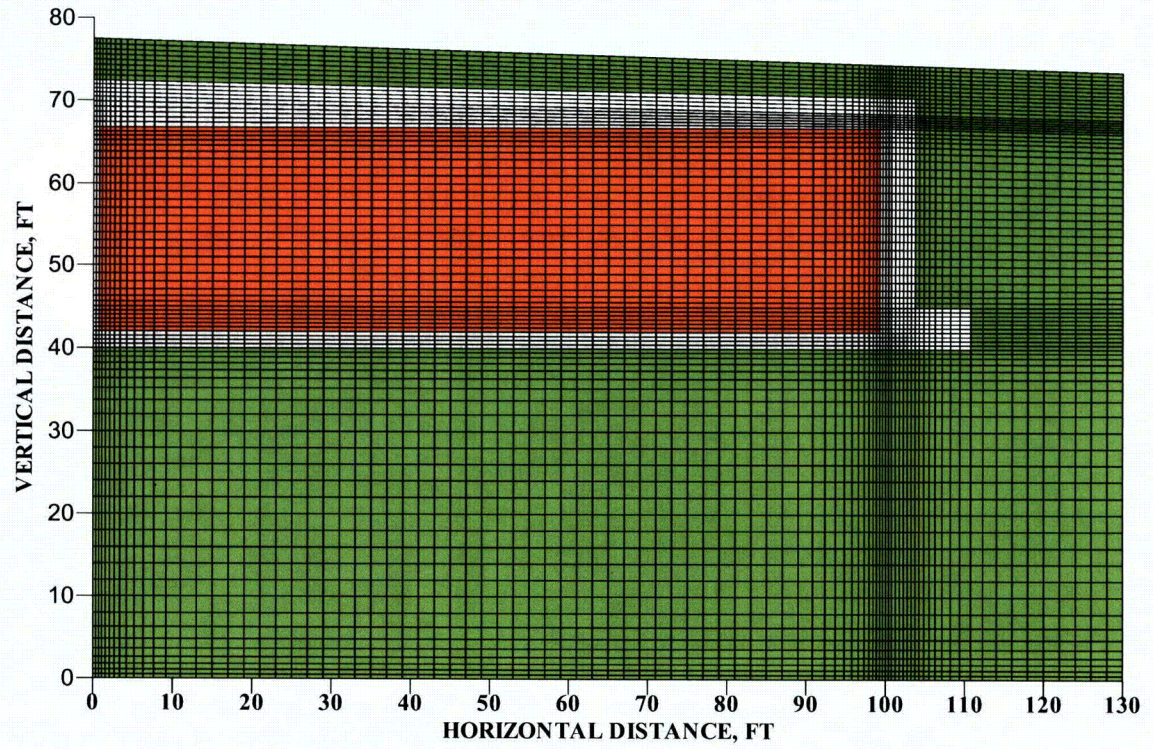


Figure 2-2. Modeling Grid

contaminant transport mechanism is downward convection. Figure 2-2 shows the gridding used in the model.

The vadose zone flow simulation was performed as a sequence of steady-state runs approximating average conditions during a number of time intervals over 10,000 years based on the HELP code results. Time zero is when closure operations are complete. Material properties were varied for each time interval to represent degradation of the closure system, the Saltstone waste form, and the vault. These properties are given in Appendix A.

A total of 45 radionuclides were selected for analysis based on a screening study for the SRS Low Level Waste Facility (Cook and Wilhite 2004). Nitrate was also run in the analysis because it occurs in high concentrations and has a relatively low groundwater limit.

The new plutonium chemistry implemented for the trench disposal units in the E-Area Low-Level Waste Facility (Cook 2002, Kaplan 2004) has been included in the present special analysis. The Pu (III/IV) oxidation state is far more abundant than Pu (V/VI), but the latter is significantly more mobile in sediments: a soil-solute distribution coefficient of  $K_d = 370$  mL/g is assumed for Pu (III/IV) versus  $K_d = 15$  mL/g for Pu (V/VI). Although present in trace amounts, the relatively high mobility of Pu (V/VI) could potentially lead to a significant contribution to the dose at the 100-meter well. The two pairs of oxidation states are tracked separately in the vadose zone transport simulations to accommodate the difference in mobility.

In addition to the geochemistry modifications described above, some distribution coefficients were updated to reflect current knowledge. Appendix A provides a complete listing of  $K_d$  values used in the groundwater analysis and other key input data such as, radionuclides analyzed, half-lives, atomic mass, concentration limits, solubility limits, and assumed decay chains.

The FACT code model of the General Separations Area (GSA) was recently superseded by an equivalent model using the PORFLOW code, in order to consolidate PA subsurface flow and transport modeling to a single software product (Flach 2004). The flow field computed by GSA/PORFLOW is used in the present study. GSA/PORFLOW is a regional scale model with a mesh resolution in the horizontal plane of 200 ft, compared to a width of about 200 ft for Vault 4.

Figure 2-3 illustrates locations of the existing Vaults, 1 and 4, and the aquifer model mesh. Figure 2-3 also shows the extent of the aquifer flow and transport model (blue border) and the mesh resolution in the horizontal plane (light gray dashes). Particle tracking results starting from the four corners of the combined facility indicate the groundwater flow direction. Time markers (red dots) are shown every 10 years of travel. Figure 2-3 indicates a possibility of plume overlap, which is the subject of a sensitivity study presented in Section 7.

## 2.2 Results

The magnitude and time of maximum concentration, the Maximum Contaminant Level (MCL) (USEPA 2004) and the Vault 4 inventory limit for the key radionuclides for two time periods of interest, 1000 years and 10,000 years, are given in Tables 2-1 and 2-2, respectively. These limits for the groundwater pathway are compared with limits derived for the other pathways and with the projected Vault 4 inventory in Section 7. For the projected Vault 4 inventory, none of the radionuclides produces a significant fraction of the groundwater limit.

Plots of fractional flux and concentration for each radionuclide modeled with PORFLOW are presented in Appendix A.

WSRC-TR-2003-00436

Revision 0

**APPROVED** for Release for  
Unlimited (Release to Public)  
3/19/2004

**KEY WORDS:**

Saltstone Disposal Facility

Performance Assessment

Closure Cap

**SALTSTONE DISPOSAL FACILITY  
CLOSURE CAP CONFIGURATION AND DEGRADATION  
BASE CASE:  
INSTITUTIONAL CONTROL TO PINE FOREST SCENARIO (U)**

**SEPTEMBER 22, 2003**

**PREPARED BY:**

Mark A. Phifer<sup>a</sup>

Eric A. Nelson<sup>a</sup>

Westinghouse Savannah River Company LLC<sup>a</sup>

Westinghouse Savannah River Company LLC

Savannah River Site

Aiken, SC 29808



---

Prepared for the U.S. Department of Energy under Contract No. DE-AC09-96SR18500

## 5.0 CLOSURE CAP DEGRADATION

The following three primary closure cap degradation mechanisms have been assumed to significantly impact the infiltration through the closure cap over time:

- Pine forest succession
- Erosion
- Colloidal clay migration

Each of these degradation mechanisms is discussed in detail below.

### 5.1 Pine Forest Succession

According to the PA and Closure Plan the SDF closure cap will be vegetated with bamboo. Bamboo is a shallow-rooted species that quickly establishes a dense ground cover and evapotranspires year-round in the SRS climate. Pine trees are the most deeply rooted naturally occurring plants at SRS. (MMES 1992; Cook et al. 2000). The institutional control to pine forest, land use scenario evaluated herein assumes a 100-year institutional control period following final SDF closure during which the closure cap is maintained. It is assumed that a pine forest begins to encroach upon the bamboo at the end of institutional control, when the approximately 43-acre closure cap (approximate area (~1300 foot by ~1450 foot) over vaults 1 through 12 in Figure 2.0-1) is no longer maintained.

The following discussion of the assumed successional transition from bamboo to pine trees is derived from the following references: Bohm (1979), Burns and Hondala (1990), Ludovici et al. (2002), Taylor (1974), Ulrich et al. (1981), Walkinshaw (1999), and Wilcox (1968).

After institutional control, it is assumed that it will take approximately 100 years for loblolly pine to be established around the closure cap perimeter and for some breakup of the bamboo to begin to occur. Within 10 years of pine tree establishment around the perimeter, the pines begin shading the bamboo located along the perimeter, which allows the establishment of pine tree seedlings 50 feet in from the perimeter of the closure cap. The process of pine tree growth and bamboo shading followed by further seedling encroachment in 50-foot increments toward the cap center continues to occur on a 10-year cycle until the entire closure cap is established with pine trees. 200 years after the end of institutional control it is assumed that the entire cap is covered with pine trees, with the oldest trees near the perimeter and the youngest in the center (i.e. an uneven age distribution).

Because of the age structure difference from edge to center, the second generation, and subsequent ones, will also probably be variable across the cap. Decline of loblolly will begin around 100 years of age. After the second establishment, the new seedlings will be established as "gaps" occur in the overstory, either through the decline or death of a dominant tree, or through abiotic occurrences (wind throw, lightning strikes, fire, insect outbreak, tornado, etc.). This will tend towards making the entire acreage an uneven age, constantly re-establishing forest. In this region, fire may be quite important in the long-term ecology of the cap. Fire will reduce the smaller understory individuals and seedlings, but will have minimal impact on the dominant individuals. It may affect the age structure over long periods of time and make the 43-acre cap closer in age distribution than the original establishment period would indicate.

It is anticipated that tree density will remain fairly constant. For a natural regeneration stand, the tree density is assumed to be approximately 550 dominant and co-dominant trees per acre with approximately 400 mature (i.e. 70 to 125 years old) trees per acre. Smaller trees will be suppressed and die.

It is assumed that mature pine will have 5 deep roots, mainly near the center of the tree spread (i.e., concentrated near main trunk). Of these 5 deep roots, four go to a depth of 6 feet and one to 12 feet.

Deep roots have a diameter of 3 inches in the top foot of soil and taper with depth to 0.25 inches at depth. These roots will be maintained over the life of the tree and exhibit little turnover prior to death. They will enlarge with yearly growth, similar to branches, although anatomically different and at a slower rate. Smaller trees, which are suppressed and die, will not establish deep roots in excess of 4 to 5 feet, and primarily only 1 or 2 such roots. Hard layers and water-saturated layers will slow root penetration. A continuous water surface will stop elongation. Hard layers will eventually be penetrated.

Decomposition of roots near the ground surface should occur fairly quickly due to better microclimate for microbial populations than at depth. Decomposition of roots at depth will be fairly slow, depending on the soil environment and aeration. It is assumed that it will take 25 years for the decomposition of intermediate depth roots and 30 years at depth due to the soil environment. Some shrinkage of the deep roots may occur at depth and provide a channel for water or sediment movement along the surface. Very rapid yearly turnover of fine roots and feeder roots occurs in the soil, although these are primarily in the top 18 inches of soil and will not go vertically with any intensity or longevity.

Based upon this discussion the following assumptions are made relative to the succession of bamboo by a pine forest for this evaluation:

- 200 years after the end of institutional control it is assumed that the entire cap is dominated by pine.
- Complete turnover of the 400 mature trees per acre occurs every 100 years (in a staggered manner).
- There are 400 mature trees per acre with 4 roots to 6 feet and 1 root to 12 feet. The roots are 3 inches in diameter at a depth of 1 foot and 0.25 inches in diameter at either 6 or 12 feet, whichever is applicable.

## 5.2 Erosion

The topsoil and upper backfill layers, which are located above the erosion barrier, are subject to erosion. For the institutional control to pine forest land use scenario, it is assumed that the closure cap will be vegetated with bamboo during the institutional control period, with a combination of bamboo and pine trees for 200 years immediately following the institutional control period, and with a pine forest thereafter. The projected erosion rate for both the topsoil and upper backfill layers has been determined utilizing the Universal Soil Loss Equation (Horton and Wilhite 1978; Goldman et al. 1986). The Universal Soil Loss Equation is expressed as:

$$A = R \times K \times LS \times C \times P \quad (\text{Eq. 5.2-1})$$

where

A = soil loss (tons/acre/year)

R = rainfall erosion index (100 ft·ton/acre per in/hr)

K = soil erodibility factor, tons/acre per unit of R

LS = slope length and steepness factor, dimensionless

C = vegetative cover factor, dimensionless

P = erosion control practice factor, dimensionless

The erosion rate for the SRP Burial Grounds (i.e. current SRS E-Area) was previously estimated and documented by Horton and Wilhite (1978) as provided in Table 5.2-1.

**RESPONSE TO RAI COMMENT 30  
ROADMAP TO REFERENCES**

<b>REFERENCED DOCUMENT</b>	<b>*EXCERPT LOCATION</b>	<b>REMARK</b>
ACRI 2002	Excerpt enclosed following response	Chapter 1, section 1.1
Cook et al. 2005 (WSRC-TR-2005-00074)	Excerpt enclosed following response	Section 1.2, Figure 1.2, Section 2.1, Figure 2.1, Figure 2.2, Section A.2.1
Phifer and Nelson 2003 (WSRC-TR-2003-00436)	Excerpt enclosed following response	Section Table 4.7-1, Figure 4.7-1, Sections 5.0 and 6.0, Section 7.0 and Appendix K
USEPA 1994a	Excerpt enclosed following response	Section 1
USEPA 1994b	Excerpt enclosed following response	Sections 1 and 2

**\*Excerpt Locations:**

1. Excerpt included within response: The excerpt is included within the text of the response or is appended to the response.
2. Excerpt enclosed following response: The excerpt is enclosed on a separate sheet or sheets following the response.
3. Representative excerpt(s) enclosed following response: Representative excerpts from a document that is wholly or largely applicable are enclosed following the response.
4. Other

**APPROVED** for Release for  
Unlimited (Release to Public)

7/14/2005

**APPROVED** for Release for  
Unlimited (Release to Public)  
6/6/2005

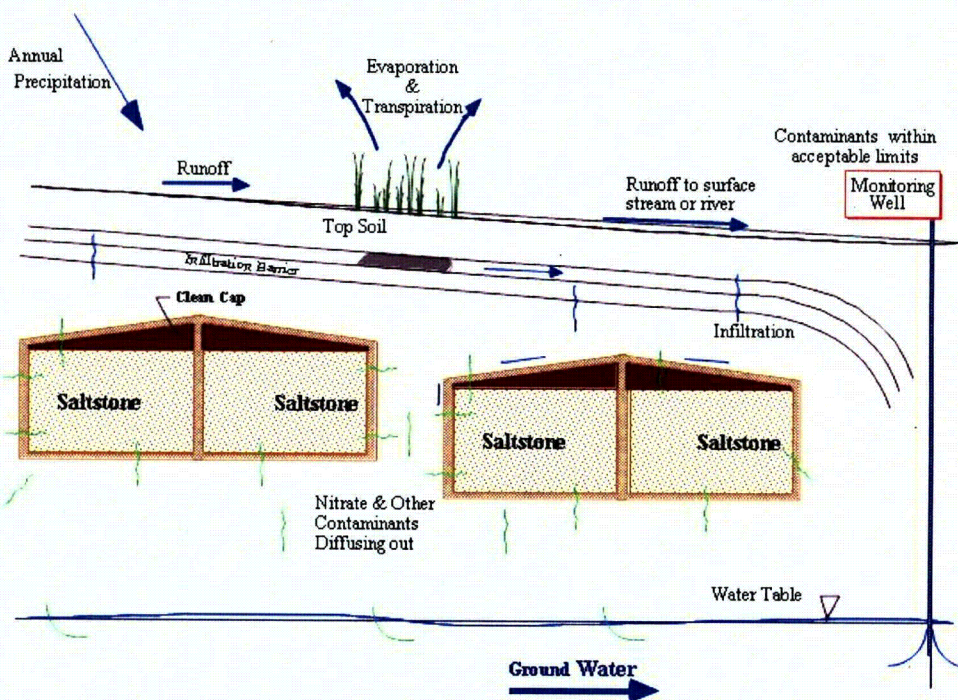
WSRC-TR-2005-00074  
Revision 0

**KEY WORDS:** Performance Assessment  
Low-level Radioactive Waste Disposal

**SPECIAL ANALYSIS:  
REVISION OF SALTSTONE VAULT 4 DISPOSAL LIMITS (U)**

**PREPARED BY:**  
James R. Cook  
Elmer L. Wilhite  
Robert A. Hiergesell  
Gregory P. Flach

**MAY 26, 2005**



Westinghouse Savannah River Company  
Savannah River Site  
Aiken, SC 29808

Prepared for the U.S. Department of Energy Under  
Contract Number DE-AC09-96SR18500



## 2.0 GROUNDWATER ANALYSIS

### 2.1 Methodology

The groundwater pathway analysis for each radionuclide involves two steps. First a vadose zone flow and transport simulation is done to estimate flux to the water table for a disposed radionuclide parent and any subsequent progeny. Then saturated zone flow and transport modeling is used to estimate the groundwater concentration(s) at a hypothetical well placed 100 meters down-gradient from the disposal unit.

The vadose zone flow model was developed to reflect the current Z-Area closure concept (Phifer and Nelson 2003), which calls for a geosynthetic cover system instead of a kaolin cap as assumed in the 1992 PA. After completion of the institutional control period, infiltration is predicted to gradually increase over time as the closure system degrades due to phenomena such as intrusion of deep-rooted plants (e.g., trees) and silting of drainage layers (Phifer 2004). While it is assumed that tree root penetration will contribute to closure system degradation, tree roots should not penetrate into the Saltstone, itself, and uptake radionuclides for the following reasons:

- Several layers of the multi-layered cover system above the vault roof are frequently at or near saturation. Since tree roots are opportunistic and seek sources of water, the roots will concentrate in these layers above the vault roof, which contain significant water.
- While roots might penetrate to the vault roof, the concrete roof presents a hardened surface over which roots are more likely to extend along rather than penetrate.
- The pore fluid within Saltstone is essentially a salt solution (brackish water) which the trees could not utilize.
- It is unlikely that roots would be able to extract water from Saltstone due to the matrix potential within Saltstone.

The purpose of the deeper roots of pine trees is to seek sources of water. The multi-layered cover system will produce local zones of saturated water in the drainage layers overlying the barrier layers. The pine tree roots will tend to follow these layers rather than attempt to penetrate to deeper levels since it is much easier for the roots to extract water from saturated soil than unsaturated soil. Therefore, pine tree roots are not expected to penetrate the vault roof.

A potential PA concern is the effects of cracks developing in the Saltstone monolith over time. A structural analysis (Peregoy 2003) predicts that cracks will develop and their aperture will increase with increasing time. However, the analysis shows that the cracks will open either at the top or at the bottom and will be pinched closed at the opposite end. Therefore, no through-wall cracks will develop. A separate modeling study (Yu and Cook 2004) concluded that cracks of this nature have very little effect on contaminant transport rate. Based on this finding cracks are not considered in this SA.

The conceptual model describes the materials, layout, and dimensions of the SDF. Figure 2-1 depicts the conceptual model used for the Vault No. 4. The Saltstone monolith is approximately 200×600×25 ft. Only half of a vault in the short dimension is modeled, taking advantage of symmetry. The top of the modeling domain is the bottom of the upper GCL layer. Infiltration through this layer as a function of time is calculated by the HELP code (USEPA 1994a, 1994b). The constant infiltration rate is used as a flow boundary condition at the top of the modeling domain. The bottom of the modeling domain is the water table. Capillary pressure at the water table is set to zero to simulate 100% water saturation. The vertical boundary through the center of the vault is modeled as a no-flow boundary due to symmetry. The right boundary is also assumed to be a no-flow boundary because it is sufficiently far away from the vault and the predominant

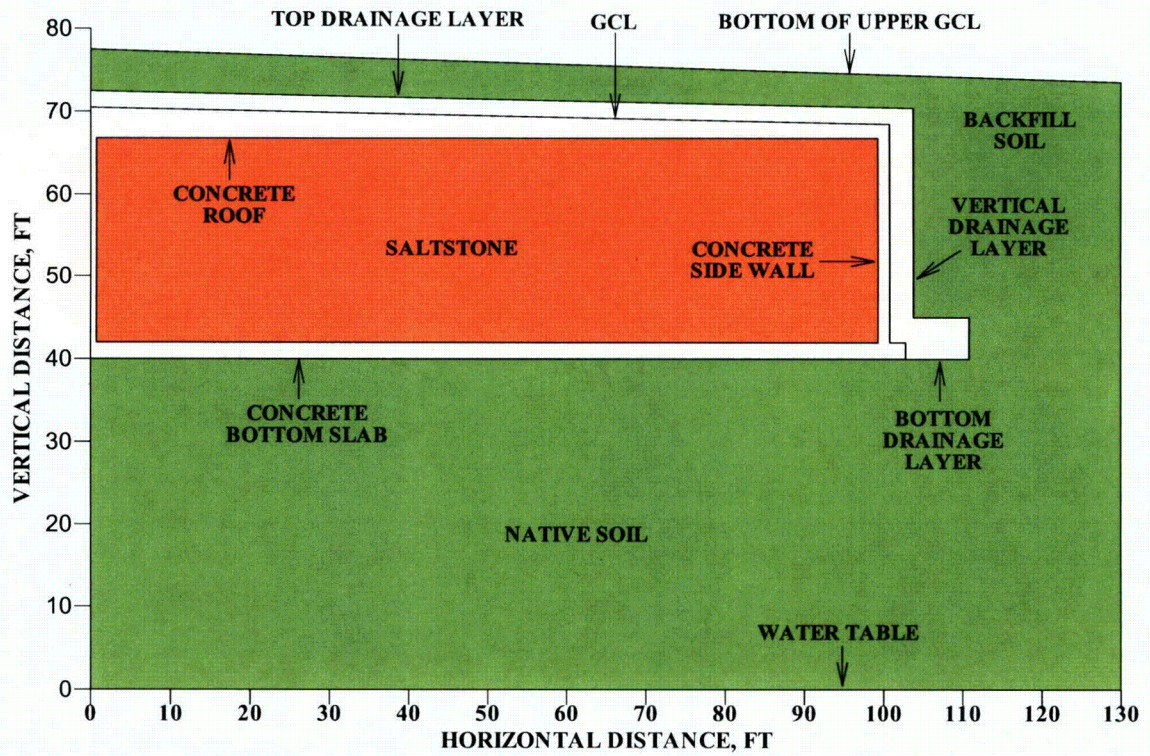


Figure 2-1. Conceptual Model for the Saltstone Vault No. 4

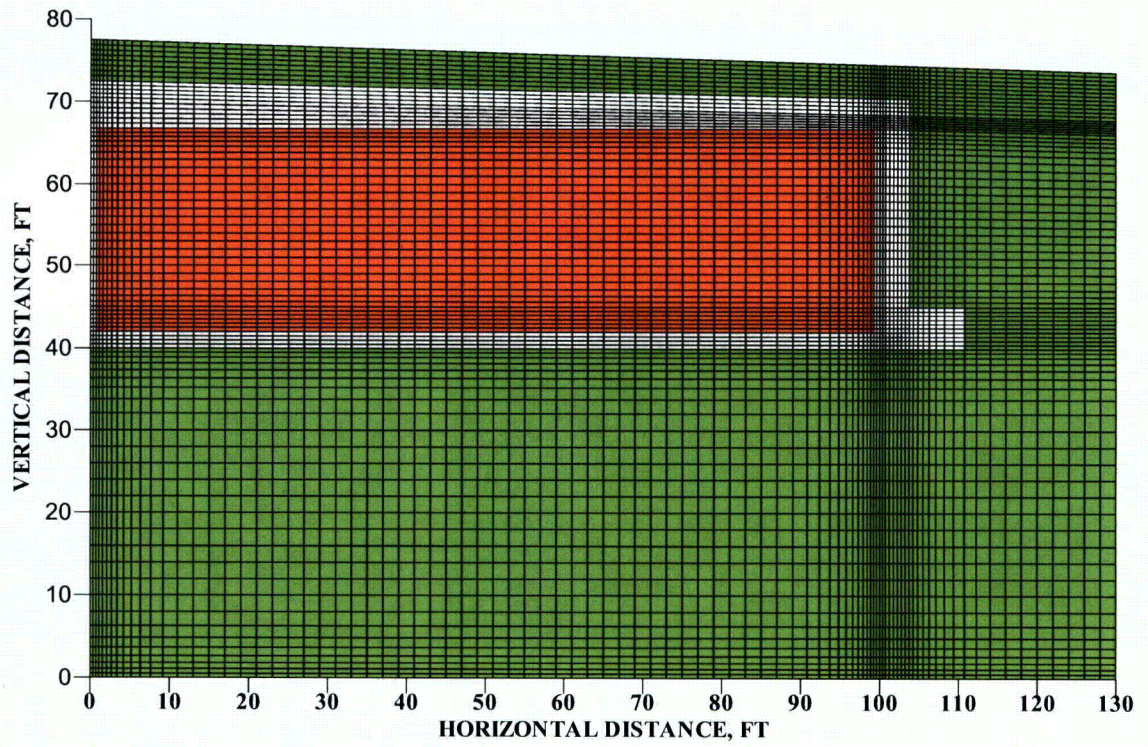


Figure 2-2. Modeling Grid

contaminant transport mechanism is downward convection. Figure 2-2 shows the gridding used in the model.

The vadose zone flow simulation was performed as a sequence of steady-state runs approximating average conditions during a number of time intervals over 10,000 years based on the HELP code results. Time zero is when closure operations are complete. Material properties were varied for each time interval to represent degradation of the closure system, the Saltstone waste form, and the vault. These properties are given in Appendix A.

A total of 45 radionuclides were selected for analysis based on a screening study for the SRS Low Level Waste Facility (Cook and Wilhite 2004). Nitrate was also run in the analysis because it occurs in high concentrations and has a relatively low groundwater limit.

The new plutonium chemistry implemented for the trench disposal units in the E-Area Low-Level Waste Facility (Cook 2002, Kaplan 2004) has been included in the present special analysis. The Pu (III/IV) oxidation state is far more abundant than Pu (V/VI), but the latter is significantly more mobile in sediments: a soil-solute distribution coefficient of  $K_d = 370$  mL/g is assumed for Pu (III/IV) versus  $K_d = 15$  mL/g for Pu (V/VI). Although present in trace amounts, the relatively high mobility of Pu (V/VI) could potentially lead to a significant contribution to the dose at the 100-meter well. The two pairs of oxidation states are tracked separately in the vadose zone transport simulations to accommodate the difference in mobility.

In addition to the geochemistry modifications described above, some distribution coefficients were updated to reflect current knowledge. Appendix A provides a complete listing of  $K_d$  values used in the groundwater analysis and other key input data such as, radionuclides analyzed, half-lives, atomic mass, concentration limits, solubility limits, and assumed decay chains.

The FACT code model of the General Separations Area (GSA) was recently superseded by an equivalent model using the PORFLOW code, in order to consolidate PA subsurface flow and transport modeling to a single software product (Flach 2004). The flow field computed by GSA/PORFLOW is used in the present study. GSA/PORFLOW is a regional scale model with a mesh resolution in the horizontal plane of 200 ft, compared to a width of about 200 ft for Vault 4.

Figure 2-3 illustrates locations of the existing Vaults, 1 and 4, and the aquifer model mesh. Figure 2-3 also shows the extent of the aquifer flow and transport model (blue border) and the mesh resolution in the horizontal plane (light gray dashes). Particle tracking results starting from the four corners of the combined facility indicate the groundwater flow direction. Time markers (red dots) are shown every 10 years of travel. Figure 2-3 indicates a possibility of plume overlap, which is the subject of a sensitivity study presented in Section 7.

## 2.2 Results

The magnitude and time of maximum concentration, the Maximum Contaminant Level (MCL) (USEPA 2004) and the Vault 4 inventory limit for the key radionuclides for two time periods of interest, 1000 years and 10,000 years, are given in Tables 2-1 and 2-2, respectively. These limits for the groundwater pathway are compared with limits derived for the other pathways and with the projected Vault 4 inventory in Section 7. For the projected Vault 4 inventory, none of the radionuclides produces a significantly large fraction of the groundwater limit.

Plots of fractional flux and concentration for each radionuclide modeled with PORFLOW are presented in Appendix A.

## A.2 SALTSTONE VAULT NUMBER 4 UNSATURATED ZONE GROUNDWATER MODELING

### A.2.1 Conceptual Model and Modeling Grid

The conceptual model describes the materials, layout, and dimensions of the SDF. Figure A-1 depicts the conceptual model used for the Vault No. 4. The Saltstone monolith is approximately  $200 \times 600 \times 25$  ft<sup>3</sup>. Only half of a vault in the short dimension is modeled, taking advantage of symmetry. The top of the modeling domain is the bottom of the upper geosynthetic clay liner (GCL) layer. Infiltration through this layer as a function of time is calculated by the HELP code (USEPA 1994a, 1994b). The constant infiltration rate is used as a flow boundary condition at the top of the modeling domain. The bottom of the modeling domain is the water table. Capillary pressure at the water table is set to zero to simulate 100% water saturation. The vertical boundary through the center of the vault at the left side of the figure is modeled as a no-flow boundary due to symmetry. The right boundary is also assumed to be a no-flow boundary because it is sufficiently far away from the vault and the predominant contaminant transport mechanism is downward convection.

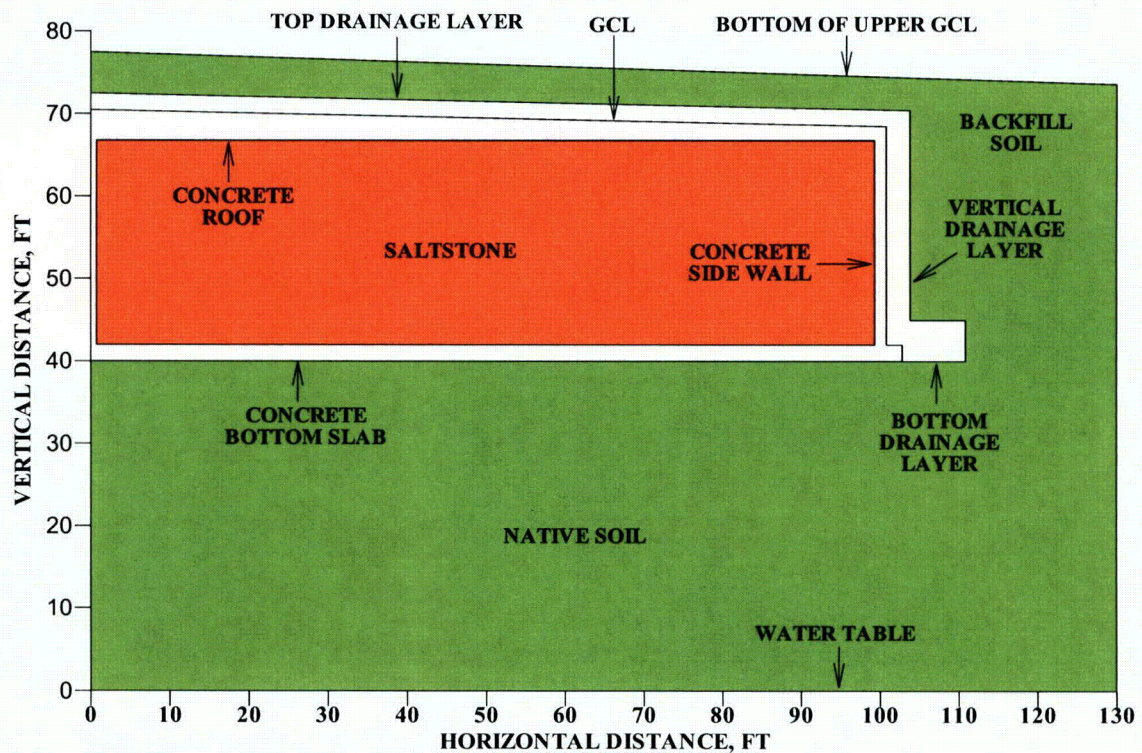


Figure A-1. Conceptual Model for the Saltstone Vault No. 4

The dimensions of the vault and lower portion of the closure are summarized in Table A-2. The “concrete” zone above the Saltstone pour level (at 66.75 ft) includes the top portion of the center and exterior walls and the concrete roof. The drainage layer is a gravel/sand mixture. It is used to reduce water perching above the vault. Test modeling results indicate that perching water can increase water flow rate through the vault, which results in a higher contaminant leaching rate.

The drainage layer is divided into three sections: top, vertical and bottom. The initial hydraulic conductivities in these sections are the same. However, these conductivities degrade at different rates (Phifer 2004) as will be described later. Because the backfill is largely soil excavated during vault construction, it is assumed that the backfill soil has the same properties as the native soil. There is a GCL above the vault roof. Since the conductivity of the Saltstone and the vault is less than or equal to the conductivity of the GCL ( $10^{-9}$  cm/sec), this GCL is ignored in the simulation.

**Table A-2. Dimensions of Saltstone Vault No. 4**

Component	Dimensions of Vertical Distances		
	From (ft)	To (ft)	Thickness (ft)
Native Soil	0.00	40.00	40.00
Bottom Concrete Slab	40.00	42.00	2.00
Saltstone	42.00	66.75	24.75
Concrete at Center <sup>1</sup>	66.75	70.50	3.75
Drainage Layer <sup>2</sup>	70.50	72.50	2.00
Drainage Layer at the Vault Base	40.00	45.00	5.00
Backfill above Drainage Layer <sup>3</sup>	72.50	77.50	5.00
	Dimensions of Horizontal Distances		
Center Slab <sup>4</sup>	0.00	0.75	0.75
Saltstone	0.75	99.25	98.50
Side Slab	99.25	100.75	1.50
Drainage Layer	100.75	103.75	3.00
Drainage Layer at the Vault Base	100.75	110.75	10.00

<sup>1</sup> Concrete includes tip of vault wall, concrete pour and concrete roof.

<sup>2</sup> Slope = 2.0%

<sup>3</sup> Slope = 3.0% at the upper boundary

<sup>4</sup> Actual center slab thickness = 1.50 ft.

The potential impact of cracks on the performance of Vault 4 is discussed in Section A.4. Over 10,000 years, the suction head is great enough that flow through cracks, whether through-wall or not, can be neglected.

The modeling grid used for PORFLOW simulation is shown in Figure A-2. Trapezoidal grid blocks are used for the concrete roof and the backfill to mimic the facility geometry.

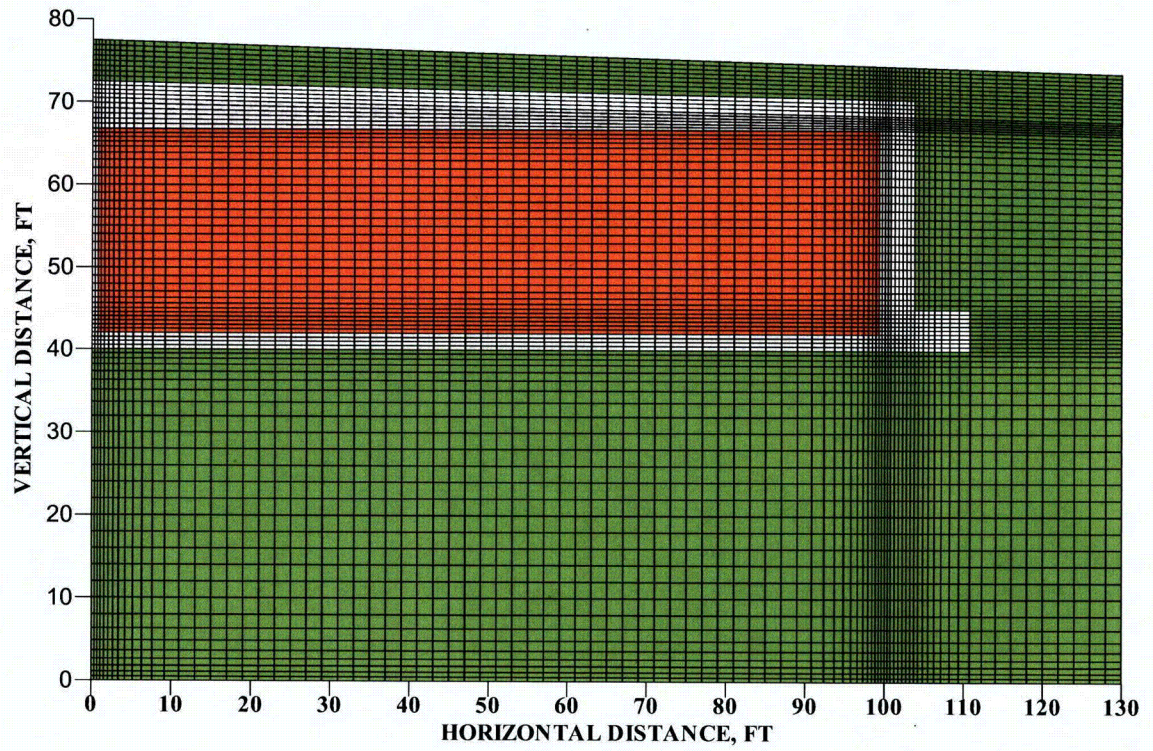


Figure A-2. Modeling Grid

### A.2.2 Time of Compliance and Simulation Time Intervals

The DOE time of compliance is 1,000 years (Wilhite 2003). However, the total time used for groundwater modeling is extended to 10,000 years to assess the impact of a longer period of compliance. The eight time intervals (Phifer 2004) used for groundwater modeling are shown in Table A-3.

Table A-3. Simulation Time Intervals

INTERVAL	TIME (YEARS)
TI01	0 to 100
TI02	100 to 300
TI03	300 to 550
TI04	550 to 1,000
TI05	1,000 to 1,800
TI06	1,800 to 3,400
TI07	3,400 to 5,600
TI08	5,600 to 10,000

### A.2.3 Flow Modeling

#### A.2.3.1 Flow Properties

The fundamental concept of the SDF (wasteform and facility features) is controlled contaminant release. Due to the low hydraulic conductivity and low molecular diffusion in cementitious materials, contaminant leaching from the SDF is very slow. This makes transformation into Saltstone an effective method for liquid waste disposal. Among all the factors affecting the SDF performance, the most important factor is hydraulic conductivity. The saturated hydraulic conductivities of the engineered porous media (Saltstone, concrete and gravel drain layers) were measured by Core Lab as described in 1993 (Yu 1993). These intact values are used for the first 100 years of simulation under the column heading TI01 in Table A-4.

Table A-4. Saturated Hydraulic Conductivities (cm/sec)

	TI01	TI02	TI03	TI04	TI05	TI06	TI07	TI08
	Horizontal conductivity:							
Nati/Back	1.00E-04	1.00E-04	1.00E-04	1.00E-04	1.00E-04	1.00E-04	1.00E-04	1.00E-04
Drain Bot	1.00E-01	9.99E-02	9.97E-02	9.90E-02	9.71E-02	9.30E-02	8.63E-02	7.46E-02
Drain Ver	1.00E-01	1.00E-01	1.00E-01	1.00E-01	1.00E-01	1.00E-01	1.00E-01	1.00E-01
Drain Top	1.00E-01	9.99E-02	9.93E-02	9.75E-02	9.28E-02	8.25E-02	6.58E-02	3.66E-02
Concrete	1.00E-12	5.20E-12	1.29E-11	3.16E-11	7.64E-11	1.98E-10	4.19E-10	1.00E-09
Saltstone	1.00E-11	3.00E-11	5.50E-11	1.00E-10	1.80E-10	3.40E-10	5.60E-10	1.00E-09
	Vertical conductivity:							
Drain Bot	9.52E-02	6.45E-02	2.70E-02	8.94E-03	3.34E-03	1.41E-03	7.25E-04	3.93E-04
Drain Top	8.89E-02	4.21E-02	1.29E-02	3.78E-03	1.36E-03	5.69E-04	2.91E-04	1.57E-04

In this SA, it is assumed the hydraulic conductivities of Saltstone and concrete will increase as time proceeds. As a result, water percolation will gradually increase through the vault. It is also assumed that the conductivities of the top and bottom drains will decrease with time due to plugging in the lower part of these drains resulting in the engineered drains becoming less effective in shedding perched water above the concrete roof. It is assumed that the effective

vertical hydraulic conductivities decrease more rapidly than the horizontal conductivities. All of the saturated hydraulic conductivities used for the simulation are summarized in Table A-4. The data, equations, and rationale used to obtain these data are discussed below.

#### NATIVE AND BACKFILL SOIL

The saturated hydraulic conductivity of native and backfill soil is revised from  $10^{-5}$  to  $10^{-4}$  cm/sec to be consistent with the generally accepted value for the SRS General Separations Area. Since soil is a geological material, its conductivity is assumed to be constant.

#### SALTSTONE AND CONCRETE

In the time interval of 0 and 100 years, the hydraulic conductivities of Saltstone and concrete are  $10^{-11}$  and  $10^{-12}$  cm/sec, respectively. Both conductivities degrade to  $10^{-9}$  cm/sec at 10,000 years. The degradation rate for concrete is faster because it is exposed to the environment and is more vulnerable to be attacked by sulfate, chloride and other chemical reactions. The decay rate is calculated by a log-log correlation:

$$\log_{10}(k/k_o) = \alpha \log_{10}(t/t_o) \quad (A-1)$$

where  $k$  = conductivity at time  $t$ , cm/sec

$k_o$  = conductivity at  $t_o = 100$  years, cm/sec

$\alpha$  = degradation rate constant ( $\alpha = 1.0$  for Saltstone and 1.5 for concrete)

Calculated  $k$  values at the end of each time interval are used as PORFLOW input data to generate the steady-state flow field for the time interval. They are summarized in Table A-4.

#### GRAVEL DRAIN LAYERS

The initial hydraulic conductivity of the gravel drain layers is  $10^{-1}$  cm/sec. As time goes on, soil particles carried by the percolation water will plug the drains from the bottom. The plugged-zone thickness will increase with increasing time. Calculated thickness (Phifer 2004) is shown in Table A-5.

**Table A-5. Plugged-Zone Thickness as a Function of Time**

<u>TIME (YEARS)</u>	<u>PLUGGED-ZONE THICKNESS, FT</u>
0	0
100	0.0005
300	0.005
550	0.022
1,000	0.08
1,800	0.21
3,400	0.49
5,600	0.88
10,000	1.66

Plugging results in reduction in effective hydraulic conductivity. Freeze and Cherry (Freeze 1979) suggested equations to calculate horizontal and vertical effective conductivities:

$$k_{h,eff} = [(H - h)k_g + hk_s] / H \quad (A-2)$$

$$k_{v,eff} = H / [(H - h)/k_g + h/k_s] \quad (A-3)$$

where  $H$  = total thickness (2 ft for top drainage layer and 5 ft for bottom drainage layer)

$h$  = plugged-zone thickness, ft

$k_g$  =conductivity of gravel ( $10^{-1}$  cm/sec)

$k_s$  =conductivity of soil ( $10^{-4}$  cm/sec)

Calculated horizontal and vertical effective hydraulic conductivities for the top and the bottom drainage layers are summarized in Table A-4. The plugged zone thickness used for the calculation is the average for the time interval. For the vertical drainage layer, conductivity remains constant at  $10^{-1}$  cm/sec.

These assumptions on the changes in hydraulic properties over time are based on professional judgment, since actual data over the time periods of interest do not exist. They were discussed during meetings of the performance assessment team and the team agreed to use these values in this analysis.

Because the SDF is constructed in the unsaturated zone, water saturation in the modeling domain is expected to be below 100%. Fluid flow is affected by the capillary pressure (or suction pressure) and relative permeability (or conductivity). Capillary pressure decreases with increasing water saturation, whereas relative permeability increases with increasing water saturation. Saturation dependence of these two parameters is often depicted as characteristic curves. The characteristic curves for Saltstone are illustrated in Figure A-3. Figures A-4 through A-6 show the same curves for the other porous media. In the unsaturated-zone flow model, the capillary pressure and relative permeability are entered as table input.

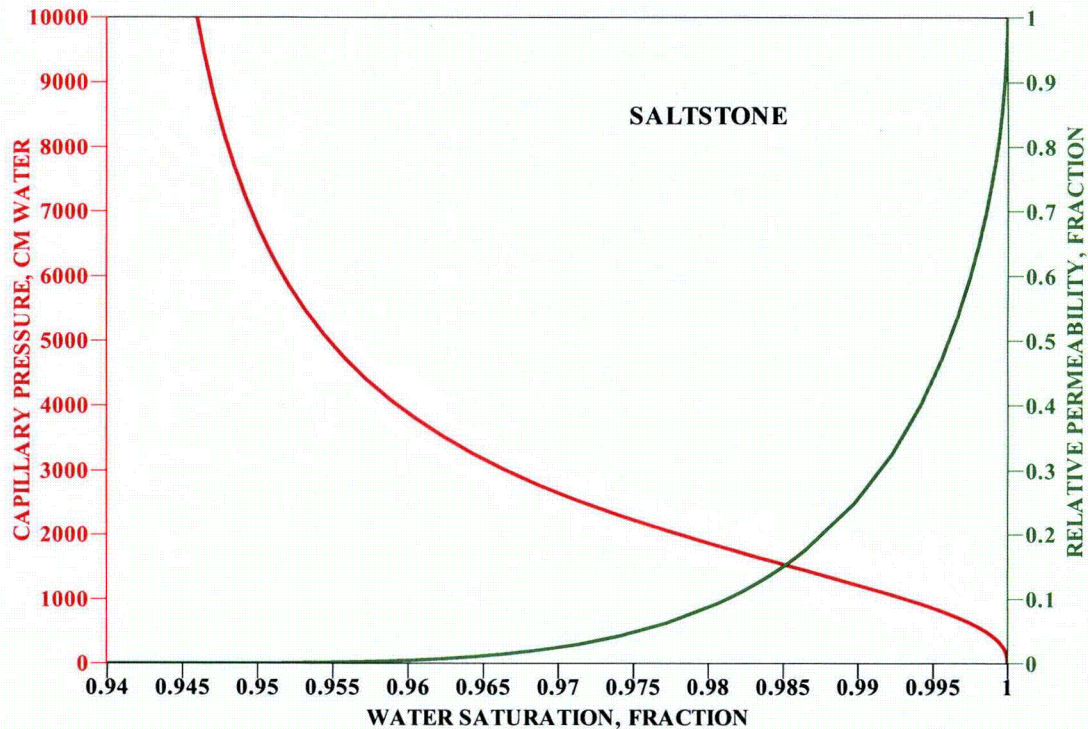


Figure A-3. Characteristic Curves for Saltstone

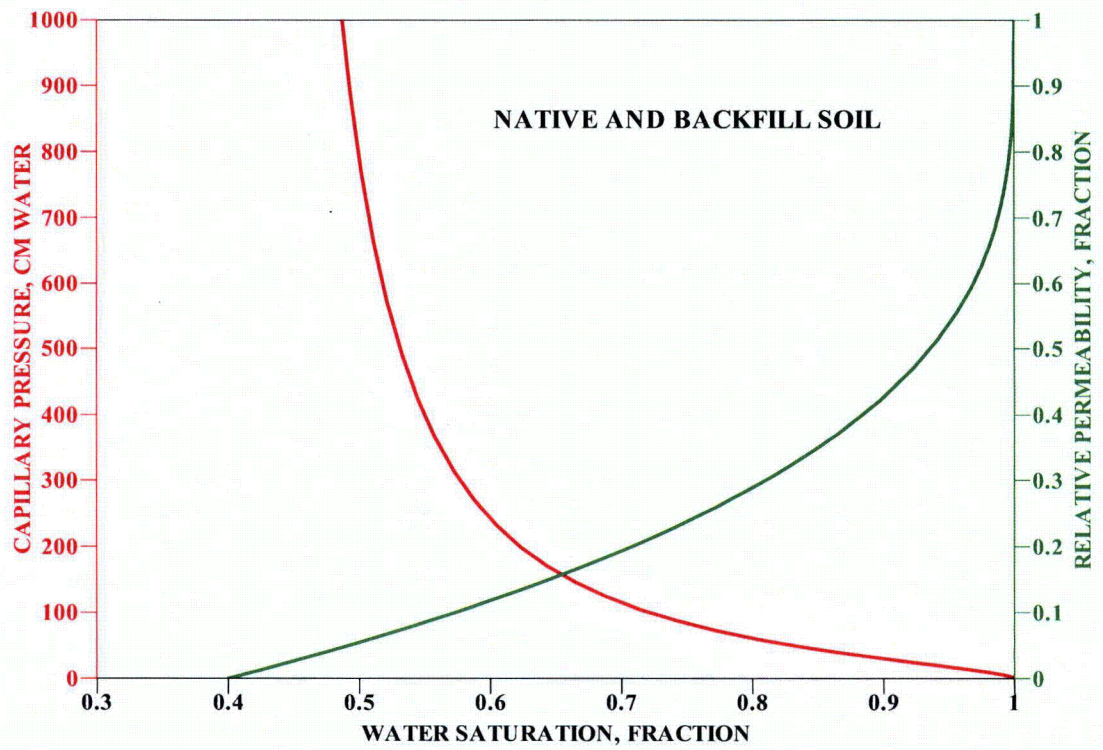


Figure A-4. Characteristic Curves for Native and Backfill Soil

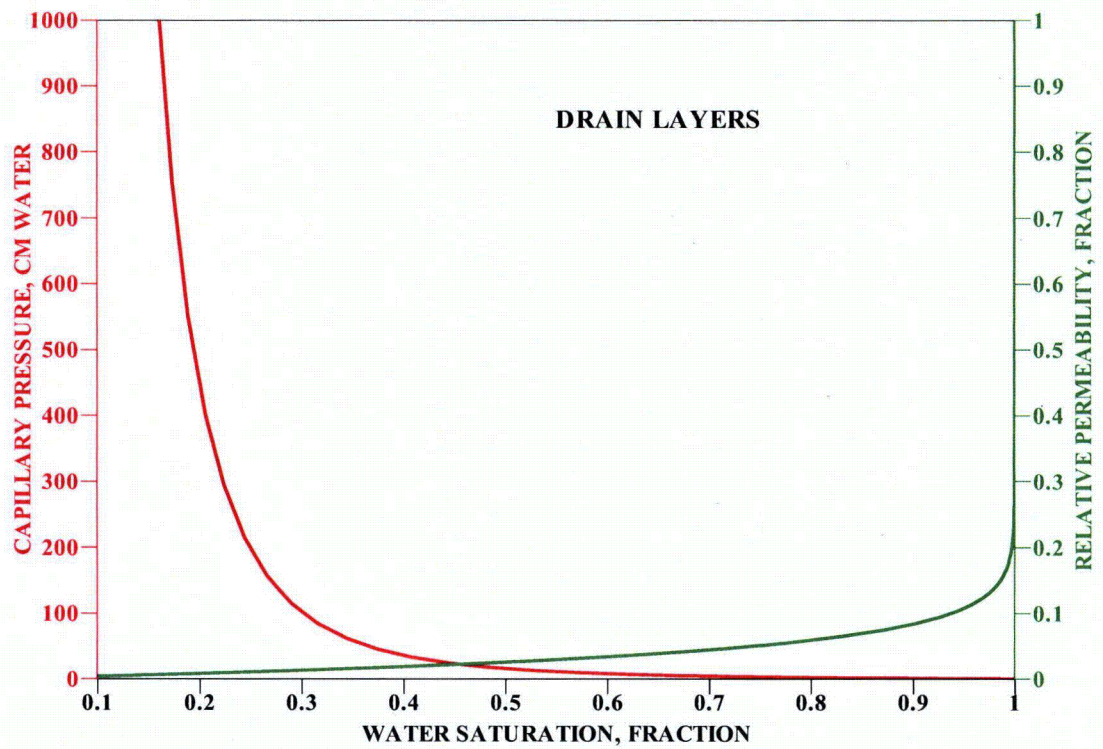


Figure A-5. Characteristic Curves for Drain Layers

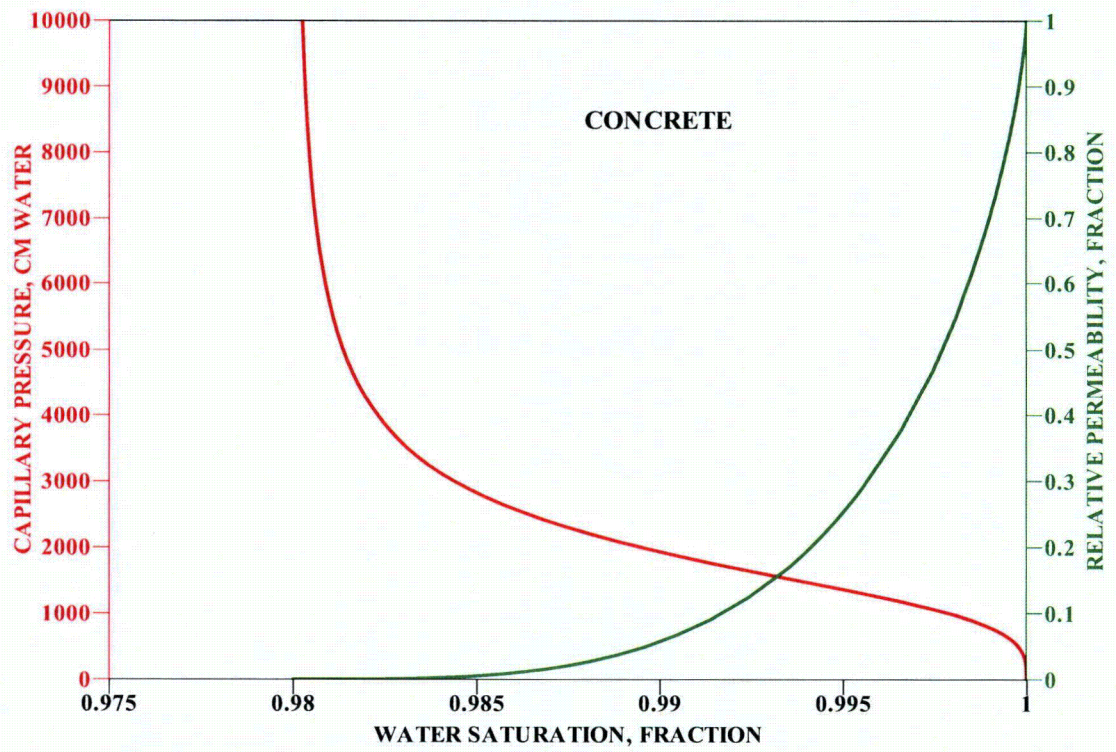


Figure A-6. Characteristic Curves for Concrete

**A.2.3.2 Infiltration Rates**

The infiltration rates (in inches/year) through the lower GCL (Phifer 2004) used for this study are summarized in Table A-6 and shown in Figure A-7.

**Table A-6. Infiltration Rates Used as Upper Boundary Conditions**

Time Interval	Infiltration Rate (in/yr)
0 to 100	0.39
100 to 300	1.73
300 to 550	5.48
550 to 1,000	9.97
1,000 to 1,800	12.90
1,800 to 3,400	13.90
3,400 to 5,600	14.06
5,600 to 10,000	14.09

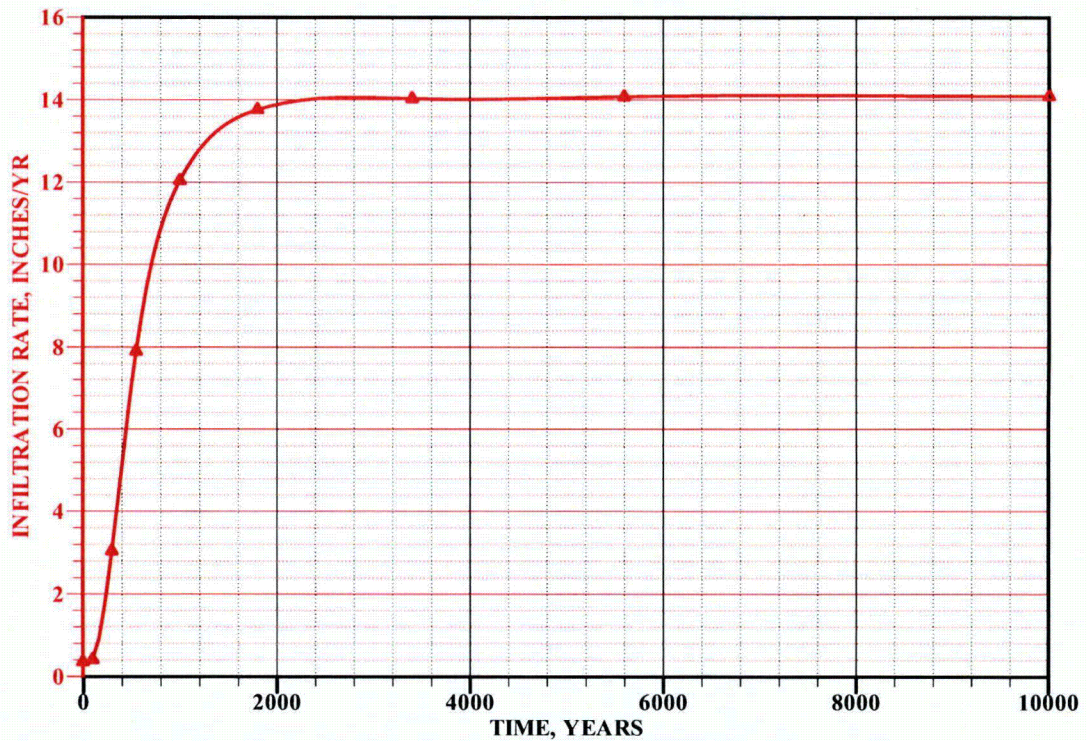


**Figure A-7. Infiltration Rate Through the Lower GCL**

WSRC-TR-2003-00436

Revision 0

**APPROVED** for Release for  
Unlimited (Release to Public)  
3/19/2004

**KEY WORDS:**

**Saltstone Disposal Facility**

**Performance Assessment**

**Closure Cap**

**SALTSTONE DISPOSAL FACILITY  
CLOSURE CAP CONFIGURATION AND DEGRADATION  
BASE CASE:  
INSTITUTIONAL CONTROL TO PINE FOREST SCENARIO (U)**

**SEPTEMBER 22, 2003**

**PREPARED BY:**

**Mark A. Phifer<sup>a</sup>**

**Eric A. Nelson<sup>a</sup>**

Westinghouse Savannah River Company LLC<sup>a</sup>

Westinghouse Savannah River Company LLC

Savannah River Site

Aiken, SC 29808



---

Prepared for the U.S. Department of Energy under Contract No. DE-AC09-96SR18500

## 1.0 EXECUTIVE SUMMARY

The Performance Assessment (PA) for the Saltstone Disposal Facility (SDF) is currently under revision. As part of the PA revision and as documented herein, the closure cap configuration has been reevaluated and closure cap degradation mechanisms and their impact upon infiltration through the closure cap have been evaluated for the institutional control to pine forest, land use scenario. This land use scenario is considered the base case land use scenario. This scenario assumes a 100-year institutional control period following final SDF closure during which the closure cap is maintained. At the end of institutional control, it is assumed that a pine forest succeeds the cap's original bamboo cover. Infiltration through the upper hydraulic barrier layer of the closure cap as determined by this evaluation will be utilized as the infiltration input to subsequent PORFLOW vadose zone contaminant transport modeling, which will also be performed as part of the PA revision.

The reevaluation of the closure cap configuration has resulted in the following primary changes to the closure cap configuration:

- The previous kaolin hydraulic barriers have been replaced with geosynthetic clay liners (GCL).
- The drainage system configuration has been revised to decrease the drainage slope lengths.
- An erosion barrier separate from and above the upper drainage layer has been added.
- A backfill layer has been added between the erosion barrier and the upper drainage layer to help promote evapotranspiration.
- The previous grout layer directly above the vault has been replaced with soil.
- The thickness of the lower drainage layer has been increased, a vertical drainage layer has been added along the sides of the vaults, and a drainage layer has been added at the base of the vaults to minimize the hydraulic head on top of the vaults.

The impacts of pine forest succession, erosion, and colloidal clay migration as degradation mechanisms on the hydraulic properties of the closure cap layers over time have been estimated and the resulting infiltration through the closure cap has been evaluated. The primary changes caused by the degradation mechanisms that result in increased infiltration are the formation of holes in the upper GCL by pine forest succession and the reduction in the saturated hydraulic conductivity of the drainage layers due to colloidal clay migration into the layers. Erosion can also result in significant increases in infiltration if it causes the removal of soil layers, which provide water storage for the promotion of evapotranspiration. For this scenario, infiltration through the upper GCL was estimated at approximately 0.29 inches/year under initial intact conditions, it increased to approximately 11.6 inches/year at year 1000 in nearly a linear fashion, and it approached an asymptote of around 14.1 inches/year at year 1800 and thereafter. At year 1800, it was estimated that holes covered approximately 0.3 percent of the GCL due to root penetration, and that this resulted in an infiltration near that of typical background infiltration (i.e. as though the GCL were not there at all). This demonstrated that a very small area of holes essentially controlled the hydraulic performance of the GCL.

Deep roots have a diameter of 3 inches in the top foot of soil and taper with depth to 0.25 inches at depth. These roots will be maintained over the life of the tree and exhibit little turnover prior to death. They will enlarge with yearly growth, similar to branches, although anatomically different and at a slower rate. Smaller trees, which are suppressed and die, will not establish deep roots in excess of 4 to 5 feet, and primarily only 1 or 2 such roots. Hard layers and water-saturated layers will slow root penetration. A continuous water surface will stop elongation. Hard layers will eventually be penetrated.

Decomposition of roots near the ground surface should occur fairly quickly due to better microclimate for microbial populations than at depth. Decomposition of roots at depth will be fairly slow, depending on the soil environment and aeration. It is assumed that it will take 25 years for the decomposition of intermediate depth roots and 30 years at depth due to the soil environment. Some shrinkage of the deep roots may occur at depth and provide a channel for water or sediment movement along the surface. Very rapid yearly turnover of fine roots and feeder roots occurs in the soil, although these are primarily in the top 18 inches of soil and will not go vertically with any intensity or longevity.

Based upon this discussion the following assumptions are made relative to the succession of bamboo by a pine forest for this evaluation:

- 200 years after the end of institutional control it is assumed that the entire cap is dominated by pine.
- Complete turnover of the 400 mature trees per acre occurs every 100 years (in a staggered manner).
- There are 400 mature trees per acre with 4 roots to 6 feet and 1 root to 12 feet. The roots are 3 inches in diameter at a depth of 1 foot and 0.25 inches in diameter at either 6 or 12 feet, whichever is applicable.

## 5.2 Erosion

The topsoil and upper backfill layers, which are located above the erosion barrier, are subject to erosion. For the institutional control to pine forest land use scenario, it is assumed that the closure cap will be vegetated with bamboo during the institutional control period, with a combination of bamboo and pine trees for 200 years immediately following the institutional control period, and with a pine forest thereafter. The projected erosion rate for both the topsoil and upper backfill layers has been determined utilizing the Universal Soil Loss Equation (Horton and Wilhite 1978; Goldman et al. 1986). The Universal Soil Loss Equation is expressed as:

$$A = R \times K \times LS \times C \times P \quad (\text{Eq. 5.2-1})$$

where

A = soil loss (tons/acre/year)

R = rainfall erosion index (100 ft-ton/acre per in/hr)

K = soil erodibility factor, tons/acre per unit of R

LS = slope length and steepness factor, dimensionless

C = vegetative cover factor, dimensionless

P = erosion control practice factor, dimensionless

The erosion rate for the SRP Burial Grounds (i.e. current SRS E-Area) was previously estimated and documented by Horton and Wilhite (1978) as provided in Table 5.2-1.

**Table 5.2-1. Previous SRP Burial Grounds Estimated Erosion Rate (Horton and Wilhite 1978)**

Parameter	Value Utilized	Comment
R	260	-
K	0.28	Dothan subsoil
LS	0.67	1000 foot long 2% slope
C	0.001	Natural successional forest
P	1	No supporting practices
A (soil loss)	0.05 tons/acre/year	-
A (soil loss)	0.0007 cm/year	Assuming dry bulk density of 1.6 g/cm <sup>3</sup>

The following are estimated parameter values based upon Horton and Wilhite 1978 and Goldman et al. 1986:

- From Figure 5.2 of Goldman et al. (1986), R is slightly greater than 250 but significantly less than 300 100 ft-ton/acre per in/hr. Therefore will utilize the Horton and Wilhite 1978 R value of 260 100 ft-ton/acre per in/hr
- From Figure 5.6 of Goldman et al. (1986):
  - If topsoil is assumed to consist of 70% sand, 25% silt, and 5% clay, K equals 0.28 tons/acre per unit of R.
  - If backfill is assumed to consist of 70% sand, 20% silt, and 10% clay, K equals 0.20 tons/acre per unit of R.
- With a slope length of 350 feet (see Figure 4.2-2) and a slope of 3% the LS value equals 0.40 as determined from Table 5.5 of Goldman et al. (1986).
- Will assume that both bamboo and a pine forest, have C values of a natural successional forest, therefore the C value equals 0.001 as utilized by Horton and Wilhite (1978).
- No supporting practices are associated with the closure cap therefore P equals 1.

Based upon the Universal Soil Loss Equation and the parameter values listed above the following are the estimated soil losses:

- Topsoil with a natural successional forest has an estimated soil loss of 0.0291 tons/acre/year ( $A = 260 \times 0.28 \times 0.40 \times 0.001 \times 1$ ). Based upon the dry bulk density the estimated soil loss can be converted to a loss in terms of depth of loss per year. From Jones and Phifer (2002), the dry bulk density of topsoil was taken as 90 lbs/ft<sup>3</sup>. Topsoil with a natural successional forest has an estimated depth of soil loss of approximately 1.8E-04 inches/year ( $Loss = \frac{0.0291 \text{ tons / acre / year} \times 2000 \text{ lbs / ton} \times 12 \text{ inches / foot}}{43560 \text{ ft}^2 / \text{acre} \times 90 \text{ lbs / ft}^3}$ ).
- Backfill with a natural successional forest has an estimated soil loss of 0.0208 tons/acre/year ( $A = 260 \times 0.20 \times 0.40 \times 0.001 \times 1$ ). Based upon the dry bulk density the estimated soil loss can be converted to a loss in terms of depth of loss per year. From Jones and Phifer (2002), the dry bulk density of backfill was taken as 104 lbs/ft<sup>3</sup>. Backfill with a natural successional forest has an

estimated depth of soil loss of approximately 1.1E-04 inches/year  
 (Loss =  $\frac{0.0208 \text{ tons / acre / year} \times 2000 \text{ lbs / ton} \times 12 \text{ inches / foot}}{43560 \text{ ft}^2 / \text{acre} \times 104 \text{ lbs / ft}^3}$ ).

The previous estimated erosion rate of 0.0007 cm/year (2.8E-04 inches/year) for the SRP Burial Grounds (Horton and Wilhite 1978) compares well with the current estimates for the SDF closure cap of 1.8E-04 and 1.1E-04 inches/year for topsoil and backfill, respectively. The primary difference in input between the two estimates is associated with the site-specific slopes and slope lengths.

### 5.3 Colloidal Clay Migration

It is assumed that colloidal clay migrates from overlying backfill layers and accumulates in the drainage layers reducing the saturated hydraulic conductivity of the drainage layers over time. The clay minerals (in order of predominance) at SRS are shown in Table 5.3-1 along with the percentage range of the clay mineral fraction and typical range in particle size for each. Colloids can be mineral grains such as clays, which have particle sizes between 0.01 and 10  $\mu\text{m}$  (Looney and Falta 2000). Colloidal clay can exist in groundwater in concentrations up to 63 mg/L as measured by suspended solids (Puls and Powell 1991). Based upon this information and the previous assumption, it will be assumed that water flux driven colloidal clay migration at a concentration of 63 mg/L occurs from overlying backfill layers to the drainage layers. It will be further assumed that the colloidal clay accumulates in the drainage layer from the bottom up filling the void space of the drainage layer with clay at a density of 1.1 g/cm<sup>3</sup> (Hillel 1982). These assumptions are analogous to the formation of the B soil horizon as documented in the soil science literature. Clay translocation is a very slow process where discrete clay particles are washed out in slightly acidic conditions and deposited lower in the soil profile (McRae 1988). Evidence has been found that the B-horizon where the translocated clay is deposited may form at a rate of 10 inches per 5,000 years (Buol et al. 1973).

**Table 5.3-1: SRS Clay Minerals**

Clay Mineral	Percentage Range of the Clay Mineral Fraction <sup>1</sup> (%)	Typical Particle Size Range <sup>2</sup> ( $\mu\text{m}$ )
Kaolinite	62.6 to 98.8	0.1 to 4
Vermiculite	0.7 to 34.3	0.1 to 2
Illite	0 to 7.1	0.1 to 2

<sup>1</sup> Looney et al. (1990), Table 6.31

<sup>2</sup> Mitchell (1993)

### 5.4 Closure Cap Degradation Summary

Base upon the assumed closure cap degradation mechanisms, pine forest succession, erosion, and colloidal clay migration, an assumed degradation scenario has been assumed for each layer as outlined in Table 5.4-1. These degradation scenarios form the basis for modifying the thickness and hydraulic properties of each layer over time. This information will be utilized in section 6.0 to determine infiltration through the upper GCL over time.

**Table 6.2-1. Inputs for PORFLOW Vadose Zone Modeling**

Year	Infiltration through Upper GCL (in/yr)	Lower Drainage Layer Saturated Hydraulic Conductivity (cm/s)	Side Vertical Drainage Layer Saturated Hydraulic Conductivity (cm/s)	Thickness of Upper Portion of the Vault Base Drainage Layer with a K of 0.1 cm/s (feet)	Thickness of Lower Portion of the Vault Base Drainage Layer with a K of 0.0001 cm/s (feet)
0	0.29165	1.00E-01	1.00E-01	5	0
100	0.33135	1.00E-01	1.00E-01	4.9996	0.0004
300	2.48161	9.98E-02	1.00E-01	4.996	0.004
550	7.01335	9.91E-02	1.00E-01	4.98	0.02
1,000	11.55066	9.64E-02	1.00E-01	4.93	0.07
1,800	13.65308	9.01E-02	1.00E-01	4.8	0.2
3,400	14.00566	7.62E-02	1.00E-01	4.52	0.48
5,600	14.05202	5.68E-02	1.00E-01	4.14	0.86
10,000	14.09426	1.81E-02	1.00E-01	3.36	1.64

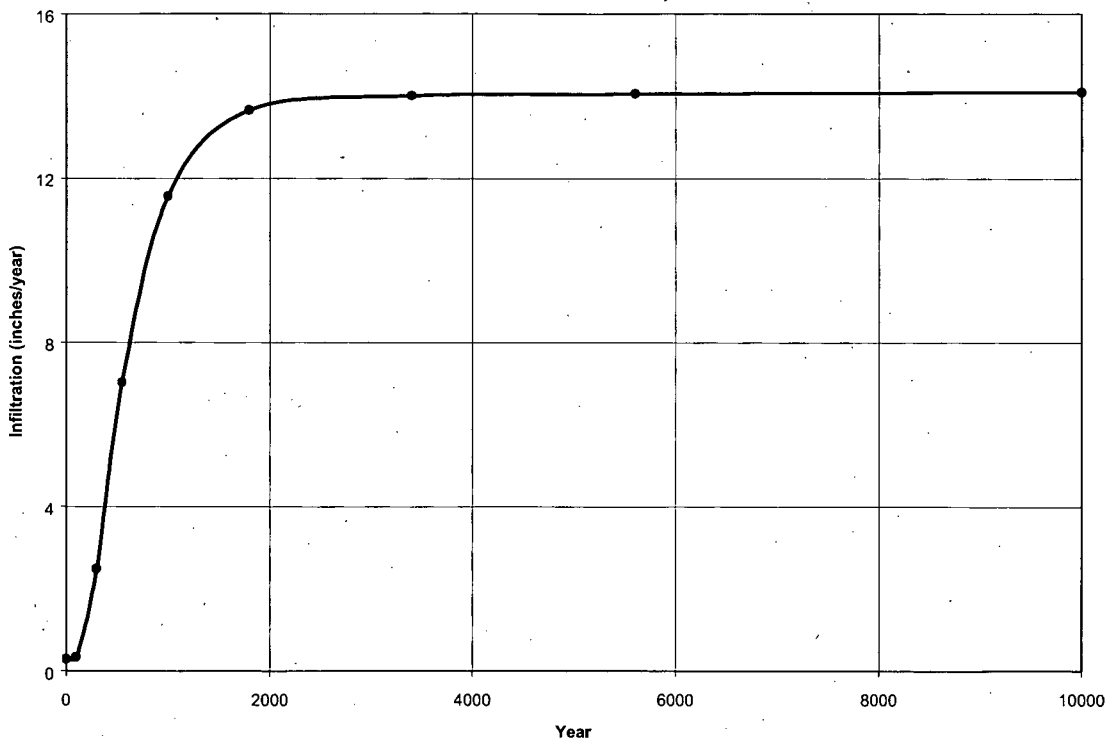


**Figure 6.2-1. Infiltration through Upper GCL**

**APPROVED** for Release for  
Unlimited (Release to Public)  
3/19/2004

WSRC-TR-2003-00523

Revision 0

**KEY WORDS:**

Saltstone Disposal Facility

Performance Assessment

Closure Cap

**SALTSTONE DISPOSAL FACILITY  
MECHANICALLY STABILIZED EARTH VAULT  
CLOSURE CAP DEGRADATION BASE CASE:  
INSTITUTIONAL CONTROL TO PINE FOREST SCENARIO (U)**

**DECEMBER 18, 2003**

**PREPARED BY:**

**Mark A. Phifer<sup>a</sup>**

Westinghouse Savannah River Company LLC<sup>a</sup>

ADC and Reviewing Official

---

M. K. Harris, Manager, Geo-Modeling  
Environmental Restoration Technology Section

Westinghouse Savannah River Company LLC  
Savannah River Site  
Aiken, SC 29808



---

Prepared for the U.S. Department of Energy under Contract No. DE-AC09-96SR18500

## 1.0 EXECUTIVE SUMMARY

As part of the current Saltstone Disposal Facility (SDF) Performance Assessment (PA) revision, the closure cap configuration was reevaluated and closure cap degradation mechanisms and their impact upon infiltration through the closure cap was evaluated for the existing SDF concrete vaults (i.e. vaults 1 and 4) for the base case land use scenario (i.e. institutional control to pine forest scenario) and documented in Phifer and Nelson (2003). The closure cap configuration was modified from a compacted kaolin barrier layer concept to a geosynthetic clay layer (GCL) barrier layer concept. The degradation mechanisms developed included pine forest succession, erosion, and colloidal clay migration. These degradation mechanisms resulted in changes in the hydraulic properties of the closure cap layers and resulting increases in infiltration through the closure cap over time.

Subsequently, Winship (2003) recommended that future SDF vaults be based upon Mechanically Stabilized Earth (MSE) technology rather than poured in place concrete technology. Due to these recommended SDF vault changes, the closure cap degradation mechanisms and their impact upon infiltration through the closure cap has been reevaluated for the proposed MSE vaults for the base case land use scenario (i.e. institutional control to pine forest scenario). This has been conducted as part of the PA revision and as documented herein. This land use scenario assumes a 100-year institutional control period following final SDF closure during which the closure cap is maintained. At the end of institutional control, it is assumed that a pine forest succeeds the cap's original bamboo cover. Infiltration through the upper hydraulic barrier layer of the closure cap as determined by this evaluation will be utilized as the infiltration input to subsequent PORFLOW vadose zone contaminant transport modeling, which will also be performed as part of the PA revision.

The impact of pine forest succession, erosion, and colloidal clay migration as degradation mechanisms on the hydraulic properties of the closure cap layers over time has been estimated and the resulting infiltration through the MSE vault closure cap has been evaluated. The primary changes caused by the degradation mechanisms that result in increased infiltration are the formation of holes in the upper GCL by pine forest succession and the reduction in the saturated hydraulic conductivity of the drainage layers due to colloidal clay migration into the layers. Erosion can also result in significant increases in infiltration if it causes the removal of soil layers, which provide water storage for the promotion of evapotranspiration.

For the institutional control to pine forest, land use scenario, infiltration through the upper GCL was estimated at approximately 0.36 inches/year under initial intact conditions. Such infiltration increased from approximately 0.41 inches/year at the end of institutional control (i.e. year 100) to approximately 12.0 inches/year at year 1000 in nearly a linear fashion. From year 1800 to year 10,000 the infiltration approaches 14.1 inches/year. At year 1800 approximately 0.3 percent of the GCL area had holes due to root penetration resulting in an infiltration near that of typical background infiltration (i.e. as though the GCL were not there at all). A very small area of holes essentially controlled the hydraulic performance of the GCL. It is assumed that the infiltration remains at 14.1 inches/year until approximately year 97,000, at which point the thickness of the upper backfill above the erosion barrier is equal to the assumed evapotranspiration zone depth of 22 inches (Phifer and Nelson 2003). After year 97,000 it is assumed that infiltration through the upper GCL increases linearly from 14.1 inches/year to a maximum of 18.1 inches/year in year 280,000. As the thickness of the upper backfill layer decreases below 22 inches the evapotranspiration zone extends into the erosion barrier, which provides inadequate water storage for the promotion of evapotranspiration. This results in the infiltration increase over 14.1 inches/year after year 97,000.

## 4.0 CLOSURE CAP DEGRADATION

The following three primary closure cap degradation mechanisms have been assumed to significantly impact the infiltration through the closure cap over time:

- Pine forest succession
- Erosion
- Colloidal clay migration

Phifer and Nelson (2003) discussed each of these degradation mechanisms in detail.

### 4.1 Pine Forest Succession

According to the PA and Closure Plan the SDF closure cap will be vegetated with bamboo. Bamboo is a shallow-rooted species that quickly establishes a dense ground cover and evapotranspires year-round in the SRS climate. Pine trees are the most deeply rooted naturally occurring plants at SRS. (MMES 1992; Cook et al. 2000). The institutional control to pine forest, land use scenario evaluated herein assumes a 100-year institutional control period following final SDF closure during which the closure cap is maintained. It is assumed that a pine forest begins to encroach upon the bamboo at the end of institutional control, when the closure cap is no longer maintained.

The following assumptions, which were made relative to the succession of bamboo by a pine forest by Phifer and Nelson (2003), have also been utilized for this evaluation:

- 200 years after the end of institutional control it is assumed that the entire cap is dominated by pine.
- Complete turnover of the 400 mature trees per acre occurs every 100 years (in a staggered manner).
- There are 400 mature trees per acre with 4 roots to 6 feet and 1 root to 12 feet. The roots are 3 inches in diameter at a depth of 1 foot and 0.25 inches in diameter at either 6 or 12 feet, whichever is applicable.

### 4.2 Erosion

The topsoil and upper backfill layers, which are located above the erosion barrier, are subject to erosion. For the institutional control to pine forest land use scenario, it is assumed that the closure cap will be vegetated with bamboo during the institutional control period, with a combination of bamboo and pine trees for 200 years immediately following the institutional control period, and with a pine forest thereafter. The projected erosion rate for both the topsoil and upper backfill layers has been determined utilizing the Universal Soil Loss Equation (Horton and Wilhite 1978; Goldman et al. 1986). The Universal Soil Loss Equation (USLE) is expressed as:

$$A = R \times K \times LS \times C \times P \quad (\text{Eq. 5.2-1})$$

where

A = soil loss (tons/acre/year)

R = rainfall erosion index (100 ft-ton/acre per in/hr)

K = soil erodibility factor, tons/acre per unit of R

LS = slope length and steepness factor, dimensionless

C = vegetative cover factor, dimensionless

P = erosion control practice factor, dimensionless

Table 4.2-1 presents the USLE parameter values utilized and the source of the values for both the topsoil and backfill.

**Table 4.2-1. USLE Parameter Values**

USLE Parameter	Value Utilized	Source
R for SRS location	260	Horton and Wilhite 1978
K for topsoil	0.28	Phifer and Nelson 2003 and Goldman et al. 1986 Figure 5.6
K for backfill	0.20	Phifer and Nelson 2003 and Goldman et al. 1986 Figure 5.6
LS for 450-foot 3% slope (see Figure 3.1-2)	0.45	Goldman et al. 1986 Table 5.5
C for both bamboo and pine forest	0.001	Horton and Wilhite 1978
P for no supporting practices	1	Not applicable

Based upon the Universal Soil Loss Equation and the Table 4.2-1 parameter values the following soil losses were estimated:

- Topsoil with a natural successional forest has an estimated soil loss of 0.0328 tons/acre/year ( $A = 260 \times 0.28 \times 0.45 \times 0.001 \times 1$ ). Based upon the dry bulk density the estimated soil loss can be converted to a loss in terms of depth of loss per year. From Jones and Phifer (2002), the dry bulk density of topsoil was taken as 90 lbs/ft<sup>3</sup>. Topsoil with a natural successional forest has an estimated depth of soil loss of approximately 2.0E-04 inches/year.

$$\left( \text{Loss} = \frac{0.0328 \text{ tons / acre / year} \times 2000 \text{ lbs / ton} \times 12 \text{ inches / foot}}{43560 \text{ ft}^2 / \text{acre} \times 90 \text{ lbs / ft}^3} \right).$$

- Backfill with a natural successional forest has an estimated soil loss of 0.0234 tons/acre/year ( $A = 260 \times 0.20 \times 0.45 \times 0.001 \times 1$ ). Based upon the dry bulk density the estimated soil loss can be converted to a loss in terms of depth of loss per year. From Jones and Phifer (2002), the dry bulk density of backfill was taken as 104 lbs/ft<sup>3</sup>. Backfill with a natural successional forest has an estimated depth of soil loss of approximately 1.2E-04 inches/year.

$$\left( \text{Loss} = \frac{0.0234 \text{ tons / acre / year} \times 2000 \text{ lbs / ton} \times 12 \text{ inches / foot}}{43560 \text{ ft}^2 / \text{acre} \times 104 \text{ lbs / ft}^3} \right).$$

### 4.3 Colloidal Clay Migration

It is assumed that colloidal clay migrates from overlying backfill layers and accumulates in the drainage layers reducing the saturated hydraulic conductivity of the drainage layers over time. As previously documented in Phifer and Nelson (2003), it will be assumed that water-flux driven colloidal clay migration at a concentration of 63 mg/L occurs from overlying backfill layers to the drainage layers. It will be further assumed that the colloidal clay accumulates in the drainage layer from the bottom up filling the void space of the drainage layer with clay at a density of 1.1 g/cm<sup>3</sup> (Hillel 1982).

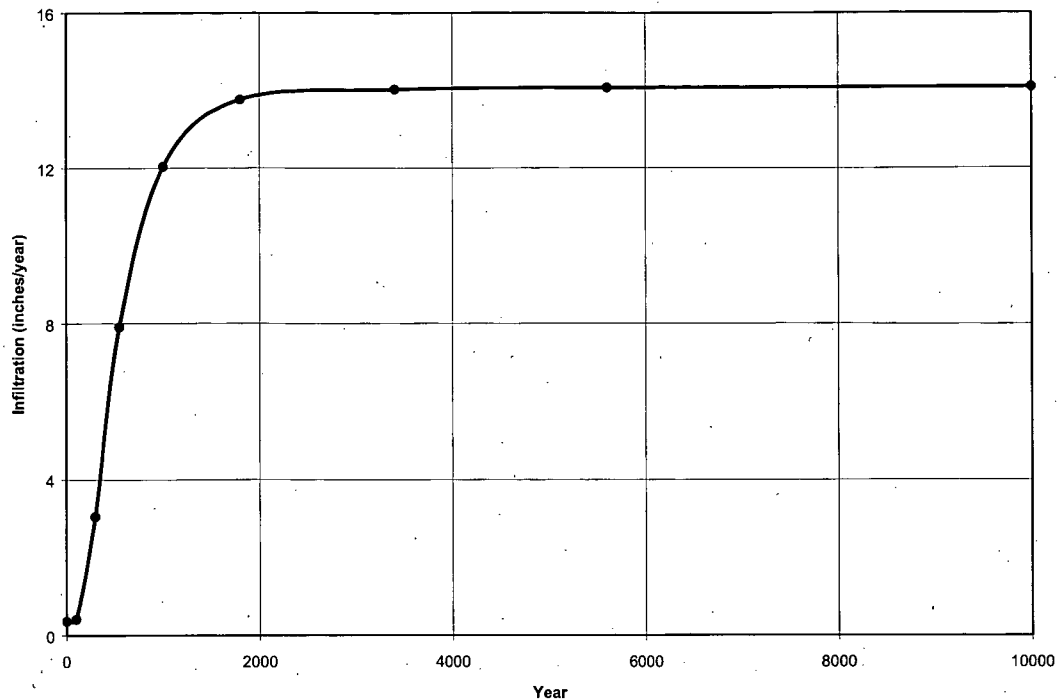


**Figure 5.2-1. Infiltration through Upper GCL**

### 5.3 Worse Case Infiltration

The worse case infiltration through the upper GCL and the associated time of occurrence have been determined based upon the following:

- As documented in Phifer and Nelson (2003), worse case infiltration occurs when both the topsoil and upper backfill have eroded away, since the underlying erosion barrier does not provide as efficient water storage for the promotion of evapotranspiration as the topsoil and upper backfill.
- Since degradation of the erosion barrier is assumed to be caused by intrusion of the overlying backfill following root decomposition, erosion barrier degradation will be assumed to cease once the upper backfill is eroded to three inches thick. Therefore erosion barrier properties will be taken as those at complete erosion of the topsoil and upper backfill for determination of the worse case infiltration through the upper GCL. (see Table 4.4-1)
- As outlined in Appendix F, it is assumed that the material properties of the middle backfill and upper drainage layer become the same at year 2246 and remain constant thereafter. Therefore the middle backfill and upper drainage layer material properties will be taken as those determined at year 2246 for determination of the worse case infiltration through the upper GCL.
- The upper GCL becomes ineffective as a barrier layer at year 1800 when holes comprise 0.29 percent of the layer's area (see Appendix F). Therefore for determination of the worse case infiltration the GCL will be assigned as a barrier soil liner with the same material properties as the overlying middle backfill and upper drainage layer at year 2246.

WSRC-TR-2004-00049

Revision 0

**APPROVED** for Release for  
Unlimited (Release to Public)  
3/19/2004

**KEY WORDS:**  
Saltstone Disposal Facility  
Performance Assessment  
Closure Cap

**SALTSTONE DISPOSAL FACILITY  
MECHANICALLY STABILIZED EARTH VAULT  
CLOSURE CAP DEGRADATION:  
SENSITIVITY ANALYSIS (U)**

**FEBRUARY 12, 2004**

**PREPARED BY:**

**Mark A. Phifer**

Westinghouse Savannah River Company LLC

ADC and Reviewing Official

---

M. K. Harris, Manager, Geo-Modeling  
Environmental Restoration Technology Section

Westinghouse Savannah River Company LLC  
Savannah River Site  
Aiken, SC 29808



---

Prepared for the U.S. Department of Energy under Contract No. DE-AC09-96SR18500

## 1.0 EXECUTIVE SUMMARY

As part of the current Saltstone Disposal Facility (SDF) Performance Assessment (PA) revision, Mechanically Stabilized Earth (MSE) vault closure cap degradation mechanisms and their impact upon infiltration through the MSE vault closure cap were evaluated for the base case land use scenario (i.e. institutional control to pine forest). The degradation mechanisms evaluated included pine forest succession, erosion, and colloidal clay migration (Phifer 2003). Infiltration through the upper hydraulic barrier layer of the closure cap as determined by this evaluation will be utilized as the infiltration input to subsequent PORFLOW vadose zone contaminant transport modeling, which will also be performed as part of the PA revision.

Additionally as part of the PA revision, a sensitivity analysis has been performed and documented herein, to bound the previous base case land use scenario results. The same degradation mechanisms utilized for the base case, as appropriate, have been utilized in the sensitivity analysis. The bounding sensitivity analysis includes the following two MSE vault, closure cap, land use scenarios:

- Continuous bamboo cover (this scenario bounds the lower end of infiltration), and
- Institutional control to farm to pine forest (this scenario bounds the upper end of infiltration).

The estimated infiltration through the upper GCL for the lower bounding, base case, and upper bounding scenarios at year 1000 were 1.75, 12.04, and 19.46 inches/year, respectively. The maximum infiltration estimated through the upper GCL within the first 10,000 years infiltration for the lower bounding, base case, and upper bounding scenarios were 6.46 inches/year at year 3,400, 14.09 inches/year at year 10,000, and 21.42 inches/year at year 3,400, respectively. The estimated infiltration through the upper GCL at complete degradation of the closure cap for the lower bounding, base case, and upper bounding scenarios were 4.75 inches/year at year 280,000, 18.12 inches/year at year 280,000, and 18.60 at approximately year 38,250.

Based upon the results of this sensitivity analysis, it was estimated that the pine forest succession, degradation mechanism results in the greatest increase in infiltration at approximately 13.5 inches/year. It was estimated that colloidal clay migration into the drainage layer results in an infiltration increase of approximately 6 inches/year. Finally it was estimated that erosion results in the least infiltration increase of the degradation mechanisms at approximately 1 inch/year. Based upon this, it is evident that elimination of the pine forest succession, degradation mechanism would do the most to minimize increases in the infiltration over time.

In addition to infiltration over time, the saturated hydraulic conductivity of the lower drainage layer over time is an important parameter. It is estimated that the lower drainage layer completely silts-in (i.e. has a saturated hydraulic conductivity of 0.0001 cm/s) in year 26,000 for the lower bounding scenario, in year 12,000 for the base case scenario, and in year 8,300 for the upper bounding scenario.

#### 4.0 CLOSURE CAP DEGRADATION

The following two primary closure cap degradation mechanisms have been assumed to significantly impact the infiltration through the MSE vault closure cap over time for the continuous bamboo cover land use scenario (i.e. lower bounding scenario):

- Erosion
- Colloidal clay migration

The pine forest succession, degradation mechanism is not applicable to the continuous bamboo cover land use scenario.

The following three primary closure cap degradation mechanisms have been assumed to significantly impact the infiltration through the MSE vault closure cap over time for the institutional control to farm to pine forest land use scenario (i.e. upper bounding scenario):

- Pine forest succession
- Erosion
- Colloidal clay migration

Phifer and Nelson (2003) discussed each of these degradation mechanisms in detail.

##### 4.1 Pine Forest Succession

Pine forest succession is only a degradation mechanism for the upper bounding scenario as outlined above. Corn is a shallow-rooted, single harvest per year farm crop in the vicinity of SRS. For the upper bounding scenario, it is assumed that pine trees succeed corn farming after erosion exposes the erosion barrier. Pine trees are the most deeply rooted naturally occurring plants at SRS. (MMES 1992; Cook et al. 2000). The following assumptions, which were made relative to pine forest succession by Phifer and Nelson (2003), have also been utilized for this evaluation as appropriate:

- 200 years after the end of farming it is assumed that the entire cap is dominated by pine.
- Complete turnover of the 400 mature trees per acre occurs every 100 years (in a staggered manner).
- There are 400 mature trees per acre with 4 roots to 6 feet and 1 root to 12 feet. The roots are 3 inches in diameter at a depth of 1 foot and 0.25 inches in diameter at either 6 or 12 feet, whichever is applicable.

##### 4.2 Erosion

The topsoil and upper backfill layers, which are located above the erosion barrier, are subject to erosion. For the lower bounding scenario erosion is assumed to occur with a bamboo vegetative cover only. For the upper bounding scenario erosion is assumed to occur with a bamboo vegetative cover for the first 100 years followed by erosion with corn cover until both the topsoil and upper backfill layers are completely eroded. The projected erosion rate for both the topsoil and upper backfill layers has been determined utilizing the Universal Soil Loss Equation for both bamboo and corn vegetative covers. The Universal Soil Loss Equation (USLE) is expressed as:

$$A = R \times K \times LS \times C \times P \quad (\text{Eq. 5.2-1})$$

where

A = soil loss (tons/acre/year)

R = rainfall erosion index (100 ft-ton/acre per in/hr)

K = soil erodibility factor, tons/acre per unit of R

LS = slope length and steepness factor, dimensionless

C = vegetative cover factor, dimensionless

P = erosion control practice factor, dimensionless

Table 4.2-1 presents the USLE parameter values utilized and the source of the values for both the topsoil and backfill cover with bamboo and corn.

**Table 4.2-1. USLE Parameter Values**

USLE Parameter	Value Utilized	Source
R for SRS location	260	Horton and Wilhite 1978
K for topsoil	0.28	Phifer and Nelson 2003 and Goldman et al. 1986 Figure 5.6
K for backfill	0.20	Phifer and Nelson 2003 and Goldman et al. 1986 Figure 5.6
LS for 450-foot 3% slope (see Figure 3.1-2)	0.45	Goldman et al. 1986 Table 5.5
C for bamboo <sup>1</sup>	0.001	Horton and Wilhite 1978
C for corn	0.54	Horton and Wilhite 1978
P for no supporting practices	1	Not applicable

<sup>1</sup> Assumed to be the same as a natural successional forest.

Based upon the Universal Soil Loss Equation and the Table 4.2-1 parameter values the following soil losses were estimated:

- Topsoil with bamboo has an estimated soil loss of 0.0328 tons/acre/year ( $A = 260 \times 0.28 \times 0.45 \times 0.001 \times 1$ ). Based upon the dry bulk density the estimated soil loss can be converted to a loss in terms of depth of loss per year. From Jones and Phifer (2002), the dry bulk density of topsoil was taken as 90 lbs/ft<sup>3</sup>. Topsoil with bamboo has an estimated depth of soil loss of approximately 2.0E-04 inches/year.

$$(\text{Loss} = \frac{0.0328 \text{ tons / acre / year} \times 2000 \text{ lbs / ton} \times 12 \text{ inches / foot}}{43560 \text{ ft}^2 / \text{acre} \times 90 \text{ lbs / ft}^3})$$

- Topsoil with corn has an estimated soil loss of 17.69 tons/acre/year ( $A = 260 \times 0.28 \times 0.45 \times 0.54 \times 1$ ). Based upon the dry bulk density the estimated soil loss can be converted to a loss in terms of depth of loss per year. From Jones and Phifer (2002), the dry

bulk density of topsoil was taken as 90 lbs/ft<sup>3</sup>. Topsoil with corn has an estimated depth of soil loss of approximately 0.11 inches/year.

$$\left( \text{Loss} = \frac{17.69 \text{ tons / acre / year} \times 2000 \text{ lbs / ton} \times 12 \text{ inches / foot}}{43560 \text{ ft}^2 \text{ / acre} \times 90 \text{ lbs / ft}^3} \right).$$

- Backfill with bamboo has an estimated soil loss of 0.0234 tons/acre/year ( $A = 260 \times 0.20 \times 0.45 \times 0.001 \times 1$ ). Based upon the dry bulk density the estimated soil loss can be converted to a loss in terms of depth of loss per year. From Jones and Phifer (2002), the dry bulk density of backfill was taken as 104 lbs/ft<sup>3</sup>. Backfill with bamboo has an estimated depth of soil loss of approximately 1.2E-04 inches/year.

$$\left( \text{Loss} = \frac{0.0234 \text{ tons / acre / year} \times 2000 \text{ lbs / ton} \times 12 \text{ inches / foot}}{43560 \text{ ft}^2 \text{ / acre} \times 104 \text{ lbs / ft}^3} \right).$$

- Backfill with corn has an estimated soil loss of 12.64 tons/acre/year ( $A = 260 \times 0.20 \times 0.45 \times 0.54 \times 1$ ). Based upon the dry bulk density the estimated soil loss can be converted to a loss in terms of depth of loss per year. From Jones and Phifer (2002), the dry bulk density of backfill was taken as 104 lbs/ft<sup>3</sup>. Backfill with corn has an estimated depth of soil loss of approximately 0.067 inches/year.

$$\left( \text{Loss} = \frac{12.64 \text{ tons / acre / year} \times 2000 \text{ lbs / ton} \times 12 \text{ inches / foot}}{43560 \text{ ft}^2 \text{ / acre} \times 104 \text{ lbs / ft}^3} \right).$$

### 4.3 Colloidal Clay Migration

It is assumed that colloidal clay migrates from overlying backfill layers and accumulates in the drainage layers reducing the saturated hydraulic conductivity of the drainage layers over time. As previously documented in Phifer and Nelson (2003), it will be assumed that water flux driven colloidal clay migration at a concentration of 63 mg/L occurs from overlying backfill layers to the drainage layers. It will be further assumed that the colloidal clay accumulates in the drainage layer from the bottom up filling the void space of the drainage layer with clay at a density of 1.1 g/cm<sup>3</sup> (Hillel 1982).

### 4.4 Closure Cap Degradation Summary

Based upon the erosion and colloidal clay migration degradation mechanisms, degradation assumptions for each closure cap layer has been made as outlined in Table 4.4-1 for the lower bounding scenario (i.e. continuous bamboo cover). Based upon the pine forest succession, erosion, and colloidal clay migration degradation mechanisms, degradation assumptions for each closure cap layer has been made as outlined and in Table 4.4-2 for the upper bounding scenario (i.e. institutional control to farm to pine forest). These degradation scenarios form the basis for modifying the thickness and hydraulic properties of each layer over time. This information has been utilized in Section 5.0 to determine infiltration through the upper GCL over time.

**Table 7.0-1. Base Case, Lower Bounding, and Upper Bounding Infiltration over Time**

Lower Bounding Scenario		Base Case Scenario		Upper Bounding Scenario	
Year	Infiltration <sup>1</sup> (in/yr)	Year	Infiltration <sup>1</sup> (in/yr)	Year	Infiltration <sup>1</sup> (in/yr)
0	0.36	0	0.36	0	0.36
100	0.41	100	0.41	100	0.43
300	0.55	300	3.05	154	0.42
550	0.80	550	7.90	300	0.56
1,000	1.75	1,000	12.04	550	1.22
1,800	5.05	1,800	13.76	602	1.37
3,400	6.46	3,400	14.03	802	16.12
5,600	6.44	5,600	14.08	1,000	19.46
10,000	6.40	10,000	14.09	1,800	21.32
280,000 <sup>3</sup>	4.75	96,667 <sup>2</sup>	14.10	3,400	21.42
		280,000 <sup>3</sup>	18.12	5,600	21.13
				10,000	20.05
				38,254 <sup>3</sup>	18.60

<sup>1</sup> Infiltration through upper GCL

<sup>2</sup> The year 96,667 is not a calculated value; it is an assumed value. It is assumed that infiltration remains at 14.10 inches/year until the upper backfill erodes to the assumed evapotranspiration zone depth of 22 inches in year 96,667. At that point it is assumed that infiltration increases linearly from 14.10 inches/year to the year 280,000 infiltration of 18.12 inches/year.

<sup>3</sup> Infiltration at complete degradation of the closure cap

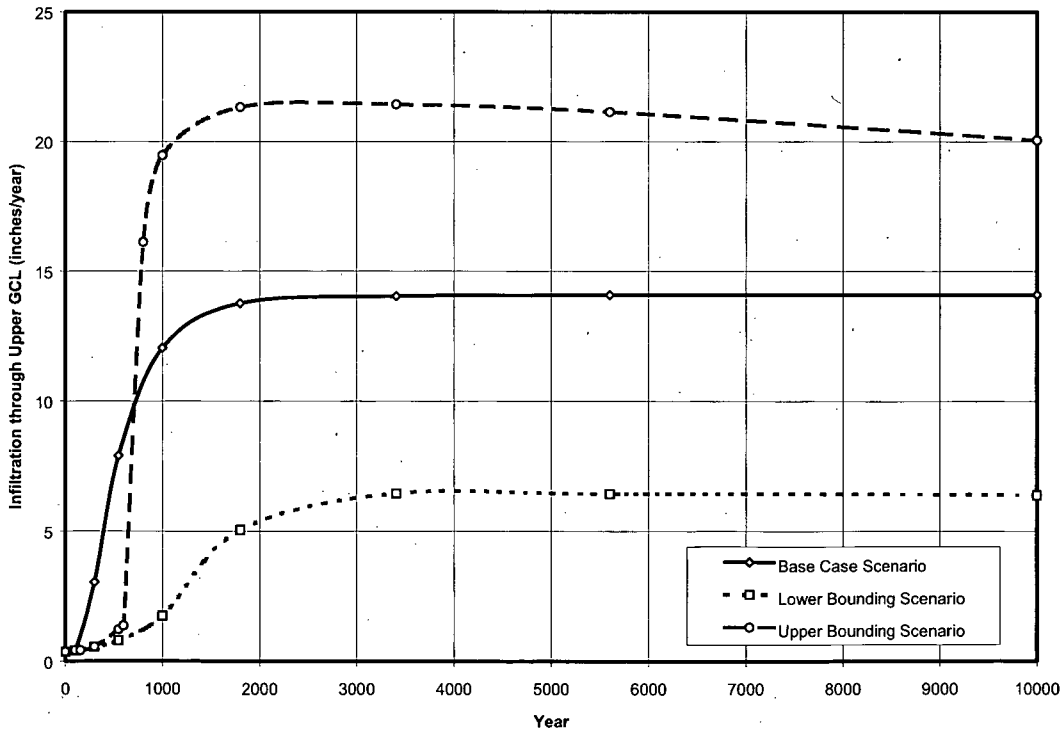
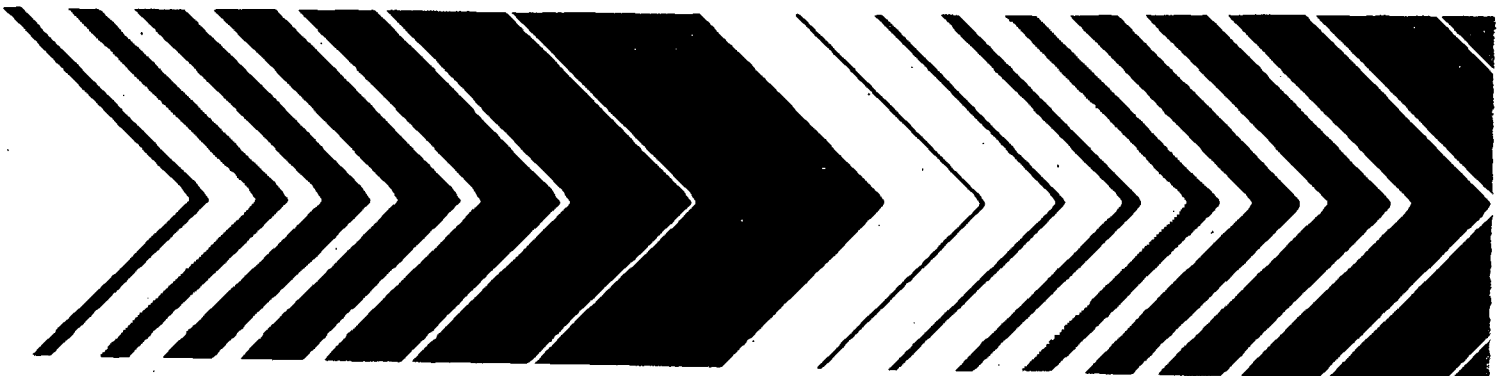


**Figure 7.0-1. Base Case, Lower Bounding, and Upper Bounding Infiltration over Time**



# The Hydrologic Evaluation of Landfill Performance (HELP) Model

## User's Guide for Version 3



EPA/600/R-94/168a  
September 1994

**THE HYDROLOGIC EVALUATION OF LANDFILL  
PERFORMANCE (HELP) MODEL**

***USER'S GUIDE FOR VERSION 3***

by

**Paul R. Schroeder, Cheryl M. Lloyd, and Paul A. Zappi**  
Environmental Laboratory  
U.S. Army Corps of Engineers  
Waterways Experiment Station  
Vicksburg, Mississippi 39180-6199

and

**Nadim M. Aziz**  
Department of Civil Engineering  
Clemson University  
Clemson, South Carolina 29634-0911

Interagency Agreement No. DW21931425

Project Officer

**Robert E. Landreth**  
Waste Minimization, Destruction and Disposal Research Division  
Risk Reduction Engineering Laboratory  
Cincinnati, Ohio 45268

**RISK REDUCTION ENGINEERING LABORATORY  
OFFICE OF RESEARCH AND DEVELOPMENT  
U.S. ENVIRONMENTAL PROTECTION AGENCY  
CINCINNATI, OHIO 45268**

 Printed on Recycled Paper

## SECTION 1

### INTRODUCTION

The Hydrologic Evaluation of Landfill Performance (HELP) computer program is a quasi-two-dimensional hydrologic model of water movement across, into, through and out of landfills. The model accepts weather, soil and design data, and uses solution techniques that account for the effects of surface storage, snowmelt, runoff, infiltration, evapotranspiration, vegetative growth, soil moisture storage, lateral subsurface drainage, leachate recirculation, unsaturated vertical drainage, and leakage through soil, geomembrane or composite liners. Landfill systems including various combinations of vegetation, cover soils, waste cells, lateral drain layers, low permeability barrier soils, and synthetic geomembrane liners may be modeled. The program was developed to conduct water balance analysis of landfills, cover systems and solid waste disposal and containment facilities. As such, the model facilitates rapid estimation of the amounts of runoff, evapotranspiration, drainage, leachate collection and liner leakage that may be expected to result from the operation of a wide variety of landfill designs. The primary purpose of the model is to assist in the comparison of design alternatives as judged by their water balances. The model, applicable to open, partially closed, and fully closed sites, is a tool for both designers and permit writers.

#### 1.1 BACKGROUND

The HELP program, Versions 1, 2 and 3, was developed by the U.S. Army Engineer Waterways Experiment Station (WES), Vicksburg, MS, for the U.S. Environmental Protection Agency (EPA), Risk Reduction Engineering Laboratory, Cincinnati, OH, in response to needs in the Resource Conservation and Recovery Act (RCRA) and the Comprehensive Environmental Response, Compensation and Liability Act (CERCLA, better known as Superfund) as identified by the EPA Office of Solid Waste, Washington, DC.

HELP Version 1 (Schroeder et al., 1984) represented a major advance beyond the Hydrologic Simulation on Solid Waste Disposal Sites (HSSWDS) program (Perrier and Gibson, 1980; Schroeder and Gibson, 1982), which was also developed at WES. The HSSWDS model simulated only the cover system, did not model lateral flow through drainage layers, and handled vertical drainage only in a rudimentary manner. The infiltration, percolation and evapotranspiration routines were almost identical to those used in the Chemicals, Runoff, and Erosion from Agricultural Management Systems (CREAMS) model, which was developed by Knisel (1980) for the U.S. Department of Agriculture (USDA). The runoff and infiltration routines relied heavily on the Hydrology Section of the National Engineering Handbook (USDA, Soil Conservation Service, 1985). Version 1 of the HELP model incorporated a lateral subsurface drainage model and improved unsaturated drainage and liner leakage models into the HSSWDS model. In

addition, the HELP model provided simulation of the entire landfill including leachate collection and liner systems.

Version 2 (Schroeder et al., 1988) represented a great enhancement of the capabilities of the HELP model. The WGEN synthetic weather generator developed by the USDA Agricultural Research Service (ARS) (Richardson and Wright, 1984) was added to the model to yield daily values of precipitation, temperature and solar radiation. This replaced the use of normal mean monthly temperature and solar radiation values and improved the modeling of snow and evapotranspiration. Also, a vegetative growth model from the Simulator for Water Resources in Rural Basins (SWRRB) model developed by the ARS (Arnold et al., 1989) was merged into the HELP model to calculate daily leaf area indices. Modeling of unsaturated hydraulic conductivity and flow and lateral drainage computations were improved. Accuracy was increased with the use of double precision. Default soil data were improved, and the model permitted use of more layers and initialization of soil moisture content. Input and editing were simplified. Output was clarified, and standard deviations were reported.

In Version 3, the HELP model has been greatly enhanced beyond Version 2. The number of layers that can be modeled has been increased. The default soil/material texture list has been expanded to contain additional waste materials, geomembranes, geosynthetic drainage nets and compacted soils. The model also permits the use of a user-built library of soil textures. Computation of leachate recirculation between soil layers and groundwater drainage into the landfill have been added. Moreover, HELP Version 3 accounts for leakage through geomembranes due to manufacturing defects (pinholes) and installation defects (punctures, tears and seaming flaws) and by vapor diffusion through the liner. The estimation of runoff from the surface of the landfill has been improved to account for large landfill surface slopes and slope lengths. The snowmelt model has been replaced with an energy-based model; the Priestly-Taylor potential evapotranspiration model has been replaced with a Penman method, incorporating wind and humidity effects as well as long wave radiation losses (heat loss at night). A frozen soil model has been added to improve infiltration and runoff predictions in cold regions. The unsaturated vertical drainage model has also been improved to aid in storage computations. Input and editing have been further simplified with interactive, full-screen, menu-driven input techniques.

In addition, the HELP Version 3 model provides a variety of methods for specifying precipitation, temperature and solar radiation data. Now, data from the most commonly available government and commercial sources can be imported easily. Moreover, data used in HELP Version 2 can still be used with minimum user effort. Specifying weather data manually and editing previously entered weather data can be easily done by using built-in spreadsheet facilities.

The use of data files in Version 3 is much simpler and more convenient than HELP Version 2 because data are saved permanently in user defined file names at a user-specified location. Similarly, the user has more flexibility to define units for every type

of data needed to run the HELP model. Finally, Version 3 of the HELP model provides on-line help at every step of the data preparation process.

Although applicable to most landfill applications, the HELP model was developed specifically to perform hazardous and municipal waste disposal landfill evaluations as required by RCRA. Hazardous waste disposal landfills generally should have a liner to prevent migration of waste from the landfill, a final cover to minimize the production of leachate following closure, careful controls of runoff and runoff, and limits on the buildup of leachate head over the liner to no more than 1 ft. The HELP model is useful for predicting the amounts of runoff, drainage, and leachate expected for reasonable designs as well as the buildup of leachate above the liner. However, the model should not be expected to produce credible results from input unrepresentative of landfills.

## **1.2 OVERVIEW**

The principal purpose of this User's Guide is to provide the basic information needed to use the computer program. Thus, while some attention must be given to definitions, descriptions of variables and interpretation of results, only a minimal amount of such information is provided. Detailed documentation providing in-depth coverage of the theory and assumptions on which the model is based and the internal logic of the program is also available (Schroeder et al., 1994). Potential HELP users are strongly encouraged to study the documentation and this User's Guide before attempting to use the program to evaluate a landfill design. Additional documentation concerning the sensitivity of program inputs, application of the model and verification of model predictions are under development.

## **1.3 SYSTEM AND OPERATING DOCUMENTATION**

### **1.3.1 Computer Equipment**

The model entitled "The Hydrologic Evaluation of Landfill Performance" (HELP) was written to run on IBM-compatible personal computers (PC) under the DOS environment.

### **1.3.2 Required Hardware**

The following IBM-compatible CPU (8088, 80286, 80386 or 80486) hardware is required:

1. Monitor, preferably color EGA or better
2. Floppy disk drive (5.25-inch double-sided, double- or high-density; or 3.5-inch

double-sided, double- or high-density)

3. Hard disk drive or a second floppy disk drive
4. 400k bytes or more of available RAM memory
5. 8087, 80287, 80387 or 80486 math co-processor
6. Printer, if a hard copy is desired

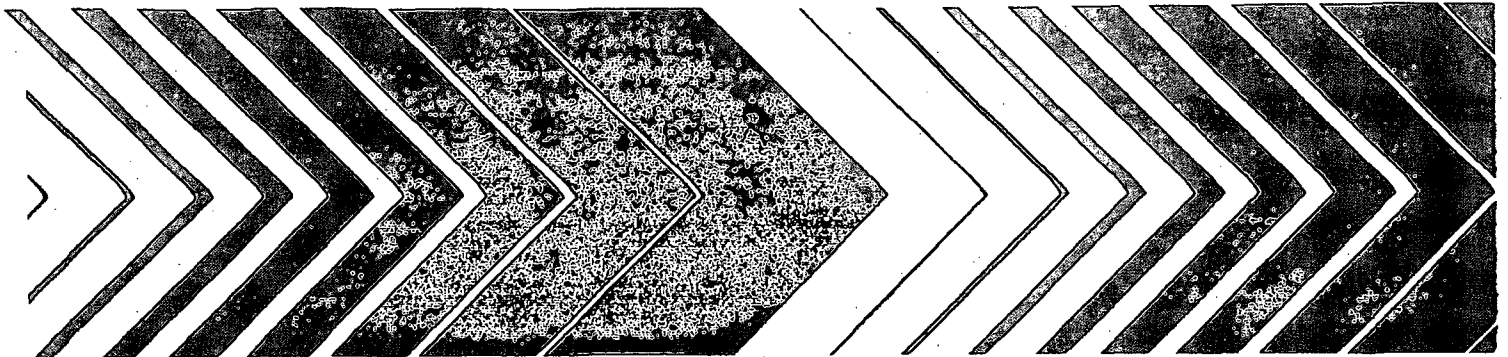
### **1.3.3 Software Requirements**

The user must use Microsoft or compatible Disk Operating Systems (MS-DOS) Version 2.10 or a higher version. The user interface executable module was compiled and linked with Microsoft Basic Professional Development System 7.1. Other executable components were compiled with the Ryan-McFarland FORTRAN Version 2.42. The Microsoft Basic Professional Development System and Ryan-McFarland FORTRAN compiler are not needed to run the HELP Model.



# The Hydrologic Evaluation of Landfill Performance (HELP) Model

Engineering  
Documentation for  
Version 3



EPA/600/R-94/168b  
September 1994

**THE HYDROLOGIC EVALUATION OF LANDFILL  
PERFORMANCE (HELP) MODEL**

***ENGINEERING DOCUMENTATION FOR VERSION 3***

by

Paul R. Schroeder, Tamsen S. Dozier, Paul A. Zappi,  
Bruce M. McEnroe, John W. Sjoström and R. Lee Peyton  
Environmental Laboratory  
U.S. Army Corps of Engineers  
Waterways Experiment Station  
Vicksburg, MS 39180-6199

Interagency Agreement No. DW21931425

Project Officer

Robert E. Landreth  
Waste Minimization, Destruction and Disposal Research Division  
Risk Reduction Engineering Laboratory  
Cincinnati, Ohio 45268

**RISK REDUCTION ENGINEERING LABORATORY  
OFFICE OF RESEARCH AND DEVELOPMENT  
U.S. ENVIRONMENTAL PROTECTION AGENCY  
CINCINNATI, OHIO 45268**

 Printed on Recycled Paper

## SECTION 1

### PROGRAM IDENTIFICATION

**PROGRAM TITLE:** Hydrologic Evaluation of Landfill Performance (HELP) Model

**WRITERS:** Paul R. Schroeder, Tamsen S. Dozier, John W. Sjostrom and Bruce M. McEnroe

**ORGANIZATION:** U.S. Army Corps of Engineers, Waterways Experiment Station (WES)

**DATE:** September 1994

**UPDATE:** None Version No.: 3.00

**SOURCE LANGUAGE:** The simulation code is written in ANSI FORTRAN 77 using Ryan-McFarland Fortran Version 2.44 with assembly language and Spindrift Library extensions for Ryan-McFarland Fortran to perform system calls, and screen operations. The user interface is written in BASIC using Microsoft Basic Professional Development System Version 7.1. Several of the user interface support routines are written in ANSI FORTRAN 77 using Ryan-McFarland Fortran Version 2.44, including the synthetic weather generator and the ASCII data import utilities.

**HARDWARE:** The model was written to run on IBM-compatible personal computers under the DOS environment. The program requires an IBM-compatible 8088, 80286, 80386 or 80486-based CPU (preferably 80386 or 80486) with an 8087, 80287, 80387 or 80486 math co-processor. The computer system must have a monitor (preferably color EGA or better), a 3.5- or 5.25-inch floppy disk drive (preferably 3.5-inch double-sided, high-density), a hard disk drive with 6 MB of available storage, and 400k bytes or more of available low level RAM. A printer is needed if a hard copy is desired.

**AVAILABILITY:** The source code and executable code for IBM-compatible personal computers are available from the National Technical Information Service (NTIS). Limited distribution immediately following the initial distribution will be available from the USEPA Risk Reduction Engineering Laboratory, the USEPA Center for Environmental Research Information and the USAE Waterways Experiment Station.

**ABSTRACT:** The Hydrologic Evaluation of Landfill Performance (HELP) computer program is a quasi-two-dimensional hydrologic model of water movement across, into, through and out of landfills. The model accepts weather, soil and design data and uses solution techniques that account for surface storage, snowmelt, runoff, infiltration, vegetative growth, evapotranspiration, soil moisture storage, lateral subsurface drainage, leachate recirculation, unsaturated vertical drainage, and leakage through soil, geomembrane or composite liners. Landfill systems including combinations of vegetation, cover soils, waste cells, lateral drain layers, barrier soils, and synthetic geomembrane liners may be modeled. The program was developed to conduct water balance analyses of landfills, cover systems, and solid waste disposal facilities. As such, the model facilitates rapid estimation of the amounts of runoff, evapotranspiration, drainage, leachate collection, and liner leakage that may be expected to result from the operation of a wide variety of landfill designs. The primary purpose of the model is to assist in the comparison of design alternatives as judged by their water balances. The model, applicable to open, partially closed, and fully closed sites, is a tool for both designers and permit writers.

The HELP model uses many process descriptions that were previously developed, reported in the literature, and used in other hydrologic models. The optional synthetic weather generator is the WGEN model of the U.S. Department of Agriculture (USDA) Agricultural Research Service (ARS) (Richardson and Wright, 1984). Runoff modeling is based on the USDA Soil Conservation Service (SCS) curve number method presented in Section 4 of the National Engineering Handbook (USDA, SCS, 1985). Potential evapotranspiration is modeled by a modified Penman method (Penman, 1963). Evaporation from soil is modeled in the manner developed by Ritchie (1972) and used in various ARS models including the Simulator for Water Resources in Rural Basins (SWRRB) (Arnold et al., 1989) and the Chemicals, Runoff, and Erosion from Agricultural Management System (CREAMS) (Knisel, 1980). Plant transpiration is computed by the Ritchie's (1972) method used in SWRRB and CREAMS. The vegetative growth model was extracted from the SWRRB model. Evaporation of interception, snow and surface water is based on an energy balance. Interception is modeled by the method proposed by Horton (1919). Snowmelt modeling is based on the SNOW-17 routine of the National Weather Service River Forecast System (NWSRFS) Snow Accumulation and Ablation Model (Anderson, 1973). The frozen soil submodel is based on a routine used in the CREAMS model (Knisel et al., 1985). Vertical drainage is modeled by Darcy's (1856) law using the Campbell (1974) equation for unsaturated hydraulic conductivity based on the Brooks-Corey (1964) relationship. Saturated lateral drainage is modeled by an analytical approximation to the steady-state solution of the Boussinesq equation employing the Dupuit-Forchheimer (Forchheimer, 1930) assumptions. Leakage through geomembranes is modeled by a series of equations based on the compilations by Giroud et al. (1989, 1992). The processes are linked together in a sequential order starting at the surface with a surface water balance; then evapotranspiration from the soil profile; and finally drainage and water routing, starting at the surface with infiltration and then proceeding downward through the landfill profile to the bottom. The solution procedure is applied repetitively for each day as it simulates the water routing throughout the simulation period.

## SECTION 2

### NARRATIVE DESCRIPTION

The HELP program, Versions 1, 2 and 3, was developed by the U.S. Army Engineer Waterways Experiment Station (WES), Vicksburg, MS, for the U.S. Environmental Protection Agency (EPA), Risk Reduction Engineering Laboratory, Cincinnati, OH, in response to needs in the Resource Conservation and Recovery Act (RCRA) and the Comprehensive Environmental Response, Compensation and Liability Act (CERCLA, better known as Superfund) as identified by the EPA Office of Solid Waste, Washington, DC. The primary purpose of the model is to assist in the comparison of landfill design alternatives as judged by their water balances.

The Hydrologic Evaluation of Landfill Performance (HELP) model was developed to help hazardous waste landfill designers and regulators evaluate the hydrologic performance of proposed landfill designs. The model accepts weather, soil and design data and uses solution techniques that account for the effects of surface storage, snowmelt, runoff, infiltration, evapotranspiration, vegetative growth, soil moisture storage, lateral subsurface drainage, leachate recirculation, unsaturated vertical drainage, and leakage through soil, geomembrane or composite liners. Landfill systems including various combinations of vegetation, cover soils, waste cells, lateral drain layers, low permeability barrier soils, and synthetic geomembrane liners may be modeled. Results are expressed as daily, monthly, annual and long-term average water budgets.

The HELP model is a quasi-two-dimensional, deterministic, water-routing model for determining water balances. The model was adapted from the HSSWDS (Hydrologic Simulation Model for Estimating Percolation at Solid Waste Disposal Sites) model of the U.S. Environmental Protection Agency (Perrier and Gibson, 1980; Schroeder and Gibson, 1982), and various models of the U.S. Agricultural Research Service (ARS), including the CREAMS (Chemical Runoff and Erosion from Agricultural Management Systems) model (Knisel, 1980), the SWRRB (Simulator for Water Resources in Rural Basins) model (Arnold et al., 1989), the SNOW-17 routine of the National Weather Service River Forecast System (NWSRFS) Snow Accumulation and Ablation Model (Anderson, 1973), and the WGEN synthetic weather generator (Richardson and Wright, 1984).

HELP Version 1 (Schroeder et al., 1984a and 1984b) represented a major advance beyond the HSSWDS program (Perrier and Gibson, 1980; Schroeder and Gibson, 1982), which was also developed at WES. The HSSWDS model simulated only the cover system, did not model lateral flow through drainage layers, and handled vertical drainage only in a rudimentary manner. The infiltration, percolation and evapotranspiration routines were almost identical to those used in the Chemicals, Runoff, and Erosion from Agricultural Management Systems (CREAMS) model, which was developed by Knisel (1980) for the U.S. Department of Agriculture (USDA). The runoff and infiltration routines relied heavily on the Hydrology Section of the National Engineering Handbook

(USDA, Soil Conservation Service, 1985). Version 1 of the HELP model incorporated a lateral subsurface drainage model and improved unsaturated drainage and liner leakage models into the HSSWDS model. In addition, the HELP model provided simulation of the entire landfill including leachate collection and liner systems.

Version 1 of the HELP program was tested extensively using both field and laboratory data. HELP Version 1 simulation results were compared to field data for 20 landfill cells from seven sites (Schroeder and Peyton, 1987a). The lateral drainage component of HELP Version 1 was tested against experimental results from two large-scale physical models of landfill liner/drain systems (Schroeder and Peyton, 1987b). The results of these tests provided motivation for some of the improvements incorporated into HELP Version 2.

Version 2 (Schroeder et al., 1988a and 1988b) presented a great enhancement of the capabilities of the HELP model. The WGEN synthetic weather generator developed by the USDA Agricultural Research Service (ARS) (Richardson and Wright, 1984) was added to the model to yield daily values of precipitation, temperature and solar radiation. This replaced the use of normal mean monthly temperature and solar radiation values and improved the modeling of snow and evapotranspiration. Also, a vegetative growth model from the Simulator for Water Resources in Rural Basins (SWRRB) model developed by the ARS (Arnold et al., 1989) was merged into the HELP model to calculate daily leaf area indices. Modeling of unsaturated hydraulic conductivity and flow and lateral drainage computations were improved. Default soil data were improved, and the model permitted use of more layers and initialization of soil moisture content.

In Version 3, the HELP model has been greatly enhanced beyond Version 2. The number of layers that can be modeled has been increased. The default soil/material texture list has been expanded to contain additional waste materials, geomembranes, geosynthetic drainage nets and compacted soils. The model also permits the use of a user-built library of soil textures. Computations of leachate recirculation and groundwater drainage into the landfill have been added. Moreover, HELP Version 3 accounts for leakage through geomembranes due to manufacturing defects (pinholes) and installation defects (punctures, tears and seaming flaws) and by vapor diffusion through the liner based on the equations compiled by Giroud et al. (1989, 1992). The estimation of runoff from the surface of the landfill has been improved to account for large landfill surface slopes and slope lengths. The snowmelt model has been replaced with an energy-based model; the Priestly-Taylor potential evapotranspiration model has been replaced with a Penman method, incorporating wind and humidity effects as well as long wave radiation losses (heat loss at night). A frozen soil model has been added to improve infiltration and runoff predictions in cold regions. The unsaturated vertical drainage model has also been improved to aid in storage computations. Input and editing have been further simplified with interactive, full-screen, menu-driven input techniques.

The HELP model requires daily climatologic data, soil characteristics, and design specifications to perform the analysis. Daily rainfall data may be input by the user,

generated stochastically, or taken from the model's historical data base. The model contains parameters for generating synthetic precipitation for 139 U.S. cities. The historical data base contains five years of daily precipitation data for 102 U.S. cities. Daily temperature and solar radiation data are generated stochastically or may be input by the user. Necessary soil data include porosity, field capacity, wilting point, saturated hydraulic conductivity, and Soil Conservation Service (SCS) runoff curve number for antecedent moisture condition II. The model contains default soil characteristics for 42 material types for use when measurements or site-specific estimates are not available. Design specifications include such things as the slope and maximum drainage distance for lateral drainage layers, layer thicknesses, leachate recirculation procedure, surface cover characteristics and information on any geomembranes.

Figure 1 is a definition sketch for a somewhat typical closed hazardous waste landfill profile. The top portion of the profile (layers 1 through 4) is the cap or cover. The bottom portion of the landfill is a double liner system (layers 6 through 11), in this case composed of a geomembrane liner and a composite liner. Immediately above the bottom composite liner is a leakage detection drainage layer to collect leakage from the primary liner, in this case, a geomembrane. Above the primary liner are a geosynthetic drainage net and a sand layer that serve as drainage layers for leachate collection. The drain layers composed of sand are typically at least 1-ft thick and have suitably spaced perforated or open joint drain pipe embedded below the surface of the liner. The leachate collection drainage layer serves to collect any leachate that may percolate through the waste layers. In this case where the liner is solely a geomembrane, a drainage net may be used to rapidly drain leachate from the liner, avoiding a significant buildup of head and limiting leakage. The liners are sloped to prevent ponding by encouraging leachate to flow toward the drains. The net effects are that very little leachate should leak through the primary liner and virtually no migration of leachate through the bottom composite liner to the natural formations below. Taken as a whole, the drainage layers, geomembrane liners, and barrier soil liners may be referred to as the leachate collection and removal system (drain/liner system) and more specifically a double liner system.

Figure 1 shows eleven layers--four in the cover or cap, one as the waste layers, three in the primary leachate collection and removal system (drain/liner system) and three in the secondary leachate collection and removal system (leakage detection). These eleven layers comprise three subprofiles or modeling units. A subprofile consists of all layers between (and including) the landfill surface and the bottom of the top liner system, between the bottom of one liner system and the bottom of the next lower liner system, or between the bottom of the lowest liner system and the bottom of the lowest soil layer modeled. In the sketch, the top subprofile contains the cover layers, the middle subprofile contains the waste, drain and liner system for leachate collection, and the bottom subprofile contains the drain and liner system for leakage detection. Six subprofiles in a single landfill profile may be simulated by the model.

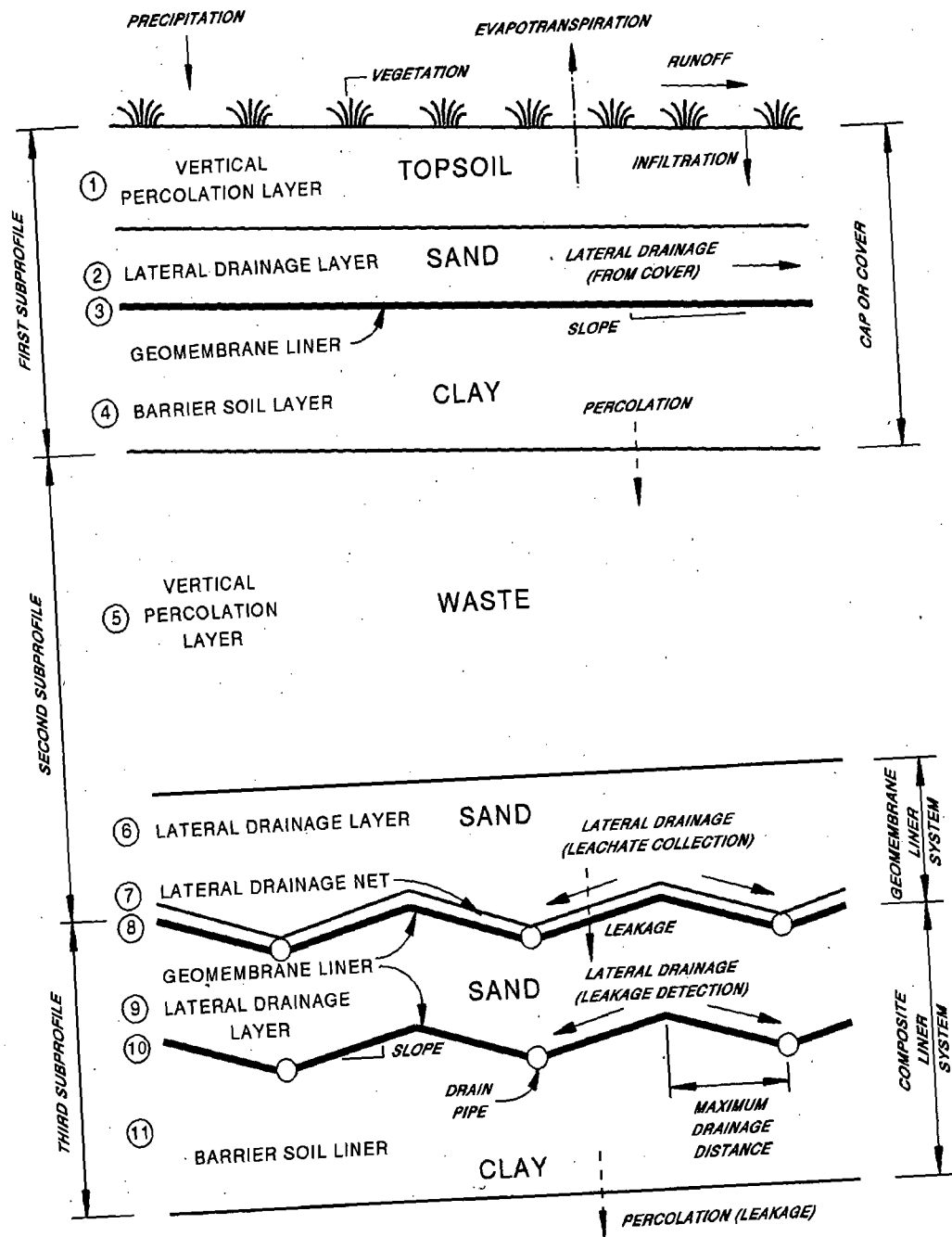


Figure 1. Schematic Profile View of a Typical Hazardous Waste Landfill

The layers in the landfill are typed by the hydraulic function that they perform. Four types of layers are available: vertical percolation layers, lateral drainage layers, barrier soil liners and geomembrane liners. These layer types are illustrated in Figure 1. The topsoil and waste layers are generally vertical percolation layers. Sand layers above liners are typically lateral drainage layers; compacted clay layers are typically barrier soil liners. Geomembranes are typed as geomembrane liners. Composite liners are modeled as two layers. Geotextiles are not considered as layers unless they perform a unique hydraulic function.

Flow in a vertical percolation layer (e.g., layers 1 and 5 in Figure 1) is either downward due to gravity drainage or extracted by evapotranspiration. Unsaturated vertical drainage is assumed to occur by gravity drainage whenever the soil moisture is greater than the field capacity (greater than the wilting point for soils in the evaporative zone) or when the soil suction of the layer below the vertical percolation layer is greater than the soil suction in the vertical percolation layer. The rate of gravity drainage (percolation) in a vertical percolation layer is assumed to be a function of the soil moisture storage and largely independent of conditions in adjacent layers. The rate can be restricted when the layer below is saturated and drains slower than the vertical percolation layer. Layers, whose primary hydraulic function is to provide storage of moisture and detention of drainage, should normally be designated as vertical percolation layers. Waste layers and layers designed to support vegetation should be designated as vertical percolation layers, unless the layers provide lateral drainage to collection systems.

Lateral drainage layers (e.g., layers 2, 6, 7 and 9 in Figure 1) are layers that promote lateral drainage to collection systems at or below the surface of liner systems. Vertical drainage in a lateral drainage layer is modeled in the same manner as for a vertical percolation layer, but saturated lateral drainage is allowed. The saturated hydraulic conductivity of a lateral drainage layer generally should be greater than  $1 \times 10^{-3}$  cm/sec for significant lateral drainage to occur. A lateral drainage layer may be underlain by only a liner or another lateral drainage layer. The slope of the bottom of the layer may vary from 0 to 40 percent.

Barrier soil liners (e.g., layers 4 and 11 in Figure 1) are intended to restrict vertical flow. These layers should have hydraulic conductivities substantially lower than those of the other types of layers, typically below  $1 \times 10^{-6}$  cm/sec. The program allows only downward flow in barrier soil liners. Thus, any water moving into a liner will eventually percolate through it. The leakage (percolation) rate depends upon the depth of water-saturated soil (head) above the base of the layer, the thickness of the liner and the saturated hydraulic conductivity of the barrier soil. Leakage occurs whenever the moisture content of the layer above the liner is greater than the field capacity of the layer. The program assumes that barrier soil liner is permanently saturated and that its properties do not change with time.

Geomembrane liners (e.g., layers 3, 8 and 10 in Figure 1) are layers of nearly

impermeable material that restricts significant leakage to small areas around defects. Leakage (percolation) is computed to be the result from three sources: vapor diffusion, manufacturing flaws (pinholes) and installation defects (punctures, cracks, tears and bad seams). Leakage by vapor diffusion is computed to occur across the entire area of the liner as a function of the head on the surface of the liner, the thickness of the geomembrane and its vapor diffusivity. Leakage through pinholes and installation defects is computed in two steps. First, the area of soil or material contributing to leakage is computed as a function of head on the liner, size of hole and the saturated hydraulic conductivity of the soils or materials adjacent to the geomembrane liner. Second, the rate of leakage in the wetted area is computed as a function of the head, thickness of soil and membrane and the saturated hydraulic conductivity of the soils or materials adjacent to the geomembrane liner.

**RESPONSE TO RAI COMMENT 31  
ROADMAP TO REFERENCES**

<b>REFERENCED DOCUMENT</b>	<b>*EXCERPT LOCATION</b>	<b>REMARK</b>
Cook et al. 2005	Other	Referenced in general in this response, no excerpts included for this response.
McIntyre and Wilhite, 1987 figure 2.4-2.	Excerpt included within response.	
MMES 1992 (Saltstone PA 1992)	Excerpt enclosed following response.	Page 2-54 and Section 2.4.1.3

**\*Excerpt Locations:**

1. Excerpt included in response: The excerpt is included within the text of the response or is appended to the response.
2. Excerpt enclosed following response: The excerpt is enclosed on a separate sheet or sheets following the response.
3. Representative excerpt(s) enclosed following response: Representative excerpts from a document that is wholly or largely applicable are enclosed following the response.
4. Other

**APPROVED** for Release for  
Unlimited (Release to Public)

7/15/2005

4/10980

APPROVED for Release for  
Unlimited (Release to Public)  
6/23/2005

WSRC-RP-92-1360

**RADIOLOGICAL  
PERFORMANCE ASSESSMENT FOR THE Z-AREA  
SALTSTONE DISPOSAL FACILITY (U)**

RC  
2/4/93

Prepared for the  
**WESTINGHOUSE SAVANNAH RIVER COMPANY**  
Aiken, South Carolina

by

**MARTIN MARIETTA ENERGY SYSTEMS, INC.  
EG&G IDAHO, INC.  
WESTINGHOUSE HANFORD COMPANY  
WESTINGHOUSE SAVANNAH RIVER COMPANY**

December 18, 1992

Rev. 0

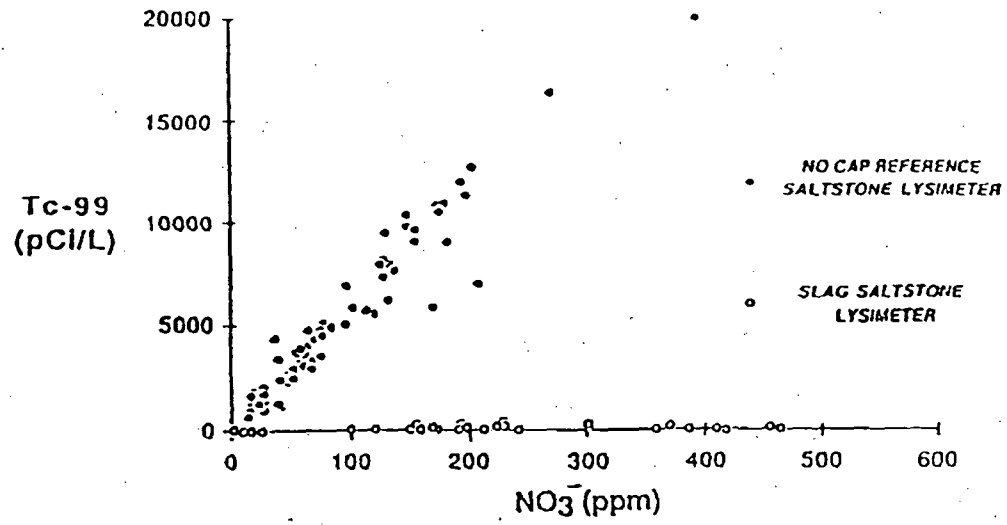


Fig. 2.4-2 Comparison of Technetium vs. Nitrate Leaching for Slag- and Cement-Based Saltstone Lysimeters.

### → 2.4.1.3 Evolution of the Landfill Design

#### Slit Trenches (1979)

In the initial concept of the disposal site proposed in 1979, slit trenches would be opened, filled with saltcrete grout, and backfilled with native soil. Trenches would be sized to enable filling with saltcrete and a portable trench cover would remain in place until the waste had solidified. After the waste had solidified, trenches would be backfilled with native soil, consistent with commercial landfill operations and regulations of that era (Benjamin and Roggenkamp 1979).

#### Slit Trenches Lined and Capped with Clay (1982)

With the evolution of disposal and groundwater protection regulations through the implementation of the Resource Conservation and Recover Act (RCRA), modeling, laboratory leaching tests, and lysimeter tests showed a need for improved waste disposal methods to minimize the rate of release of contaminants from the waste to the general environment and into the underlying groundwater. Contaminants of principal concern were nitrate (due to the projected high inventory), technetium-99 (due to its long half-life), and chromate (due to a hazardous waste classification, if chromate leach rates were too high). The slag formulation for saltstone eliminated concerns with chromium and technetium leaching (see Sect. 2.4.1.2), but modeling results indicated nitrate releases might be too high to meet the groundwater standards that were to be imposed by the state of South Carolina.

#### Concrete Vaults (1984)

Continuing modeling studies (Wilhite 1986) showed that disposal in concrete vaults was likely to effectively reduce the rate of nitrate release from the saltstone waste form, thus, eliminating a key environmental concern with the disposal of saltstone. Vaults would be constructed above grade and backfilling would be delayed until most or all of the vaults were filled with waste. Final site closure would be done in a manner that would comply with landfill regulatory requirements imposed by the state of South Carolina. A general closure concept was described in the permit application to the state, but detailed engineering was deferred until a future date prior to beginning final closure operations.

### 2.4.2 Physical Characteristics of Saltstone

For this performance assessment a composition containing 47 wt% salt solution, 25 wt% slag, 25 wt% fly ash, and 3 wt% cement is used to represent the average projected composition of the saltstone that will be sent to the SDF for disposal. When first prepared, the saltstone grout has the consistency and flow characteristics of

**RESPONSE TO RAI COMMENT 32  
ROADMAP TO REFERENCES**

<b>REFERENCED DOCUMENT</b>	<b>*EXCERPT LOCATION</b>	<b>REMARK</b>
Cook et al. 2005	Excerpt enclosed following response.	Section A.4
Peregoy 2003	Excerpt enclosed following response.	Pages 1-21 of calculation T-CLC-Z-00009.
Saltstone PA 1992	Excerpt enclosed following response.	Appendix B

**\*Excerpt Locations:**

1. Excerpt included in response: The excerpt is included within the text of the response or is appended to the response.
2. Excerpt enclosed following response: The excerpt is enclosed on a separate sheet or sheets following the response.
3. Representative excerpt(s) enclosed following response: Representative excerpts from a document that is wholly or largely applicable are enclosed following the response.
4. Other

**APPROVED** for Release for  
Unlimited (Release to Public)

7/14/2005

APPROVED for Release for  
Unlimited (Release to Public)  
6/6/2005

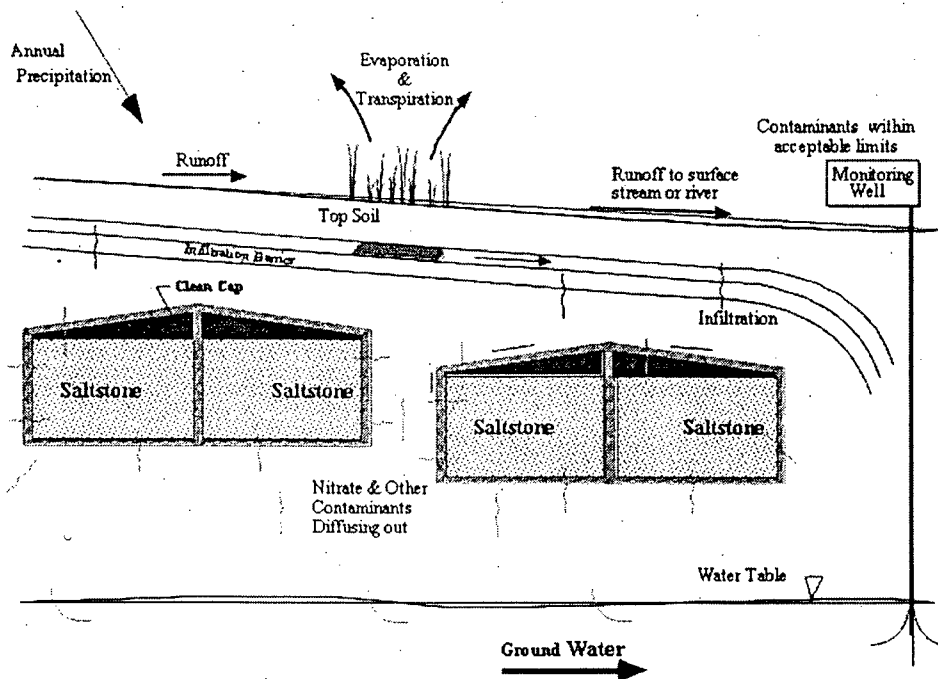
WSRC-TR-2005-00074 ←  
Revision 0

KEY WORDS: Performance Assessment  
Low-level Radioactive Waste Disposal

## SPECIAL ANALYSIS: REVISION OF SALTSTONE VAULT 4 DISPOSAL LIMITS (U)

PREPARED BY:  
James R. Cook  
Elmer L. Wilhite  
Robert A. Hiergesell  
Gregory P. Flach

MAY 26, 2005



Westinghouse Savannah River Company  
Savannah River Site  
Aiken, SC 29808

Prepared for the U.S. Department of Energy Under  
Contract Number DE-AC09-96SR18500



#### A.4 Impact of Macroscopic Cracks on Saltstone Vault 4 Performance

Vertical cracks or fractures spanning the entire Saltstone Vault 4 width and height are predicted to occur at 30 ft intervals, coinciding with construction joints, in response to static settlement and earthquakes. For the assumed properties of saltstone ( $10^{-11}$  cm/s conductivity), the literature indicates cracks can be neglected when the suction head exceeds approximately 200 cm in saltstone. Such conditions are predicted to occur during the 0-10,000 year period. This conclusion applies regardless of crack geometry, i.e., open at top, open at bottom, or through-crack.

##### A.4.1 Introduction

Peregoy (2003) analyzed the structural behavior of Saltstone Vault 4 in response to forecast static settlement and earthquakes. Approximately vertical cracks or fractures spanning the entire Vault 4 width and height were predicted to occur at 30 ft intervals, coinciding with construction joints. In the structural simulations, these macroscopic cracks were observed to open at either the top or bottom, while remaining in close contact at the opposite end of the fracture face, the latter forming a "hinge" of sorts. The cracks developed gradually over time (Peregoy 2003, Figure 9, Figure 10 and Table 2). Predicted mean crack sizes are summarized in Table A-20.

Table A-20. Summary of mean crack sizes at specific times.

##### Cracks open at bottom

Time (yr)	Crack width at open end (in)	Average width (in)
100	0.06	0.03
500	0.18	0.09
1000	0.30	0.15
2500	0.63	0.31
5000	1.15	0.58
10000	2.18	1.09

##### Cracks open at top

Time (yr)	Crack width at open end (in)	Average width (in)
100	0.01	0.004
500	0.03	0.015
1000	0.06	0.03
2500	0.16	0.08
5000	0.31	0.16
10000	0.62	0.31

Under a positive pressure condition, cracks or fractures in the saltstone monolith would be liquid-filled and form preferential pathways for infiltrating water compared to the surrounding low permeability matrix ( $10^{-11}$  cm/s). Under negative pressure or suction, the impact of cracks on saltstone performance is not immediately clear. The purpose of this Section is to assess the effect of macroscopic cracks on moisture movement through Saltstone Vault 4 under a range of hydraulic conditions and crack dimensions.

#### A.4.2 Flow Regimes

Water flow through a rough walled crack in a porous medium occurs in at least three distinct regimes:

1. Saturated flow, that is, liquid completely filling the aperture.
2. "Thick" film flow on each crack wall, where water is present as a film completely filling surface pits and grooves and the air-water interface is relatively flat.
3. "Thin" film flow, where water recedes into surface pits/grooves by capillary forces and adheres to flat surfaces by adsorption.

The saturated flow regime occurs at positive or very slightly negative pressures. The "thick" and "thin" film flow regimes occur at increasing negative pressures or suction in the surrounding porous medium. Each flow regime is analyzed separately below in the context of a uniform crack width.

An implicit assumption in these analyses is that the source of liquid to the crack is steady rather than episodic/transient, and that the resulting fracture flow is steady. Unsteady fracture flow has been observed at laboratory scale and inferred at field scale (Persoff and Pruess 1995; Su et al. 2001; Nativ et al. 1995; Fabryka-Martin et al. 1996; Pruess 1999). At laboratory scale, unsteady flow appears to be associated with relatively low suctions in a variable aperture setting. Under these conditions, water fills the smaller apertures while larger apertures are desaturated. At field scale (e.g. Yucca Mountain), unsteady flow has been inferred under high matrix suction. Temporal and spatial variations in infiltration and physical heterogeneity are thought to be factors leading to episodic flow.

The planned Saltstone closure cover system is expected to insulate cracks from episodic rainfall and lead to a relatively steady influx of water. Saltstone itself is expected to exhibit uniform properties in comparison with fractured geologic media. Cracks forming from differential settlement and seismic events are expected to be unsaturated. All of these conditions favor steady flow in Saltstone Vault 4.

#### A.4.3 Saturated Flow

The height of capillary liquid rise  $H$  between two parallel surfaces of aperture  $b$  is given by (e.g. Looney and Falta 2000)

$$H = \frac{2\sigma}{\rho g b} \quad (\text{A-20})$$

where  $\sigma$  is surface tension,  $\rho$  is liquid density, and  $g$  is gravitational acceleration. In the context of a fracture subject to a given pressure  $P$  in the surrounding matrix, the aperture will be liquid filled under the condition

$$P > -\frac{2\sigma}{b} \tag{A-21}$$

where suction is indicated by a negative pressure value (e.g. Wang and Narasimhan 1985). The equivalent permeability of the fracture is

$$k = \frac{b^2}{12} \tag{A-22}$$

and the hydraulic conductivity is

$$K = \frac{\rho g k}{\eta} = \frac{\rho g b^2}{12\eta} \tag{A-23}$$

where  $\eta$  is liquid viscosity. Figure 1 shows hydraulic conductivity as a function of aperture for water at 20°C. Note that even narrow cracks have a high conductivity compared to cementitious materials.

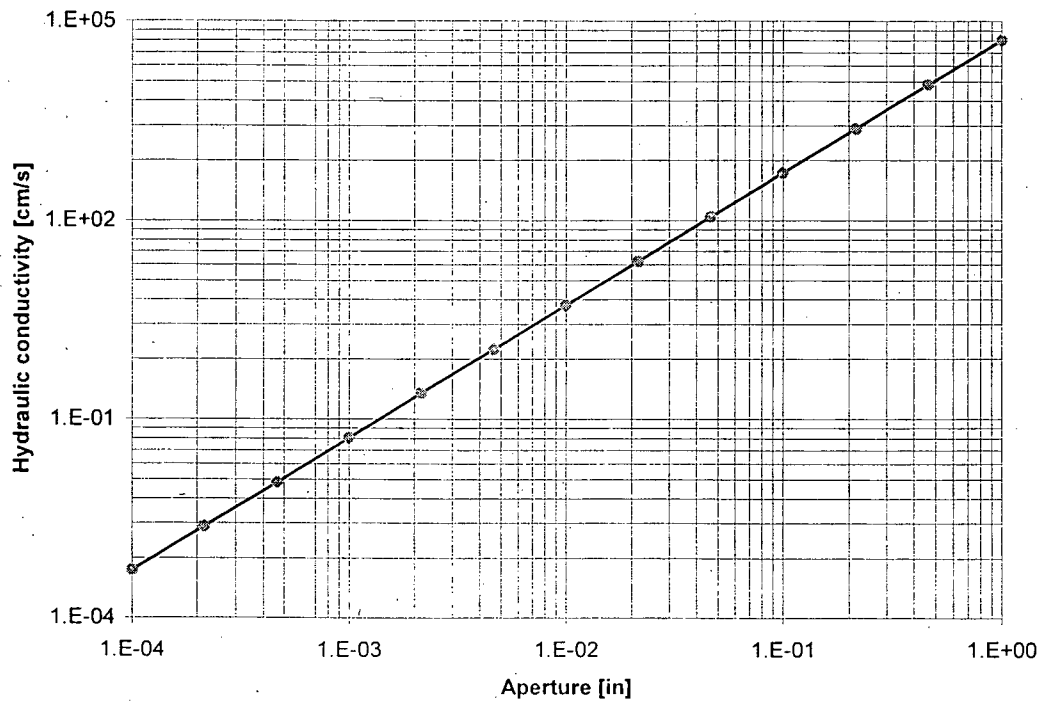


Figure A-77. Hydraulic conductivity of saturated cracks as a function of aperture.

#### A.4.4 Film Flow

When  $P < -2\sigma/b$ , liquid can no longer span an aperture and the crack will desaturate. For this condition, a rough fracture face can be conceptually simplified as a repeating series of vertical flat surfaces and V-shaped grooves to facilitate further analysis, following Or and Tuller (2000, Figure 1). At pressures slightly below  $-2\sigma/b$ , liquid will completely fill a groove and form a flat liquid-vapor interface. At a sufficiently low pressure, liquid will recede into the corner of the groove and be retained by capillary forces. Under this condition, the matric potential

$$\mu = \frac{P}{\rho} = gH \quad (\text{A-24})$$

determines the radius of the liquid vapor interface in a groove (Or and Tuller 2000, Figure 2):

$$r(\mu) = -\frac{\sigma}{\rho\mu} \quad (\text{A-25})$$

For a groove of depth  $L$  and angle  $\gamma$ , the maximum radius accommodated by the groove geometry is

$$r_c = \frac{L \tan(\gamma/2)}{\cos(\gamma/2)} \quad (\text{A-26})$$

The critical pressure defining the transition between flat and curved interfaces is

$$P_c = -\frac{\sigma}{r_c} \quad (\text{A-27})$$

and is the result of combining equations (A-24) through (A-26). Thus the three flow regimes identified earlier occur over the following pressure ranges for the assumed geometry of the fracture face:

1. Saturated flow:  $P > -\frac{2\sigma}{b}$
2. "Thick" film flow:  $-\frac{\sigma}{r_c} < P < -\frac{2\sigma}{b}$
3. "Thin" film flow:  $P < -\frac{\sigma}{r_c}$

Liquid not being held by capillary suction will adhere to the remaining surfaces of the fracture face as a thin film. Considering only van der Waal forces, liquid adsorption on solid surfaces can be characterized by

$$h(\mu) = \left[ \frac{A_{svl}}{6\pi\rho\mu} \right]^{1/3} \quad (\text{A-28})$$

where  $h$  is film thickness and  $A_{sv}$  is a Hamaker constant.

Liquid held in groove corners by capillary suction and adhering as a thin film to remaining surfaces flows downward under the force of gravity. Or and Tuller (2000) present a detailed analysis of the liquid area and average velocity associated with corner and film flows, which is summarized in the Appendix. Figures A-78a and A-78b illustrate equivalent film thickness and average hydraulic conductivity for a representative "rough" fracture surface (Or and Tuller 2000, Figure 6a). The critical matric potential defining the transition between "thick" and "thin" film flow is  $\mu_c = -0.22$  J/kg or approximately 2 cm of suction head. A discontinuity in film thickness is observed in Figure 6a at this matric potential.

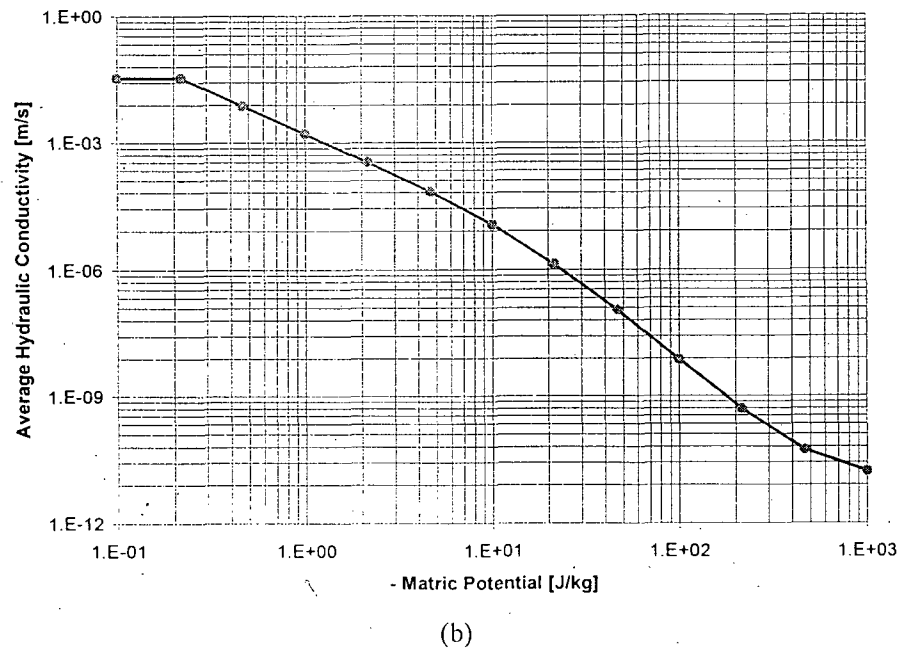
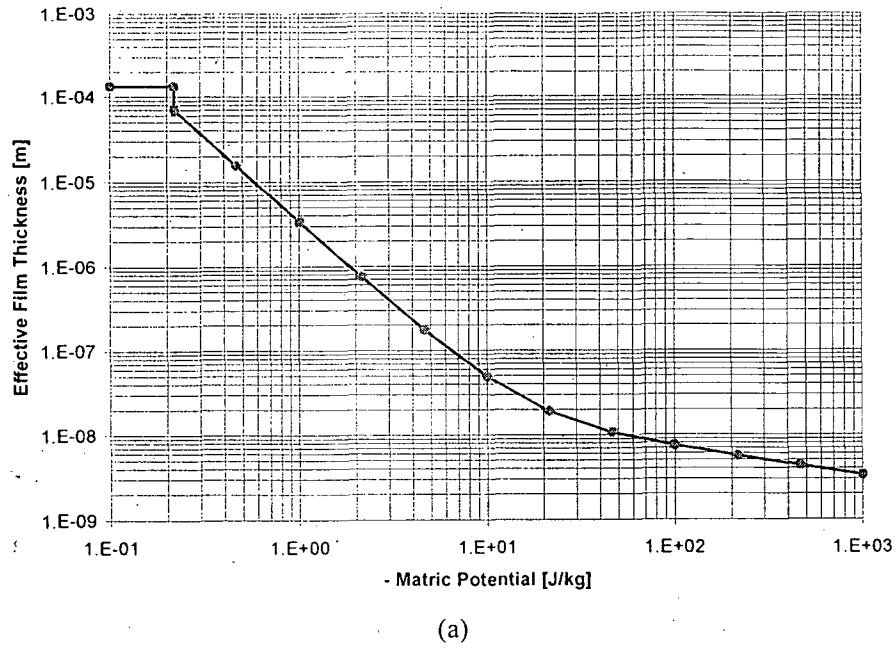


Figure A-78. Predicted film flow behavior for a representative “rough” fracture face with  $L = 5 \times 10^{-4}$  m and  $\gamma = 60^\circ$ : a) equivalent film thickness, and b) average hydraulic conductivity.

#### A.4.5 Application to Saltstone Vault 4

Under saturated flow conditions, the thickness of saltstone transmitting the same flow as a saturated crack under the same hydraulic gradient is

$$D_{saltstone} = \frac{K_{crack} b}{K_{saltstone}} \quad (A-29)$$

where  $b$  is the aperture and  $K_{crack}$  is defined by Figure A-77. For the assumed Saltstone Vault 4 hydraulic conductivity of  $10^{-11}$  cm/s, even a small crack is significant because of the extreme conductivity contrast. During the 10,000-50,000 year period, Saltstone Vault 4 is predicted to experience ponding on the upper surface. Cracks should be considered under these positive pressure conditions.

Similarly, the equivalent thickness of saltstone for unsaturated flow is

$$D_{saltstone} = \frac{2K_A D_A}{K_{saltstone}} \quad (A-30)$$

where the factor of two results from consideration of flow down both sides of the crack,  $D_A$  the average film thickness (e.g. Figure A-78a), and  $K_A$  is average conductivity (e.g. Figure 2b). Figure 3 defines the suction head required to desaturate a fixed width crack and the equivalent saltstone thickness, for the aperture conditions assumed in Figure A-78.

For example, at a suction of 100 cm, cracks larger than  $6 \times 10^{-4}$  inches will be unsaturated according to equation (A-27). Therefore the exact geometry of the crack, i.e. open at top or bottom, has little impact on the end result. The equivalent saltstone thickness, assuming a conductivity of  $10^{-11}$  cm/s, would be about 3 ft. At lower suctions, the equivalent thickness increases rapidly. Conversely, thickness rapidly decreases at higher suction. During the 0-10,000 year period, Saltstone Vault 4 is predicted to experience a suction of around 1200 cm. At this suction, unsaturated crack flow is predicted to be negligible ( $D_{saltstone} \approx 10^{-3}$  ft from Figure A-79). An informal sensitivity study that varied groove depth ( $L$ ), angle ( $\gamma$ ), and spacing ( $\beta$  in Or and Tuller (2000)) indicates this conclusion is not sensitive to the particular values assumed in Figure A-79.

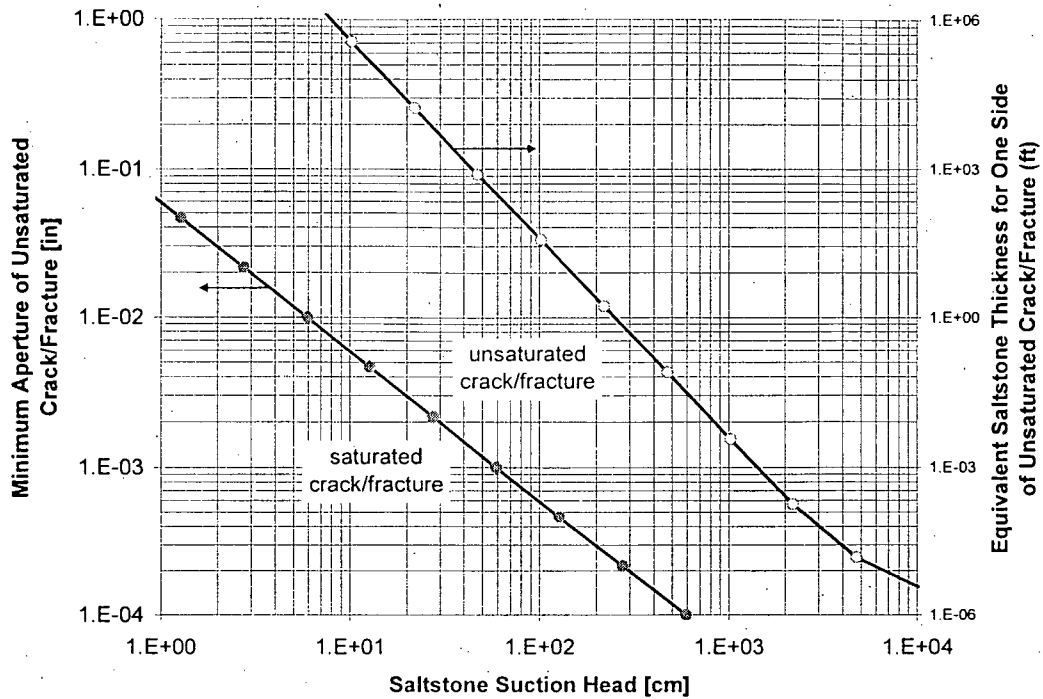


Figure A-79. Minimum unsaturated aperture and equivalent saltstone thickness for film flow down crack faces.

**A.4.6 Conclusions**

Macroscopic cracks forming in Saltstone Vault 4, whether pinched at top or bottom or through-wall, can be neglected when the suction head exceeds approximately 200 cm. Such conditions are predicted to occur during the 0-10,000 year period. At lower suction or positive pressure conditions, crack flow may be significant.

#### A.4.7 Details from Or and Teller Reference

The key equations and relationships needed to reproduce Figure 6a in Or and Tuller (2000) are summarized below:

Matric potential

$$\mu = \frac{P}{\rho} = gH \quad (\text{A-31})$$

Film thickness adsorbed to surface under tension

$$h(\mu) = \left[ \frac{A_{svl}}{6\pi\rho\mu} \right]^{1/3} \quad (\text{A-32})$$

Corner radius under capillary retention

$$r(\mu) = -\frac{\sigma}{\rho\mu} \quad (\text{A-33})$$

Critical matric potential

$$\mu_c = -\frac{\sigma \cos(\gamma/2)}{\rho L \tan(\gamma/2)} \quad (\text{A-34})$$

Critical radius of curvature ( $r < r_c$ )

$$r_c = \frac{L \tan(\gamma/2)}{\cos(\gamma/2)} \quad (\text{A-35})$$

Corner area for  $\mu < \mu_c$

$$A_{C1}(\mu) = r(\mu)^2 \left[ \frac{1}{\tan(\gamma/2)} - \frac{\pi(180-\gamma)}{360} \right] \quad (\text{A-36})$$

Corner area for  $\mu \geq \mu_c$

$$A_{C2} = L^2 \tan(\gamma/2) \quad (\text{A-37})$$

Film area for  $\mu < \mu_c$

$$A_{F1}(\mu) = h(\mu) \left\{ \beta L + 2 \left[ \frac{L}{\cos(\gamma/2)} - \frac{r(\mu)}{\tan(\gamma/2)} \right] \right\} \quad (\text{A-38})$$

Film area for  $\mu \geq \mu_c$

$$A_{F2}(\mu) = h(\mu) \{ \beta L + 2(1-\delta)L \tan(\gamma/2) \} \quad (\text{A-39})$$

Smooth vertical surface film flow (Tokunaga and Wan 1997; Or and Tuller 2000)

$$\bar{v} = \frac{\rho g}{3\eta} h^2 \quad (\text{A-40})$$

Corner vertical flow (Or and Tuller 2000)

$$\bar{v} = \frac{\rho g}{\varepsilon \eta} r^2 \quad (\text{A-41})$$

where

$$\varepsilon = \exp \left[ \frac{b + d\gamma}{1 + c\gamma} \right] \quad (\text{A-42})$$

and  $b = 2.124$ ,  $c = -0.00415$  and  $d = 0.00783$  for  $10^\circ < \gamma < 150^\circ$ .

Hydraulic conductivity

$$K \equiv \bar{v} \quad (\text{A-43})$$

Average hydraulic conductivity (velocity) for  $\mu < \mu_c$

$$K_{A1} = \frac{K_F A_{F1} + K_C A_{C1} \delta}{A_{F1} + A_{C1}} \quad (\text{A-44})$$

Average hydraulic conductivity (velocity) for  $\mu \geq \mu_c$

$$K_{A1} = \frac{K_F A_{F2} + K_C A_{C2} \delta}{A_{F2} + A_{C2}} \quad (\text{A-45})$$

Width of representative surface element

$$W = \beta L + 2L \tan(\gamma/2) \quad (\text{A-46})$$

Effective film thickness

$$D = \frac{A_F + A_C}{W} \quad (\text{A-47})$$

APPROVED for Release for  
 Unlimited (Release to Public)  
 6/23/2005

Calculation Cover Sheet

Project Saltstone Vault Performance Assessment		Calculation Number T-CLC-Z-00006	Project Number N/A	
Title Saltstone Vault Structural Degradation Prediction		Functional Classification PS	Sheet 1 of 615	
Discipline Structural Mechanics				
<input type="checkbox"/> Preliminary <input checked="" type="checkbox"/> Confirmed				
Computer Program: ANSYS      NA <input type="checkbox"/>		Version/Release: 7.0		
Purpose and Objective This calculation predicts the performance of the Saltstone Vault Number 4 over time, considering static settlement and the effects of earthquakes. A statistical approach combined with non-linear structural analysis is used. The objective is to estimate structural cracking and associated statistical uncertainty during the next 10,000 years.				
Summary of Conclusion See page 21				
		<b>UNCLASSIFIED</b>		
Rev. No.	Revision Description	DOES NOT CONTAIN UNCLASSIFIED CONTROLLED NUCLEAR INFORMATION		
0	Original Issue	ADC & Reviewing Officer: <u>J. R. JOHNS</u> (Name and Title) Date: <u>6/23/03</u>		
Rev. No.	Originator (Print) Sign/Date	Verification/Checking Method	Verifier/Checker (Print) Sign/Date	Manager (Print) Sign/Date
0	W. L. Peregoy <i>W. Peregoy 7/9/03</i>	Document Review of FE Analysis	Roger Parish <i>[Signature] 7/10/03</i>	Greg Mertz <i>[Signature] 7.10.03</i>
0		Independent Review of Statistical Analysis	Greg Mertz <i>[Signature] 7/10/03</i> Sec 1-7, 8, 3, A-D, H	FRED LOEFF <i>[Signature] 7.10.03</i>
Design Authority - (Print) <u>NA</u>		Signature		Date
Release to Outside Agency - (Print) <u>NA</u>		Signature		Date
Security Classification of the Calculation <u>Unclassified</u>				

ENGINEERING DOC. CONTROL - SRS



00575702

## Calculation Continuation Sheet

Calculation No. <b>T-CLC-Z-00006</b>	Sheet No. <b>2</b>	Rev. <b>0</b>
---	-----------------------	------------------

### Table of Contents

Section	Description	Page
	Open Items	3
1.0	Introduction and Scope	4
2.0	Input	5
3.0	Methodology	6
4.0	Assumptions	15
5.0	Results	17
6.0	Conclusion	21
7.0	References	21
8.0	Body of Calculation	22
8.1	2-D Axisymmetric Model	22
8.2	Structural Model	52
8.3	Statistical Model	165
Appendix A	Saltstone Properties	287
Appendix B	Soil Layer Properties and DWPF Settlement Data	291
Appendix C	Closure Cap Configuration	336
Appendix D	SGS Geotechnical Data for Differential Settlement	342
Appendix E	Structural Analysis Results	347
Appendix F	ANSYS Model Data	491
Appendix G	2-D/3-D Preliminary Model Study	572
Appendix H	Independent Verification of Statistical Approach	589

## Calculation Continuation Sheet

Calculation No. T-CLC-Z-00006	Sheet No. 4	Rev. 0
----------------------------------	----------------	-----------

**1 INTRODUCTION AND SCOPE**

Saltstone Vault Number 4 is a rectangular monolith 200-ft. wide by 600-ft. long by 27-ft. high. It is constructed of reinforced concrete with a 2-ft. base slab and 1 ½-ft. thick walls. The roof is nominally 6-in. thick, but is not considered as a structural element. Its purpose is for weather protection only.

The vault is filled with a saltstone grout mix that solidifies to form a weak concrete.

Prediction of structural cracking with time in this calculation is used in conjunction with groundwater flow modeling (by others) to estimate the potential leaching of radiological and chemical contaminants over time. The calculation is intended to cover times up to 10,000 years from the present. Since the time frame is so long, there are significant probabilities of large earthquakes that exceed those normally considered for production support facilities.

In its final configuration, the vault is completely filled with saltstone covered by clean grout and surrounded with soil backfill. Inertial loading of the vault itself does not induce significant structural stress since it is a monolithic structure. The only structural mechanism that causes cracking is settlement of the foundation soil.

This calculation covers cracks induced by settlement of the ground beneath the vault. There are two types of settlement: first, static settlement over time caused by the initial response of the soil to the loading imposed by the vaults and the consolidation of the soil layers, and second, differential settlement of local areas under the vault caused by earthquakes. The cracking caused by the static settlement is induced by a dishing effect that produces a curvature at the base of the vault. The differential settlement also causes a curvature, but over a small area. Geotechnical investigations did not find liquefaction potential and soft zones that could cause larger and more extensive settlements during a seismic event.

This calculation is based on the vault geometry as of January 1, 2003. Changes in configuration after that date are not considered. The cracks observed during and after filling the cells in the vault are assumed to be 100% repaired. Cracks caused by degradation of materials, weathering, chemical reactions, etc. are addressed elsewhere.

A typical cross section of the vault is shown in Figure 1. The locations of construction joints and the locations assumed for earthquake induced differential settlements are shown on this figure. Note that this cross section represents half of the overall vault. The vault is symmetrical at its center and the two halves are separated by a 3in expansion joint.

The analysis is performed in three parts:

**Static Settlement Model.** An axisymmetric model is run with appropriate soil properties to determine the static settlement pattern over time. Soil properties are based on actual settlement recorded for the Defense Waste Processing Facility (DWPF).

**Structural Model.** A structural model of the vault, including the structural concrete and saltstone, determines the extent of cracking for both static and earthquake induced settlements. Location, extent, and magnitude of differential settlement are considered as parameters.

## Calculation Continuation Sheet

Calculation No. T-CLC-Z-00006	Sheet No. 5	Rev. 0
----------------------------------	----------------	-----------

**Statistical Model.** The relationships of extent of cracking to the input parameters is determined from the results of multiple structural analyses. A Monte Carlo analysis utilizing these relationships is performed to determine the behavior of the vault over time.

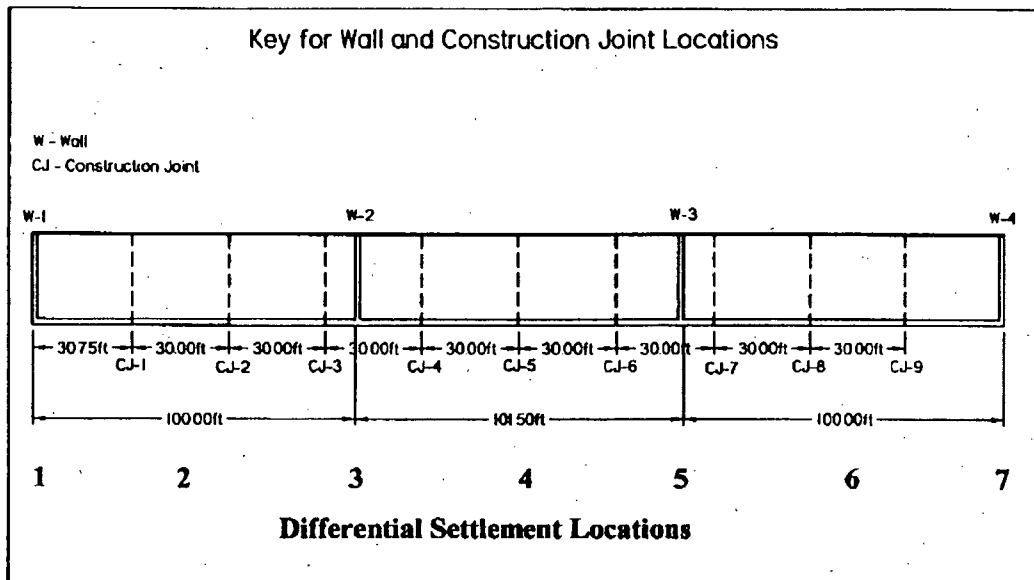


Figure 1. Typical Vault No. 4 Cross Section

## 2 INPUT

### 2.1 Drawings

The following drawings are used for the structural data in this calculation:

C-CC-Z-0011, through 14.      Saltstone Vault #4 Roof  
W828992, 993, and 999      Saltstone Vault #4 Concrete and Steel

### 2.2 Materials

**Concrete:** Concrete strength is taken as 4000 pounds per square inch (psi) and steel reinforcement is assumed to be Grade 60 (yield strength = 60,000psi).

**Saltstone:** Structural properties are taken from WSRC-TR-2003-00082. Relevant pages are included in Appendix A.

**Soil:** Appendix B contains the soil data and DWPF settlement data used in the analysis.

## Calculation Continuation Sheet

Calculation No. <b>T-CLC-Z-00006</b>	Sheet No. <b>6</b>	Rev. <b>0</b>
---	-----------------------	------------------

**Vault Cover:** The soil cover for Vault No. 4 is taken from The Revision 2 Closure Cap Configuration Report issued on 04/02/2003 by Mark Phifer. This report is included as Appendix C.

**3 METHODOLOGY**

The calculation is performed in three parts as noted in Section 1. A description of each of these parts follows.

**3.1 Axisymmetric Analysis**

**3.1.1 Purpose of Analysis**

A 2-D axisymmetric non-linear analysis is performed on the soil beneath Vault No. 4. The intent of this analysis is to train the properties of the soil with the DWPF data to obtain representative settlement displacements for Vault No. 4. The displacements are used in the structural model of the vault.

**3.1.2 Model Details**

The model is prepared with initial soil properties based on the shear wave velocities from Site Geotechnical Services (SGS) reports (References 7.3, 7.4, and 7.5). Relevant sections of these reports are included in Appendix B.

Settlement is the result of short-term elastic response of the soil layers beneath the structure and long-term secondary soil consolidation. Non-linear elements using elastic properties and kinematic hardening creep behavior are used to model the initial elastic response and the secondary consolidation, respectively.

The lateral extent of the model is sufficient to obtain horizontal boundary conditions that do not affect the area beneath the load application. The overall depth of the model is controlled by bedrock location at elevation -700-ft. The finite element mesh size is increased as a function of distance from the load application. A fine mesh is not needed in areas where the stress gradients are small.

Initial properties for the soil layers are calculated from the shear wave velocity data as discussed above. The initial properties are used as a starting point to verify that the model is working correctly and converging properly.

**3.1.3 DWPF Load Analysis**

SGS has calculated the DWPF construction load sequence for correlation with settlement monument data. The load application data and monument settlement readings are taken from Reference 7.3 and included in Appendix B.

Following the analysis with the calculated initial properties, the elastic and creep properties are varied until a displacement pattern is obtained that matches actual settlements. The relative relationships of properties from layer to layer are maintained.

## Calculation Continuation Sheet

Calculation No. <b>T-CLC-Z-00006</b>	Sheet No. <b>7</b>	Rev. <b>0</b>
---	-----------------------	------------------

Figure 2 shows the actual settlements measured for the DWPF and the settlement of the axisymmetric model at node 9 (120 ft. from centerline) for the DWPF load application. Node 9 was chosen because it is about midway between the model center and the edge of the DWPF. Three cases were run, representing a high, low and mean settlement. These three cases are shown as the dashed lines in Figure 2.

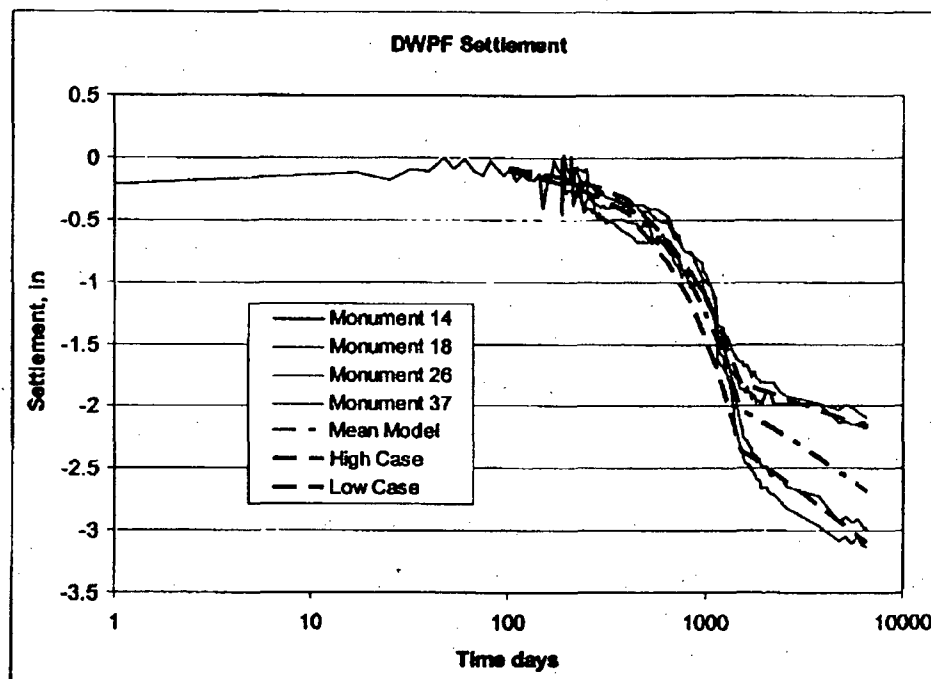


Figure 2. Comparison of DWPF Settlement with Axisymmetric Model Results

A stress contour plot for vertical normal stress and the deformed shape is shown in Figure 3. Note that the vertical scale is greatly exaggerated. The maximum displacement occurs at the model centerline (DMX) and is 0.24-ft. or 2.9-in. at a time of 6500 days.

## Calculation Continuation Sheet

Calculation No. T-CLC-Z-00006	Sheet No. 8	Rev. 0
----------------------------------	----------------	-----------

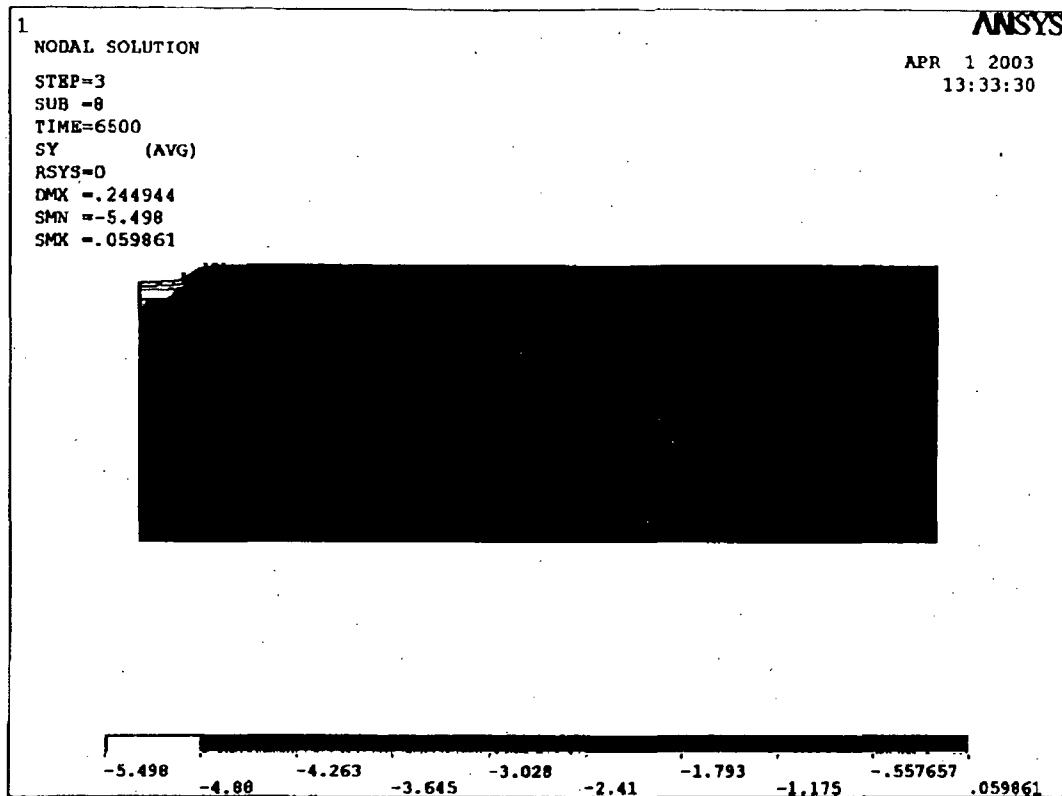


Figure 3. DWPF Non-linear Soil Model Results. This plot shows vertical stress plotted as contours on an exaggerated deformed shape.

### 3.1.4 Vault No. 4 Load Analysis

The result of the analysis for DWPF loads is a soil model that is representative of elastic and non-linear consolidation behavior of the underlying strata. To use this model to predict long-term static settlement of Vault No. 4, loads are calculated from the proposed closure cap cover plan detailed in Appendix C and applied as surface pressures. The calculated surface pressures vary from 0 to 7.3 kips per square foot (ksf).

Figure 4 shows the response of the model to the vault loads at a time of 10,000 years. The maximum soil pressure is 6.6 ksf. For Vault No. 4 the maximum displacement (DMX) is 0.61-ft., or 7.3-in. A comparison of Figure 4 and Figure 3 shows that the stress at bedrock for vault loads is significantly higher than the stress caused by DWPF loads. This difference does

## Calculation Continuation Sheet

Calculation No. T-CLC-Z-00006	Sheet No. 9	Rev. 0
----------------------------------	----------------	-----------

not affect the results since the bedrock is stiffer than the overlying strata and its long term consolidation is judged to be negligible.

The calculated displacements are in agreement with geotechnical predictions of initial and long-term settlement. (reference 7.7, attached in Appendix D)

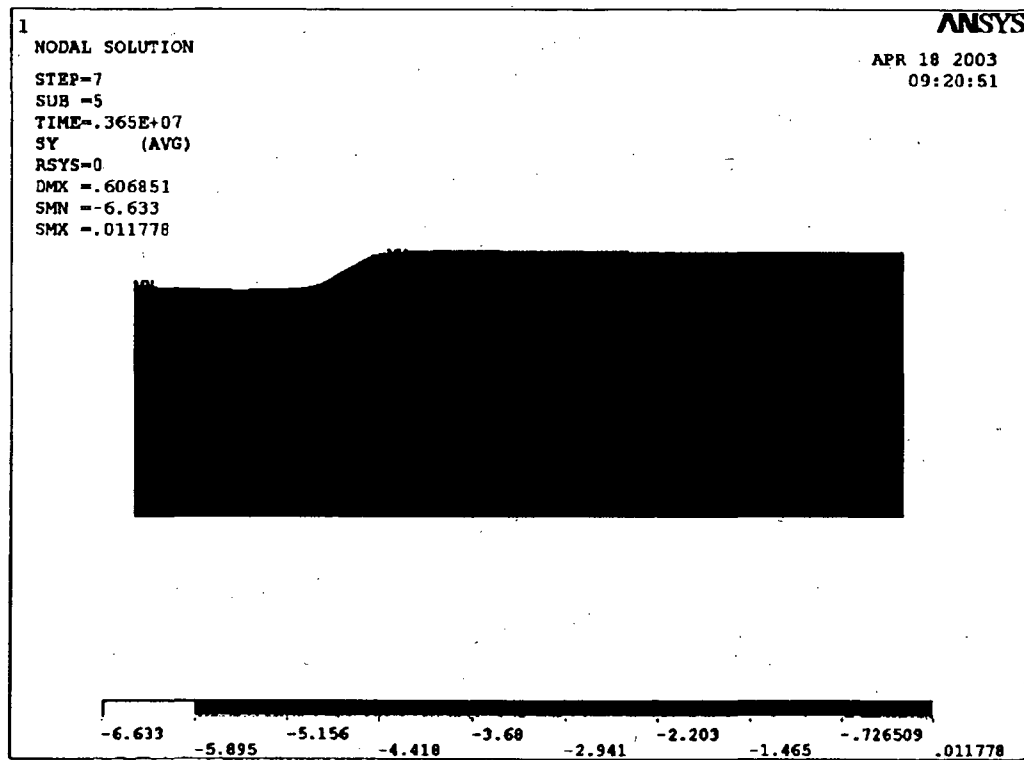


Figure 4. Non-linear Soil Model Results for Vault No. 4.

### 3.2 Structural Analysis

#### 3.2.1 Purpose of Analysis

Once the settlement displacements over time are obtained from the axisymmetric model, the next step is to determine the effects of both static settlement and earthquake induced differential settlement. The intent is to relate cracking in the vault to settlement and to determine the influence of variations in parameters, such as material properties, settlement

## Calculation Continuation Sheet

Calculation No. <b>T-CLC-Z-00006</b>	Sheet No. <b>10</b>	Rev. <b>0</b>
---	------------------------	------------------

rate, magnitude and extent of differential settlement, etc. These parameters are discussed in detail later.

**3.2.2 Model Description**

The structural analysis is performed with a 2-D plane strain model. The choice of a 2-D model is based on a preliminary comparison between 2-D and 3-D models presented in Appendix G. The study showed that stress and strains in the 2-D model are slightly higher than the 3-D model, but only by 5% or less.

An important aspect of the vault construction is that there are construction joints on 30-ft. centers in the base slab and walls. These joints are considered as discontinuities that are locations for crack initiation. The saltstone grout mix is almost an order of magnitude weaker than the structural concrete. It is therefore assumed that the cracks in the grout would tend to follow the pattern initiated by cracking in the structural concrete slab and walls.

The construction joints effectively subdivide the structure into blocks. Because of their aspect ratios (30-ft. wide and 27-ft. tall), the blocks have low bending stress between the joints for the static and differential displacements. If the blocks were larger, say 100-ft., there would be a potential for cracking between joints. There are also joints between the saltstone and the concrete walls. There is no bond assumed between at these joints.

The structural model uses non-linear contact elements for the joints between the walls and the saltstone and at the construction joint locations in the base slab. Crack propagation in the saltstone is modeled with non-linear elements that are elastic under compressive load and have a small elastic tensile strength. When the tensile strength is exceeded, the capacity of the element is zero.

The interface between the soil and the vault is represented by soil spring elements whose properties are based on the soil bulk modulus. These elements are simple unidirectional springs. The displacement boundary conditions are imposed on the structure through these springs to simulate the actual soil behavior in distributing the settlement to the structure. Since displacements are applied to nodal points, applying the displacements directly to the structure would give artificially high results, unless an extremely fine mesh is used.

Figure 5 shows a plot of the model used for the structural analysis. The non-linear interface elements do not appear in graphical representations since they have zero length.

Some of the structural model properties were considered parametrically as shown in Table 1. These properties are bulk modulus for the soil and Young's modulus and cracking strain for saltstone.

## Calculation Continuation Sheet

Calculation No. <b>T-CLC-Z-00006</b>	Sheet No. <b>11</b>	Rev. <b>0</b>
---	------------------------	------------------

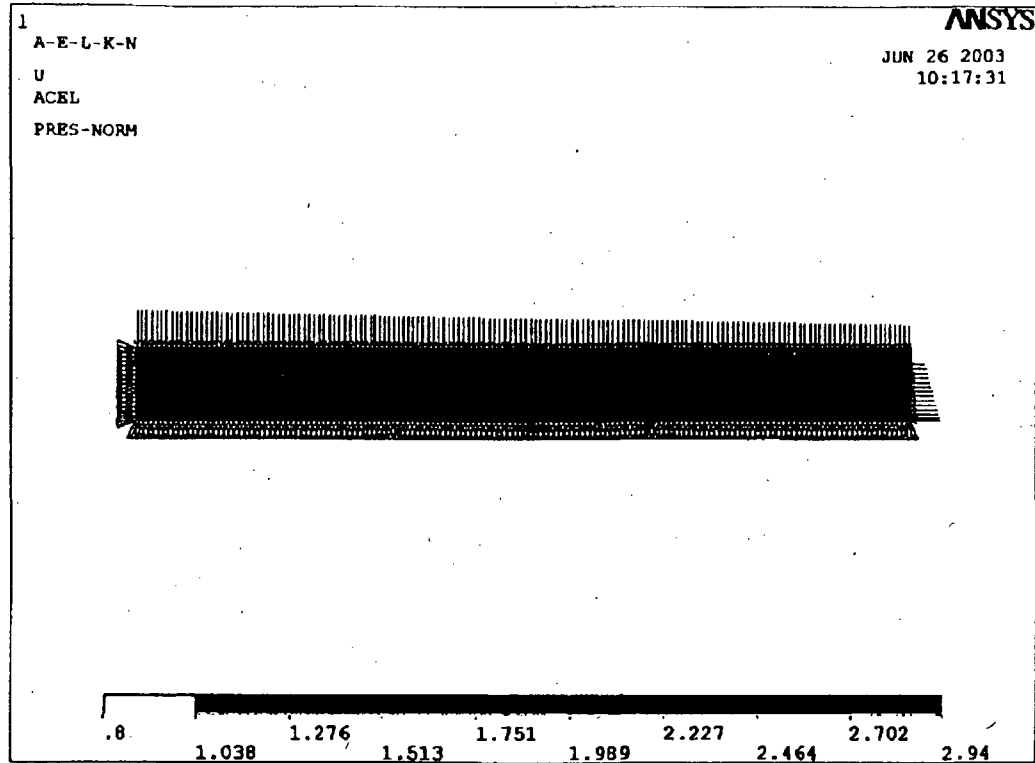


Figure 5. Structural Model. Applied pressures and boundary conditions are shown. The self weight of the structure is applied as a gravity load.

### 3.2.3 Static Settlement Analysis

The static settlement displacements from the axisymmetric model are applied to the structural model. The model is run by stepping through time with the displacements changed at discrete points in time corresponding to the axisymmetric model results. Since the mesh size is different for the structural model, displacements are linearly interpolated between nodal points of the axisymmetric model. The displacements from the axisymmetric model and the interpolations are shown graphically in Figure 8.

The static settlement rate is varied between the mean, high, and low cases discussed in Section 3.1.3. The settlement rate is used as a variable parameter in the statistical analysis and is given in Table 1.

## Calculation Continuation Sheet

Calculation No. T-CLC-Z-00006	Sheet No. 12	Rev. 0
----------------------------------	-----------------	-----------

Table 1. Parameters used in the Structural Analyses

Parameter	Units	Mean	1 sigma	Coefficient of variation
<b>Basic Parameters</b>				
Soil Bulk Modulus	kcf	30	15	0.5
Grout Compressive Strength	psi	524	196.8	0.38
Grout Modulus	ksf	2.05E+05	dependent on sqrt(Comp. Strength)	
Grout Cracking Strain	in/in	1.21E-04	dependent on sqrt(Comp. Strength)	
Static Settlement	ft	1.0807	0.53	0.5
<b>Earthquake Parameters</b>				
<b>Differential Settlement</b>				
Magnitude, PC-3	in	0.75	N/A	N/A
Magnitude, PC-4	in	2.75	N/A	N/A
Surface Extent	ft	62	31	0.5
Location	N/A	1 of 7	N/A	Uniform Distribution

## 3.2.4 Differential Settlement Analysis

The major effect of an earthquake on a monolithic structure of this type is to cause settlement beneath the structure. Differential settlement causes structural deformations that can lead to cracking. In the time span being analyzed, there is a likelihood of the occurrence of significant earthquakes.

To quantify the effects of differential settlement, there are three parameters of interest. First, the magnitude of settlement is related to the size of the event. The settlement magnitude for PC-3 and PC-4 events have been calculated by SGS (Reference 7.7 and Appendix D). These values are 0.75 inches for PC-3 and 2.75 inches for PC-4.

The second parameter is the extent of settlement. In reference 7.1, SGS shows the depth to the major earthquake induced settlement to be about 62-ft. for boring ZCP-27. This is the only boring that shows a fairly significant settlement of the six borings listed. Because of this observation, the settlement is treated as a point source with a 2:1 vertical cone of influence. The result of this assumption is a settlement diameter of 62-ft. at the surface. The settlement shape is a standard normal curve per Reference 7.2.

The third parameter is the location of the settlement with respect to the structure. Seven locations for potential differential settlement during earthquakes are chosen for the analysis. These locations are evenly spaced at 50-ft. intervals as shown on Figure 1.

The differential settlements are superimposed on the static settlements at specific times. The times chosen for the differential settlements are 100, 1000, and 5000 years.

The parameters for the differential settlement analysis are also shown in Table 1.

## Calculation Continuation Sheet

Calculation No. T-CLC-Z-00006	Sheet No. 13	Rev. 0
----------------------------------	-----------------	-----------

### 3.2.5 Structural Analysis Results Format

The results of multiple finite element analyses are summarized on spreadsheets by graphing nodal displacements at the construction joints and at the saltstone-concrete interface. The displacement patterns at the cracks are noted to be predominately linear. The cross sectional area for each crack is calculated by the length times the width divided by 2.

A typical plot of the finite element model deformed shape is shown on Figure 6. Note that the deformed shape plot is highly exaggerated. A corresponding plot showing the crack size vs. height is shown as Figure 7. Figure 7 is produced by plotting

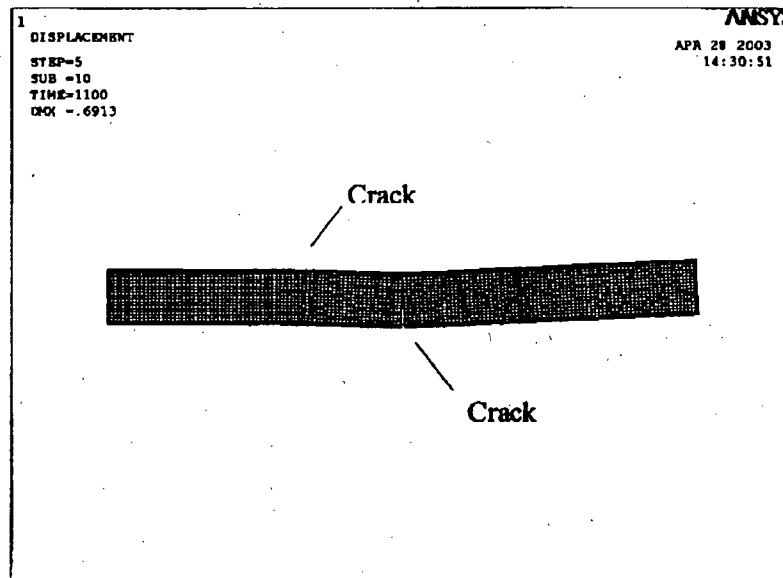


Figure 6. Typical Deformed Shape Plot. Differential settlement is at location 4 with PC-4 magnitude. All parameters are mean values.

For example, for the crack at construction joint 5 shown in Figure 7, the width is about 1.15 inches and the length is about 27 ft. The calculated area is  $1.15 \times 27 \times 1/2 = 186 \text{ in}^2$ .

## Calculation Continuation Sheet

Calculation No. T-CLC-Z-00006	Sheet No. 14	Rev. 0
----------------------------------	-----------------	-----------

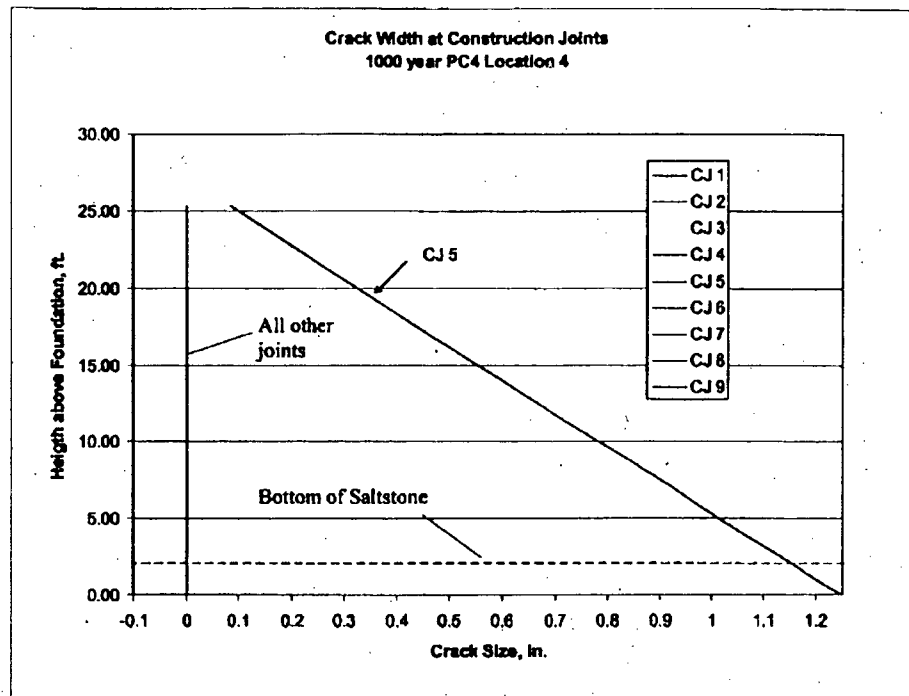


Figure 7. Typical Plot of Crack Size at CJ 5.

### 3.3 Statistical Analysis

#### 3.3.1 Purpose

The structural analysis generates multiple results for the various parameters discussed above. The results are generated by varying each parameter independently while holding the others at their mean values. To arrive at a statistical result that reflects crack sizes with respect to time, a Monte Carlo analysis is performed.

#### 3.3.2 Reduction of Structural Data

The first step in this process is to reduce the structural data to a form usable for the iterative analysis. Spreadsheet compilations of the structural data relate observed cracks to the parameters. Observed cracks were expressed in terms of cross sectional area for the two types observed: Cracks open at the top at the joint between the walls and the grout, and cracks open at the bottom at the construction joint locations.

There were some cases noted where there were multiple cracks. In these cases the data was simplified by adding the crack areas. The two basic premises in calculating crack areas are

## Calculation Continuation Sheet

Calculation No.	Sheet No.	Rev.
T-CLC-Z-00006	15	0

that static and differential settlement cracks were considered as independent and once a crack opens it remains open. The latter premise is discussed further in Section 4.

The results of the data reduction is a series of mathematical relationships that relate crack size to each of the parameters in Table 1.

**3.3.3 Monte Carlo Analysis**

Once the relationships between the parameters and the resulting crack areas are established, the next step is to apply statistical distributions to the data. In general, normal, or truncated normal distributions were used. The data was mapped onto these distributions.

The analysis is an iterative process where random numbers are used to set parameters for each iteration in accordance with the mapped distributions. Each iteration establishes values for saltstone modulus and cracking strain, soil bulk modulus, and static settlement rate. Once these parameters are set, the analysis is stepped through 10,000 years in 10 year increments.

As the analysis proceeds through the time steps, a random number generator is used to determine if a seismic event occurs, and if so, the magnitude of differential settlement associated with the event.

If an event occurs, random number generators are used to establish the location and extent of settlement.

The results of the Monte Carlo are a relationship between crack area and time with a statistical distribution. The model is iterated until a low convergence criterion in terms of percentage variation of mean and standard deviation of the results is met. The results are calculated at times of 100, 500, 1000, 2500, 5000, and 10000 years.

**3.3.4 Calculation of Crack Size**

The output of most interest for flow modeling is the crack width. To determine representative crack widths from the crack areas, a comparison is made between the statistical analysis results and the plots of the structural analysis cracks (see Figure 7). Empirical relationships are established that relate the areas and dimensions of the cracks.

**4 ASSUMPTIONS**

4.1 The starting point for this calculation is that the vault is in an as designed condition with all repairs complete.

4.2 Since the soil profiles for the Saltstone Vault area and the DWPF are similar, and the facilities are in close proximity on the site, the settlement data for the DWPF are considered applicable to the Saltstone Vault.

4.3 The static settlement for the DWPF is modeled by adjusting non-linear creep and linear elastic response in the axisymmetric model until a representative settlement curve is obtained as shown in Figure 2. This curve is considered the mean. The high and low settlement measurements of the DWPF are assumed to be a one sigma variation each way.

## Calculation Continuation Sheet

Calculation No.	Sheet No.	Rev.
T-CLC-Z-00006	16	0
<p>4.4 The loading used for soil cover considers the current information for the entire vault area. The vault area is projected to contain 15 vaults. Appendix G presents the results of various trial load combinations. The loading configuration that caused the greatest static displacement curvature is the inclusion of Vaults No. 1 through 12, but the exclusion of 13 through 15.</p> <p>4.5 Since the vault is symmetric about its centerline in the long direction, only one half of the vault is used in the structural analysis. However, the loads are not entirely axisymmetric about the Vault No. 4 centerline when considering the effects of the other proposed vaults. The static load case is slightly conservative since the half of the vault with the greatest static settlement curvature is used as shown in Appendix G.</p> <p>4.6 Assumptions regarding the coefficients of variation of the input to the analysis are explained in the body of the calculation.</p> <p>4.7 As discussed in Section 3.2, the structural behavior of the model is controlled by preexisting construction joints spaced on 30-ft. centers. Since these joints represent discontinuities in the structure, they provide locations for crack initiation. Because of the length of time considered in this analysis, the waterstop and reinforcing dowels are considered to be ineffective in reducing the cracking or leakage through the joints. These joints are also assumed to control the saltstone cracking in that cracks in the much weaker saltstone will tend to follow the joints in the concrete floor and walls.</p> <p>4.8 The reinforcing dowels in the structure tying the construction joints would initially provide some resistance to crack propagation. However, the displacements of the underlying soil are permanent, so the reinforcing bars are not credited since corrosion is likely given the long time spans in this analysis.</p> <p>4.9 The 2-D model does not consider the effects of cracking initiated by longitudinal construction joints. However, the assumption of 2-D behavior is conservative in that the joint is considered to extend through the width of the structure. If one assumes that a mean differential settlement with radius of 31 ft. occurs at the conjunction of a longitudinal and a transverse construction joint, the result could be a crack in each joint of approximately 62-ft. for a total of 124-ft. The model is conservative in that a transverse crack would be 200-ft. in length across the transverse section.</p> <p>4.10 The loads applied to the structural model are the same loads that are applied to the axisymmetric model. This is done to ensure that there is a consistent load application for the differential settlement case. The static results are checked and the absolute displacements at the base of the structure are found to be about 16% conservative with vault loads included. The actual conservatism is somewhat less, since static settlement cracking is induced by curvature rather than absolute displacement.</p> <p>4.11 There are certain conditions where a differential displacement tends to close a previously opened crack. Credit is not taken for closing cracks since, in the time frame under consideration, they would eventually fill in with solids and not be capable of closing.</p>		

## Calculation Continuation Sheet

Calculation No. <b>T-CLC-Z-00006</b>	Sheet No. <b>17</b>	Rev. <b>0</b>
---	------------------------	------------------

4.12 There is no credit taken for increase in concrete or saltstone compressive strength with time. This is a known effect in concrete, but there is not enough data for saltstone. Since the time span of this calculation is so long, there is no basis for either an increase or decrease of strength with time, so the initial strength is used.

### 5 RESULTS

#### 5.1 Axisymmetric Analysis

The results from the axisymmetric analysis for DWPF loading are shown on Figure 2. This shows the comparison between actual settlements measured over 10 years and the settlement calculated from the model.

The results from the same model for the vault loads are shown on Figure 8. The mean settlement rate is shown. The symbols represent the discrete settlement points calculated in the axisymmetric model at the various times noted on the legend. The lines connecting the symbols represent displacements interpolated for the finer mesh in the structural model.

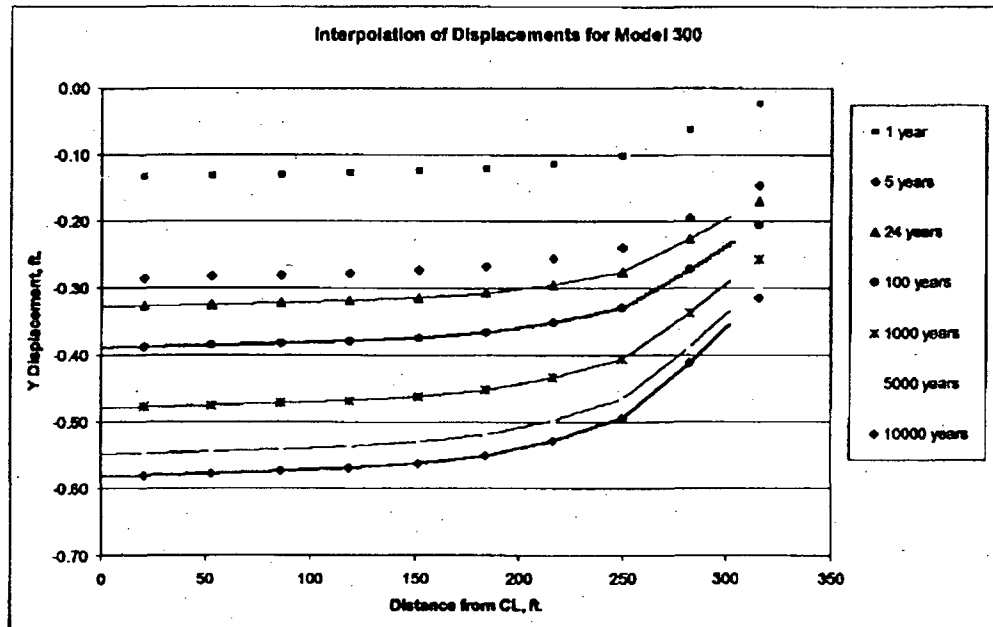


**Figure 8. Settlements for Vault 4 from Axisymmetric Model. Symbols show model results and the connecting lines are interpolations for application to the structural model.**

## Calculation Continuation Sheet

Calculation No. T-CLC-Z-00006	Sheet No. 18	Rev. 0
----------------------------------	-----------------	-----------

### 5.2 Structural Analysis

The results of the structural analysis are given in Appendix E. The plots shown indicate the formation of a cracks by the relative displacements between pairs of nodes on each end or surface of the non-linear elements.

A typical plot is shown in Figure 7. The plots are produced by exporting the ANSYS displacement results into EXCEL and plotting the relative displacements between the pairs of nodes associated with the construction joint locations and the saltstone-concrete interfaces. Appendix E shows results for the parameters listed in Table 1. Each parameter is varied independently while the others are held at their mean values.

### 5.3 Statistical Analysis

The results of the statistical analysis are shown in Figures 9 and 10. These figures represent the two types of cracks observed. The relationship of crack area and width and length is given Table 2.

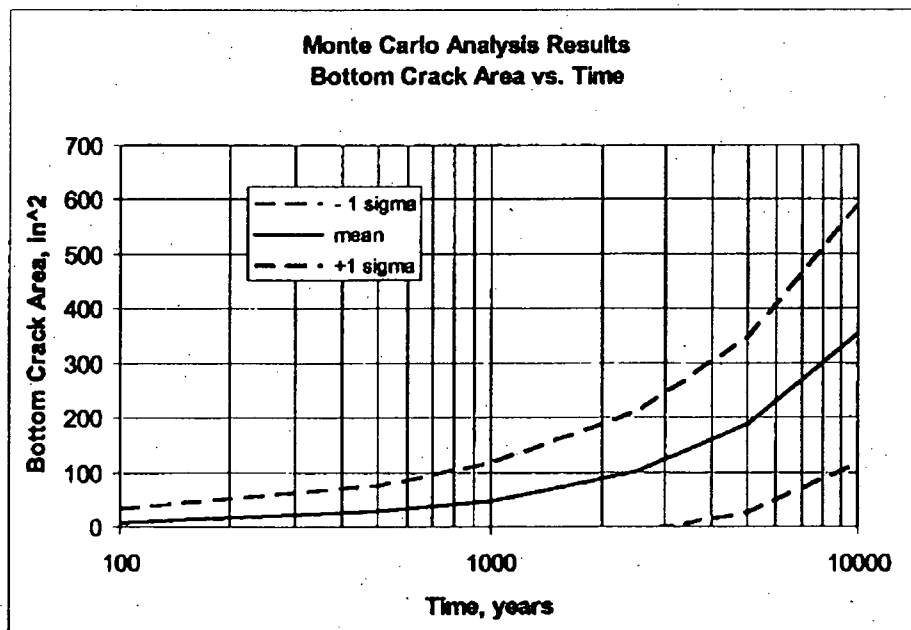


Figure 9. Cracks Open at Bottom

### Calculation Continuation Sheet

Calculation No. T-CLC-Z-00006	Sheet No. 19	Rev. 0
----------------------------------	-----------------	-----------

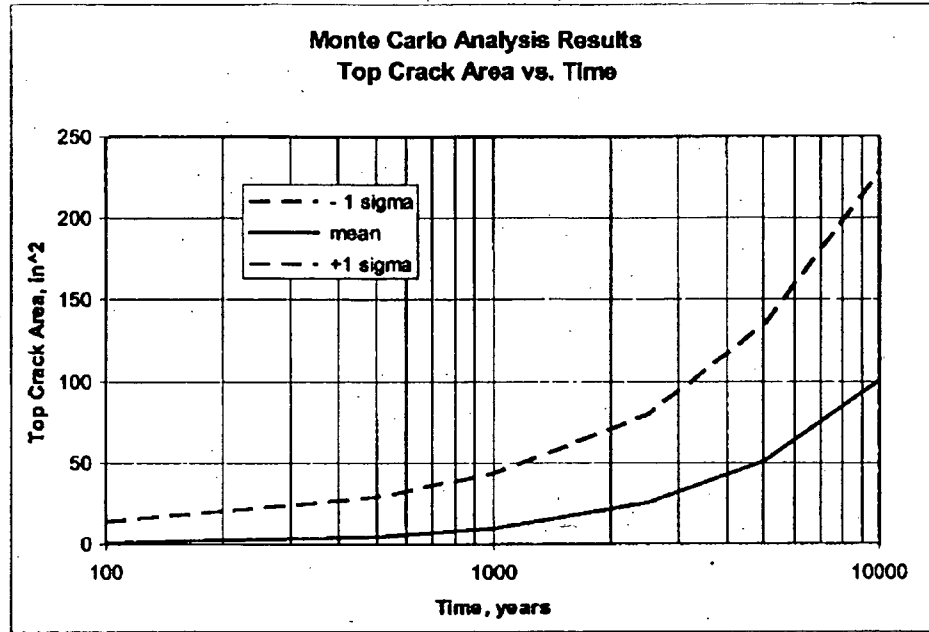


Figure 10. Cracks Open at Top

## Calculation Continuation Sheet

Calculation No. <b>T-CLC-Z-00006</b>	Sheet No. <b>20</b>	Rev. <b>0</b>
---	------------------------	------------------

Table 2. Summary of crack areas and sizes for specific time intervals.

**Cracks Open at Bottom**

Time	Mean Crack Size		Mean Crack Size		+1 sigma Crack Size	
	Mean	+1 sigma	Length ft.	Width in.	Length ft.	Width in.
<b>100</b>	8.48	33.02	24.30	0.06	25.74	0.21
<b>500</b>	27.39	75.60	25.42	0.18	27.00	0.47
<b>1000</b>	47.87	116.88	26.54	0.30	27.00	0.72
<b>2500</b>	101.50	211.98	27.00	0.63	27.00	1.31
<b>5000</b>	186.53	347.05	27.00	1.15	27.00	2.14
<b>10000</b>	353.26	588.72	27.00	2.18	27.00	3.63

**Cracks Open at  
Top**

Time	Mean Crack Size		Mean Crack Size		+1 sigma Crack Size	
	Mean	+1 sigma	Length ft.	Width in.	Length ft.	Width in.
<b>100</b>	1.14	14.02	27	0.01	27	0.09
<b>500</b>	4.70	28.80	27	0.03	27	0.18
<b>1000</b>	10.00	43.86	27	0.06	27	0.27
<b>2500</b>	25.21	79.94	27	0.16	27	0.49
<b>5000</b>	50.78	133.98	27	0.31	27	0.83
<b>10000</b>	100.55	227.80	27	0.62	27	1.41

## Calculation Continuation Sheet

Calculation No.	Sheet No.	Rev.
T-CLC-Z-00006	21	0

**6 CONCLUSIONS**

The results of the analysis predict the vault cracking over time as required by the calculation objective. The statistics provide the standard deviation and 95% confidence level for use in the flow net analysis and overall probabilistic evaluation of vault performance. The results are slightly biased towards a conservative estimate of crack size.

**7 REFERENCES**

- 7.1 K-CLC-Z-00001, "Liquefaction Potential for Saltstone Disposal Facility Vault No. 4", 8/22/2002.
- 7.2 K-CLC-H-00154, "Differential Settlement for CLWR-TEF Product Transfer Trench", Feb. 2000.
- 7.3 WSRC-TR-00072, Rev. 0, "Geotechnical Assessment Report for Defense Waste Processing Facility", February, 1995.
- 7.4 K-CLC-G-00060, Rev. 0, "General SRS Strain Compatible Soil Properties for 1886 Charleston Earthquake", October 1998.
- 7.5 K-CLC-H-00134, "Application of SRS Site-wide PC-3 Spectra to the Tritium Extraction Facility", June, 1998.
- 7.6 K-ESR-S-00002, Rev. 0, "Settlement of Defense Waste Processing Facility Vitrification Building", September 1998.
- 7.7 Memorandum FSS-GED-2003-00005, "Geotechnical Input for Saltstone Vault No. 4 Structural Analysis", May 1, 2003.

410980

APPROVED for Release for  
Unlimited (Release to Public)  
6/23/2005

WSRC-RP-92-1360

**RADIOLOGICAL  
PERFORMANCE ASSESSMENT FOR THE Z-AREA  
SALTSTONE DISPOSAL FACILITY (U)**

RC  
2/4/93

Prepared for the  
**WESTINGHOUSE SAVANNAH RIVER COMPANY**  
Aiken, South Carolina

by

**MARTIN MARIETTA ENERGY SYSTEMS, INC.**  
**EG&G IDAHO, INC.**  
**WESTINGHOUSE HANFORD COMPANY**  
**WESTINGHOUSE SAVANNAH RIVER COMPANY**

December 18, 1992

Rev. 0

## B.1. CODE SELECTION CRITERIA AND CONSIDERATIONS

Listed below are criteria that were considered in selecting computer codes for use in the RPA of the SDF at the Savannah River Plant. The first list, which follows directly, consists of absolute requirements for any code (1R = #1, Required); any code not meeting any one of these requirements was rejected.

1R. The theoretical framework of the selected computer code(s) should be based on appropriate fundamental principles of chemistry and physics (e.g., conservation of mass, momentum, and energy) and well established constitutive equations (e.g., Darcy's law, Fick's law, etc.).

2R. The selected code(s) should be verified (i.e., simulation results compared against known analytical solutions of the underlying equations) to demonstrate correctness of the source code. Such verification should be fully documented in a technical report made available, at a minimum, to SRS and the Peer Review Panel.

3R. The selected code should be documented in a technical report and contain descriptions of: 1) model theory, governing equations and assumptions, 2) computational techniques and algorithm, and 3) example applications.

4R. All simulation codes(s) selected for use in the performance assessments must be maintained under a software QA and management program that assures that modifications and updates are traceable, auditable and documented, and that all production versions have been verified and validated.

This second list contains criteria describing attributes of computer codes that, though desirable, may not be presently attainable (1S = #1, Suggested). Consideration was given to these criteria, and justification for using a code not meeting them is given in this appendix.

1S. The code(s) should allow site- and facility-specific applications; i.e., be capable of simulating the hydrologic, geologic and/or geochemical setting of the site, as well as specific design features of the facility over time.

2S. A contaminant transport code should be capable of: 1) tracking waste inventory over time, including radioactive daughter products, and 2) computing the contaminant fluxes at designated locations as a function of driving hydrologic processes and mass transport phenomena.

3S. The code(s) should be validated (e.g., simulation results compared with field data) for a system similar to that being modeled whenever possible. Benchmarking (i.e., code-to-code comparisons) is also useful in demonstrating code capabilities.

4S. The degree of complexity of the computer code(s) should be consistent with the quantity and quality of data, and the objectives of the computation. Screening calculations and sensitivity analyzes should be used to simplify conceptual models, and ultimately direct code selection.

5S. Hardware requirements for the selected code should not be exotic ( i.e., codes should run on readily accessible mainframe, mini, or personal computers (PC); convertibility is highly desirable).

6S. Proprietary codes should be used only if they provide a distinct advantage over public domain codes and only if the author(s)/custodian(s) allow inspection and verification of the source code. If a proprietary code is used, it must be made available by lease or purchase to WSRC-IWT.

7S. Consideration must be given to the ease of interfacing code output with other codes. For example, it is often desirable to use a groundwater code that simulates unsaturated and saturated flow, as well as mass transport, as coupling of output from each simulation type has already been accomplished.

8S. Familiarity with the code(s) should also be a consideration in selection, in light of time constraints that may be imposed for completion of a given Performance Assessment, and the need to revise the code if problems arise.

## B.2 GEOCHEMICAL COMPUTER CODE

The composition of saltstone pore fluids have been measured by Malek et al. (1987). Because the release rate of contaminants from saltstone is governed by aqueous concentration gradients in the saltstone pore fluids, potential geochemical controls on saltstone pore fluid composition were calculated. The analysis was done using the MINTEQ geochemical code and the measurements and observations of Malek et al. (1987).

### I. Code Description - MINTEQ

**Purpose and Scope:** MINTEQ is a geochemical computer code used to predict and evaluate the equilibrium behavior of inorganic pollutants in a variety of geochemical environments. The code can model complex equilibrium relationships that exist among soluble species, insoluble solids, gases, and adsorbed species. The code can also be used to calculate the consequences of equilibrium mass transfer between aqueous and solid phases. However, the code does not have the capability to calculate reaction path models nor can it calculate reaction kinetics. MINTEQ is useful for calculating the source term concentrations and speciation of inorganic contaminants. In addition, MINTEQ contains algorithms that predict the sorption of contaminants on soils and sediments. The sorption algorithms include: activity  $K_d$ , Langmuir isotherm, Freundlich isotherm, ion exchange, and surface complexation models. The code incorporates a

Newton-Raphson iteration scheme to solve the set of mass-action and mass-balance expressions.

**Development History:** The MINTEQ code was originally developed at Pacific Northwest Laboratory (Felmy et al. 1984a) by combining the mathematical structure of the MINEQL and the geochemical attributes of the WATEQ geochemical codes. MINTEQ was developed to solve geochemical equilibria problems by applying fundamental principles of thermodynamics. Changes to the code since its creation have been confined to improving ease of input and the flexibility of the output. Additional thermodynamic data has also been added to the database.

**Code Attributes:** The code is written in FORTRAN 77 programming language and includes several input data files containing data necessary for the operation of the code, such as: thermodynamic data, component identification numbers, ion charge and size, and formula weights.

**Computer Requirements:** Many applications of MINTEQ can be performed effectively and efficiently on a PC with a 286 central processor unit (cpu). More complex calculations will be more efficiently processed on a PC with a 386 cpu or on a work station. MINTEQ can also be run on mainframe computer systems.

**Restrictions:** The MINTEQ code was developed by Pacific Northwest Laboratory for the U.S. NRC and the EPA; the code is public domain software. The code is documented in Felmy et al. (1984a), Brown and Allison (1987), and Peterson et al. (1987).

## II. Code Selection Basis

**General Critique:** MINTEQ is one of several computer codes that have been developed to calculate equilibrium aqueous speciation and mineral mass transfer. Mechanistic adsorption models are included in the MINTEQ code, a major advantage over other geochemical codes such as EQ3/EQ6. The fundamental limitation of MINTEQ and other equilibrium based geochemical codes is that equilibrium conditions are often not obtained in low temperature systems. Furthermore, metastable conditions may persist for long periods of times in experimental systems, and experimentally observed concentrations may differ from those predicted by the code.

**Code Verification:** MINTEQ calculates the equilibrium speciation for an aqueous composition. Verification can be performed by using the MINTEQ output and hand calculations to evaluate equilibrium. In addition, the MINTEQ code was verified during its development by comparison calculations against WATEQ4 (Felmy et al. 1984a, b)

**Code Benchmarking:** The code has been benchmarked using the river water test case of Nordstrom et al. (1979; see Peterson et al. 1987). In addition, the code was benchmarked against WATEQ4 during development (Krupka and Morrey 1985).

**Code Validation:** The MINTEQ code has been partially validated for aqueous systems containing Cu(II), Pu, and U (Krupka and Morrey 1985). The code has not been validated for highly saline high-pH conditions found in saltstone pore fluids.

### III. Theoretical Framework

**Governing Equation and Assumptions:** The MINTEQ code calculates equilibrium speciation of aqueous phases. Speciation is defined as the chemical form of an element in an aqueous solution. The code solves mass balance expressions for each component ion (e.g.,  $\text{Ca}^{2+}$ ,  $\text{HCO}_3^-$ ,  $\text{Na}^+$ , etc.) using mass action relationships and equilibrium constants relating each species (such as  $\text{CO}_3^{2-}$ , a species of the  $\text{HCO}_3^-$  component) to MINTEQ components. Equilibrium constants for species are provided in the THERMO.DAT data base for calculations at a reference temperature of 25°C and infinite dilution. For temperatures that differ from 25°C, equilibrium constants are calculated either by using the Van't Hoff equation and enthalpies of reaction included in the data base or from analytical expressions relating equilibrium constants to temperature (Smith 1988). The concentration dependence of equilibrium constants are derived from individual ion activity coefficients calculated from the modified Debye-Huckel equation (Trusdell and Jones 1974), the Davies equation (Trusdell and Jones 1974), or the B-dot equation (Smith 1988).

**Initial Conditions:** The algorithm used in MINTEQ requires estimated starting values for the activities of component species. If these activity estimates are too far from the true values, the algorithm may fail to converge.

**Numerical Techniques:** MINTEQ uses a Newton-Raphson iteration method to simultaneously solve the non-linear mass balance equations.

### IV. Code Inputs and Outputs

**Input Data Structure:** To execute the MINTEQ computer code, an input data file is prepared for each problem. The data file consists of

- title or run identifier,
- analytical units and temperature,
- run-specific user options,
- component identification and concentrations, and
- component modifications (e.g., concentration of  $\text{H}^+$  fixed by pH).

**Output Options:** The MINTEQ code outputs the following:

- Echo of the data file input
- progress of the Newton-Raphson iterations
- full speciation of the input water composition
- charge balance and ionic strength for the aqueous composition
- saturation state of the water with respect to minerals in the data base

The user can also specify that the thermodynamic data base be printed. Debugging printing options are supported.

### **B.3 VAULT DEGRADATION COMPUTER CODE**

#### **I. Code Description - Concrete Degradation and Steel Reinforcement Corrosion**

**Purpose and Scope:** The code used to estimate concrete degradation and rebar corrosion is designed to model the important degradation processes that can affect the long-term performance of concrete barriers. The processes modeled include: (1) concrete attack by sulfate and magnesium, 2) concrete leaching (both concrete and geologically controlled), 3) carbonation, and 4) rebar corrosion.

**Development History:** The current model consists of analytical solutions for concrete degradation processes. These solutions were selected as the best available means of predicting long-term concrete barrier performance.

**Code Attributes:** The code is written in Mathematica programming language (Wolfram 1988) and consists of four separate modules. Three of the modules are used to estimate concrete degradation and one is used to predict corrosion of steel reinforcement.

Sulfate and magnesium attack on concrete is described by an empirical relationship determined by Atkinson and Hearne (1984). Leaching of concrete components is described by a shrinking core model, in the case of concrete-controlled leaching, and by diffusional mass transport for geologic-controlled leaching (Atkinson and Hearne 1984). Walton et al. (1990) derived a shrinking core model to describe concrete carbonation. Rebar corrosion is described by an empirical correlation to determine time to onset of corrosion from chloride attack (Clear 1976) and a one dimensional diffusion calculation for actual corrosion (Walton et al. 1990).

**Computer Requirements:** The code was developed on an Apple Macintosh IIcx and has also been run using a NEXT workstation. The code will run on any workstation, mainframe or PC that runs Mathematica. The degradation code will run on any system running the Mathematica software package. The Macintosh version 1.2.2 recommends a minimum of 4 megabytes of RAM.

**Restrictions:** The code has been developed in the Mathematica software package and is therefore restricted by the purchase of the software.

## II. Code Selection Basis

**General Critique:** The code is a compilation of analytical solutions for important concrete degradation processes (Clear 1976; Atkinson and Hearne 1984; Walton et al. 1990) selected based on the work of Walton et al. (1990). These analytical solutions are considered to be the best available means of predicting concrete degradation. The equations that are used to represent the degradation processes are based on observed conditions (i.e., sulfate, magnesium, chloride and dissolved oxygen concentrations in groundwater, etc.). However, in some cases the conditions encountered in a performance assessment are very different from the conditions on which the empirical relationships are based. Also, the observations that form the basis of the equation are for much shorter periods of time (tens of years) than is needed for performance assessments (thousands of years).

**Code Verification:** The Mathematica version of the code has been verified against the results of Walton et al. 1990.

**Code Benchmarking:** The code is made up of analytical solutions, therefore the benchmarking process does not apply.

**Code Validation:** The code is made up of analytical solutions, therefore the validation process does not apply.

## III. Theoretical Framework

### Governing Equation and Assumptions:

**Sulfate and Magnesium Attack.** The equations that form the basis for the calculations are based on chemical reactions between concrete and rebar with chemical constituents from the monolith and/or the geologic media surrounding the vault. Sulfate attack on concrete is the result of reactions of sulfate with hydrated tricalcium aluminate ( $C_3A$ ) and portlandite [ $Ca(OH)_2$ ] to form compounds of larger volume leading to expansion and disruption of the concrete. The reactions between sulfate and cement

compounds can be written as

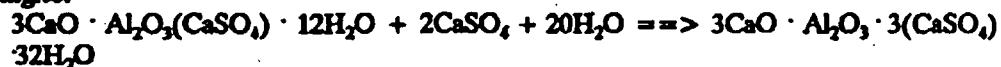
**Gypsum:**



**Monosulphoaluminate:**

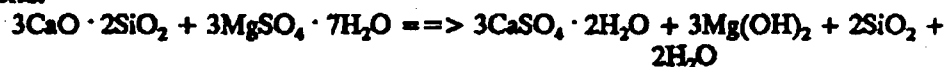


**Ettringite:**



An example of a reaction between cement paste and magnesium sulfate is

**Brucite:**



The low solubility of  $\text{Mg(OH)}_2$  causes the reaction to proceed to completion, making the attack more severe.

The depth of sulfate and magnesium attack is described by the equation

$$x = 0.55 C_3 (\text{Mg}^{2+} + \text{SO}_4^{2-})t$$

where

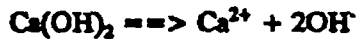
- x = depth of deterioration (cm),
- $C_3$  = weight percent of  $C_3A$  in non-hydrated cement,
- $\text{Mg}^{2+}$  = concentration of magnesium in the bulk solution (mol/L),
- $\text{SO}_4^{2-}$  = concentration of sulfate in the bulk solution (mol/L), and
- t = time (years).

**Assumptions:** The rate of attack is proportional to sulfate and magnesium concentration in the solution and  $C_3A$  content of the cement.

**Limitations:** Correlations are only valid over the time/system parameters tested. Application outside this range is highly questionable.

The empirical correlation does not include the impacts of advective transport and/or the known importance of water cement ratio (WCR) on durability. Application of the model is not clearly conservative.

Concrete-Controlled Leaching of Calcium Hydroxide. Cement components will be leached from concrete in environments in contact with water and have significant percolation rates. The alkalis are the first components to be leached followed by calcium hydroxide. The leaching of calcium hydroxide from the cement is described by



The equation that describes concrete controlled leaching is

$$x = [2D_1 \{(C_1 - C_{pw})/C_1\}t]^{1/2}$$

where

- x = depth of leaching (cm),
- D<sub>1</sub> = intrinsic diffusion coefficient of Ca<sup>2+</sup> in concrete solid (mol/cm<sup>2</sup>),
- C<sub>1</sub> = concentration of Ca<sup>2+</sup> in concrete pore water (mol/cm<sup>3</sup>),
- C<sub>pw</sub> = concentration of Ca<sup>2+</sup> in the groundwater or soil moisture (mol/cm<sup>3</sup>),
- C<sub>1</sub> = bulk concentration of Ca<sup>2+</sup> in the concrete solid (mol/cm<sup>3</sup>), and
- t = time (s).

**Assumptions:** The rate of calcium removal from the exterior of the concrete is assumed to be rapid relative to the movement of calcium ions through the concrete. Therefore, diffusion controls the transport rate of the calcium.

**Limitations:** Diffusional mass transport is considered, but advection through and around the concrete is not considered.

D<sub>1</sub> for the leached portion of the concrete will be substantially higher than D<sub>1</sub> for intact concrete. Permeability of the concrete will increase as leaching proceeds leading to greater flow rates through the leached area. Diffusional control may no longer be valid under these conditions.

Geology-Controlled Leaching of Calcium Hydroxide. Geology-controlled leaching occurs as a result of the diffusion being controlled by the geologic material surrounding the concrete. The resulting equation is

$$x = 2 \text{ phi } [(C_1 - C_{pw} / C_1) \{(R_d D_E t) / \text{pi}\}]^{1/2}$$

where

- x = depth of leaching (cm),
- phi = porosity of the geologic material (cm<sup>3</sup> voids/cm<sup>3</sup> total),
- C<sub>1</sub> = concentration of Ca<sup>2+</sup> in concrete pore water (mol/cm<sup>3</sup>),
- C<sub>pw</sub> = concentration of Ca<sup>2+</sup> in the groundwater or soil moisture (mol/cm<sup>3</sup>),
- C<sub>1</sub> = concentration of Ca<sup>2+</sup> in the bulk concrete (solid+pore) (mol/cm<sup>3</sup>),

- $R_d$  = retardation factor for  $\text{Ca}^{2+}$  in the geologic material,  
 $D_B$  = effective dispersivity/diffusivity of  $\text{Ca}^{2+}$  in geologic material ( $\text{cm}^2/\text{s}$ ), and  
 $t$  = time (s).

**Assumptions:** Diffusion into the surrounding geologic material controls leaching. Leaching is highest in low calcium concentration environments.

**Limitations:** Parameters for geologic material are needed ( $R_d$ ,  $D_B$ ,  $\phi$ ).

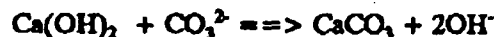
**Concrete Carbonation.** Carbonation is typically thought of as the reaction between calcium hydroxide and carbon dioxide as represented by



Carbonation can occur only as rapidly as dissolved carbonate can diffuse through the concrete. Carbonation rate is dependent on the moisture content of the concrete and the relative humidity of the ambient medium and the concentration of  $\text{CO}_2$  in the ambient medium. If diffusion in the concrete is too slow, an equilibrium is reached where the diffusion of  $\text{CO}_2$  and carbonation are stopped or severely reduced.

Carbonation rate is dependent on the moisture content of the concrete. As relative humidity changes from 0 to 100%, the rate of carbonation passes through a maximum.

Because the pH in concrete is high (>12), the carbonation reaction actually occurs as



The relationship between carbonation depth and groundwater concentration, portlandite in the concrete, and intrinsic diffusion coefficient of calcium is:

$$x = [2D_1 (C_{p^*}/C_s) t]^{1/2}$$

where

- $x$  = depth of carbonation (cm),  
 $D_1$  = intrinsic diffusion coefficient of  $\text{Ca}^{2+}$  in concrete ( $\text{cm}^2/\text{s}$ ),  
 $C_{p^*}$  = concentration of total inorganic carbon in the groundwater ( $\text{mol}/\text{cm}^3$ ),  
 $C_s$  = bulk concentration of  $\text{Ca(OH)}_2$  in the concrete solid ( $\text{mol}/\text{cm}^3$ ), and  
 $t$  = time (s).

**Assumptions:** Concrete is saturated with water.

**Limitations:** The type of cement ultimately affects the depth of carbonation. This relationship becomes increasingly invalid as the relative humidity of the concrete decreases from 100% to 50%; below this level, the reaction rates decline rapidly resulting in a reduction in carbonation rate.

**Reinforcement Corrosion/Chloride Attack.** The alkaline environment of the concrete and the isolation it provides from external corrosive agents protects the steel reinforcement from corrosion by forming a protective oxide layer on the metal surface. The passive oxide layer may undergo attack by corrosive agents as the concrete deteriorates. Historically, aqueous chloride is the corrosive agent associated with the break up of the passive layer.

Reinforcement corrosion may also be associated with reduction of concrete alkalinity in the absence of elevated chloride levels. Carbonation and leaching can cause a decrease in the concrete pH with eventual loss of passivity.

Chloride attack is modeled in two stages (a) time to breakup of the passive layer and initiation of corrosion and (b) corrosion rate subsequent to breakup of the passive layer. An empirical correlation for the time to passive layer breakup is

$$t_c = (129 x_c^{1.22}) / (WCR Cl^{0.42})$$

where

- $t_c$  = time to onset of corrosion (years),
- $x_c$  = thickness of concrete over the rebar (in.),
- WCR = water to cement ration (by mass), and
- Cl = chloride ion concentration in groundwater (ppm).

**Assumptions:** The time to onset of corrosion is related to the water to cement ratio, depth of cement cover, and chloride concentration in groundwater.

**Limitations:** Applicability to conditions outside the observed chloride concentrations on which the equation is based is questionable.

The simplest method of estimating the corrosion rate subsequent to initiation of corrosion is a one dimensional diffusion calculation assuming limitation of the corrosion rate by oxygen diffusion. The percent of reinforcement remaining at any time is given by

$$\% \text{ remaining} = 100[(4*9.4 \text{ s}D_1C_{pm}t) / (\pi d^2 \text{ delta } x)]$$

where

- $s$  = spacing between reinforcement bars (cm),
- $D_1$  = intrinsic diffusion coefficient of  $O_2$  in concrete ( $cm^2/s$ ),
- $C_{gw}$  = concentration of oxygen in the groundwater ( $mol/cm^3$ ),
- $\delta x$  = depth of reinforcement below surface (cm), and
- $t$  = time (s).

**Assumptions:** The corrosion rate is limited by oxygen diffusion.

**Limitations:** Applicable only if oxygen diffusion controls corrosion.

**Initial Conditions:** Not applicable.

**Numerical Techniques:** Not applicable.

#### IV. Code Inputs and Outputs

**Input Data Structure:** Input for the calculations is contained in the Mathematica file for degradation calculations. The values may be changed from within Mathematica and the file is evaluated as needed.

**Output Options:** Output can be in the form of numeric values, tables, two- or three-dimensional plots, and contour plots. Mathematica allows many forms of output to be displayed within the package and exported for use in other graphics packages.

### B.4 SATURATED/UNSATURATED FLOW AND TRANSPORT CODE

#### I. General Code Description

**Purpose and Scope.** The PORFLOW-3D computer code was selected and applied to predict the isolation performance of the saltstone vaults in the vadose zone, to predict transport of radionuclides released to the underlying aquifer, and to predict contaminant transport in the aquifer. Specifically, the computer code was used to model water flow through the backfill, gravel-clay barrier, vault structure, and saltstone waste form. The code was then used to model the release of contaminants from the waste form, migration through the vault structure, surrounding soils and underlying formations. The simulation results generated by the PORFLOW-3D code were then post-processed to obtain predictions of

- water pathlines and travel times to the aquifer,
- contaminant plume distributions in the vadose zone,
- contaminant fluxes to the aquifer, and
- contaminant plume distributions in the aquifer's saturated zone.

These results are then used to characterize the isolation performance of the SDF.

**Development History.** The original version of the PORFLO code (Runchal et al. 1985) was developed to analyze the isolation performance of deep geologic repositories. This early version was limited to saturated conditions and two-dimensional porous domains, and was extensively verified and benchmarked by Eyster and Budden (1984). The code was later extended to model variably saturated flow in three-dimensions and was therefore renamed PORFLO-3, version 1.0 (Sagar and Runchal 1990). Version 1.0 of the three-dimensional computer code was independently verified and benchmarked by Magnuson et al. (1990) against FEMWATER, FLASH, TRACR3D, and MAGNUM-2D for some applications. The code has been used in practical applications at the Hanford Site to model various waste disposal problems (Smoot and Sagar 1990), at an experimental waste trench site in Las Cruces, NM to evaluate the solute transport simulation capabilities (Rockhold and Wurstner 1991), and at the INEL to model a large organic vapor plume (Baca et al. 1988).

A newer version of PORFLO-3 (version 2.3) was recently developed which has a number of enhancements and new options. For example, one of the new features of version 2.3 is the capability to model multiphase flow. The commercial version of PORFLO-3 which was used to model the saltstone performance in the vadose and saturated zones is PORFLOW-3D, version 2.4 (Runchal and Sagar, 1992). This later version has not been verified and benchmarked to the same degree as the previous one. However, the Fortran source code has been checked using the INEL's KRAFT and FORWARN software QA programs (which identify coding errors and suspect programming), and benchmarking has been completed using test files from the earlier verification and benchmarking work (Magnuson et al. 1990).

**Code Attributes.** The PORFLOW-3D, version 2.4 computer code is written in Fortran 77 programming language. Some of the unique attributes of this version are

- capability to model either single or multiphase flow,
- applicable to one-, two-, or three-dimensional geometries in Cartesian or cylindrical coordinate systems,
- alternate solver techniques (such as point successive over relaxation, Cholesky decomposition, Gauss elimination, and reduced system conjugate gradient) can be selected,
- multiple porosity representations can be used, and
- discrete features (such as fractures) can be represented by line or plate elements.

The computer program is relatively portable and can be run on personal computers, workstations and mainframe computers.

**Computer Requirements.** Practical applications of the PORFLOW-3D code to realistic multidimensional flow and transport problems require the availability of a high performance workstation or mainframe computer. The vault and vadose zone simulations presented in this report were performed on an IBM workstation. Complex simulation problems such as those performed for the saltstone vault often require double precision, and are cumbersome for personal computers. For saturated flow, a PC with a 486 processor was sufficient to simulate the flow and mass transport regime.

**Restrictions.** Version 2.3 of PORFLO-3 was originally developed for the U.S. DOE and is therefore in the public domain. All versions of the PORFLO-3 code are copyright protected. Commercial versions of the code, PORFLOW-3D, which include updates of the version 2.3 are available from Analytic and Computational Research, Inc., Los Angeles, California.

## II. Code Selection Basis

The code selection criteria put forth in Sect. B.1 of this appendix were used to select PORFLOW-3D for use in the SDF RPA. The procedure followed was to identify several codes meeting requirements 1R - 4R, and subsequently evaluate those codes in terms of the remaining eight desirable criteria (1S - 8S). Table B.4.1 summarizes the results of this procedure. A more detailed explanation is given below.

**General Critique.** At present, there are relatively few general computer codes that have the capability to adequately simulate variably-saturated flow and transport in a multidimensional system. Such codes are scarce because the governing equations for flow in the unsaturated zone are highly nonlinear, and very difficult to solve. In addition to nonlinearity, this numerical difficulty is caused by such factors as:

- large contrasts in soil-hydraulic properties,
- high recharge rates and broad range of saturation conditions,
- contrasting thicknesses of soil strata, and
- advection dominated mass transport.

Advanced computational techniques (Celia et al. 1990 and Fletcher 1988) can overcome some of these difficulties; however, obtaining stable and accurate numerical solutions on a routine basis is still a modeling goal.

A number of computer codes with a demonstrated capability to model flow and transport were considered for application to the SDF study. The principal codes considered were: 1) PORFLOW-3D (Runchal and Sagar 1989 and 1992), 2) FEM-WATER/FEMWASTE (Yeh and Ward 1979; Yeh and Ward 1981; Yeh 1987), 3) FLASH (Baca and Magnuson 1992), 4) SUTRA (Voss 1984), 5) TRACR3D (Travis 1985), and 6) VAM3D-CG (Huyakorn and Panday 1990). All of these codes, with the possible exception of FEMWATER/FEMWASTE meet the first four requirements (1R-4R, see Table B.4.1). The availability of documentation of the most recent version of

Table B.4.1. Evaluation of identified alternative subsurface flow and transport codes

Selection Criteria (by number) <sup>a</sup>	Code Meets Criterion?					
	PORFLO W-3D <sup>b</sup>	FEMWAT ERFEMW ASTE <sup>c</sup>	FLAS H <sup>d</sup>	SUTR A <sup>e</sup>	TRACR3 D <sup>f</sup>	VAM3D- CG <sup>g</sup>
1R	yes	yes	yes	yes	yes	yes
2R	yes	yes	yes	yes	yes	yes
3R	yes	no	yes	yes	yes	yes
4R <sup>h</sup>	yes	yes	yes	yes	yes	yes
1S	yes	yes	yes	yes	yes	yes
2S	yes	no	yes	yes	yes	not known
3S	yes	not known	yes	not known	yes	not known
4S	yes	yes	yes	yes	yes	yes
5S	yes	yes	yes	yes	yes	yes
6S	yes	yes	yes	not known	yes	not known
7S	yes	yes	yes	yes	yes	yes
8S	yes	no	yes	no	no	no

<sup>a</sup> Described in Appendix B-1.

<sup>b</sup> Runchal, A. K. and B. Sagar 1992.

<sup>c</sup> Yeh, G. T. 1987; Yeh, G. T. and D. S. Ward 1981.

<sup>d</sup> Baca, R. G. and S. O. Magnuson 1992.

<sup>e</sup> Voss, C. I. 1984

<sup>f</sup> Travis, B. J. 1985.

<sup>g</sup> Huyakorn, P. S. and S. Panday 1990.

<sup>h</sup> Satisfying this criteria ensured by user.

FEMWATER was in question, as was support by the primary developer of the code. Thus, this code was not considered further.

The remaining codes were evaluated with respect to their probability of satisfying the eight suggested criteria (1S - 8S, Sect. B-1). Reviews of available computer codes useful to performance assessments (Kozak et al. 1989, Case et al. 1989) were consulted to assess this probability. The results are summarized in Table B.4.1. From this table, the lack of familiarity with SUTRA, TRACR3D, and VAM3D-CG is the only distinguishing characteristic between these codes and FLASH and PORFLOW-3D. Because of time constraints, this latter criteria was deemed important to code selection.

The PORFLOW-3D computer code was ultimately selected over FLASH for these reasons:

- previous successful applications to modeling waste sites (Smoot and Sagar 1990);
- quality and completeness of code documentation (Runchal and Sagar 1989 and 1991; Sagar and Runchal 1990);
- favorable results of independent verification and benchmark testing of an earlier version (Magnuson et al. 1990);
- flexibility of the code, computational efficiency and ease of use;
- rigorous testing the source code has undergone using Fortran analyzers.

Applicability to Saltstone Vaults. The hydrogeologic setting at the SRS is uniquely characterized by relatively high recharge rates, drainable soils, and a shallow vadose, or unsaturated, zone. In contrast, the vault and barrier components are typically low permeability. The PORFLOW-3D computer code allows for consideration of heterogeneity and anisotropy, and employs various numerical techniques to enhance stability under the diverse conditions encountered. PORFLOW-3D also has options for considering planar geologic features such as fractures, which is important to evaluating the possibility of vault failure during the time for which performance is being assessed.

Code Verification. Version 1.0 of the PORFLOW-3D computer code has been verified by comparing the numerical solutions against known analytical solutions. In particular, the unsaturated flow component of the code has been verified against the Philip's (1957) analytical solutions for unsaturated flow in vertical and horizontal soil columns. In a like manner, the mass transport component has been verified against a number of analytical solutions for contaminant movement in steady-state flow fields. Results of the code verification are documented in Magnuson et al. (1990).

Code Benchmarking. Version 1.0 of the PORFLOW-3D code has been benchmarked by making code-to-code comparison for various flow and transport simulations. A number of hypothetical flow and transport situations were postulated and were simulated with PORFLOW-3D and other independent computer codes. The hypothetical test problems were formulated to be representative of typical waste sites

with realistic hydrogeologic settings. The PORFLOW-3D code has been benchmark tested against such codes as TRACR3D (Travis 1985), FEMWATER (Yeh and Ward 1979), SUTRA (Voss 1984), and FLASH (Baca 1991). Results of the benchmark testing is documented in Magnuson et al. (1990).

**Code Validation.** At the present time, the PORFLOW-3D code has not been validated by comparison to laboratory or field data. There is a definite need to perform such comparisons against experimental data collected at the SRS.

### III. Theoretical Framework

**Governing Equations and Assumptions.** The governing equations solved in the PORFLOW-3D code are based on the conservation principles of continuum mechanics. These equations describe fluid flow and mass transport processes in a heterogeneous and anisotropic porous medium. The equations are well accepted mathematical representations and are found in such texts as Bear and Bachmat (1990), Freeze and Cherry (1979), and Huyakorn and Pinder (1983). The specific partial differential equation solved in PORFLOW-3D for isothermal fluid flow around and through the saltstone vault is

$$S_s \frac{\partial H}{\partial t} = \frac{\partial}{\partial x_i} \left[ K_{ij} \left( \frac{\partial H}{\partial x_j} - \delta_{ij} \right) \right] + m_v \quad (B4.1)$$

where

- $S_s$  is the fluid storage term (i.e., specific storage or moisture capacity term),
- $H$  is the total or hydraulic head,
- $K_{ij}$  is the hydraulic conductivity tensor,
- $\delta_{ij}$  is the buoyancy vector, and
- $m_v$  is the fluid source or sink term,
- $t$  is time, and
- $x_i$  is distance in the  $i$ th direction.

The quantity  $H$  is defined by:

$$H = h + z - z^* \quad (B4.2)$$

where

- $h$  = pressure head,
- $z$  = elevation head, and
- $z^*$  = reference datum.

and the quantity  $S_e$  is defined by

(B4.3)

$$S_e = S(\alpha_s + \theta_s \alpha_f) + \theta_s \frac{\partial S}{\partial H}$$

where

- $S$  = the saturation level,
- $\alpha_s$  and  $\alpha_f$  = the solid and fluid compressibilities normalized by the specific weight of the fluid, and
- $\theta_s$  = the effective porosity.

Some of the basic assumptions made in the above mathematical formulations are:

- fluid flow is laminar, slightly compressible, and single phase;
- fluid flow obeys Darcy's law for porous flow, where specific discharge is proportional to the hydraulic gradient;
- fluid viscosity is a function of temperature only;
- hydraulic properties of the porous continuum are volume averages; and
- osmotic effects (associated with salts in the waste form) are negligible.

In general, these assumptions are satisfied in the hydrogeologic environment of saltstone vaults.

The specific partial differential equation solved in PORFLOW-3D for contaminant transport from saltstone vault is

$$R_D \phi_D \frac{\partial C}{\partial t} + \frac{\partial}{\partial x_i} (V_i C) = \frac{\partial}{\partial x_i} \left[ \Gamma_{ij}^c \frac{\partial C}{\partial x_j} \right] - \phi_D R_D \lambda C + S_c + \sum_p \phi_D R_D^p \sigma^p \lambda^p C \quad (\text{B4.4})$$

where

- $C$  = contaminant concentration,
- $V_i$  = fluid pore velocities,
- $R_D$  = retardation factor,
- $\Gamma_{ij}^c$  = hydrodynamic dispersivity tensor,
- $\lambda$  = decay rate,
- $S_c$  = mass source term,
- $\sigma^p$  = fraction of decay of the parent mass species which generates the current species, and the superscript  $p$  refers to the parent mass species.

The last term in equation B4.4 represents ingrowth of mass species. The quantity  $R_D$  is defined by:

$$R_D = \left[ 1 + \frac{(1-\theta_T) \rho_s k_d}{\phi_D} \right], \quad (B4.5)$$

where

- $\rho_s$  is bulk density,
- $\theta_T$  is total porosity,
- $\phi_D$  is water filled diffusive porosity, and
- $k_d$  is sorption coefficient,

and  $\Gamma_y^c$  is defined by,

$$\Gamma_{ij}^c = \phi_D \tau_{ij} D_M + \phi_R D_{ij}, \quad (B4.6)$$

where

- $\phi_R$  is the effective pore space saturated with water,
- $\tau_{ij}$  is the tortuosity tensor,
- $D_M$  is the molecular diffusion coefficient, and
- $D_{ij}$  is the mechanical dispersion tensor.

All other coefficients are as previously defined.

Some of the key assumptions that limit the applicability of the above formulation are as follows:

- contaminant concentrations are low enough that the fluid flow is independent of mass transport, i.e., concentrations do not affect the density or viscosity of the fluid;
- diffusion of the contaminants through the fluid obeys Fick's first law, where mass flux is proportional to the concentration gradient with the constant of proportionality being the diffusion coefficient;
- mechanical dispersion is described by Scheidegger's equation, (Scheidegger 1961);
- adsorption (and desorption) of contaminants onto the porous medium is an equilibrium process described by a linear isotherm.

The model formulation is applicable to both unsaturated and saturated flow conditions.

**Initial and Boundary Conditions.** The PORFLOW-3D code accommodates the specification of standard mathematical boundary conditions. These include: 1) Dirichlet, i.e., fixed head or concentration), 2) Neumann, i.e., specified flux, and 3) Robin, i.e., mixed, boundary conditions. Detailed information on boundary condition options is given in Runchal and Sagar (1989 and 1992).

**Numerical Techniques.** In the PORFLOW-3D code, the governing equations for flow and transport are solved using a method referred to as the Nodal Point Integration, a variation of the finite volume or integrated finite difference technique (Runchal and Sagar 1991). In this method, the difference approximations to the governing equations are derived on a staggered grid system. The state variables are computed at the grid nodes whereas the fluid velocities and fluxes are computed at the cell faces (located midway between adjacent grid nodes). Three discretization schemes, or basis functions to be integrated, are provided. The user may select which of the three schemes is to be used to maximize accuracy and stability.

The system of algebraic equations produced by the finite volume method are solved in the PORFLOW-3D code using any one of five techniques

- Point successive over relaxation (Bear and Verruijt 1987),
- Alternating direction implicit (Peaceman and Rachford 1955),
- Cholesky decomposition (de Marsily 1986),
- Gauss elimination (Remson et al. 1970), or
- Reduced system conjugate gradient method (Hestenes and Stiefel 1952).

The nonlinearity of the governing equation for variably saturated flow is solved using a Picard iteration method.

#### IV. Code Inputs and Outputs

**Input Data Structure.** Input data files for the PORFLOW-3D code are relatively easy to prepare and check. The code uses a free-form input which allows the user to document the input data deck. The input file uses a keyword approach to define primary input data groups. For typical flow and transport simulations, the data groups consist of

- Title card and comments,
- Finite difference grid specification, i.e., number of grid nodes in each direction,
- Lists of grid node coordinates,
- Zone definitions that specify the grid locations of distinct strata,
- Rock and hydraulic property specifications,
- Convergence and iteration parameters,
- Initial pressures and concentrations,

- Boundary values and/or fluxes,
- Mass properties including effective diffusion coefficients and Kds,
- Source specifications, and
- Time step and output specifications.

Simulations of multidimensional flow and transport can be performed in either steady-state or time-dependent mode.

**Output Options.** Results from the PORFLOW-3D simulation consist of total head, saturation, contaminant concentration, and Darcy velocities for each grid block in the computational grid. The user can select to print out any or all of the output variables. Each of these variables can be post-processed to produce graphical output.

**Post-Processor Programs.** A number of post-processor programs have been written by EG&G Idaho, Inc. which may be used to graph the simulation results. These post-processor programs are DISSPLA based routines that plot profiles, contours, streamlines and travel times, and time histories. These programs have been used extensively by EG&G Idaho on various projects. However, no formal documentation currently exists. Analytic and Computational Research, Inc. also distributes a PLOT88-based post-processor for use with the 486 PC versions of PORFLOW-3D, documented by Runchal (1991).

**Documentation of Users Instructions.** The PORFLOW-3D, version 2.4, is documented in Runchal and Sagar (1992). This report describes the mathematical theory and numerical techniques of this version, serves as a user's manual, and provides detailed information on the code organization, selection of computational grids and time steps, input structure and keyword definitions.

## APPENDIX B REFERENCES

- Atkinson, A., and J.A. Hearne. 1984. *An Assessment of the Long-Term Durability of Concrete in Radioactive Waste Repositories*. AERE-R11465, Harwell, U.K.
- Baca, R. G., J. C. Walton, and A. S. Rood. 1988. Organic Contaminant Release from a Mixed Waste Disposal Site: Analysis of Vapor Transport through the Vadose Zone and Site Remediation. *Proceedings of Tenth Annual DOE Low-Level Waste Management Conference*. Denver, Colo.
- Baca, R. G. and S. O. Magnuson. 1992. *FLASH - Finite Element Computer Code for Variably Saturated Flow*. EGG-GEO-10274. EG&G Idaho, Inc., Idaho Falls, ID.
- Bear, J., and A. Verruijt. 1987. *Modeling Groundwater Flow and Pollution*. D. Reidel Publishing Co., Boston, Mass.
- Bear, J., and Y. Bachmat. 1990. *Introduction to Modeling of Transport Phenomena in Porous Media*. Kluwer Academic Publishers, Boston, Mass.
- Brown, D. S., and J. D. Allison. 1987. *MINTEQA1. An Equilibrium Metal Speciation Model: User's Manual*. EPA-600/3-87/012. U. S. Environmental Protection Agency, Athens, GA.
- Case, M. J., S. J. Maheras, M. D. Otis, and R. G. Baca. 1989. *A Review and Selection of Computer Codes for Establishing of the Performance Assessment Center*. DOE/LLW-83. EG&G Idaho, Inc.
- Cella, M. A., E. T. Bouloutas, and R. L. Zarba. 1990. A General Mass-Conservative Numerical Solution for the Unsaturated Flow Equation. *Water Resources Research*, 26(7):1483-1496.
- Clear, K.C. 1976. Time to Corrosion of Reinforcing Steel in Concrete Slabs, Vol. 3. Performance After 830 Daily Salt Applications. Federal Highway Administration Report No. FHWA-RD-76-70, NTIS PB-258 446.
- de Marsily, G. 1986. *Quantitative Hydrogeology*. Academic Press, Inc., New York, NY.
- Eyler, L. L., and M. J. Budden. 1984. *Verification and Benchmarking PORFLO: An Equivalent Porous Continuum Code for Repository Scale Analysis*. PNL-5044. Pacific Northwest Laboratory, Richland, Wash.
- Felmy, A. R., D. C. Girvin, and E. A. Jenne. 1984a. *MINTEQ: A Computer Program for Calculating Aqueous Geochemical Equilibria*. (NTIS PB84-157148) EPA-600/3-84-032. National Technical Information Service, Springfield, VA.

- Felmy A. R., S. M. Brown, Y. Onishi, S. B. Yabusaki, and R. S. Argo. 1984b. *MEXAMS—The Metals Exposure Analysis Modeling System*. EPA-600/3-84-031 (NTIS PB84-157155). U. S. Environmental Protection Agency, Athens, GA.
- Fletcher, C. A. J. 1988. *Computational Techniques for Fluid Dynamics*. Vols I & II, Springer-Verlag, New York, NY.
- Freeze, R. A. and J. A. Cherry. 1979. *Groundwater*. Prentice-Hall, Inc. Englewood Cliffs, NJ.
- Hestenes, M. R., and E. Stiefel. 1952. Methods of conjugate gradients for solving linear systems. *NBS J. Res.*, 49:409-436.
- Huyakorn, P. S., and G. F. Pinder. 1983. *Computational Methods in Subsurface Flow*. Academic Press, Inc., New York, NY.
- Huyakorn, P. S., and S. Panday. 1990. *VAM3D-CG - Variably Saturated Analysis Model in Three-dimensions with Preconditioned Conjugate Gradient Matrix Solvers, Documentation and User's Guide, Version 2.1*. HGL/89-02, Hydrogeologic, Inc., Herndon, VA.
- Kozak, M. W., M. S. Y. Chu, C. P. Harlan, and P. A. Mattingly. 1989. *Identification and Recommendation of Computer Codes for Low-Level Waste Performance Assessment*. Subtasks 3.0 and 4.1 of the Final Letter Report to the USNRC (August).
- Krupka, K. M., and J. R. Morrey. 1985. MINTEQ Geochemical Reaction Code: Status and Applications. *Proceedings of a Conference on the Application of Geochemical models to High-Level Nuclear Waste Repository Assessment*. G.K. Jacobs, and S. K. Whatley, Eds. NUREG/CP-0062. U.S. Nuclear Regulatory Commission, Washington, D.C.
- Magnuson, S. O., R. G. Baca, and A. J. Sondrup. 1990. *Independent Verification and Benchmark Testing of the PORFLO-3 Computer Code, Version 1.0*. EGG-BG-9175. EG&G Idaho, Inc., ID.
- Malek, R. I. A., P. H. Licastro, D. M. Roy. 1987. *Saltstone Pore Solution Analyses*. A Report to E. I. DuPont De Nemours, Savannah River Plant, Aiken, SC.
- Nordstrom, D. K., L. N. Plummer, T. M. L. Wigley, T. J. Wolery, J. W. Ball, E. A. Jenne, R. L. Basset, D. A. Crerar, T. M. Florence, B. Fritz, M. Morel, M. M. Reddy, G. Sposito, and J. Thraillkill. 1979. A Comparison of Computerized Chemical Models for Equilibrium Calculations in Aqueous Systems. *Chemical Modeling in Aqueous Systems*. E. A. Jenne, Ed. (ACS Symp. Series 93, American Chemical Society, Washington D.C.), pp. 857-892.

- Peaceman, D. W., and H. H. Rachford, Jr. 1955. The numerical solution of parabolic and elliptic differential equations. *J. Soc. of Industrial and Applied Mathematics*. 3:28-41.
- Peterson, S. R., C. J. Hostetler, W. J. Deutsch, and C. E. Cowan. 1987. MINTEQ User's Manual. (NUREG/CR-4808) PNL-6106. U.S. Nuclear Regulatory Commission, Washington, D.C.
- Phillip, J. R. 1957. Numerical Solution of Equations of the Diffusion Type with Diffusivity Concentration-Dependent II. *Australian Journal of Physics*, 10(2):29-42.
- Remson, L., G. M. Hornberger, and R. F. Molz. 1971. *Numerical Methods in Sugsurface Hydrology*. Wiley-Interscience, New York, NY.
- Rockhold, M. L., and S. K. Wurstner. 1991. *Simulation of Unsaturated Flow and Solute Transport at the Las Cruces Trench Site Using the PORFLO-3 Computer Code*. PNL-7562. Pacific Northwest Laboratory, Richland, Wash.
- Runchal, A. K., B. Sagar, R. G. Baca, and N. W. Kline. 1985. *PORFLO - A Continuum Model for Fluid Flow, Heat Transfer, Mass Transport in Porous Media*. RHO-BW-CR-150P. Rockwell Hanford Operations, Richland, Wash.
- Runchal, A. K., and B. Sagar. 1989. *PORFLO-3: A Mathematical Model for Fluid Flow, Heat and Mass Transport in Variably Saturated Geologic Media, Users Manual, Version 1.0*. WHC-EP-0042. Westinghouse Hanford Operations, Richland, Wash.
- Runchal, A. K. 1991. *acrPLOT - A General Purpose Plotting Package, User's Manual - Version 8.00*. ACRI/014/Rev. A. Analytic and computational Research, Inc., Los Angeles, Calif.
- Runchal, A. K., and B. Sagar. 1992. *PORFLOW: A Model for Fluid Flow, Heat and Mass Transport in Multifluid, Multiphase Fractured or Porous Media, Users Manual, Version 2.4*. ACRI/016/Rev. G, Analytic and Computational Research, Inc., Los Angeles, Calif.
- Sagar, B., and A. K. Runchal. 1990. *PORFLO-3: A Mathematical Model for Fluid Flow, Heat and Mass Transport in Variably Saturated Geologic Media, Theory and Numerical Methods, Version 1.0*. WHC-EP-0042. Westinghouse Hanford Operations, Richland, Wash.
- Scheidegger, A. E. 1961. General Theory of Dispersion in Porous Media. *J. Geophys. Res.* 66(10):3273-3278.

- Smith, R. W. 1988. Calculation of Equilibria at Elevated Temperatures Using the MINTEQ Geochemical Code. PNL-6700. Pacific Northwest Laboratory, Richland, Wash.
- Smoot, J. L., and B. Sagar. 1990. *Three-dimensional Contaminant Plume Dynamics in the Vadose Zone: Simulation of the 241-T-106 Single-Shell Tank Leak at Hanford*. PNL-7221. Pacific Northwest Laboratories, Richland, Wash.
- Travis, B. 1985. *TRACR3D: A Model of Flow and Transport in Porous Media*. LA-9667-MS. Los Alamos National Laboratory, Los Alamos, NM.
- Trusdell, A. H., and B. F. Jones. 1974. WATEQ, a Computer Program for Calculating Chemical Equilibria of Natural Waters. *J. Research U.S. Geol. Survey*, 2:233-348.
- Voss, C. I. 1984. *A Finite-Element Simulation Model for Saturated-Unsaturated, Fluid-Density-Dependent Ground-Water Flow and Energy Transport or Chemically-Reactive Single-Species Solute Transport*. U. S. Geological Survey, Reston, VA.
- Walton, J. C., L. E. Plansky, and R. W. Smith. 1990. *Models for Estimation of Service Life of Concrete Barriers in Low-Level Radioactive Waste Disposal*. Prepared for Division of Engineering Office of Nuclear Regulatory Research, U.S. Nuclear Regulatory Commission, Washington, DC 20555, NRC FIN A6858, NUREG/CR-5542, EGG-2597, RW,CC, 38 p.
- Wolfram, S. 1988. *Mathematica: A System for Doing Mathematics by Computer*. Addison-Wesley Publishing Company, Inc., USA, 749 p.
- Yeh, G. T., and D. S. Ward. 1979. *FEMWATER: A Finite-Element Model of Water Flow Through Saturated-Unsaturated Porous Media*. ORNL-5567. Oak Ridge National Laboratory, Oak Ridge, Tenn.
- Yeh, G. T., and D. S. Ward. 1981. *FEMWASTE: A Finite-Element Model of WASTE Transport Through Saturated-Unsaturated Porous Media*. ORNL-5601. Oak Ridge National Laboratory, Oak Ridge, Tenn.
- Yeh, G. T. 1987. *FEMWATER: a Finite-Element Model of WATER Flow Through Saturated-Unsaturated Porous Media - First Revision*. ORNL-5567/R1. Oak Ridge National Laboratory, Oak Ridge, Tenn.